NUREG/CR-1067

Design Charts for a Class of Nonlinear Systems With Gaps Under a Variety of Dynamic Loads

Prepared by J. C. Anderson and others

University of Southern California

Prepared for
U. S. Nuclear Regulatory
Commission

Available from

GPO Sales Program
Division of Technical Information and Document Control
U.S. Nuclear Regulatory Commission
Washington, D.C. 20555

and

National Technical Information Service
Springfield, Virginia 22161

NUREG/CR-1067
R0

Design Charts for a Class of Nonlinear Systems With Gaps Under a Variety of Dynamic Loads

Manuscript Completed: June 1979
Date Published: November 1979

Prepared by
J. C. Anderson and others

University of Southern California
Los Angeles, CA 90007

Prepared for
Division of Reactor Safety Research
Office of Nuclear Regulatory Research
U.S. Nuclear Regulatory Commission
Washington, D.C. 20555
NRC FIN No. B5976

ABSTRACT

An analytical investigation is made of the dynamic response of a multi-degree-of-freedom system with a displacement nonlinearity caused by a dead space gap. This class of problem can be used to model some of the mechanical equipment, piping, and components found in nuclear reactor facilities. The problem is discretized mathematically and numerical techniques are used to solve the resulting equations of motion. Displacement response spectra are developed for a variety of system parameters and dynamic loadings that include sinusoidal, random, and half-sine pulse. These response spectra form a library of design charts that provide useful information for designers and engineers.

ACKNOWLEDGEMENTS

This study was supported in part by a contract with the U.S. Nuclear Regulatory Commission.

TABLE OF CONTENTS

LIST OF FIGURES

Figure

LIST OF TABLES

Table

ABBREVIATIONS AND SYMBOLS

C_1, C_2, C_4	Damping constants
D	Clearance within which auxiliary mass can oscillate
K_1, K_2, K_4	Spring constants
M_1	Mass of primary system
M_2	Mass of auxiliary system (damper)
ζ_1	Fraction of critical damping, $C_1/\left(2\sqrt{K_1 M_1}\right)$
ζ_2	Fraction of critical damping, $C_2/\left(2\sqrt{K_2 M_2}\right)$
ζ_4	Fraction of critical damping, $C_4/\left(2\sqrt{K_4 M_2}\right)$
μ	Mass ratio (M_2/M_1)
$x_j(t)$	Displacement of j-th mass
$\dot{x}_j(t)$	Velocity of j-th mass
$\ddot{x}_j(t)$	Acceleration of j-th mass
ω_1	Frequency, $\sqrt{K_1/M_1}$
ω_2	Frequency, $\sqrt{K_2/M_2}$
ω_4	Frequency, $\sqrt{K_4/M_2}$
ω	Excitation frequency (harmonic)
ω_{di}	Damped natural frequency, $\sqrt{1 - \zeta_i^2}\,\omega_i$
i	$\sqrt{-1}$
t	Time
F_o	Amplitude of harmonic or pulse excitation force
F(t)	Excitation force applied to M_1
SDOF	Single degree of freedom
PSD	Power spectral density
RMS	Root mean square
$S_f(\omega)$	Spectral density of excitation force

S_o	Uniform spectral density, $F(t)/M_1$
$S_x(\omega)$	Spectral density of displacement response
T_1	Period of SDOF, $2\pi/\omega_1$
σ_{x_1}	RMS displacement of M_1 of the defined system model
σ_{x_o}	RMS displacement of M_1 in absence of the auxiliary mass M_2 (SDOF), $\sqrt{\pi S_o/(2\zeta_1\omega_1^3)}$
z_i	Relative displacement, $(x_i - x_B)$
x_B	Base displacement
y	Relative distance between M_1 and M_2, $(x_1 - x_2)$
τ	Duration of pulse excitation
RSMD	Root mean square displacement
SIGMAO	Equivalent to the symbol σ_{x_o} (used in graphic charts)

SECTION 1

INTRODUCTION

Spectrum analysis is an approximate method for determining the dynamic response of linear and nonlinear systems to dynamic excitations. Shock spectra have been used for many years to estimate the response of systems subjected to impulsive load. Earthquake response spectra have been widely used for the design of nuclear power plant structures and generated floor spectra have been used for the design of various mechanical equipment and systems. An important class of dynamic system that occurs frequently in mechanical equipment mounts, steam piping, pumps, and valves is the one having a gap or free space between the dynamic system and its support (see Figure 1.1).

This type of system is used as a seismic restraint in nuclear piping systems. The gap allows the piping to expand and contract in the operating condition but restrains the piping in the event of a strong earthquake. A typical run of main steam piping with gapped restraints is shown in Figure 1.2. A similar situation exists in vibration isolation mounts for mechanical equipment. In order to insure the proper functioning of equipment, it is often necessary to limit the maximum displacement. This is done by placing additional snubber restraints in parallel with the spring mounting system. The snubber restraints have an initial gap and a relatively high stiffness. This allows the isolation system to work freely over a given displacement range but limits the range when the displacements become large. A schematic of a vibration isolation system with snubber restraints is shown in Figure 1.3.

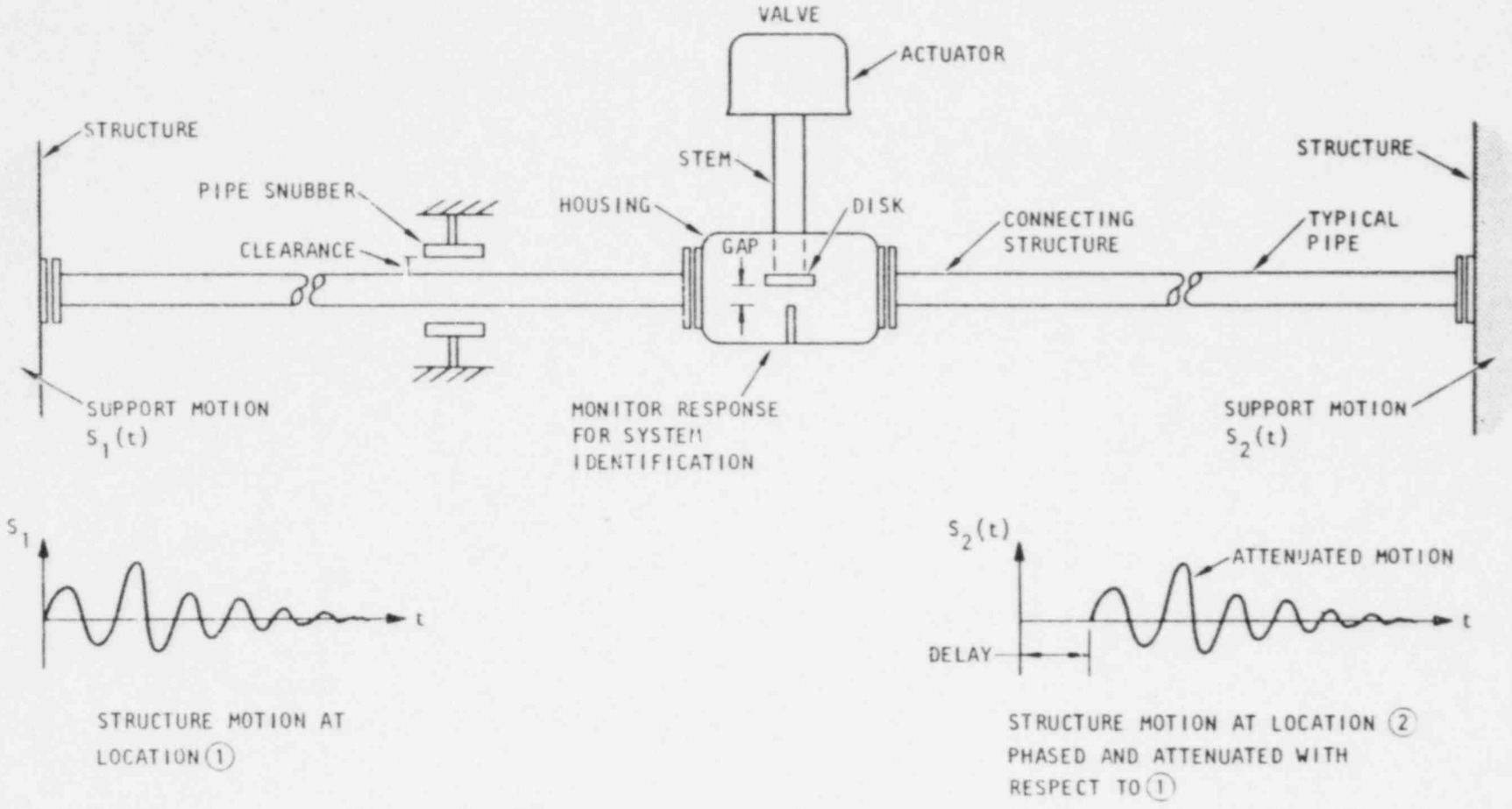

Figure 1.1 Typical Nuclear Power Plant Equipment/Structure System

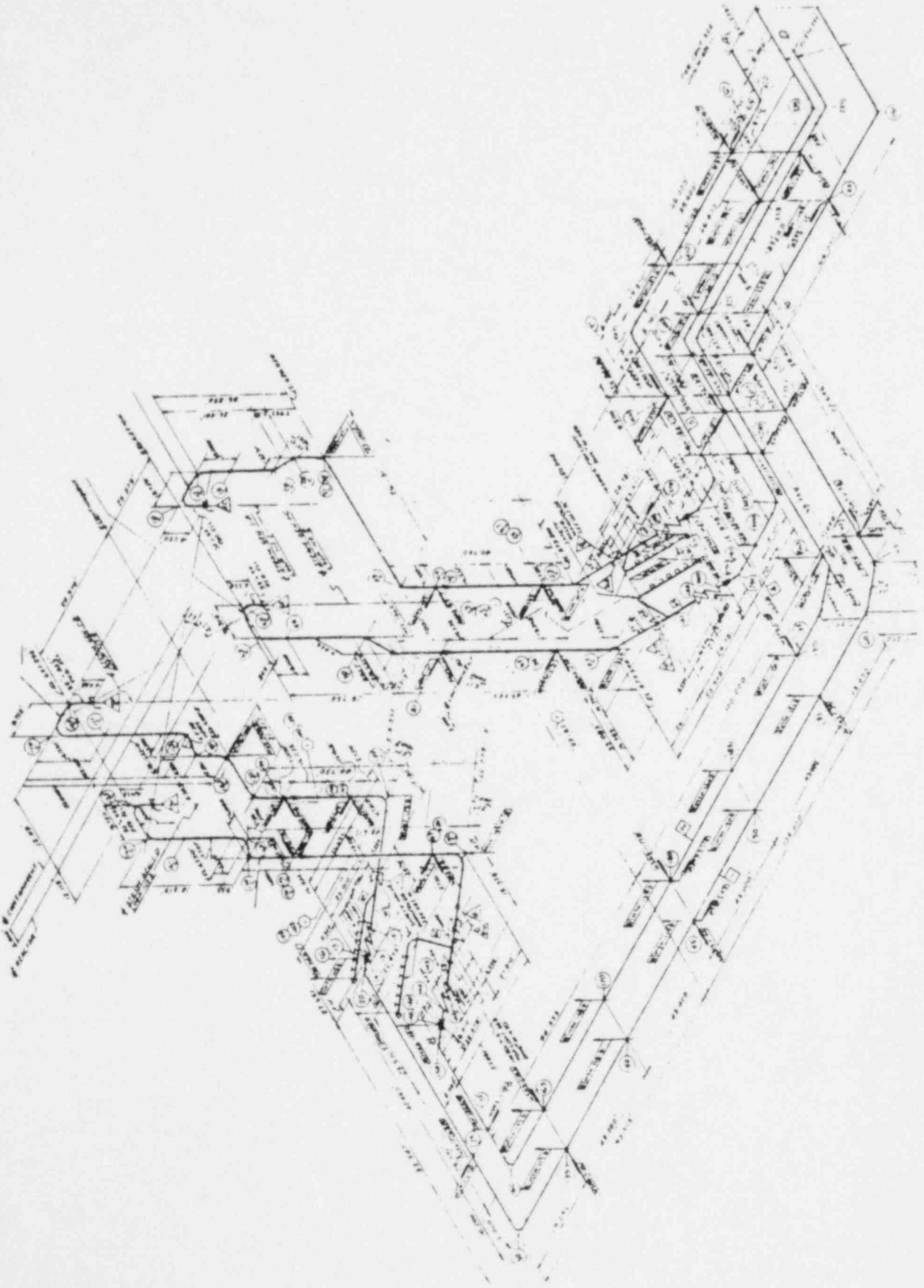

Figure 1.2 Typical Run of Main Steam Piping

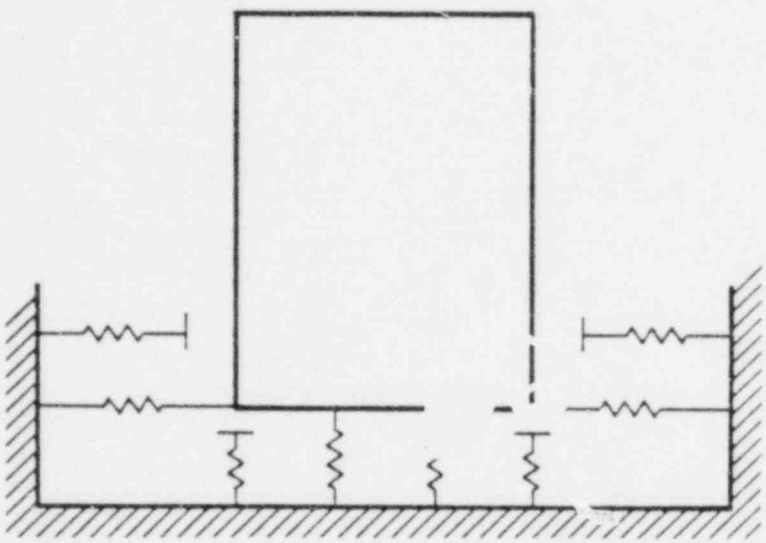

Figure 1.3 Mechanical Equipment Mount

Various valves can also be represented by this same type of dynamic system. In this case, motion in one direction is usually restricted by the valve seat; however, the system can deflect in the other direction, depending upon the stiffness of the actuator system. A typical section of a globe valve is shown in Figure 1.4 along with mathematical models of the system in Figures 1.5 to 1.. Typical arrestors and mathematical models of piping systems with gapped supports are shown in Figures 1.8 to 1.11. A representative nuclear-type valve is shown in Figure 1.12.

In all cases, it is desirable to keep the stresses in the system within the elastic range, thereby preventing permanent damage that might impair the functioning of the system. Therefore, the only nonlinearity that arises is the geometric nonlinearity due to the presence of the gap.

Model studies are also useful for evaluating the dynamic response of these systems to various types of base excitation. When system prototypes can be tested on shaking machines, the true response of the system is obtained. However, in many cases the use of a full-scale prototype is either too cumbersome or too expensive or both. Scaled models are then required to evaluate the response. Models are often difficult to scale. Owing to the nonlinear behavior, the laws of similitude between model and prototype cannot be directly applied. Furthermore, scaling of mechanical equipment models often encounters fabrication problems, which cause a distortion of the model. At best, model studies can be used to substantiate analytical techniques; however, they are not readily adaptable to the design-evaluation environment.

An attractive method for evaluating the behavior of these systems is the use of design charts, which are actually design spectra. These can be developed using a relatively simple mathematical model that in-

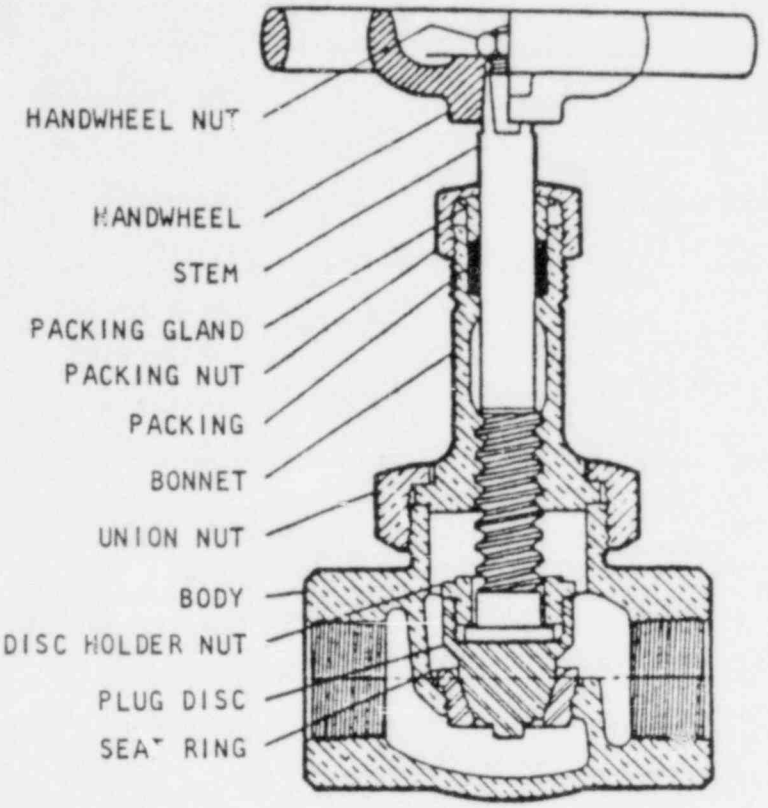

Figure 1.4 Typical Valve Configuration (Lyons, 1975)

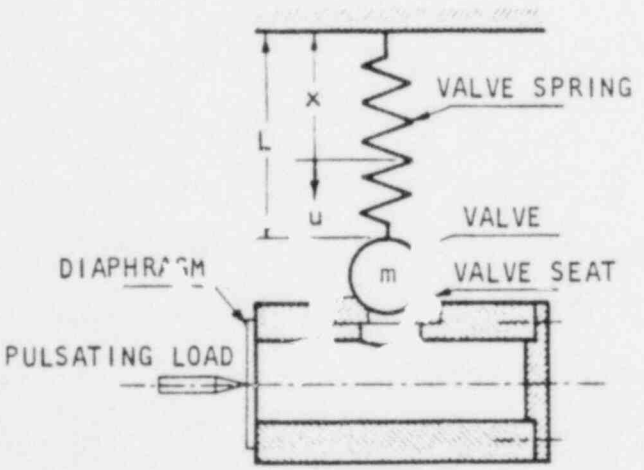

Figure 1.5 Model of a Relief Valve (Dokanish, 1978)

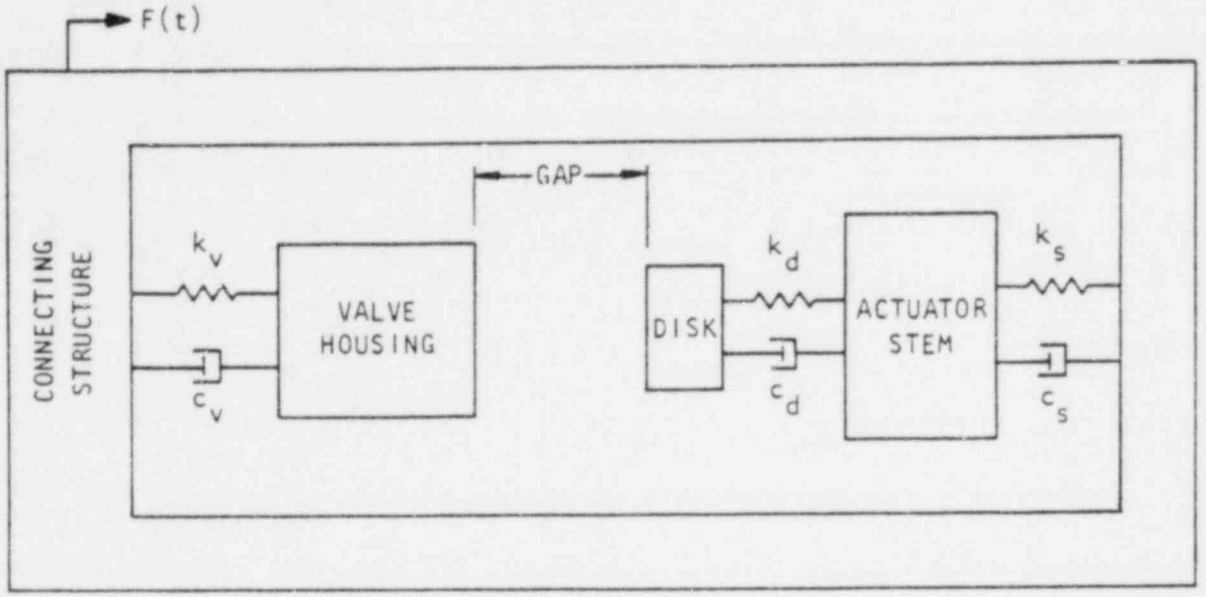

Figure 1.6 Nonlinear Lumped-Parameter Model of a Gate Valve (USC, 1976)

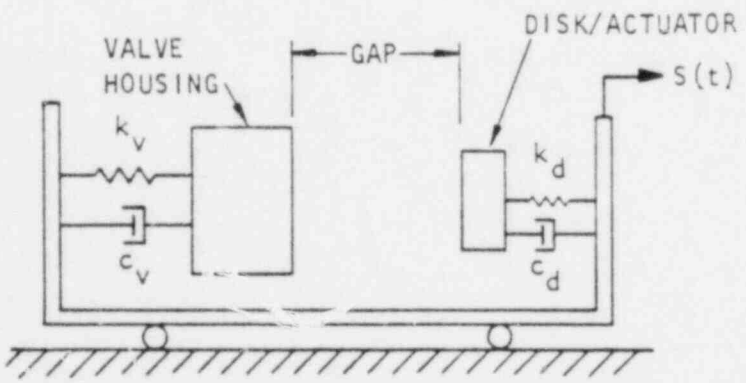

Figure 1.7 Simplified Nonlinear Valve Model (USC, 1976)

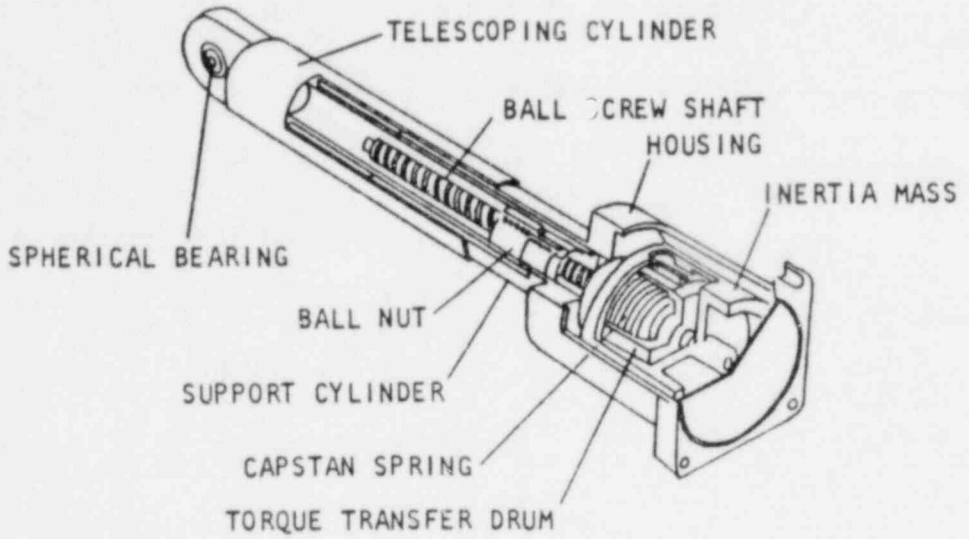

Figure 1.8 Cutaway of Typical Pacific Scientific Arrestor (Onesto, 1978)

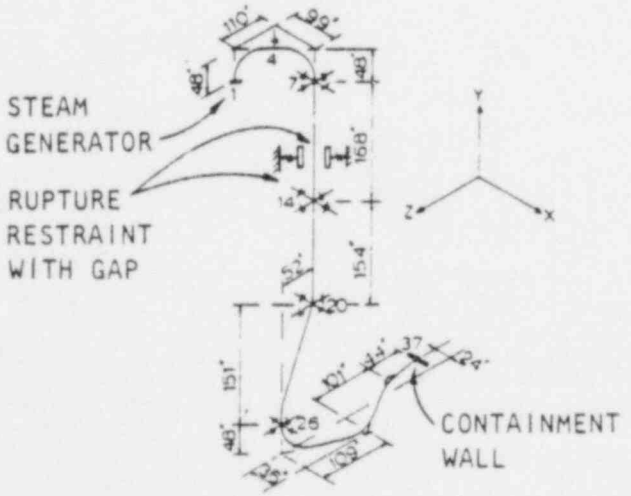

Figure 1.9 Typical Main Steam Piping (Anderson, 1976)

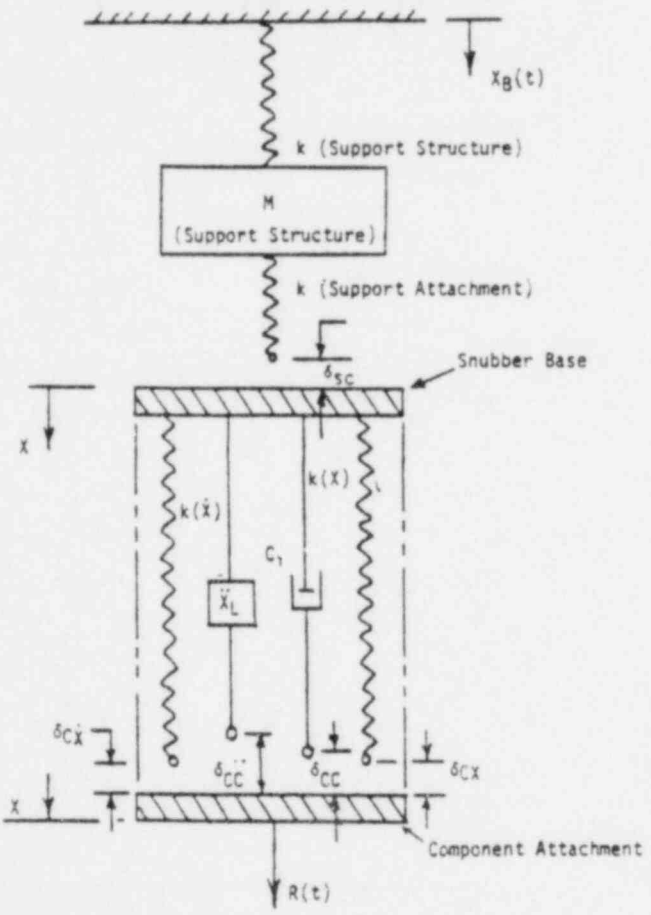

Figure 1.10 A Model of a Mechanical Snubber
(Onesto, 1978)

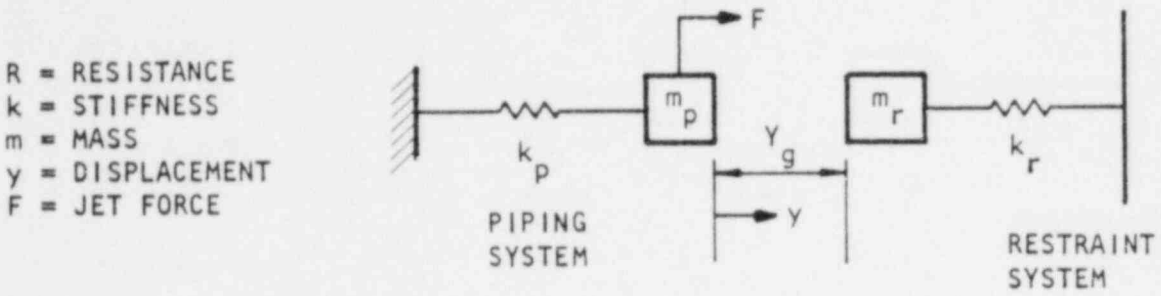

NOTE: ALL SPRINGS ARE ELASTO-PLASTIC

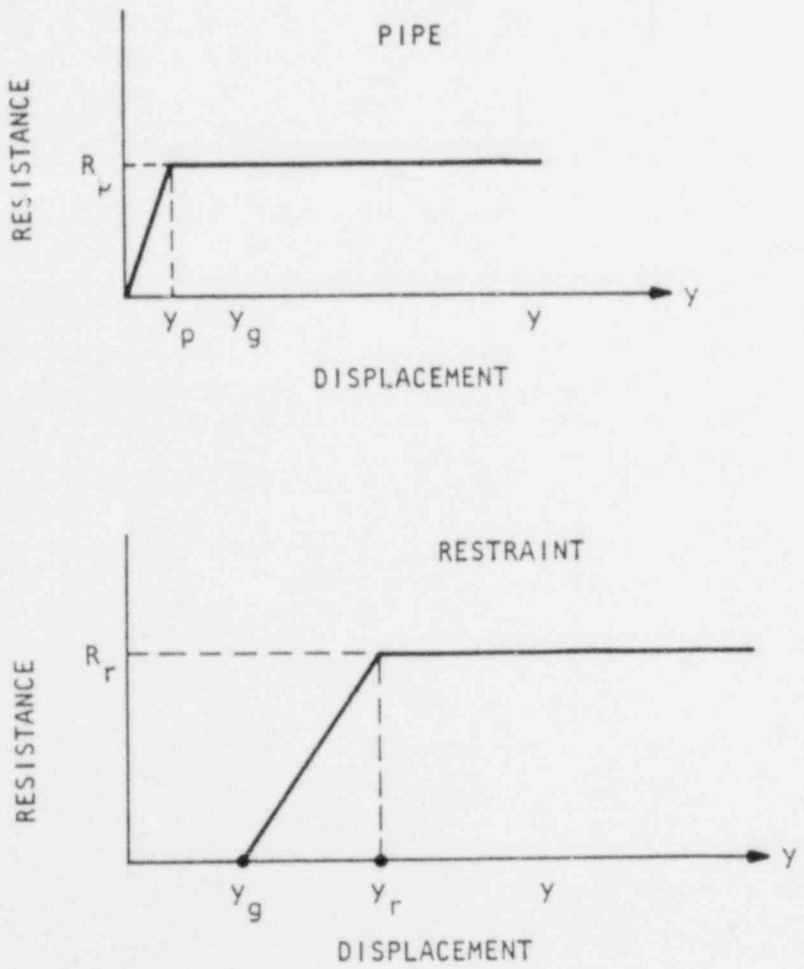

Figure 1.11 Model of a Pipe/Restraint System (Bechtel, 1974)

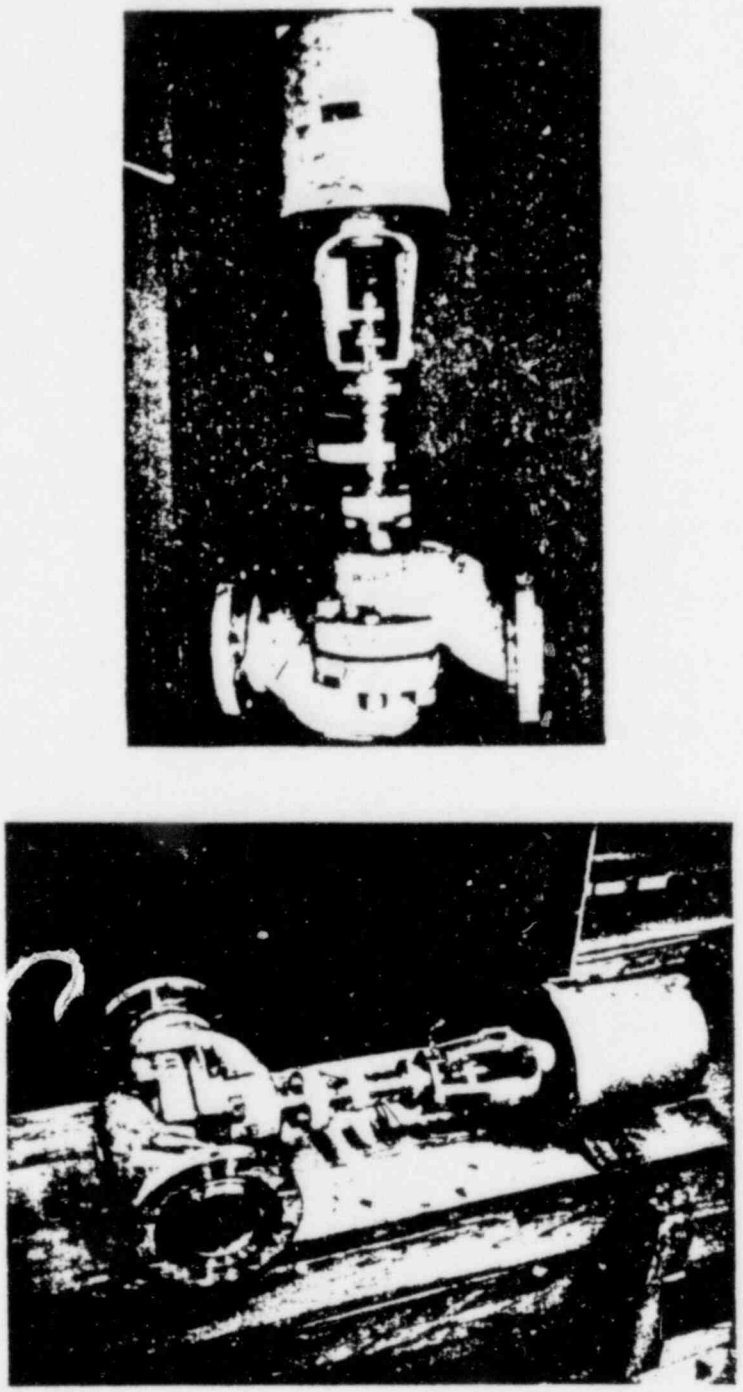

Figure 1.12 Pictures of a Typical Nuclear Valve

corporates the important aspects of the prototype system. This allows parametric studies to be made of the effect of the significant system parameters.

There are many response spectra available in the literature for linear systems (Harris and Crede, 1961; Crandall and Mark, 1963). However, there are few if any for the nonlinear problem similar to the one under consideration (Masri and Ibrahim, 1973). Even for simple dynamic systems, the inclusion of nonlinear behavior introduces several new variables that cannot be neglected. This makes the nonlinear design charts more complicated than their equivalent, and interpolation between curves becomes more difficult.

This study presents a library of typical design spectra that have been developed for three types of excitation: (1) harmonic, (2) pulse, and (3) random. Illustrative examples are presented in Appendix A which demonstrate the use of three response spectra in the solution of typical design engineering problems.

SECTION 2

DESCRIPTION OF MODEL

The system model shown in Figure 2.1 is a nonlinear multi-degree-of-freedom system that is subjected to an arbitrary random, sinusoidal, or half-sine pulse excitation forcing function F(t). The various types of forcing functions are displayed in Figures 2.2 through 2.5. The model can be used to solve the design problems discussed in Section 1.

The general equations of motion for this system model when subjected to F(t) excitation (that is, $x_B = 0$) are derived as follows.

The equation of motion for M_1 when there is no contact with the auxiliary mass M_2 is

$$M_1\ddot{x}_1 + C_1\dot{x}_1 + K_1x_1 = F(t) \tag{2.1}$$

if $(x_1 - x_2) > D$, the two masses are in contact, and the equation of motion of M_2 is

$$M_1\ddot{x}_1 + C_1\dot{x}_1 + (\dot{x}_1 - \dot{x}_2)C_4 + (x_1 - x_2 - D)K_4 = F(t) \tag{2.2}$$

The following dimensionless parameters are introduced:

$$\omega_i^2 = \frac{K_i}{M_i} \qquad i = 1,2 \tag{2.3}$$

$$2\zeta_i\omega_i = \frac{C_i}{K_i} \qquad i = 1,2 \tag{2.4}$$

$$\omega_4^2 = \frac{K_4}{M_2} \tag{2.5}$$

$$2\zeta_4\omega_4 = \frac{C_4}{M_2} \tag{2.6}$$

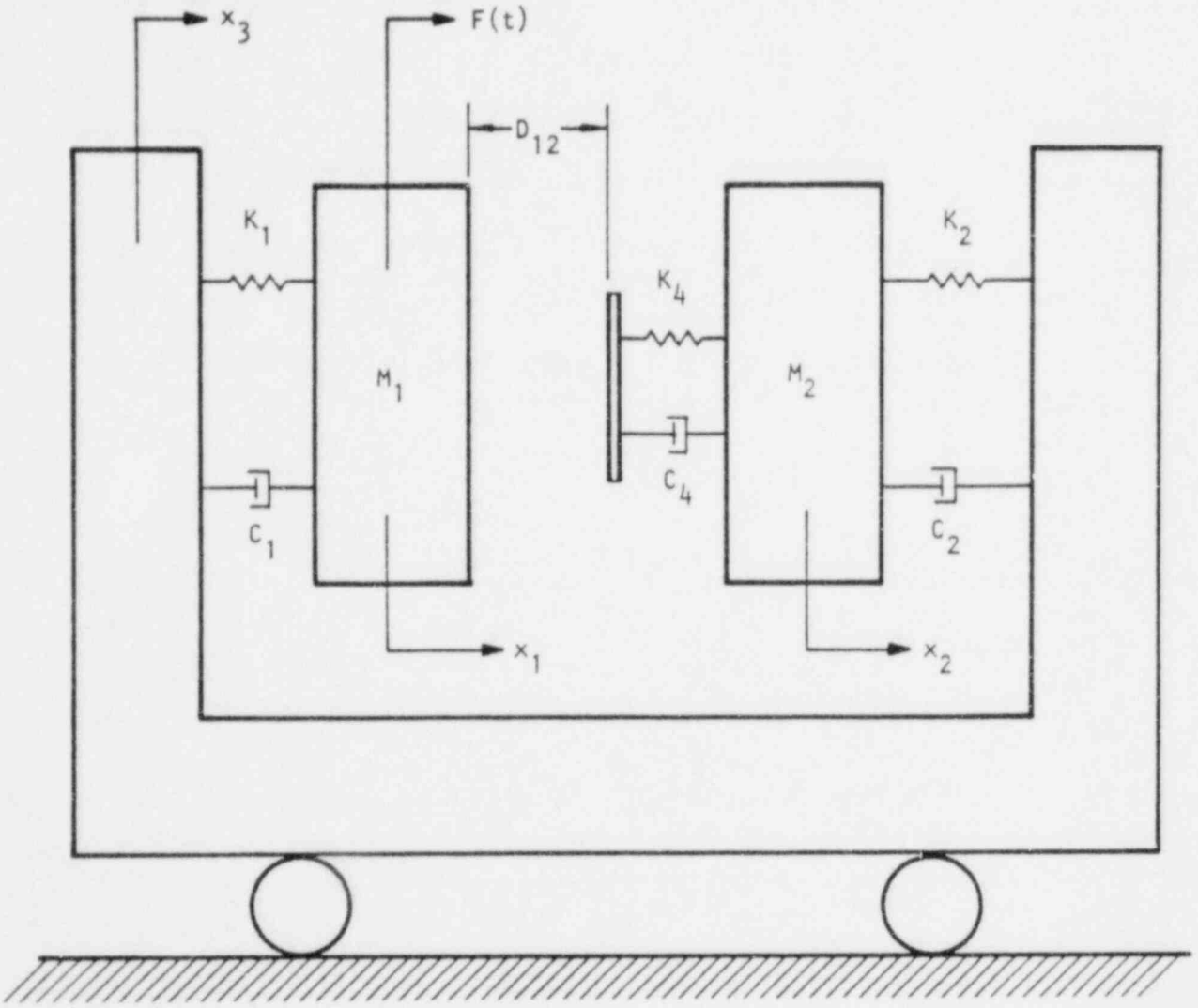

Figure 2.1 System Model

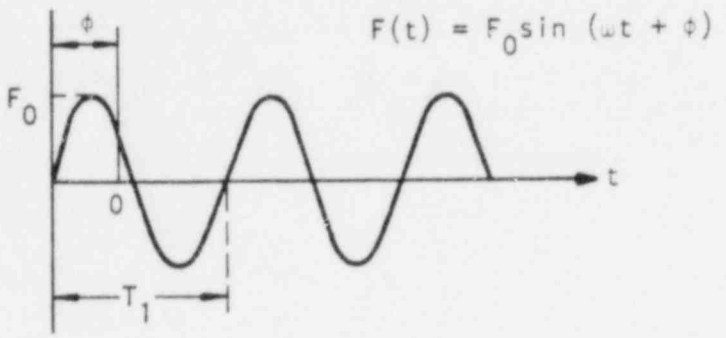

Figure 2.2 Harmonic Excitation Function

$$F(t) = \begin{cases} F_0 \sin \omega t & 0 \le t \le \tau \\ 0 & t > \tau \end{cases}$$

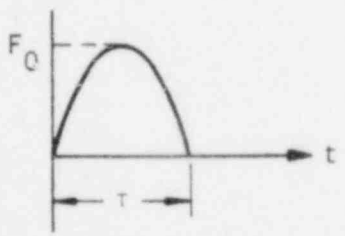

Figure 2.3 Half-Sine Pulse Excitation Function

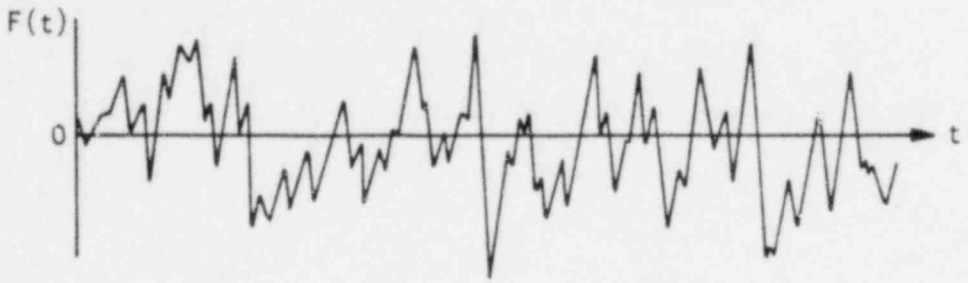

Figure 2.4 Random Forcing Function, Time History

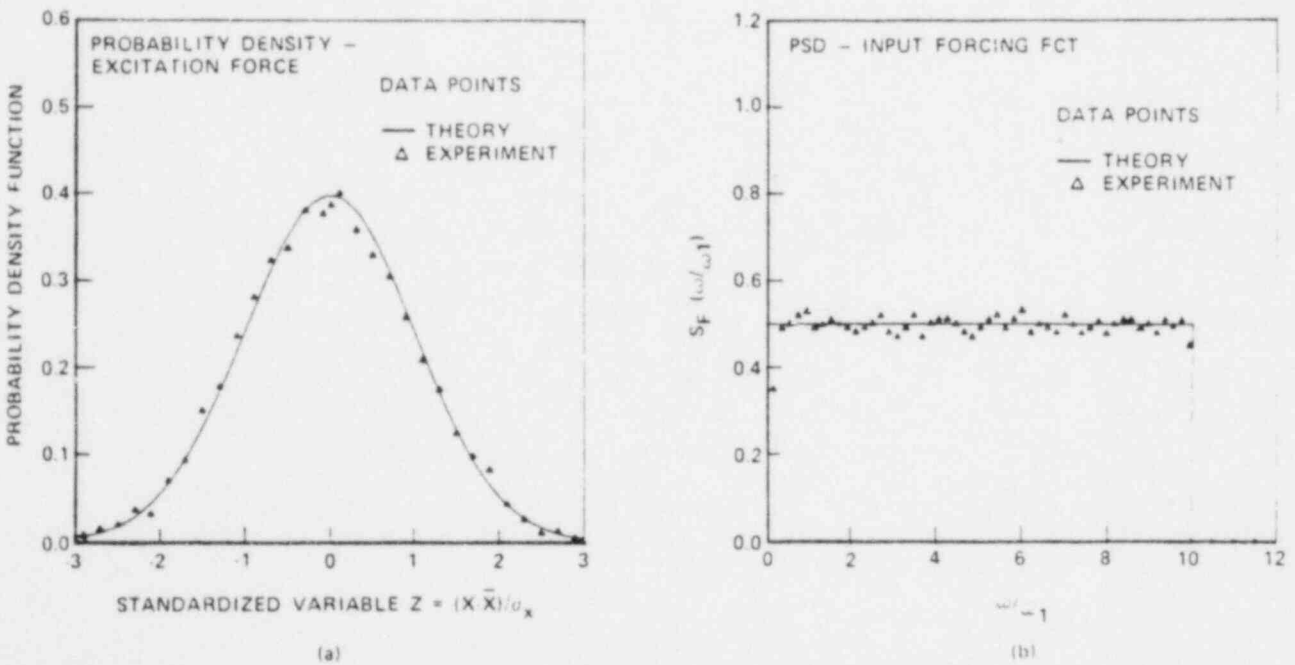

Figure 2.5 Characteristics of Computer-Generated Random Forcing Function

$$\mu = \frac{M_2}{M_1} \tag{2.7}$$

Equations (2.1) and (2.2) can thus be rewritten as

$$\ddot{x}_1 + 2\zeta_1\omega_1\dot{x}_1 + \omega_1^2 x_1 = \frac{1}{M_1} F(t) \tag{2.8}$$

$$\ddot{x}_1 + 2\zeta_1\omega_1\dot{x}_1 + \omega_1^2 x_1 + 2\zeta_4\omega_4\mu\dot{y} + \omega_4^2\ \mu(y - D) = \frac{1}{M_1} F(t) \tag{2.9}$$

where

$$y(t) = x_1(t) - x_2(t) \tag{2.10}$$

The equation of motion for M_2 when there is no contact with the primary mass M_1 is

$$M_2\ddot{x}_2 + C_2\dot{x}_2 + K_2x_2 = 0 \tag{2.11}$$

and the equation of motion for M_2 when there is contact with the primary mass M_1 is

$$M_2\ddot{x}_2 + C_2\dot{x}_2 + K_2x_2 - (\dot{x}_1 - \dot{x}_2)C_4 - (x_1 - x_2 - D)K_4 = 0 \tag{2.12}$$

Using relationships (2.3) through (2.7), equations (2.11) and (2.12) also can be rewritten as

$$\ddot{x}_2 + 2\zeta_2\omega_2\dot{x}_2 + \omega_2^2 x_2 = 0 \tag{2.13}$$

$$\ddot{x}_2 + 2\zeta_2\omega_2\dot{x}_2 + \omega_2^2 x_2 - 2\zeta_4\omega_4 - \omega_4^2(y - D) = 0 \tag{2.14}$$

Therefore, the basic system equations for force excitation F(t) (i.e., $x_B = 0$) are:

$$\ddot{x}_1 + 2\zeta_1\omega_1\dot{x}_1 + \omega_1^2 x_1 = \frac{1}{M_1} F(t) \tag{2.15}$$

$$\ddot{x}_2 + 2\zeta_2\omega_2\dot{x}_2 + \omega_2^2 x_2 \tag{2.16}$$

when $(x_1 - x_2) < D$ (i.e., no contact), and

$$\ddot{x}_1 + 2\zeta_1\omega_1\dot{x}_1 + \omega_2^2 x_1 + 2\zeta_4\omega_4\mu\dot{y} + \omega_4^2\mu(y - D) = \frac{1}{M_1} F(t) \tag{2.17}$$

$$\ddot{x}_2 + 2\zeta_2\omega_2\dot{x}_2 + \omega_2^2 x_2 - 2\zeta_4\omega_4 - \omega_4^2 (y - D) = 0 \tag{2.18}$$

when $(x_1 - x_2) \geq D$ (i.e., M_1 and M_2 contact each other).

The general equations of motion for the system model when subjected to base motion x_B (that is, $F(t) = 0$) are derived as follows.

The equation of motion for M_1 when there is no contact with the auxiliary mass M_2 is

$$M_1\ddot{x}_1 + C_1(\dot{x}_1 - \dot{x}_B) + K_1(x_1 - x_B) = 0 \tag{2.19}$$

Let

$$z_1(t) = x_1(t) - x_B(t) \tag{2.20}$$

$$z_2(t) = x_2(t) - x_B(t) \tag{2.21}$$

Using relationship (2.20), equation (2.19) can be rewritten as

$$M_1\ddot{z}_1 + C_1\dot{z}_1 + K_1 z_1 = -M_1\ddot{x}_B \tag{2.22}$$

$$\ddot{z}_1 + 2\zeta_1\omega_1\dot{z}_1 + \omega_1^2 z_1 = -\ddot{x}_B \tag{2.23}$$

The equation of motion for M_2 when there is no contact with the primary mass M_1 is

$$M_2\ddot{x}_2 + C_2(\dot{x}_2 - \dot{x}_B) + K_2(x_2 - x_B) = 0 \tag{2.24}$$

Using relationship (2.21), equation (2.24) can be rewritten as

$$M_2\ddot{z}_2 + C_2\dot{z}_2 + K_2 z_2 = -M_2\ddot{x}_B \tag{2.25}$$

$$\ddot{z}_2 + 2\zeta_2\omega_2\dot{z}_2 + \omega_2^2 z_2 = -\ddot{x}_B \tag{2.26}$$

The equation of motion for M_1 when there is a contact with M_2 is

$$M_1\ddot{x}_1 + C_1(\dot{x}_1 - \dot{x}_B) + K_1(x_1 - x_B) + K_4(x_1 - x_2 - D) + C_4(\dot{x}_1 - \dot{x}_2) = 0 \tag{2.27}$$

Using relationships (2.3) through (2.7) and (2.20), equation (2.27) can be rewritten as

$$M_1\ddot{z}_1 + C_1\dot{z}_1 + K_1 z_1 = -M_1\ddot{x}_B - K_4(y - D) - C_4\dot{y} \tag{2.28}$$

$$\ddot{z}_1 + 2\zeta_1\omega_1\dot{z}_1 + \omega_1^2 z_1 = -\ddot{x}_B - \mu\omega_4^2(y - D) - 2\zeta_4\omega_4\mu\dot{y} \tag{2.29}$$

In a similar fashion, the equation of motion for M_2 during impact is

$$M_2\ddot{x}_2 + C_2(\dot{x}_2 - \dot{x}_B) + K_2(x_2 - x_B) - K_4(x_1 - x_2 - D) - K_4(\dot{x}_1 - \dot{x}_2) = 0 \tag{2.30}$$

Using relationships (2.3) through (2.7) and (2.21), equation (2.30) can be rewritten as

$$M_2\ddot{z}_2 + C_2\dot{z}_2 + K_2 z_2 = -M_2\ddot{x}_B + K_4(y - D) + C_4\dot{y} \tag{2.31}$$

$$\ddot{z}_2 + 2\zeta_2\omega_2\dot{z}_2 + \omega_2^2 z_2 = -\ddot{x}_B + \omega_4^2(y - D) + 2\zeta_4\omega_4\dot{y} \tag{2.32}$$

Therefore, the basic system equations for base excitation $\ddot{x}_B$ (that is, $F(t) = 0$) are

$$\ddot{z}_1 + 2\zeta_1\omega_1\dot{z}_1 + \omega_1^2 z_1 = -\ddot{x}_B \tag{2.33}$$

$$\ddot{z}_2 + 2\zeta_2\omega_2\dot{z}_2 + \omega_2^2 z_2 = -\ddot{x}_B \tag{2.34}$$

when $(x_1 - x_2) < D$ (i.e., no contact), and

$$\ddot{z}_1 + 2\zeta_1\omega_1\dot{z}_1 + \omega_1^2 z_1 = -\ddot{x}_B - \mu\omega_4^2(y - D) + 2\zeta_4\omega_4\mu\dot{y} \tag{2.35}$$

$$\ddot{z}_2 + 2\zeta_2\omega_2\dot{z}_2 + \omega_2^2 z_2 = -\ddot{x}_B + \omega_4^2(y - D) + 2\zeta_4\omega_4\dot{y} \qquad (2.36)$$

when $(x_1 - x_2) \geq D$ (i.e., M_1 and M_2 contact each other).

The appropriate system equations of motion were numerically evaluated with a digital computer program, which employed Runge-Kutta integration techniques, to determine the response spectra presented in Section 4. Monte Carlo averaging was used to determine displacement response spectra for random excitation. The details of this computer program are presented in the report by Masri and Stott (1979).

SECTION 3

PROGRAM VALIDATION

The following table and figures represent numerical results used to verify the accuracy of the computer program (Masri and Stott, 1979) that was used to evaluate the system model equations of motion derived in Section 2. The data obtained from these computer runs are compared with published theoretical results as well as experimental measurements. The system model was reduced to an equivalent SDOF system (i.e., $D = \infty$ and $\mu = 0$) for some of these verifications.

Figure 3.1 contains a comparison of transmissibility (i.e., $x_{1_{max}}/(F_o/K_1)$) versus frequency ratio for various critical damping ratios corresponding to a linear SDOF system. The theoretical data values were obtained from Biggs (1964).

The verification of the nonlinear parts of the program was done by comparing the numerical results with exact solutions available for the nonlinear model shown in Figure 3.2. The comparison of numerical, experimental, and closed form solutions (USC, 1976) for this case are shown in Figure 3.3.

Table 3.1 is a comparison of the maximum displacement amplification factor of M_1 with published data (Biggs, 1964) for a sinusoidal function applied to a linear SDOF system. Comparison between analytical and experimental results for a nonlinear system with a gap under pulse excitation is shown in Figure 3.4.

Figure 3.5 displays the RMS displacement of M_1 of a linear SDOF system (σ_{x_o}) obtained from an ensemble average of 20 data samples as a function of critical damping ratio. The theoretical data values were

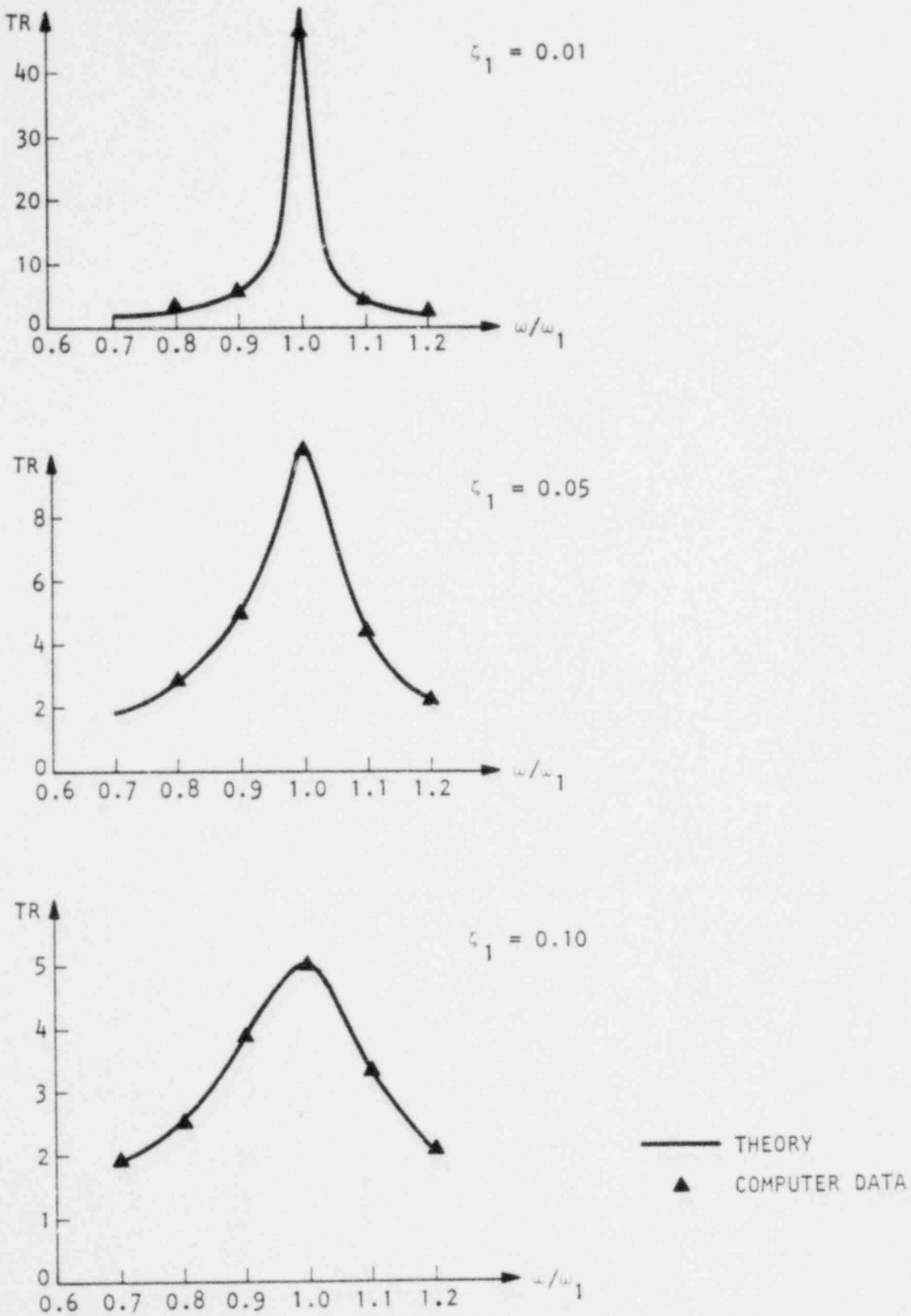

Figure 3.1 Comparison of Theoretical and Computer-Generated Data - SDOF System, Sinusoidal Excitation

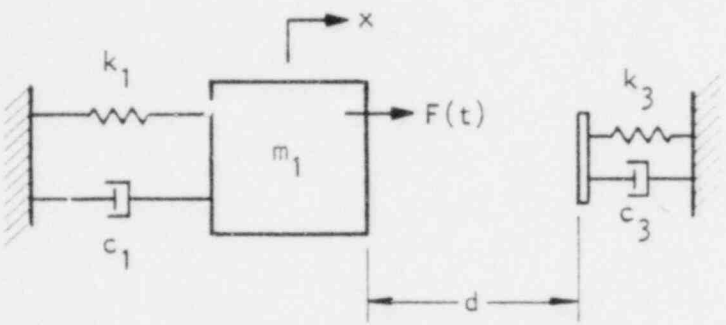

Figure 3.2 Nonlinear System with a Gap
(USC, 1976)

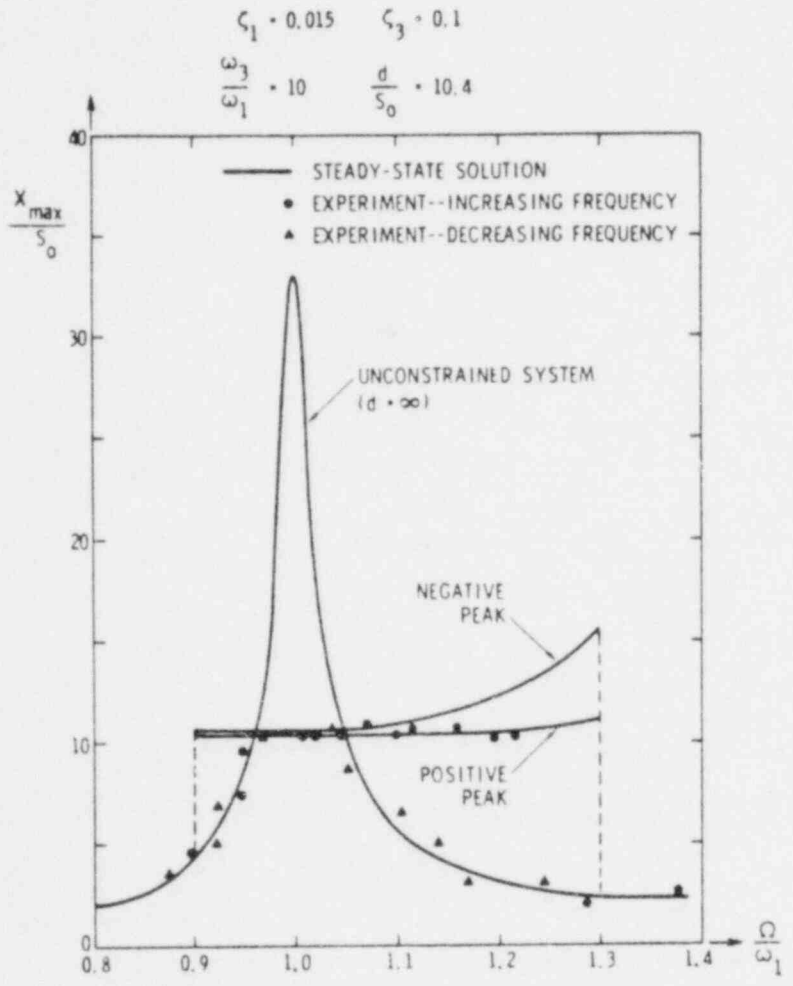

Figure 3.3 Comparison between Theory and Experiment of the Response of an SDOF System with a Gap (USC, 1976)

TABLE 3.1 Comparison of Theoretical and Computer-Generated Data: SDOF System, Pulse Excitation

τ/T	ζ_1	Maximum Displacement Amplification Factor	
		Theory	Computer
0.5	0.0	1.60	1.57
1.0		1.75	1.73
1.5		1.55	1.50
2.0		1.30	1.27
2.5		1.10	1.08
0.5	0.5	1.50	1.46
1.0		1.55	1.61
1.5		1.38	1.42
2.0		1.21	1.21
2.5		1.10	1.04
0.5	0.30	1.00	1.05
1.0		1.25	1.25
1.5		1.20	1.17
2.0		1.10	1.07
2.5		1.05	1.02

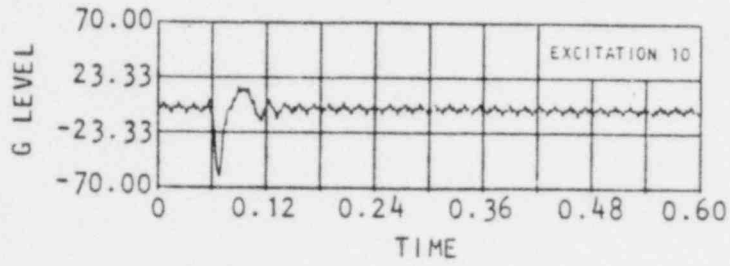

(a) Recorded base acceleration

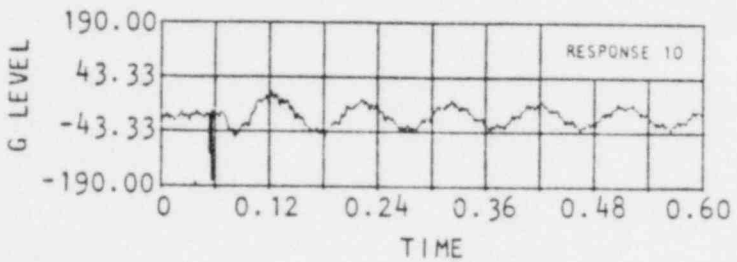

(b) Recorded tip acceleration

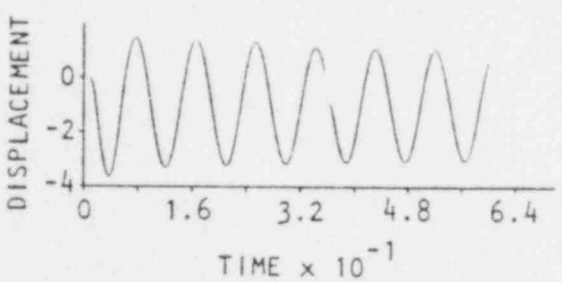

(c) Calculated tip displacement

Figure 3.4 Analytical/Experimental Response for a System with Gaps under Pulse Excitation (Anderson and Masri, 1979)

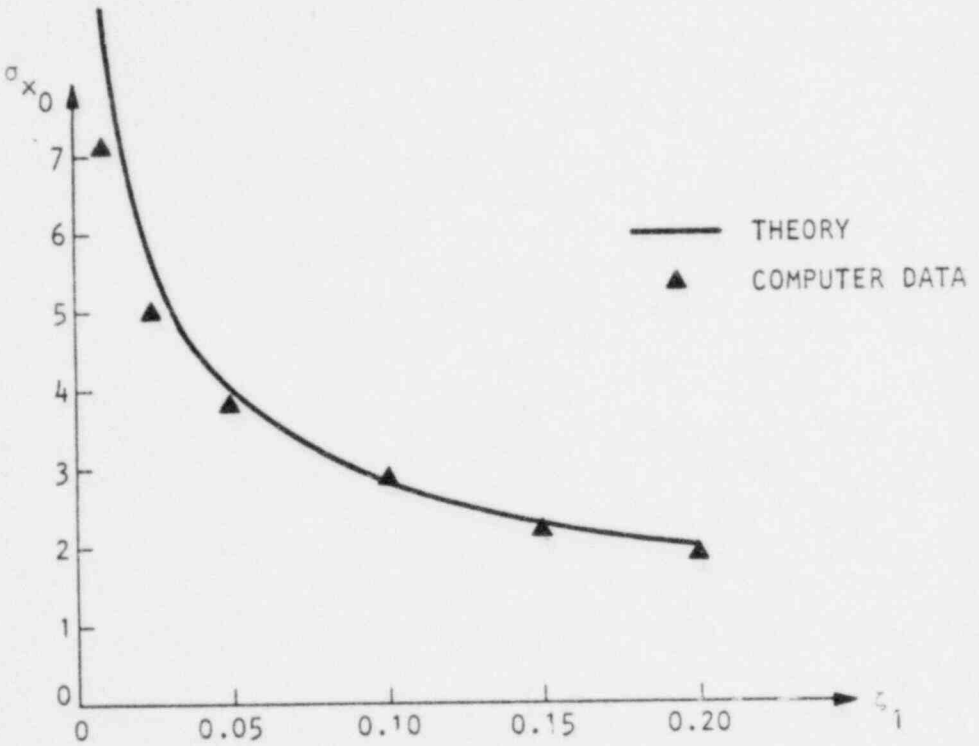

Figure 3.5 Comparison of Theoretical and Computer-Generated Data: SDOF System, Random Excitation

obtained from Crandall and Mark (1963).

The numerical results obtained from the computer code for a two-degree-of-freedom nonlinear system with a gap under stationary random excitation are compared in Figure 3.6 to published analytical and experimental results (Masri and Ibrahim, 1973).

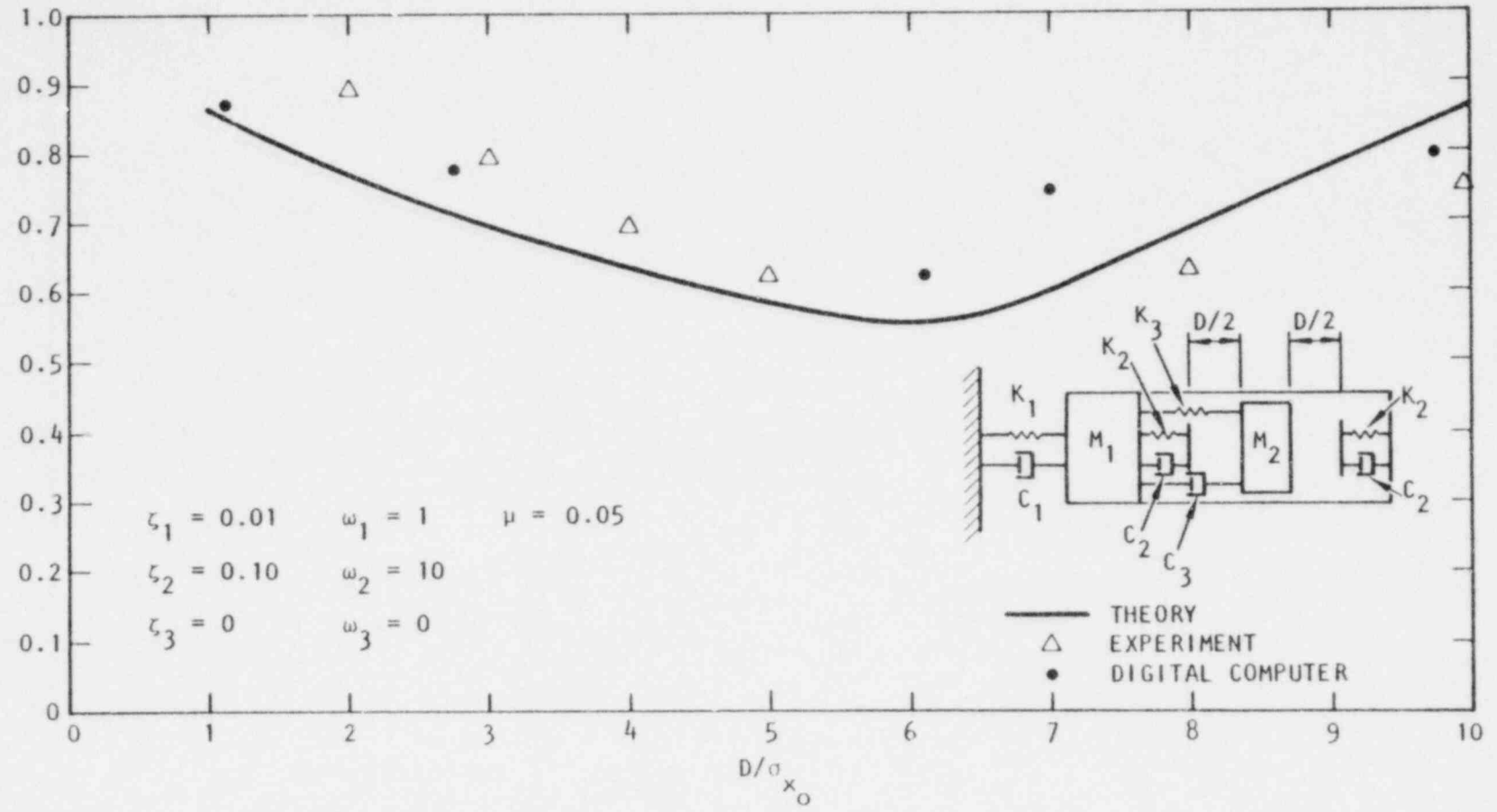

Figure 3.6 Comparison between Experimental, Approximate Theoretical and Numerical Results for a Nonlinear Two-Degree-of-Freedom System with Gaps under Random Excitation (Masri and Ibrahim, 1973)

SECTION 4

RESPONSE SPECTRA DATA

Included in this section are three subsections that contain the following information:

Section 4A Response Spectra - Harmonic Excitation

Section 4B Response Spectra - Shock Pulse Excitation

Section 4C Response Spectra - Stationary Random Excitation

All of the response spectra data contained herein were obtained by numerical integration of the system equations of motion derived in Section 2 with the digital computer program presented by Masri and Stott (1979). Table 4.1 compares the computer graphics nomenclature generated for the response spectra with that defined in the "Abbreviations and Symbols" list in this report. Tables 4.2 through 4.4 briefly describe each of the response spectra plots presented.

In Section 4.A, it was necessary to truncate at the frequency ratio (as indicated on the plots) the theoretical SDOF response of a linear system with $\zeta_1 = 0.01$ to make the plot scaling (resolution) meaningful, since this normalized response value is 50.

TABLE 4.1 Nomenclature Comparison for Section 4 Response Spectra Plots

Section 4 Plot Nomenclature (Computer-graphics generated)	Equivalent Report Symbol (See "Abbreviations and Symbols", p. xiv)
W1	ω_1
W2	ω_2
W4	ω_4
Z1	ζ_1
Z2	ζ_2
Z4	ζ_4
U	μ
FO	F_o
K1	K_1
T1	T_1
T	τ
OMEGA	ω
D/(FO/K1)	$D/(F_o/K_1)$, clearance ratio
OMEGA/W1	ω/ω_1, frequency ratio; harmonic
T/T1	τ/T_1, excitation duration ratio;pulse
SIGMAO	σx_o
D/SIGMAO	$D/\sigma x_o$, clearance ratio; random

TABLE 4.2 Plot Description for Response Spectra, Section 4.A

Plot Symbol	Computer-Printed Label	Description
ⓞ	P. P. Disp.	Normalized positive peak response for the nonlinear system, (Positive Peak Response)/(F_o/K_1)
Δ	N. P. Disp.	Normalized negative peak response for the nonlinear system, (Negative Peak Response)/(F_o/K_1)
+	D/(FO/K1)	Clearance ratio, $D/(F_o/K_1)$
x	SDOFSR	Theoretical response spectra for linear system with the same parameters as those of the nonlinear system except $D = \infty$ and $\mu = 0$

TABLE 4.3 Plot Description for Response Spectra, Section 4.B

Plot Symbol	Computer Printed Label	Description
○	P. P. Disp.	Normalized positive peak response for the nonlinear system, (Positive Peak Response)/(F_o/K_1)
△	N. P. Disp.	Normalized negative peak response for the nonlinear system, (Negative Peak Response)/(F_o/K_1)
+	D/(FO/K1)	Clearance ratio, $D/(F_o/K_1)$
x	A.M.D.	Normalized theoretical absolute maximum displacement as defined by Harris and Crede (1961), for a linear system with the same parameters as those of the nonlinear system except $D = \infty$ and $\mu = 0$ (Absolute Max. Disp.)/(F_o/K_1)
◇	R.A.	Normalized theoretical residual displacement as defined by Harris and Crede (1961) for a linear system with the same parameters as those of the nonlinear system except $D = \infty$ and $\mu = 0$. (Residual Disp.)/(F_o/K_1)

TABLE 4.4 Plot Description for Response Spectra, Section 4.C

Plot Symbol	Computer-Printed Label	Description
+, x, ◇	RMSD	Normalized RMS displacement of an equivalent SDOF linear system ($\sigma_x/\sigma_{x_o} = 1$)
+, x, o, Δ		Normalized nonlinear RMS response ($\sigma_x/\sigma_{x_o} \neq 1$)

TABLE 4A.1 DATA SUMMARY FOR RESPONSE SPECTRA:

SINUSOIDAL EXCITATION

$\frac{\omega_4}{\omega_1}$	ζ_4	$D/(F_o/K_1)$	ζ_1	ζ_2	$\mu = \frac{M_2}{M_1}$	$\frac{\omega_2}{\omega_1}$	Page	Plot No.
10.0	0.1	1.0	0.1	0.1	0.1	0.5	4A-22	S37
						1.0	4A-16	S25
						2.0	4A-10	S13
						5.0	4A-4	S1
					1.0	0.5	4A-24	S41
						1.0	4A-18	S29
						2.0	4A-12	S17
						5.0	4A-6	S5
					10.0	0.5	4A-26	S45
						1.0	4A-20	S33
						2.0	4A-14	S21
						5.0	4A-8	S9
				0.1	0.1	0.5	4A-22	S38
						1.0	4A-16	S26
						2.0	4A-10	S14
						5.0	4A-4	S2
					1.0	0.5	4A-24	S42
						1.0	4A-18	S30
						2.0	4A-12	S18
						5.0	4A-6	S6
					10.0	0.5	4A-26	S46
						1.0	4A-20	S34
						2.0	4A-14	S22
						5.0	4A-8	S10

TABLE 4A.1

(Continued)

$\frac{\omega_4}{\omega_1}$	ζ_4	$D/(F_o/K_1)$	ζ_1	ζ_2	$\mu = \frac{M_2}{M_1}$	$\frac{\omega_2}{\omega_1}$	Page	Plot No.
10.0	0.1	1.0	0.1	0.01	0.1	0.5	4A-23	S39
						1.0	4A-17	S27
						2.0	4A-11	S15
						5.0	4A-5	S3
					1.0	0.5	4A-25	S43
						1.0	4A-19	S31
						2.0	4A-13	S19
						5.0	4A-7	S7
					10.0	0.5	4A-27	S47
						1.0	4A-21	S35
						2.0	4A-15	S23
						5.0	4A-9	S11
				0.1	0.1	0.5	4A-23	S40
						1.0	4A-17	S28
						2.0	4A-11	S16
						5.0	4A-5	S4
					1.0	0.5	4A-25	S44
						1.0	4A-19	S32
						2.0	4A-13	S20
						5.0	4A-7	S8
					10.0	0.5	4A-27	S48
						1.0	4A-21	S36
						2.0	4A-15	S24
						5.0	4A-9	S12

TABLE 4A.1

(Concluded)

$\frac{\omega_4}{\omega_1}$	ζ_4	$D/(F_o/K_1)$	ζ_1	ζ_2	$\mu = \frac{M_2}{M_1}$	$\frac{\omega_2}{\omega_1}$	Page	Plot No.
10.0	0.1	0.25	0.1	0.1	0.1	5.0	4A-28	S49
↓	↓	↓	↓	↓	1.0	↓	4A-31	S55
↓	↓	↓	↓	↓	10.0	↓	4A-34	S61
↓	↓	0.5	↓	↓	0.1	↓	4A-28	S50
↓	↓	↓	↓	↓	1.0	↓	4A-31	S56
↓	↓	↓	↓	↓	10.0	↓	4A-34	S62
↓	↓	0.75	↓	↓	0.1	↓	4A-29	S51
↓	↓	↓	↓	↓	1.0	↓	4A-32	S57
↓	↓	↓	↓	↓	10.0	↓	4A-35	S63
↓	↓	2.0	↓	↓	0.1	↓	4A-29	S52
↓	↓	↓	↓	↓	1.0	↓	4A-32	S58
↓	↓	↓	↓	↓	10.0	↓	4A-35	S64
↓	↓	3.0	↓	↓	0.1	↓	4A-30	S53
↓	↓	↓	↓	↓	1.0	↓	4A-33	S59
↓	↓	↓	↓	↓	10.0	↓	4A-36	S65
↓	↓	4.0	↓	↓	0.1	↓	4A-30	S54
↓	↓	↓	↓	↓	1.0	↓	4A-33	S60
↓	↓	↓	↓	↓	10.0	↓	4A-36	S66

Figure S1

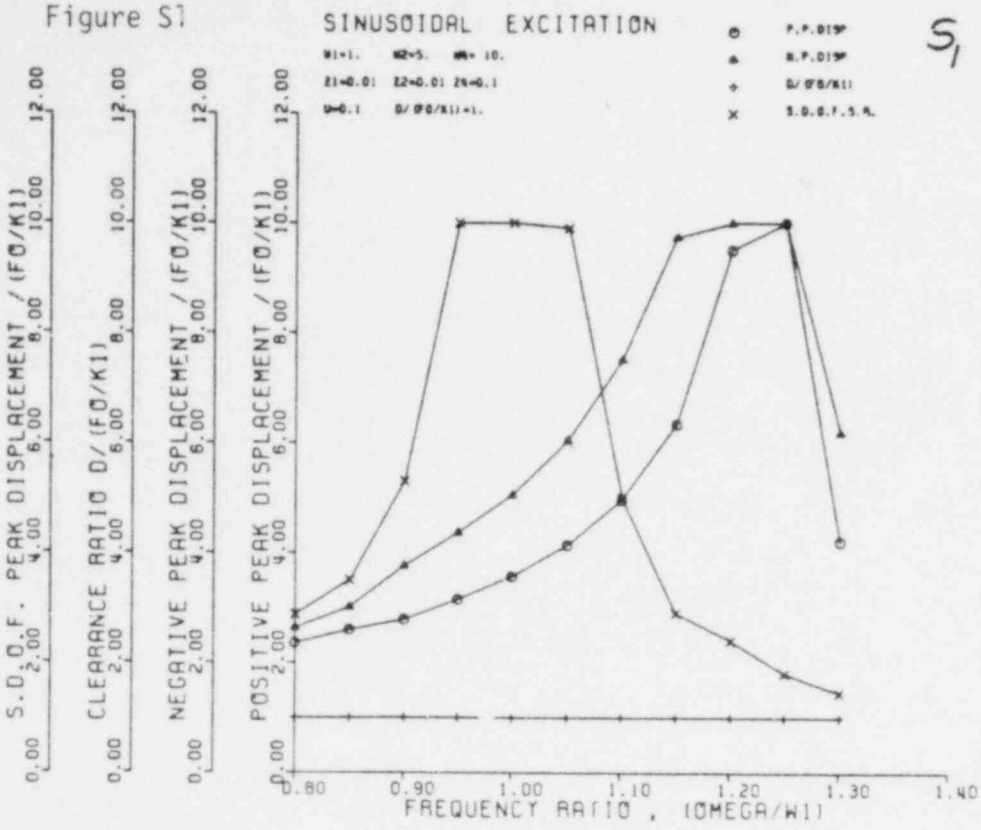

S1

Figure S2

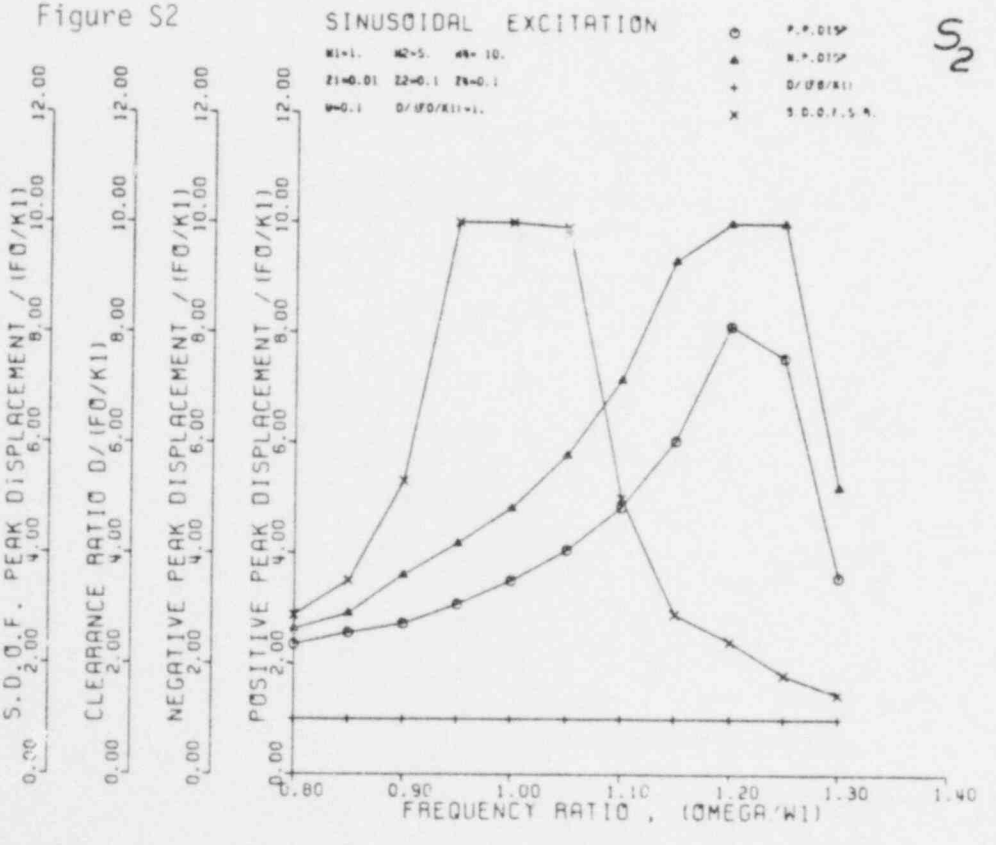

S2

Figure S3

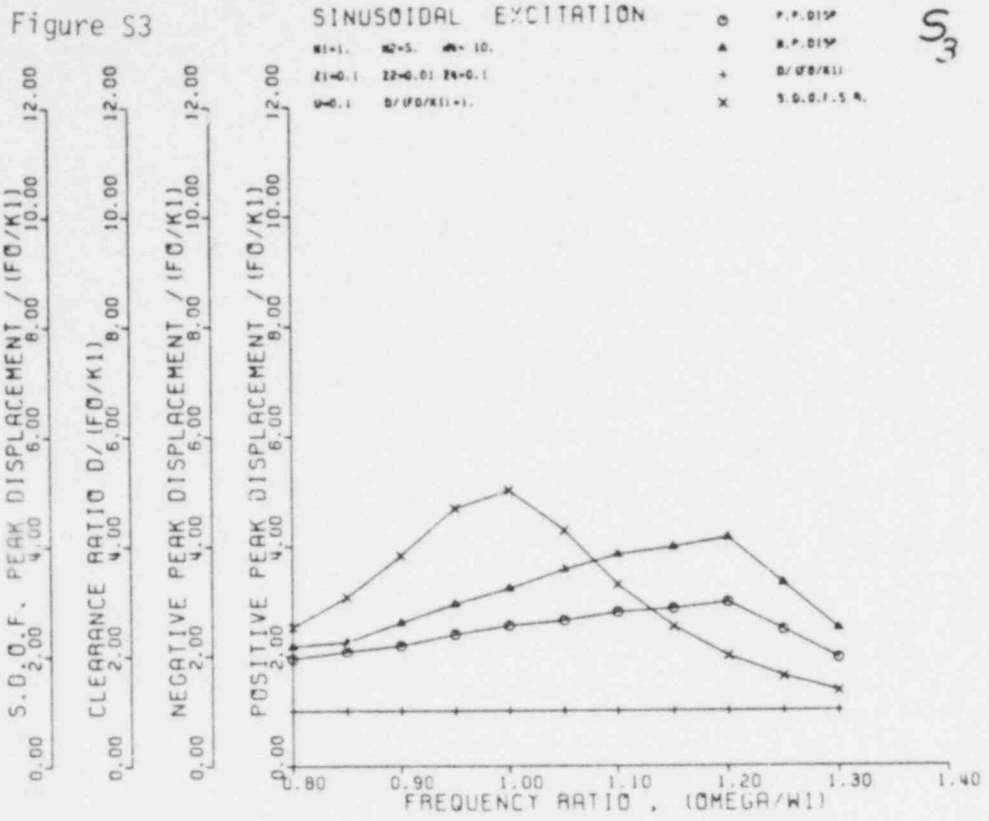

S3

Figure S4

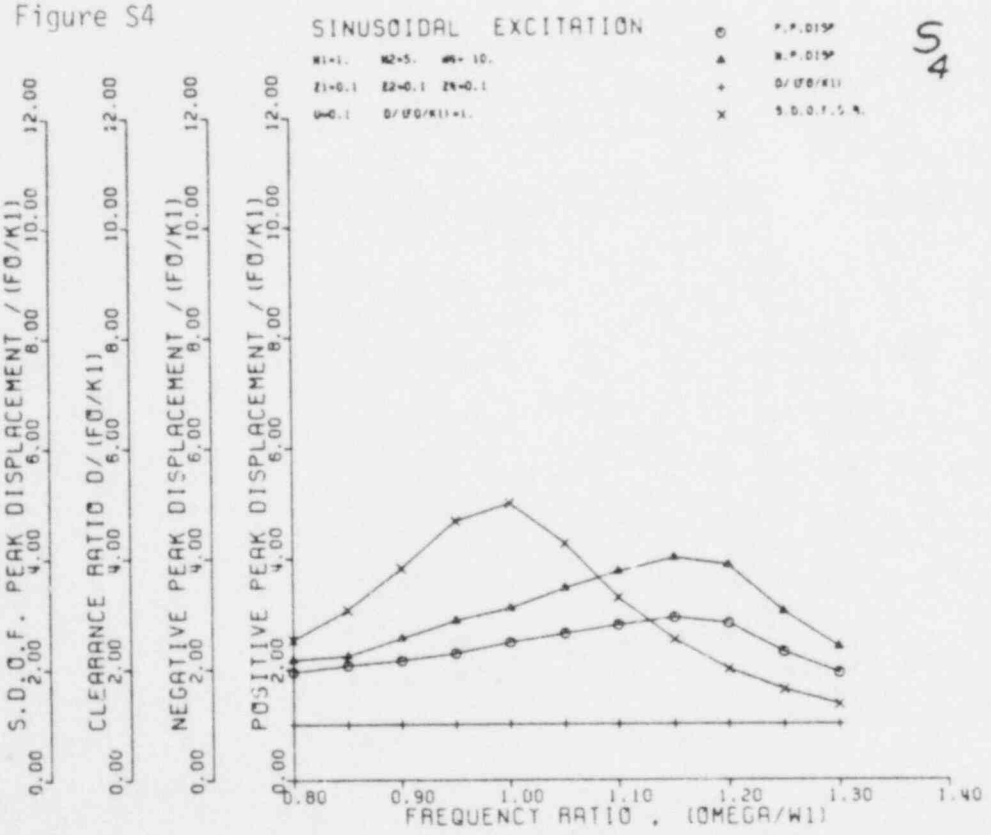

S4

Figure S5

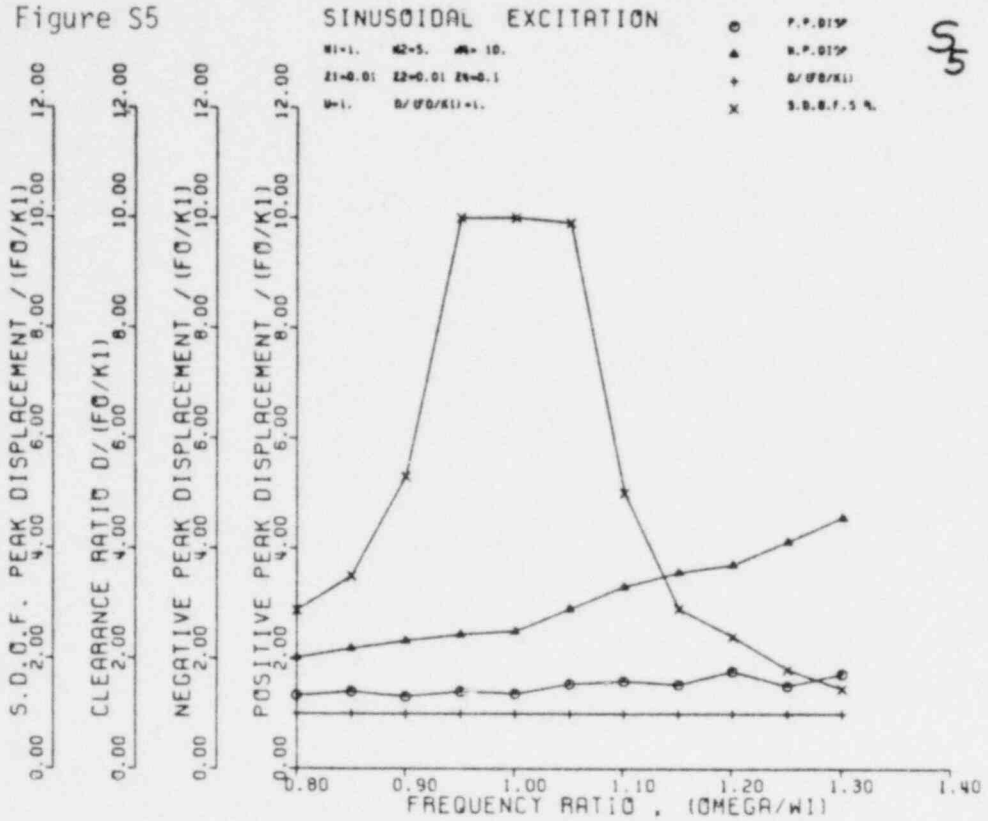

S5

Figure S6

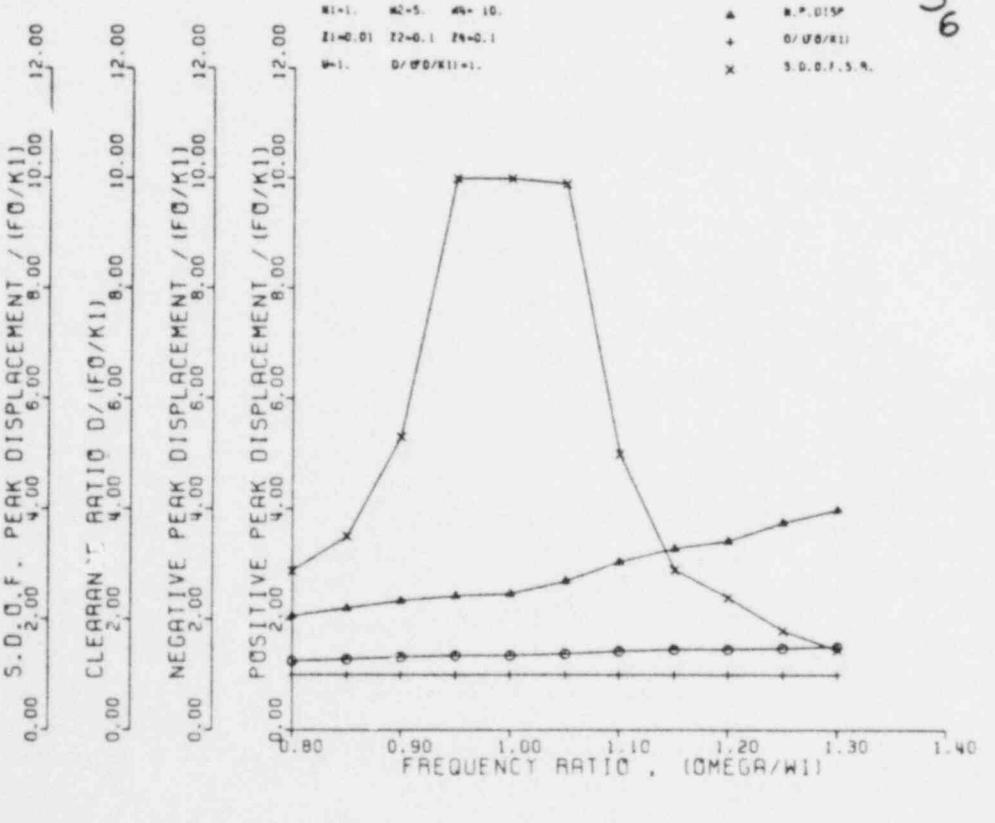

S6

Figure S7

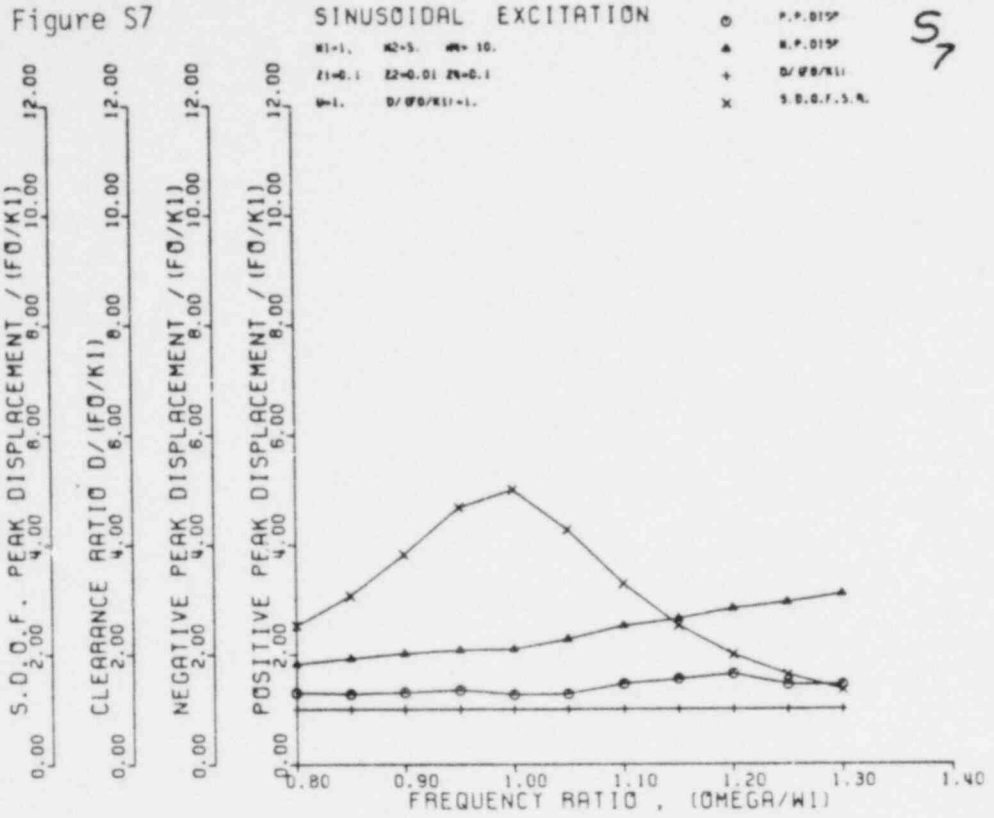

S7

Figure S8

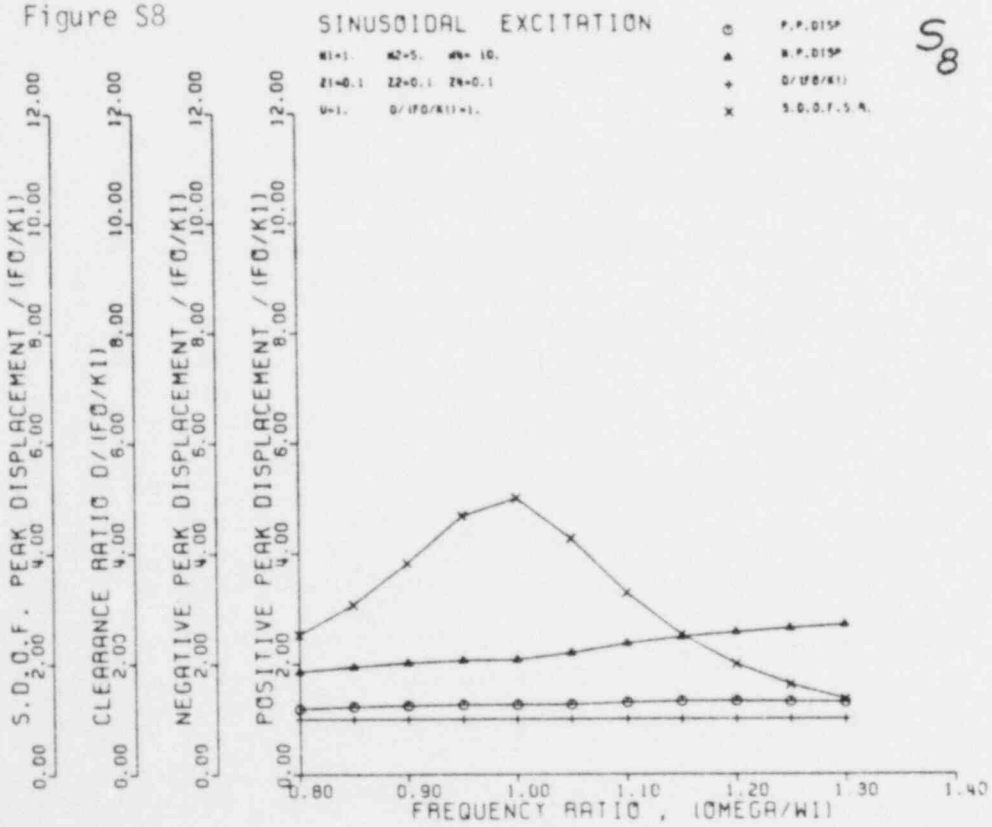

S8

Figure S9

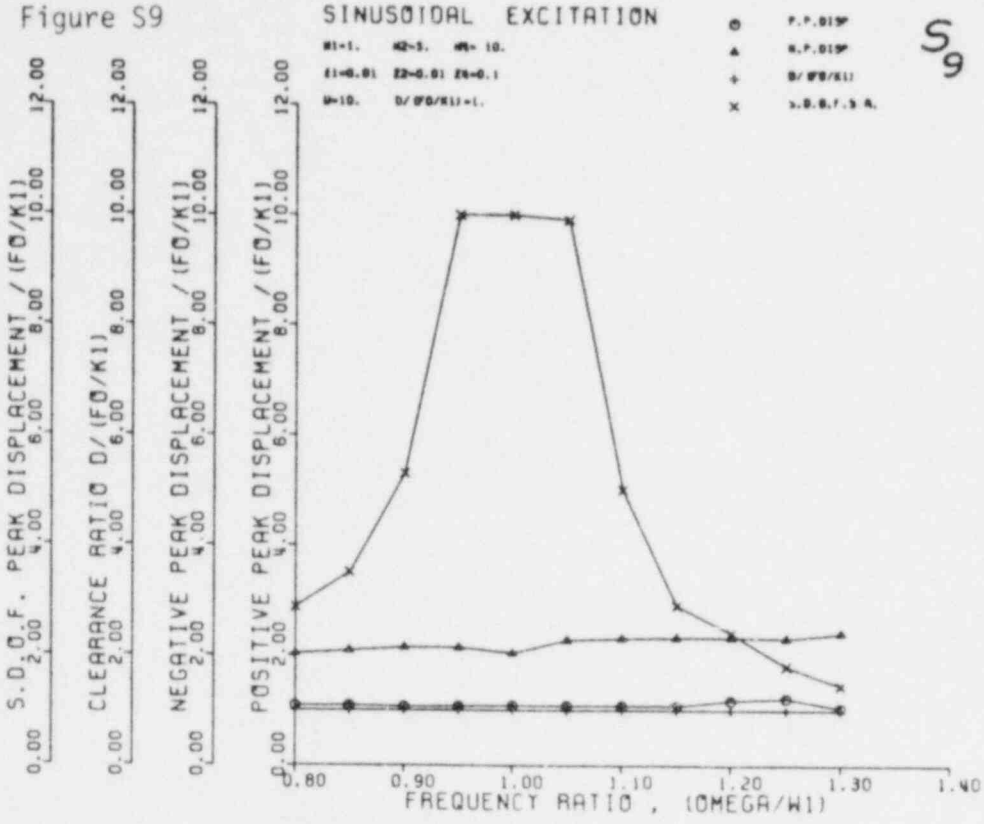

S9

Figure S10

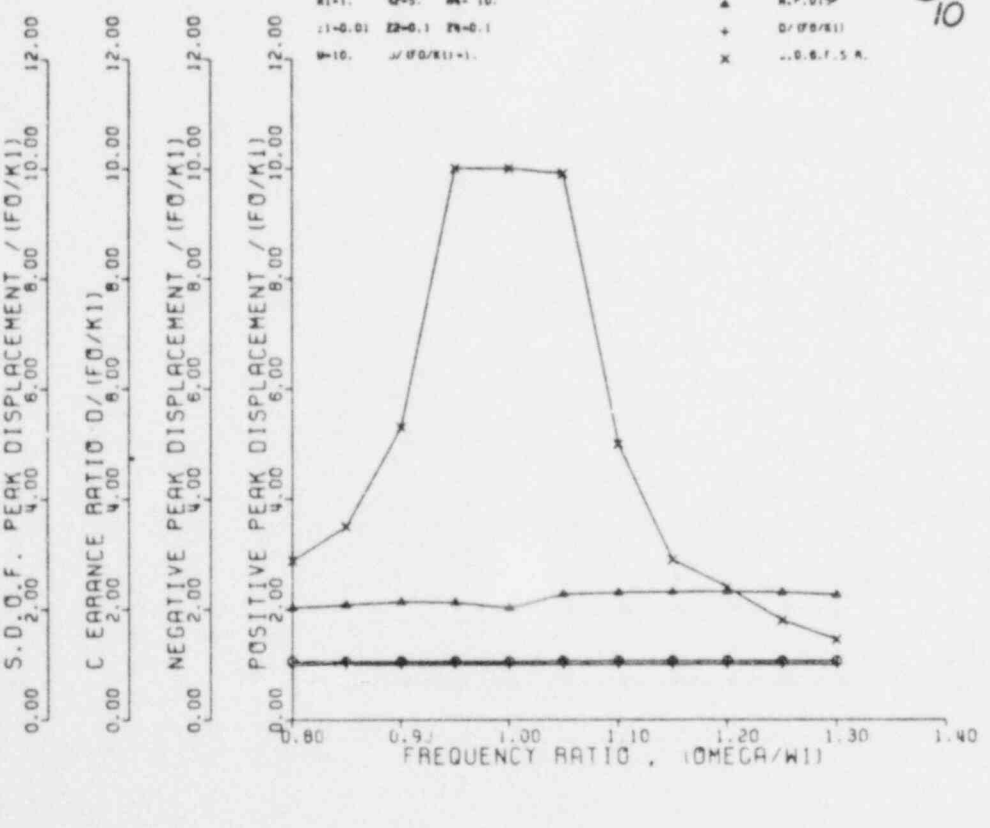

S10

Figure S11

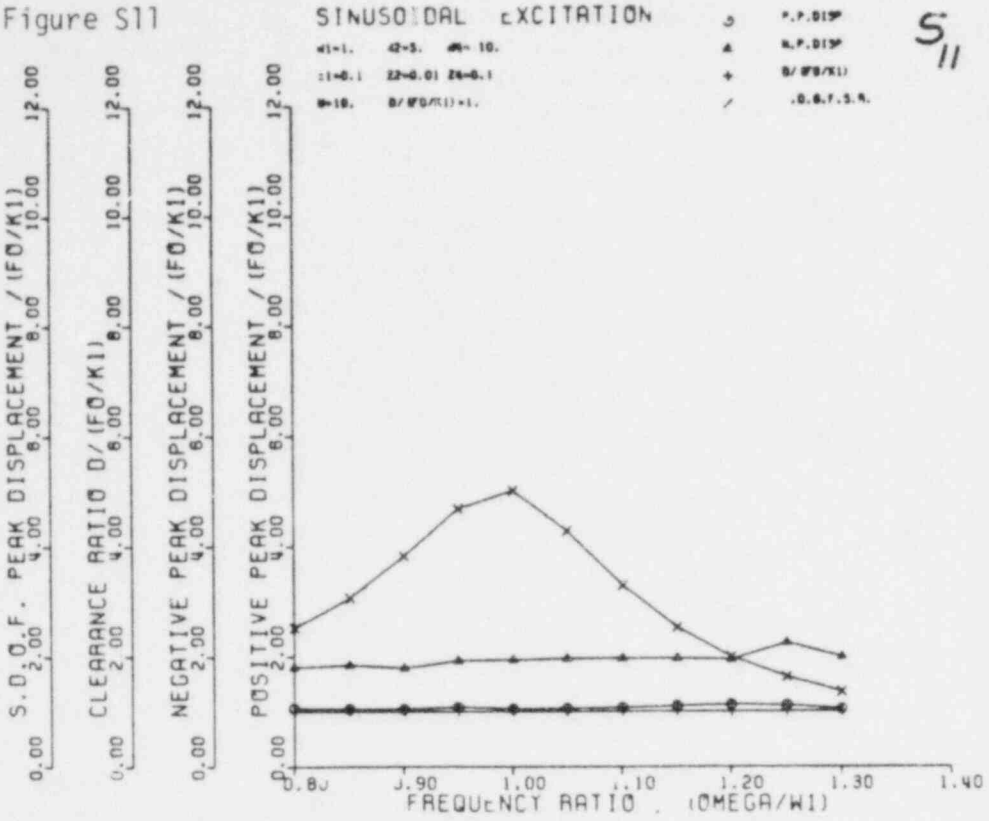

S11

Figure S12

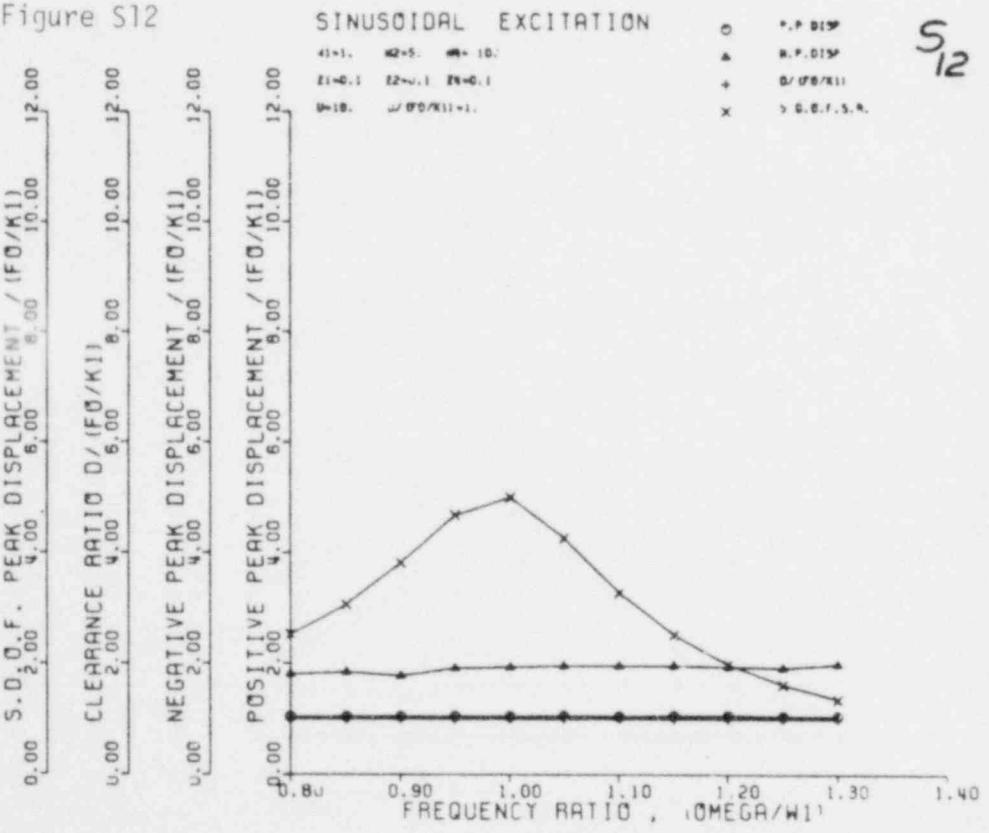

S12

Figure S13

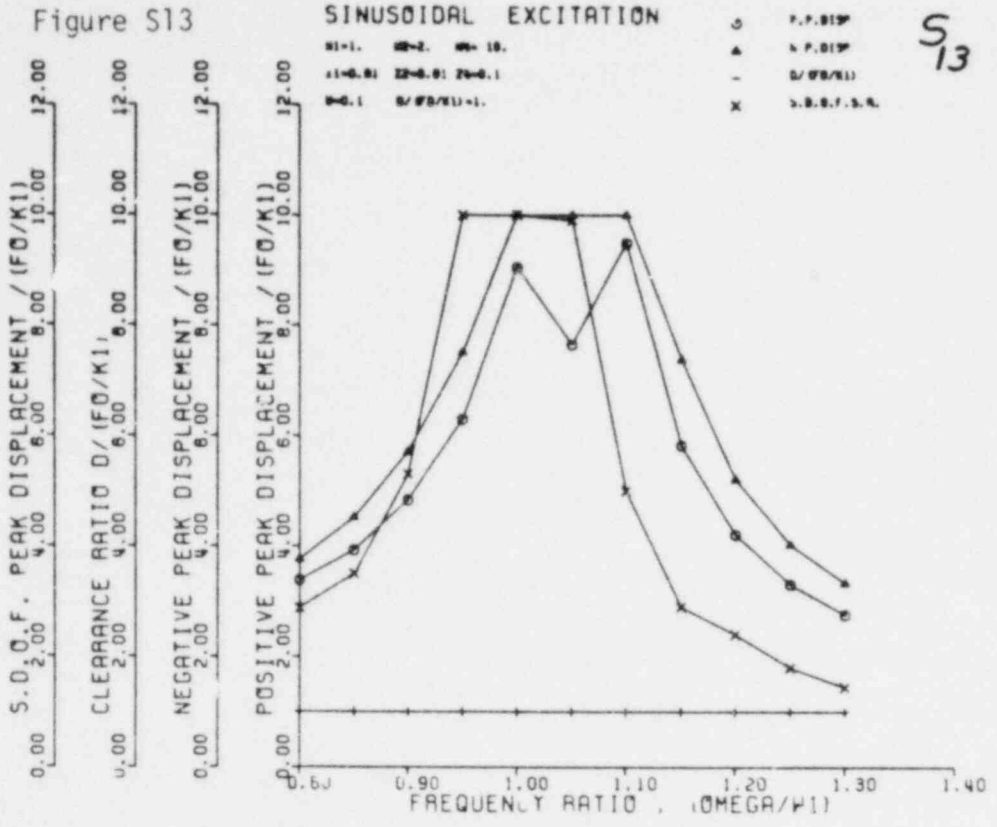

S13

Figure S14

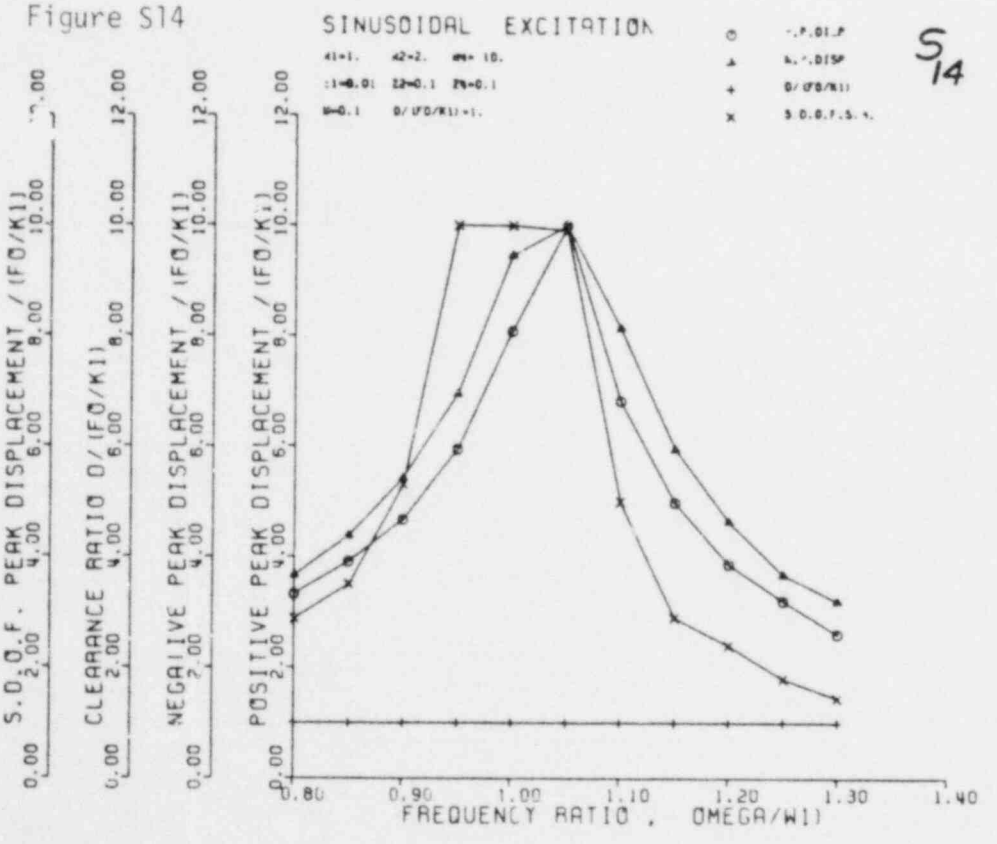

S14

Figure S15

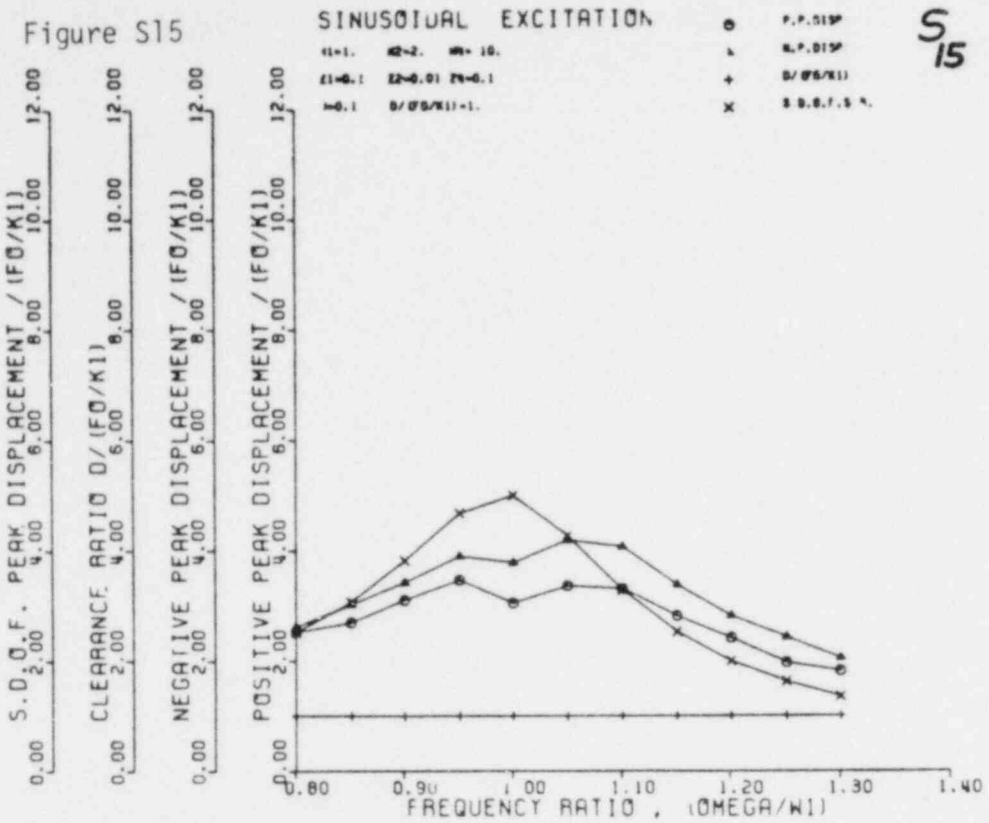

S15

Figure S16

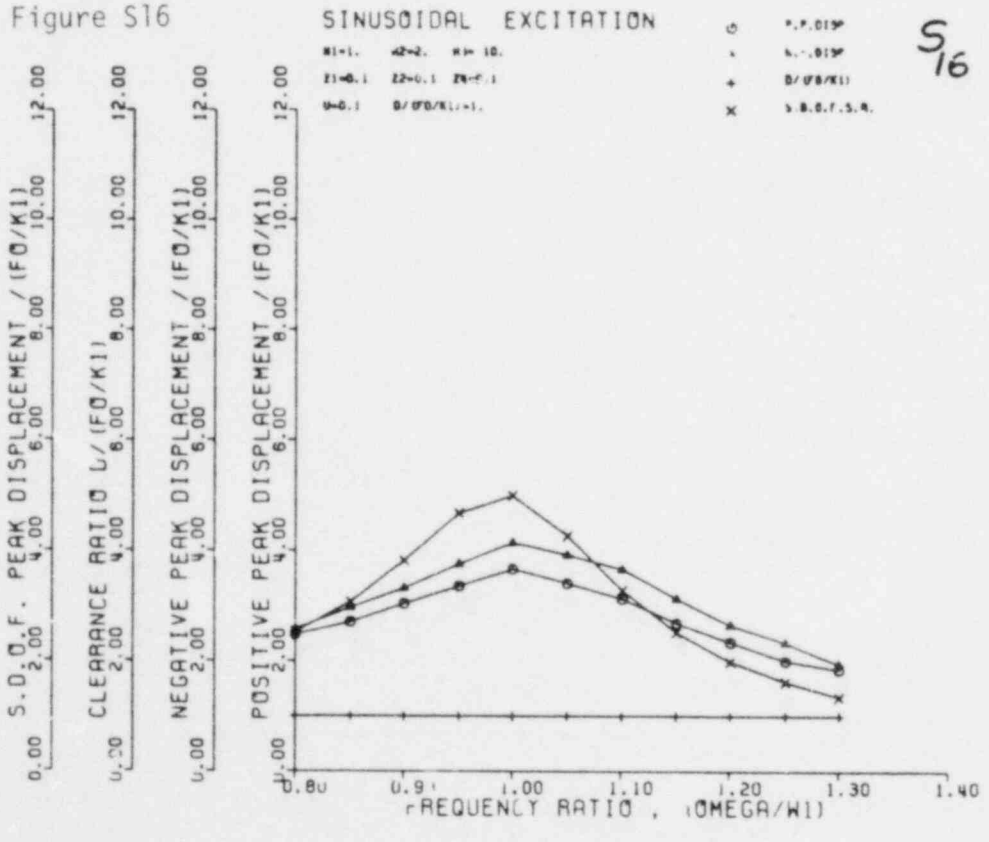

S16

Figure S17

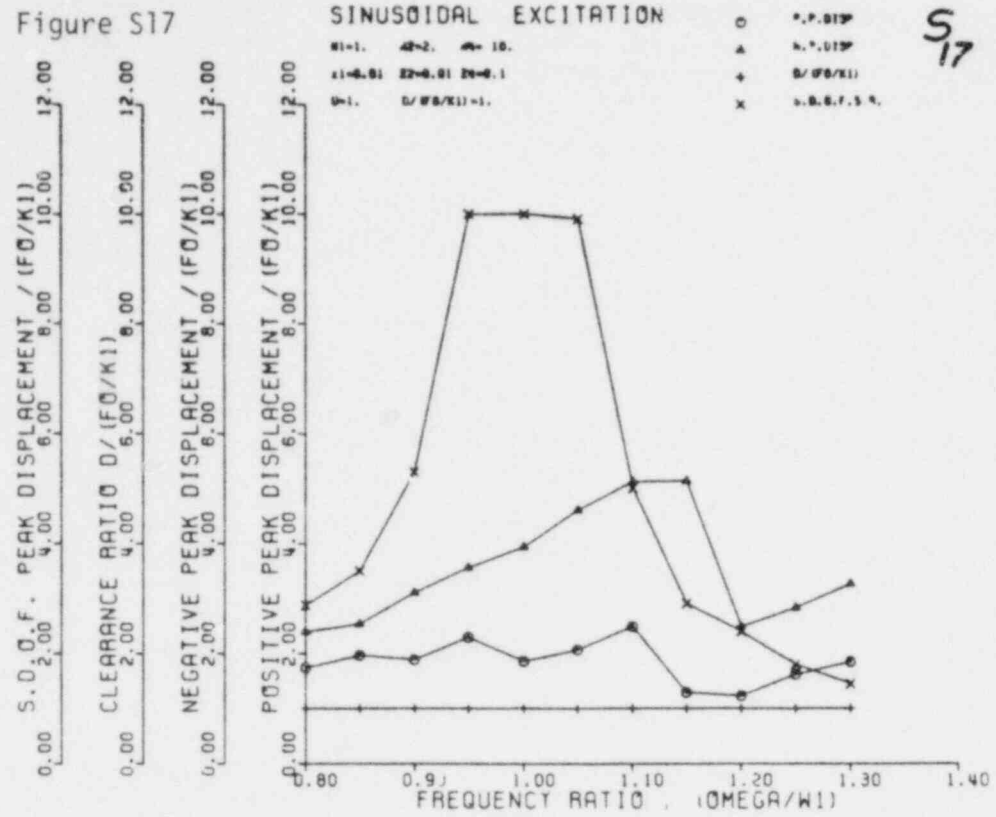

Figure S18

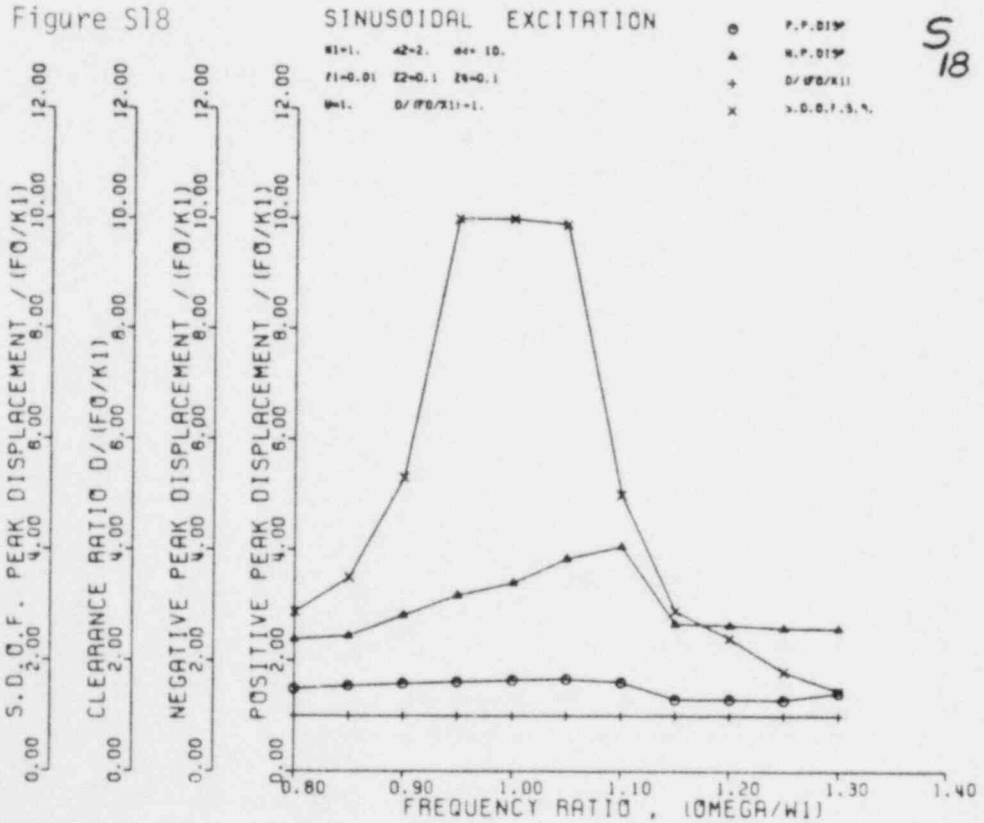

Figure S19

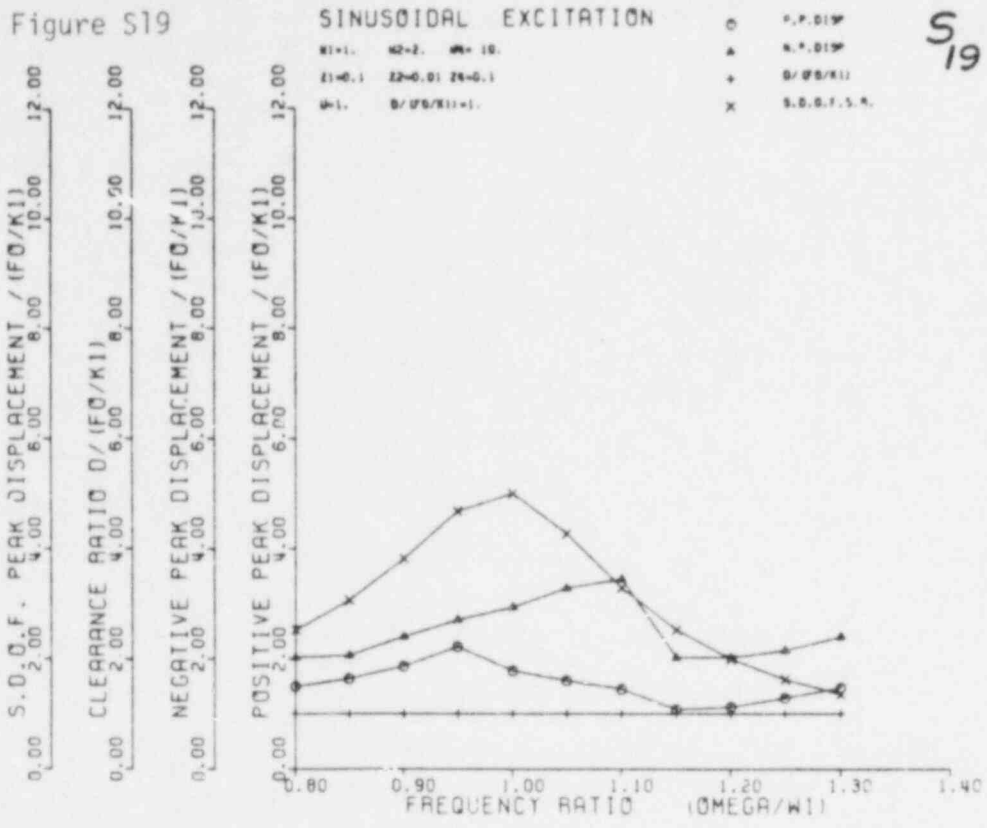

S19

Figure S20

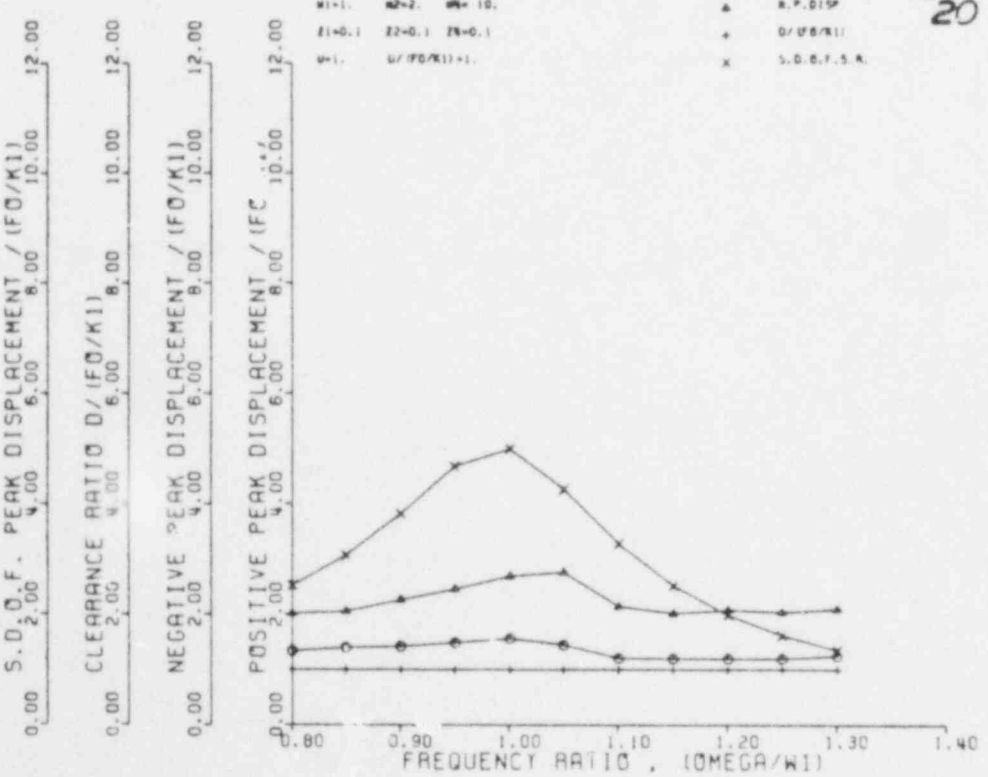

S20

Figure S21

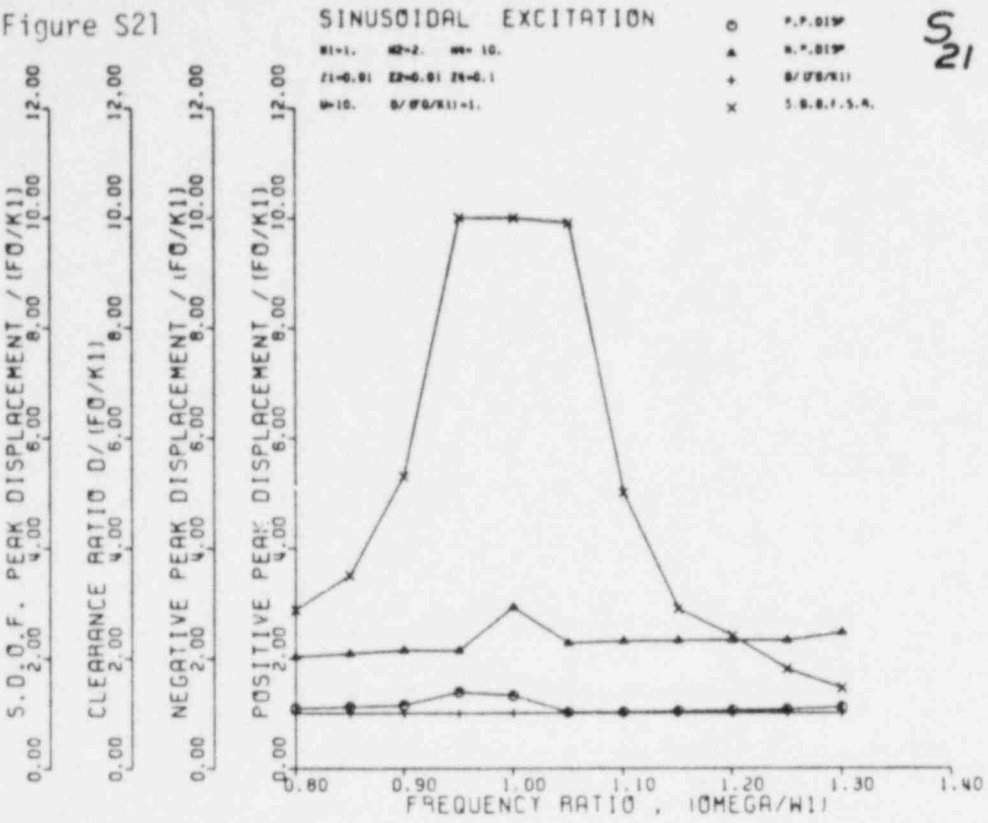

S21

Figure S22

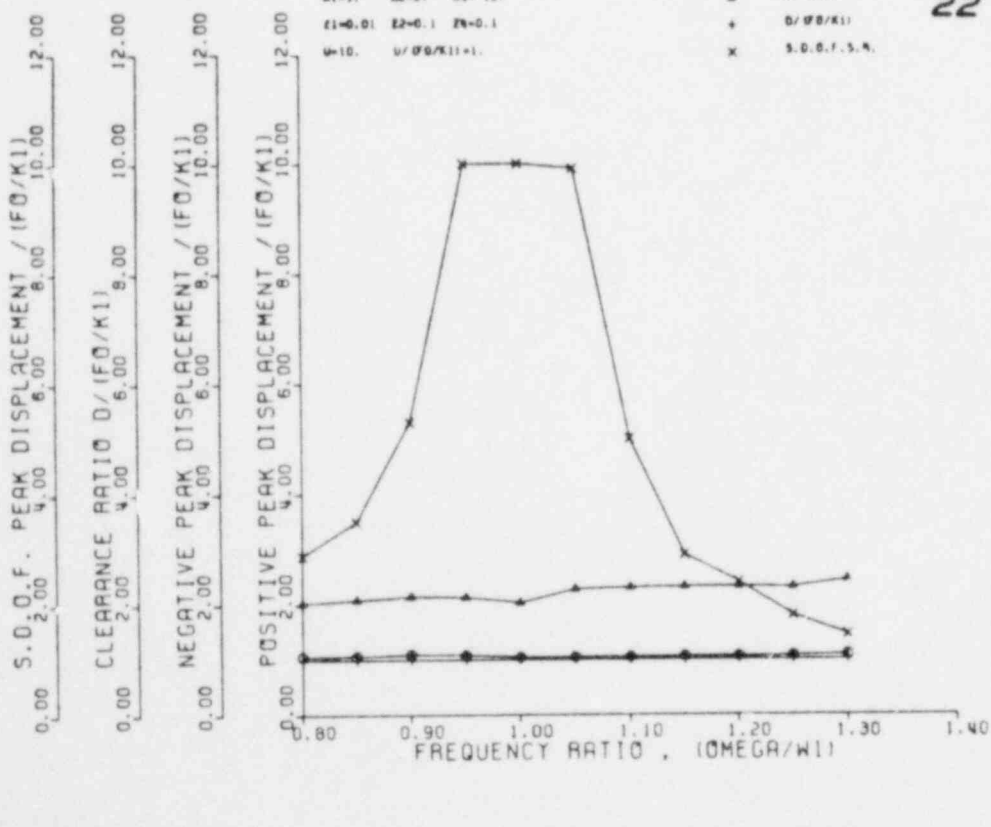

S22

Figure S23

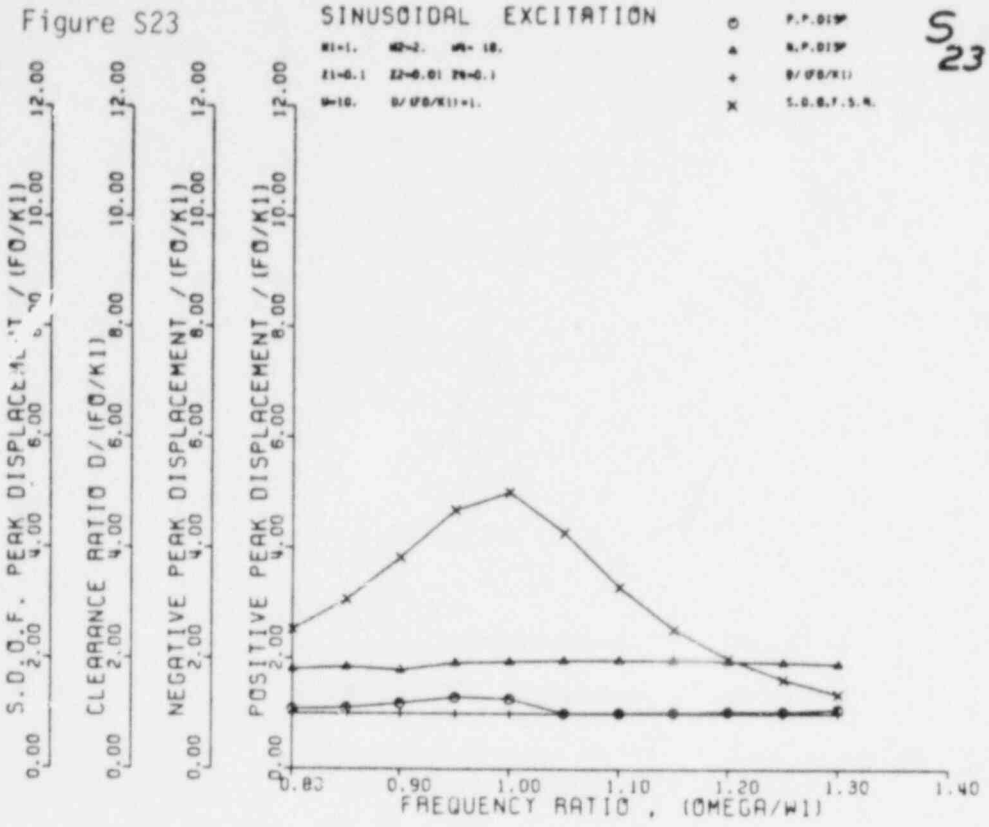

S23

Figure S24

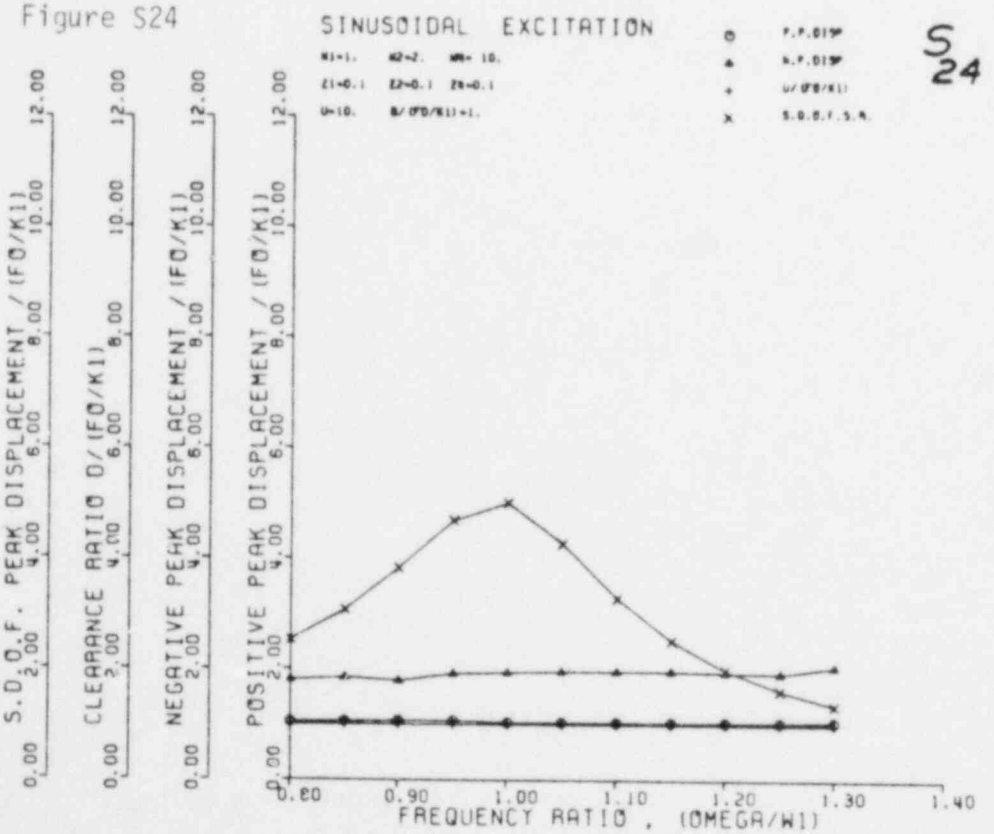

S24

Figure S25

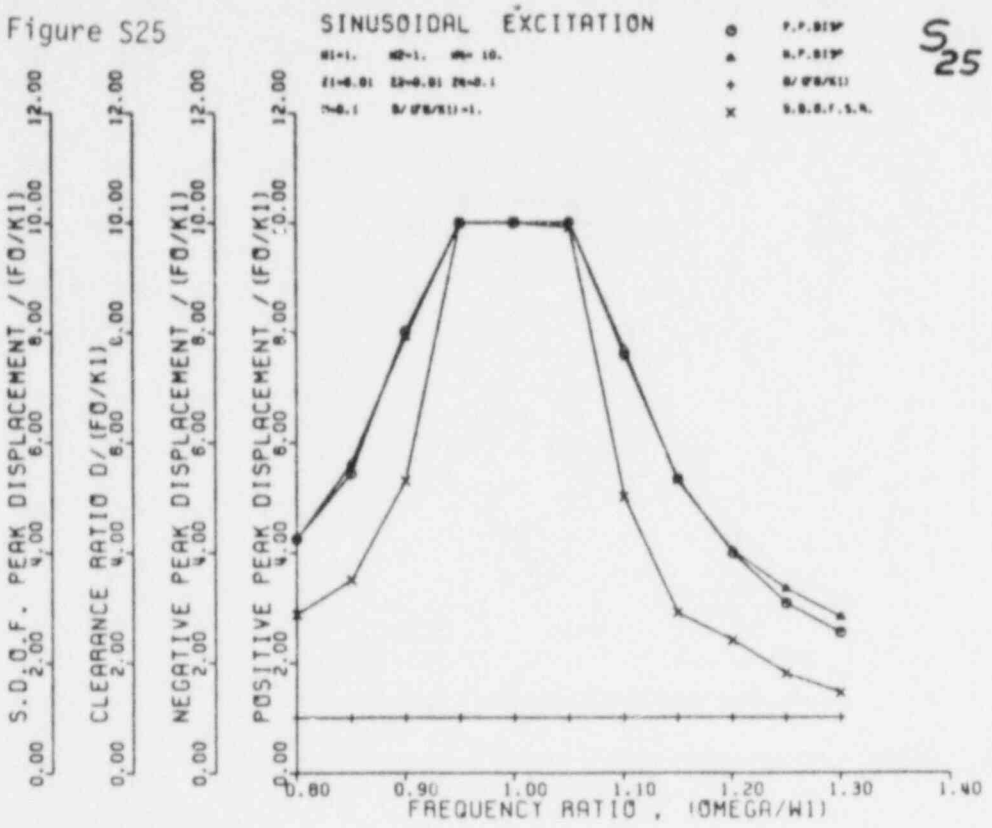

S25

Figure S26

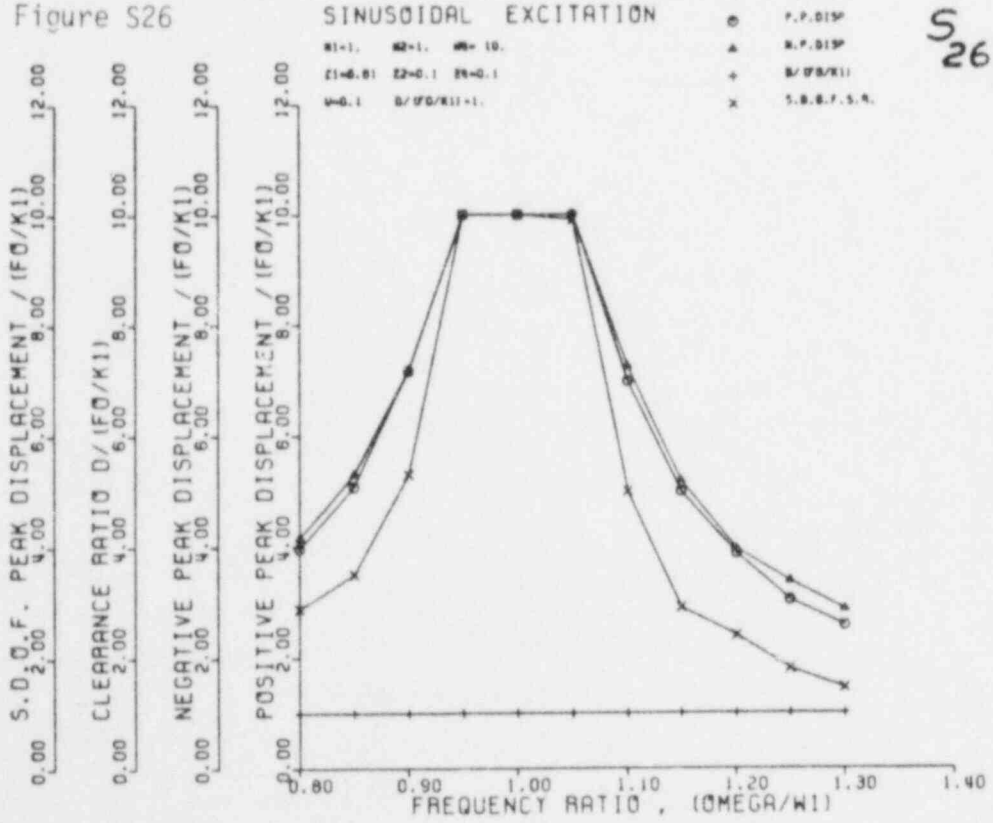

S26

Figure S27

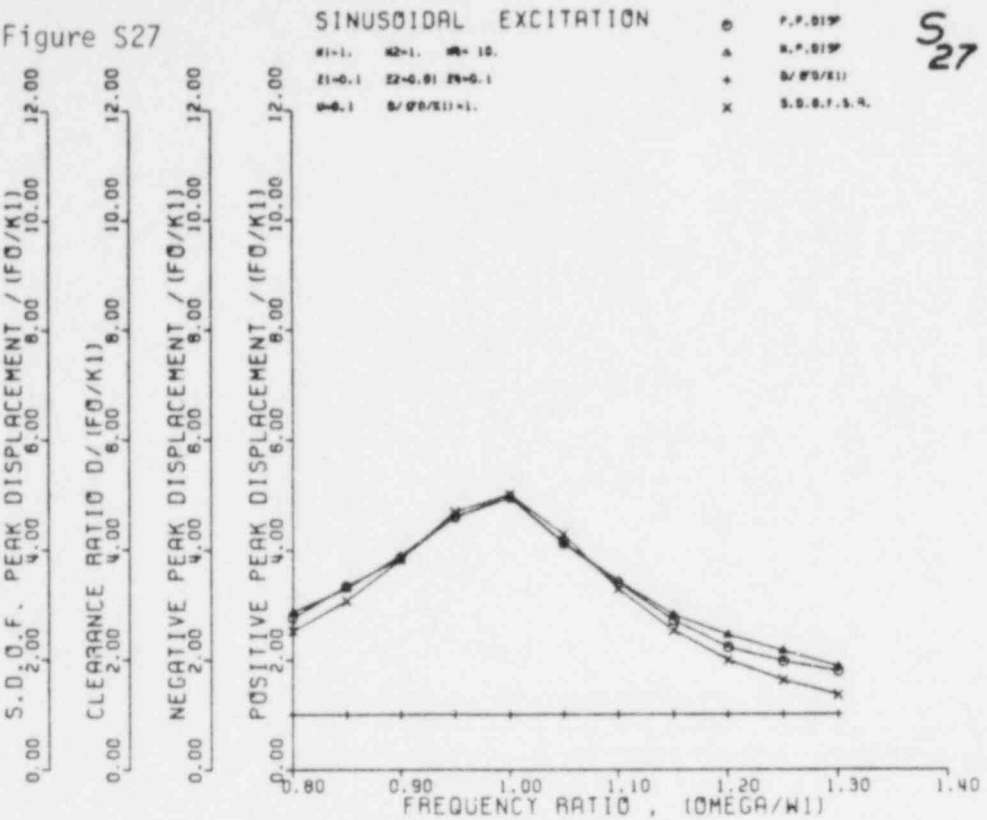

S27

Figure S28

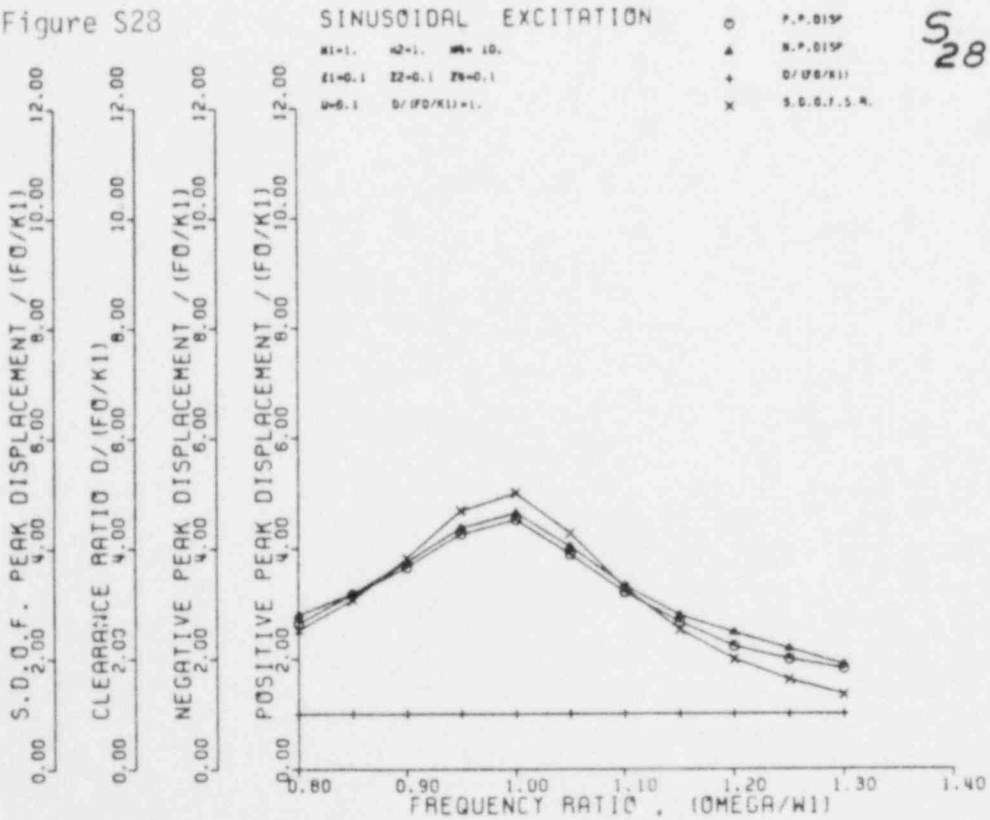

S28

Figure S29

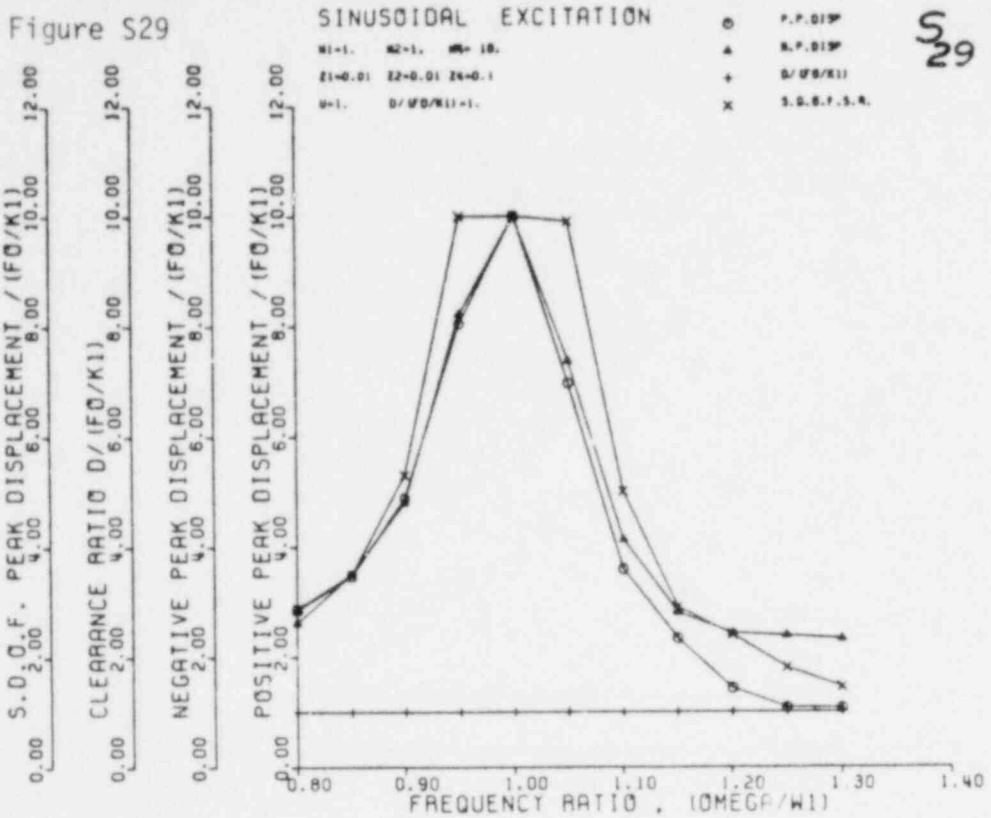

S29

Figure S30

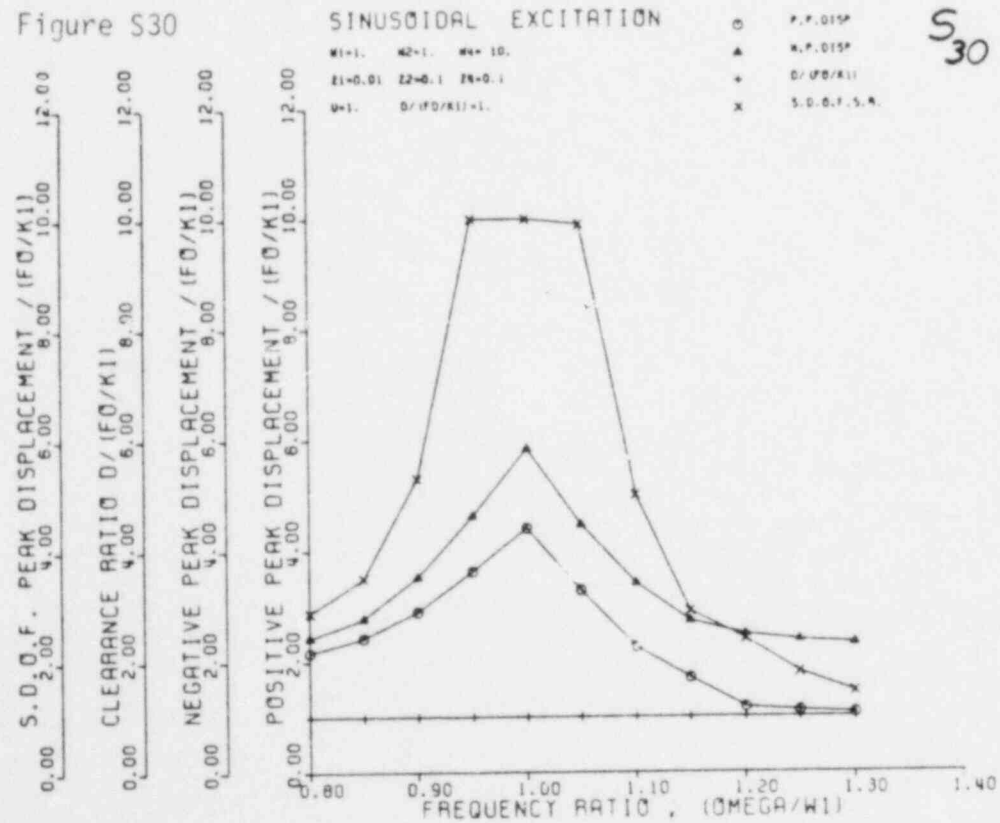

S30

Figure S31

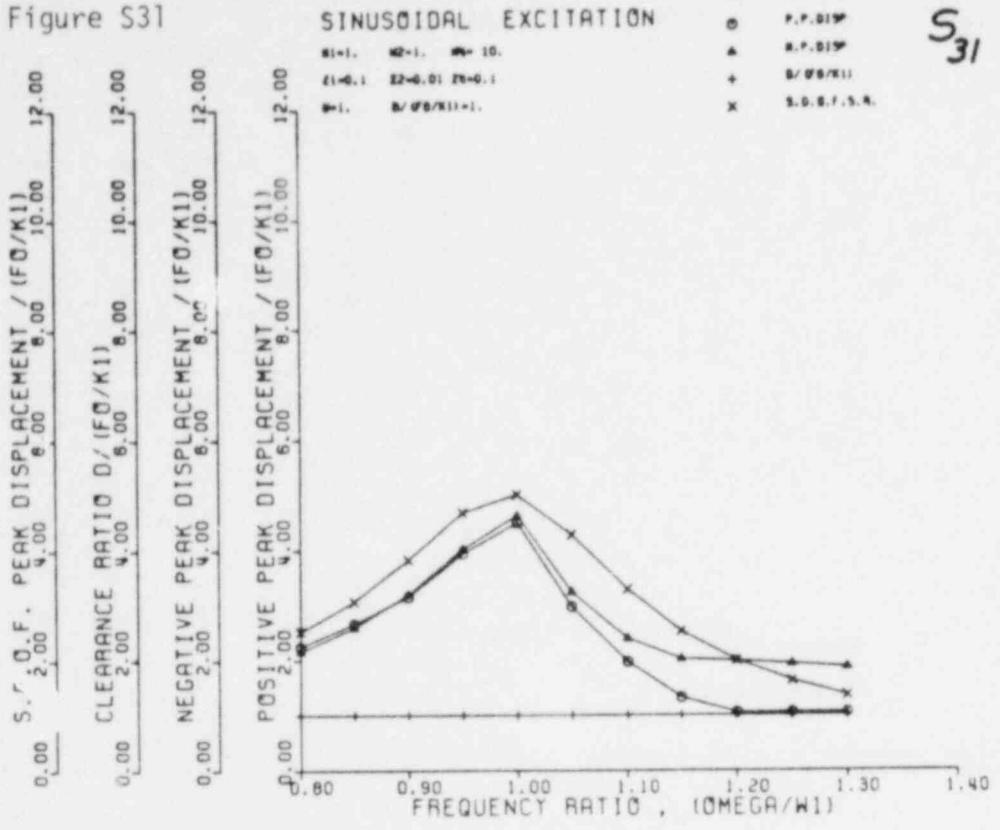

S31

Figure S32

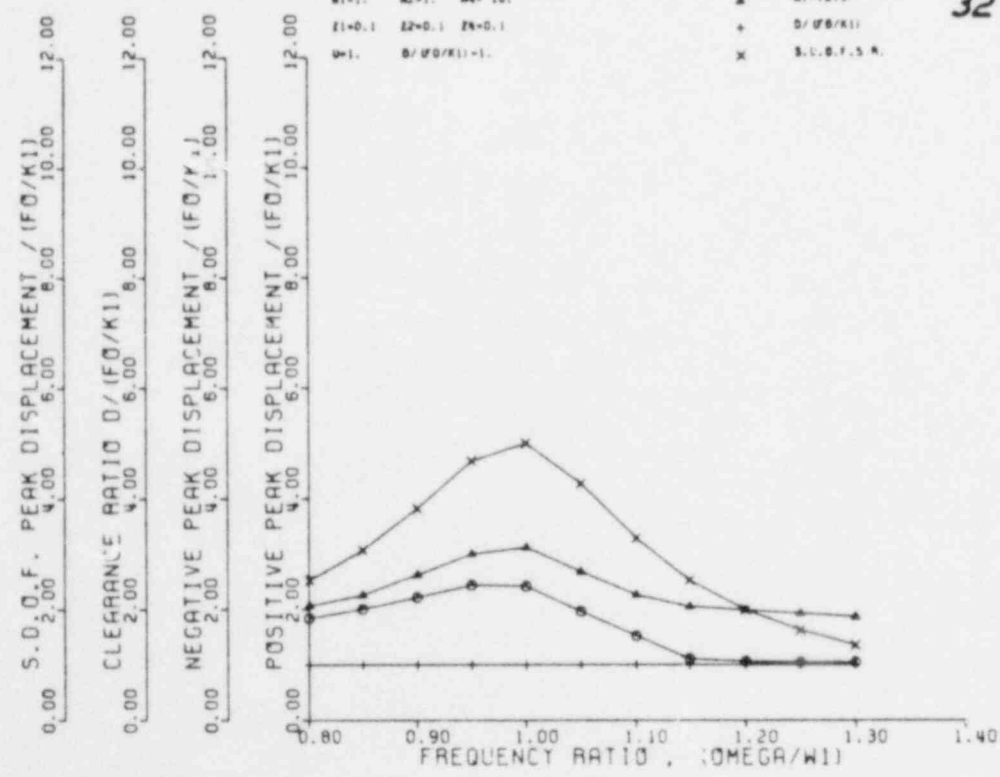

S32

Figure S33

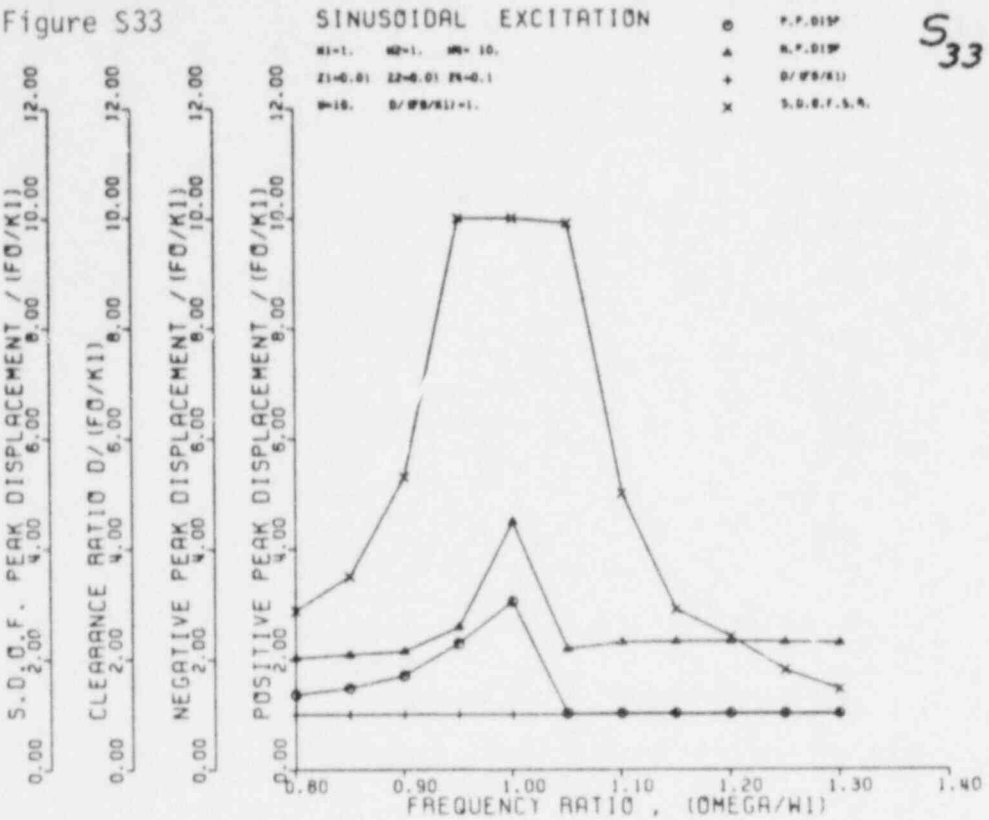

S33

Figure S34

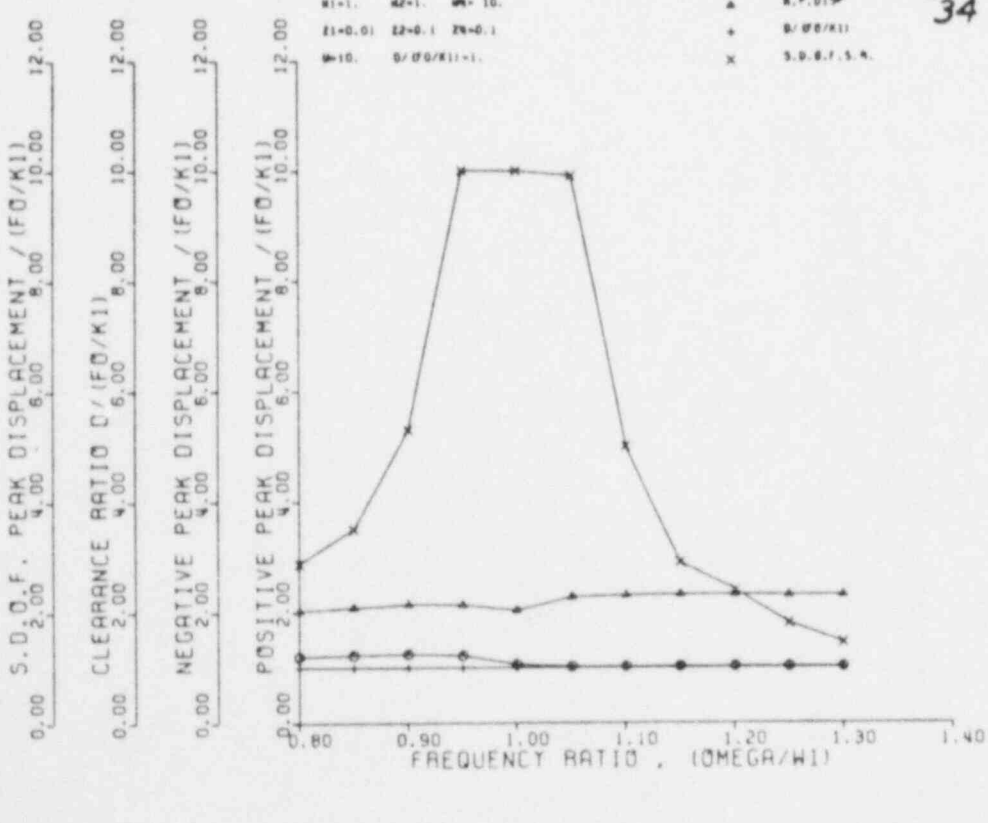

S34

Figure S35

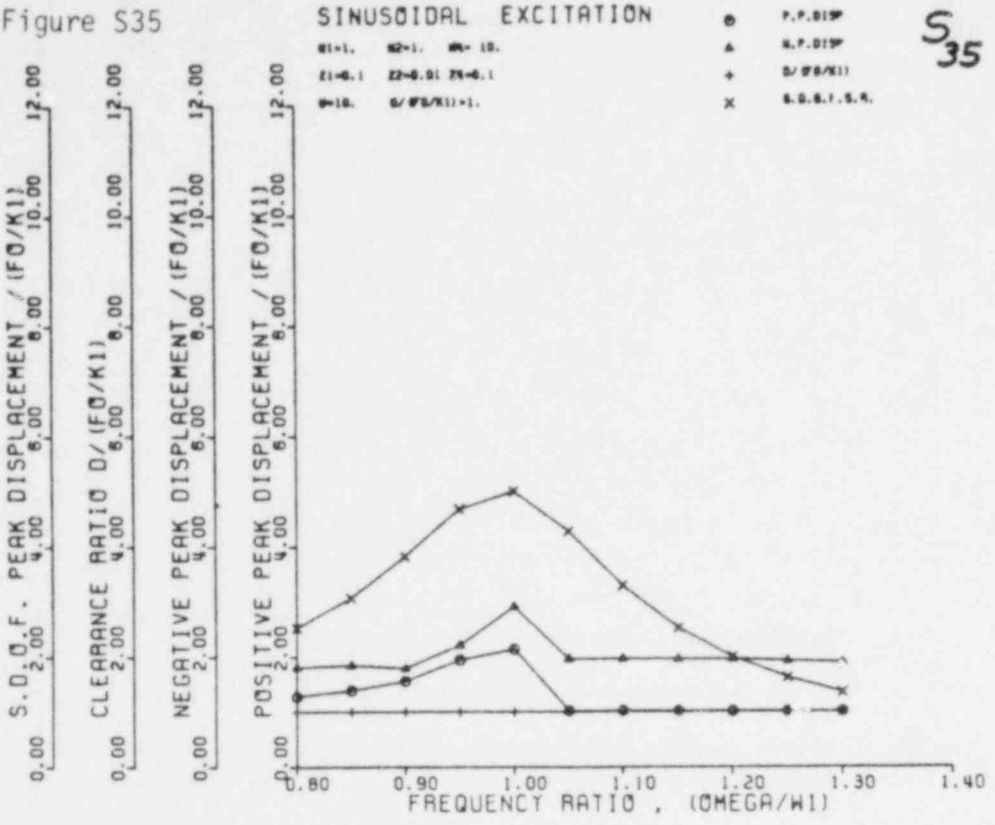

S35

Figure S36

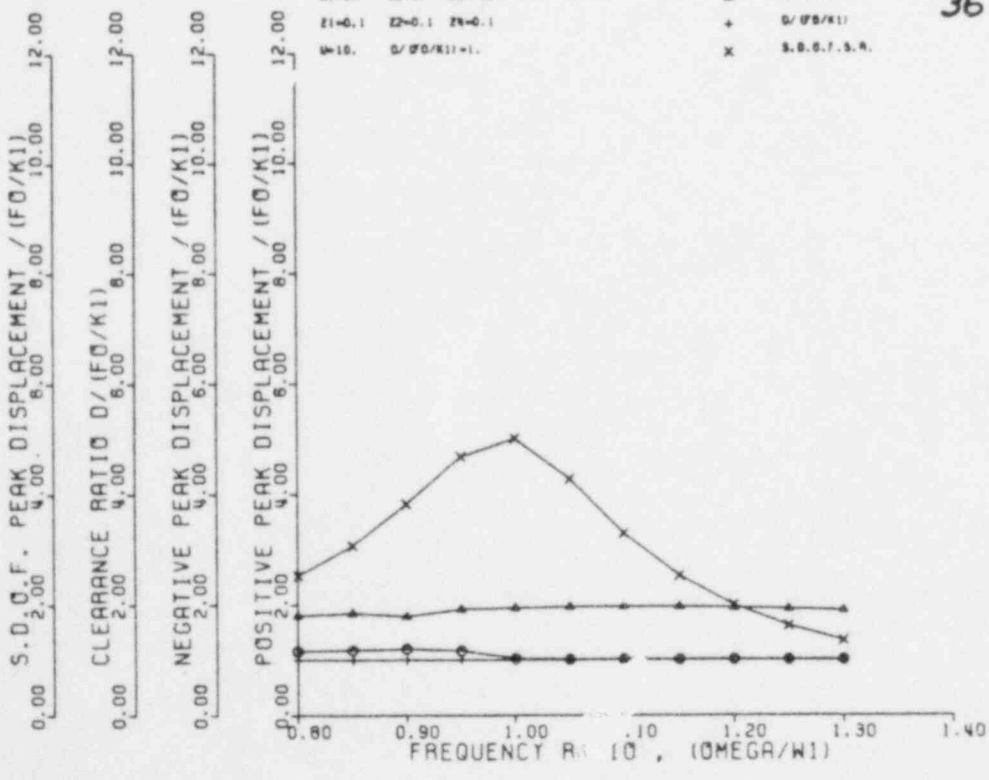

S36

Figure S37

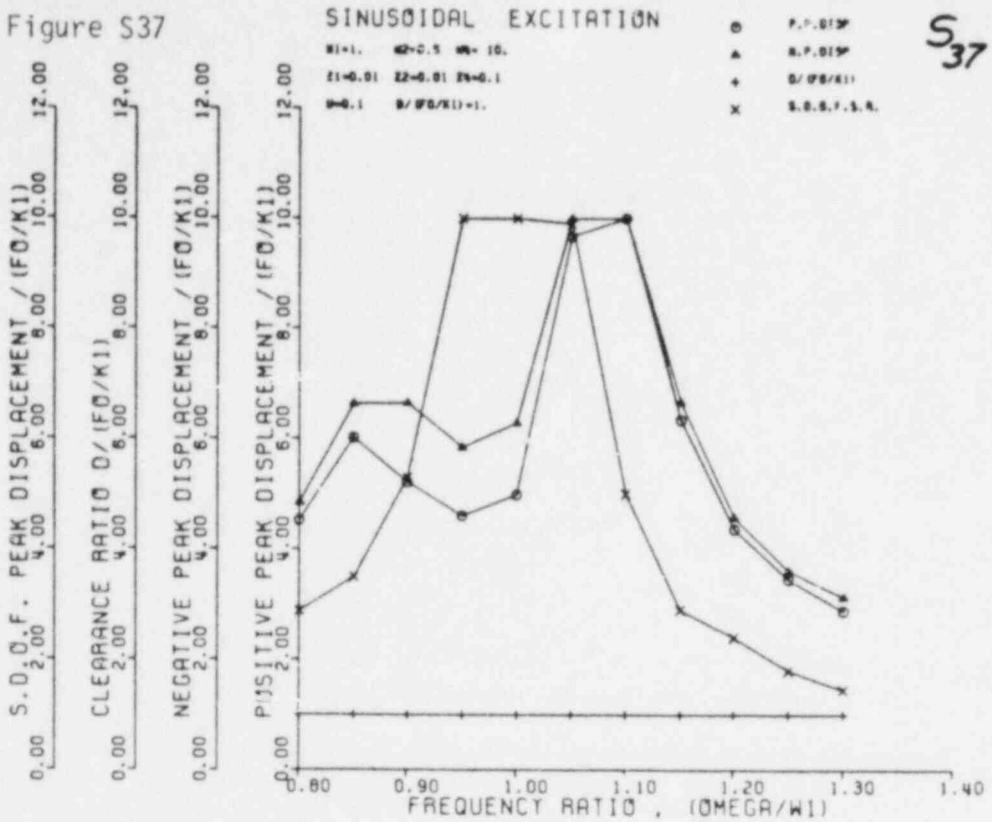

S37

Figure S38

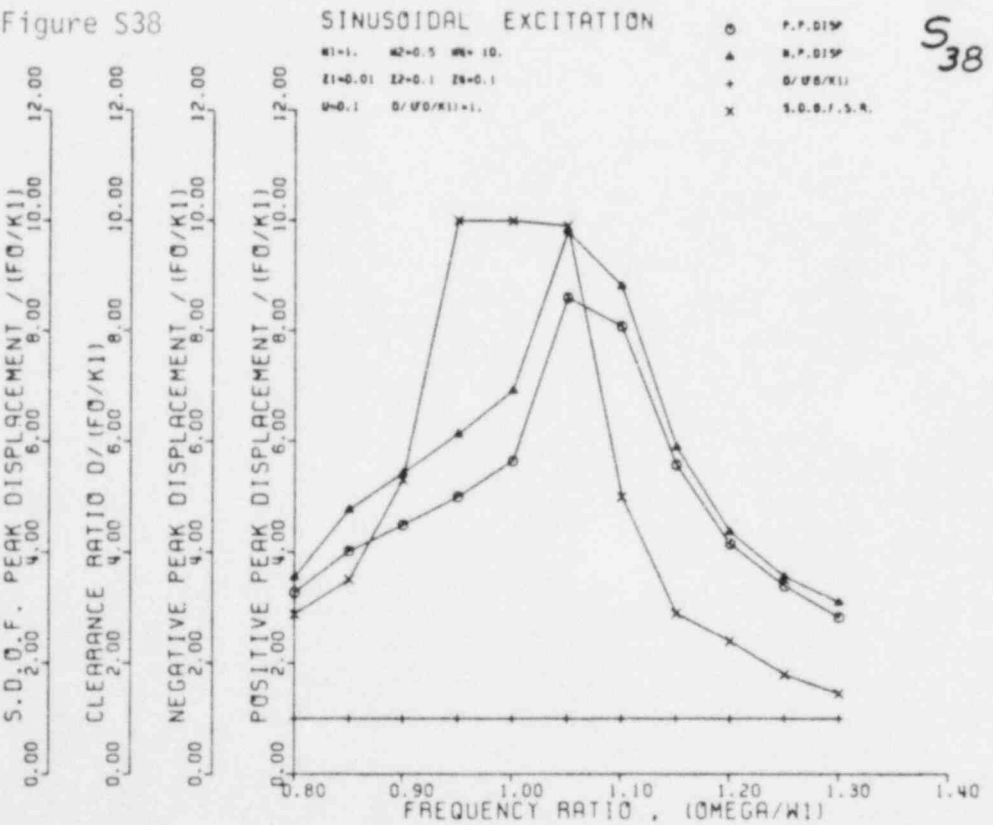

S38

Figure S39

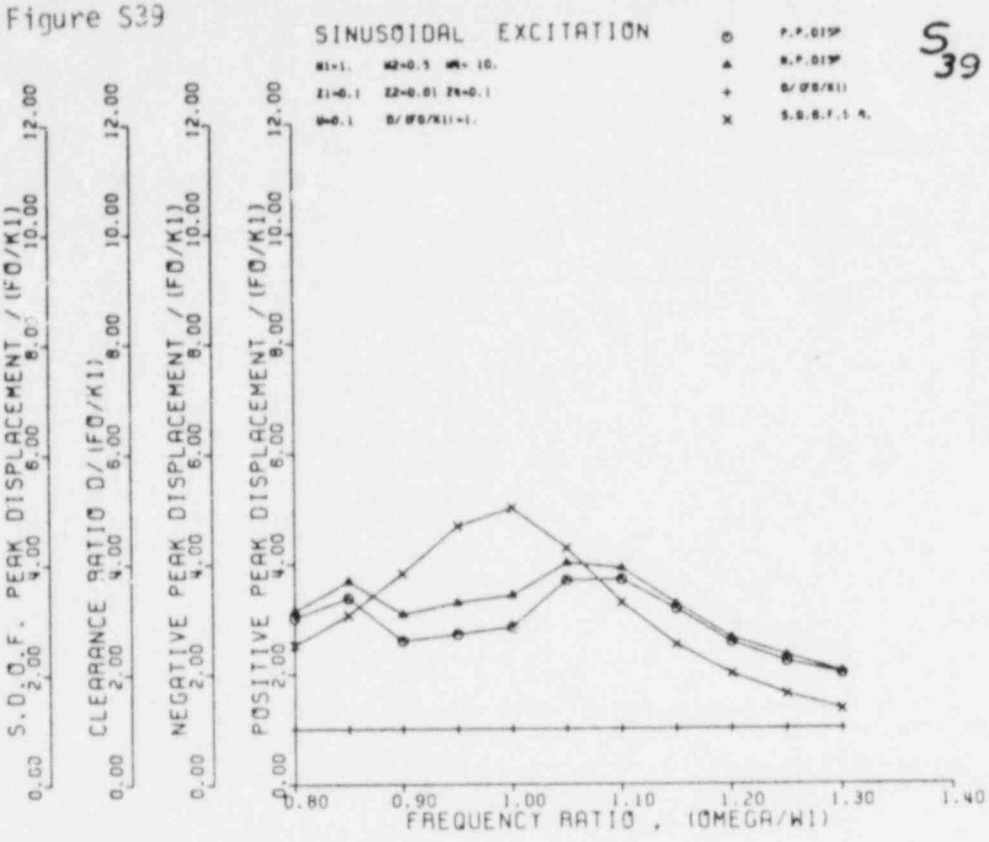

S39

Figure S40

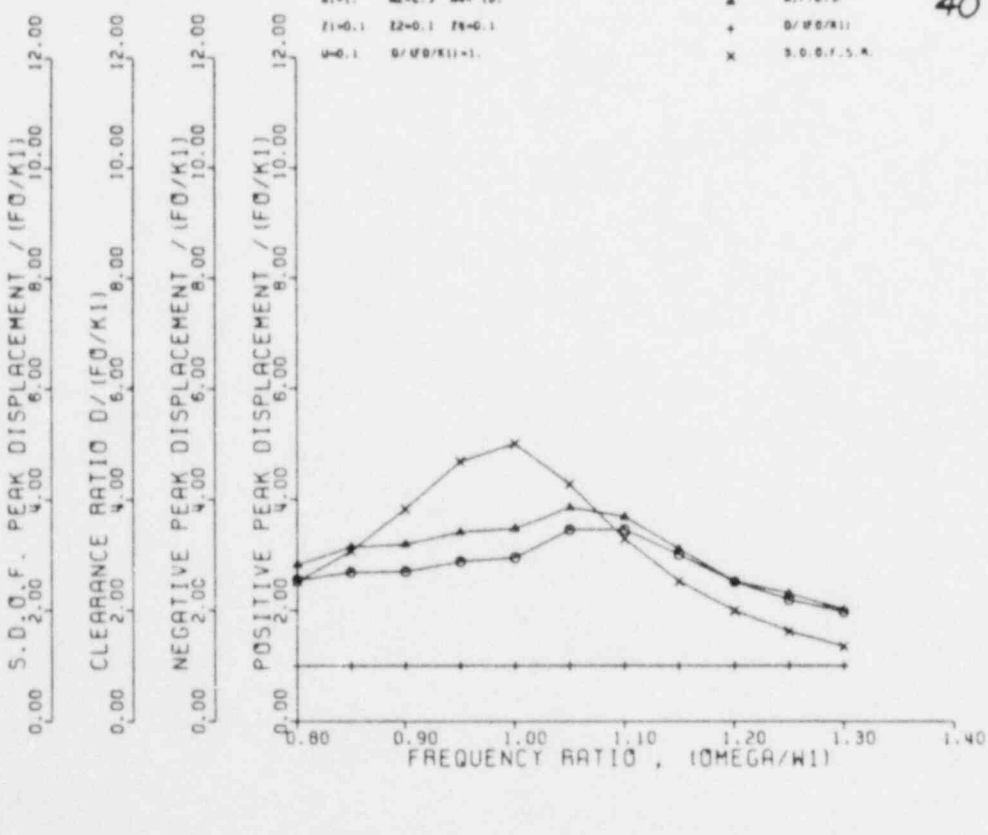

S40

Figure S41

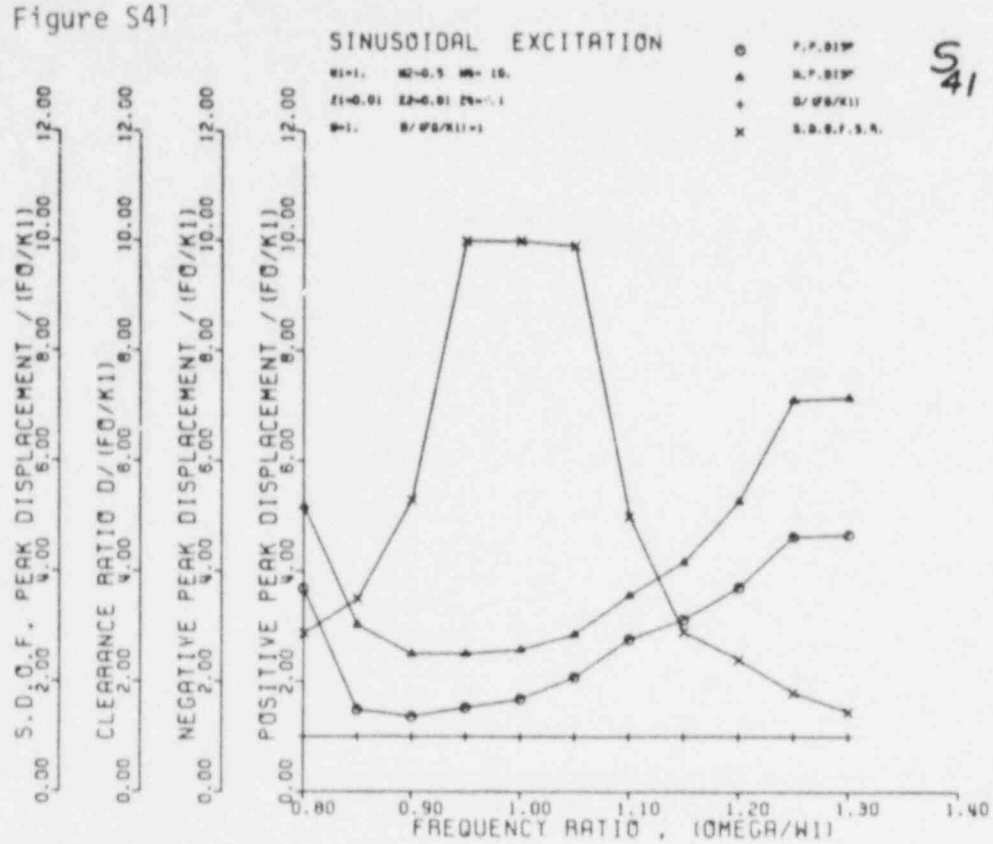

S41

Figure S42

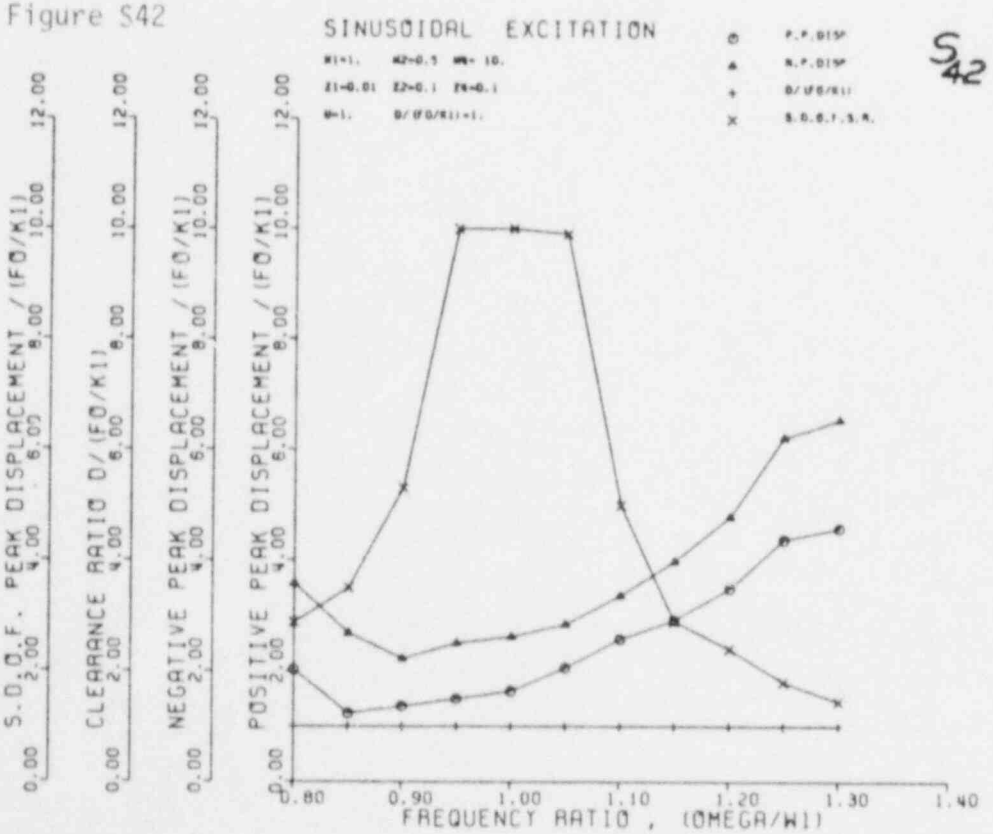

S42

Figure S43

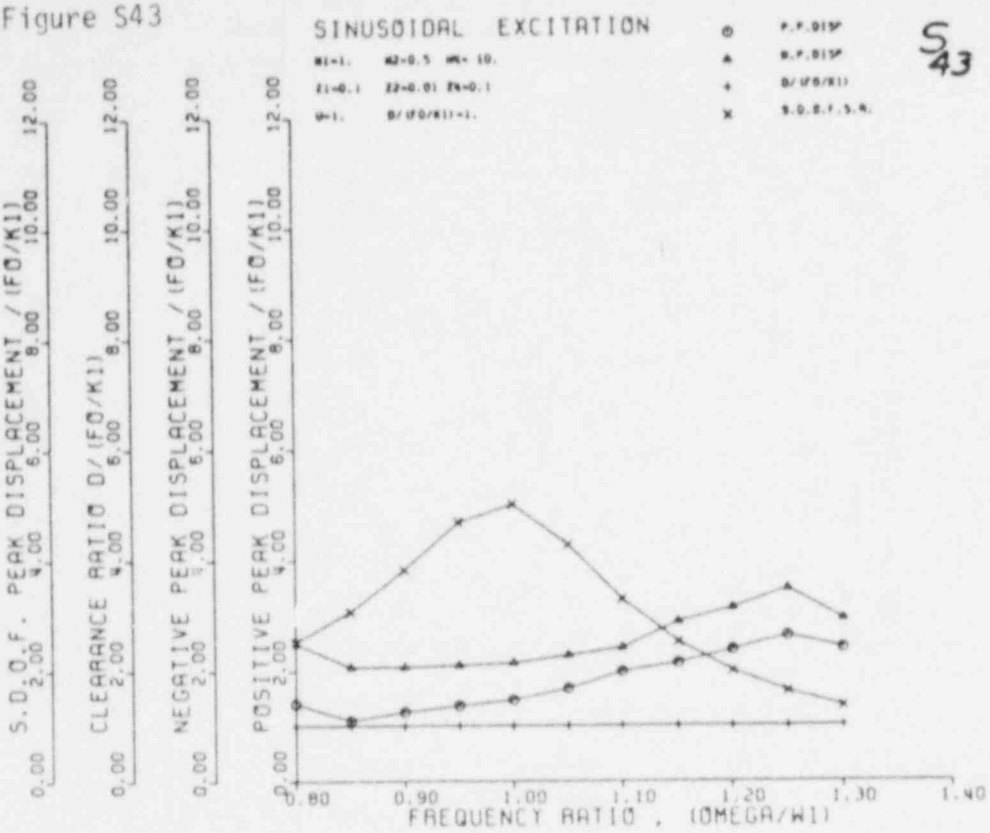

S43

Figure S44

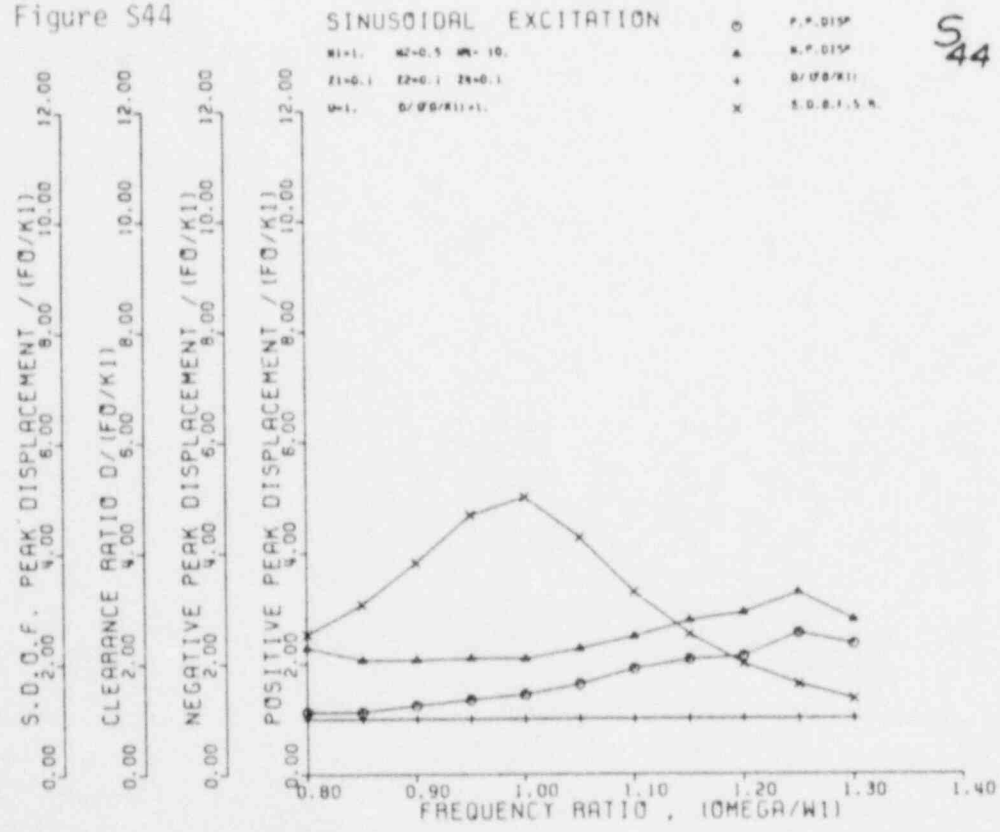

S44

Figure S45

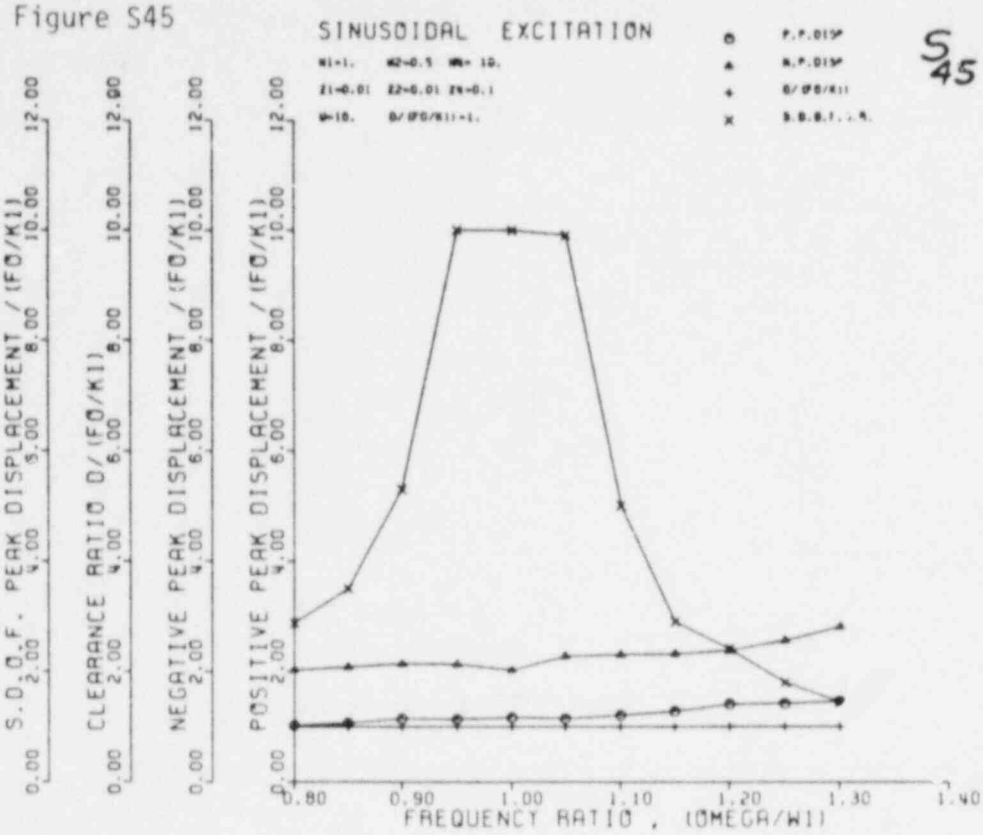

S45

Figure S46

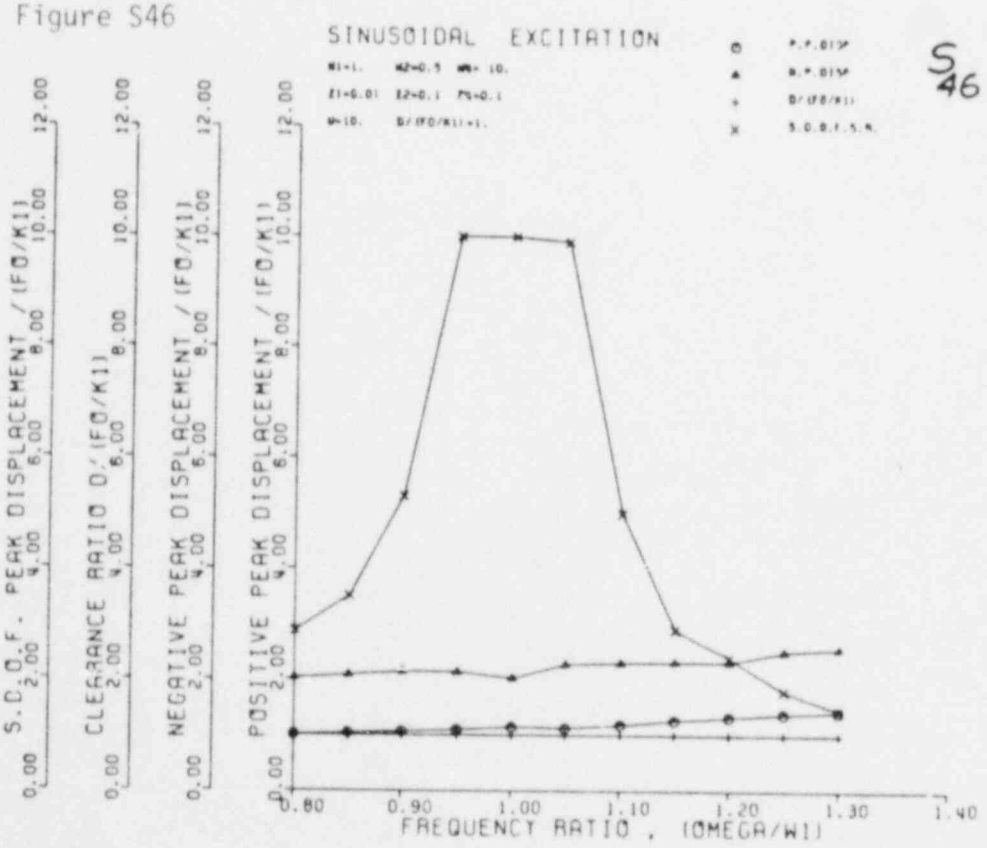

S46

Figure S47

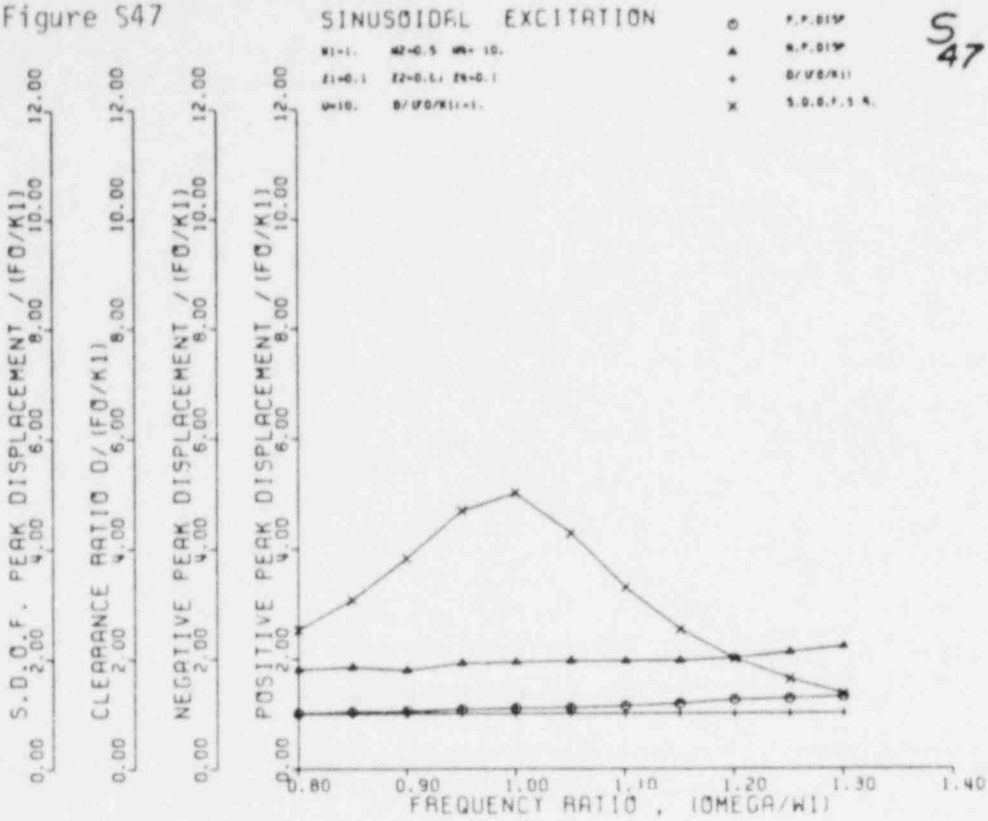

S47

Figure S48

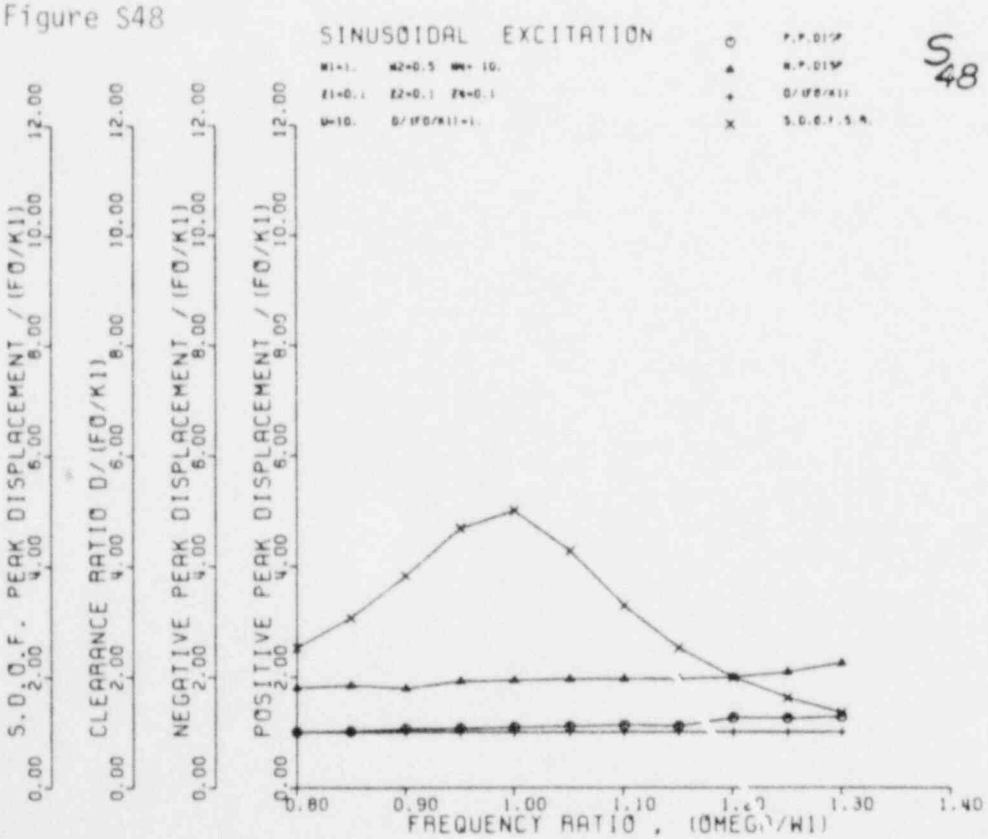

S48

Figure S49

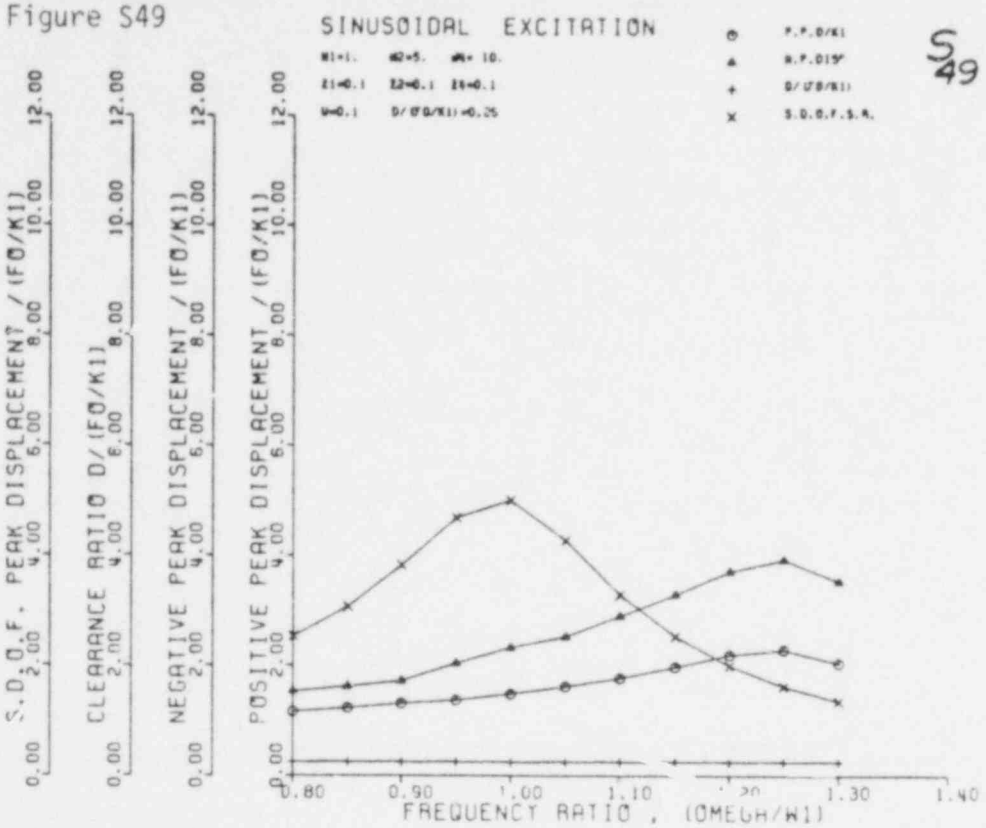

S49

Figure S50

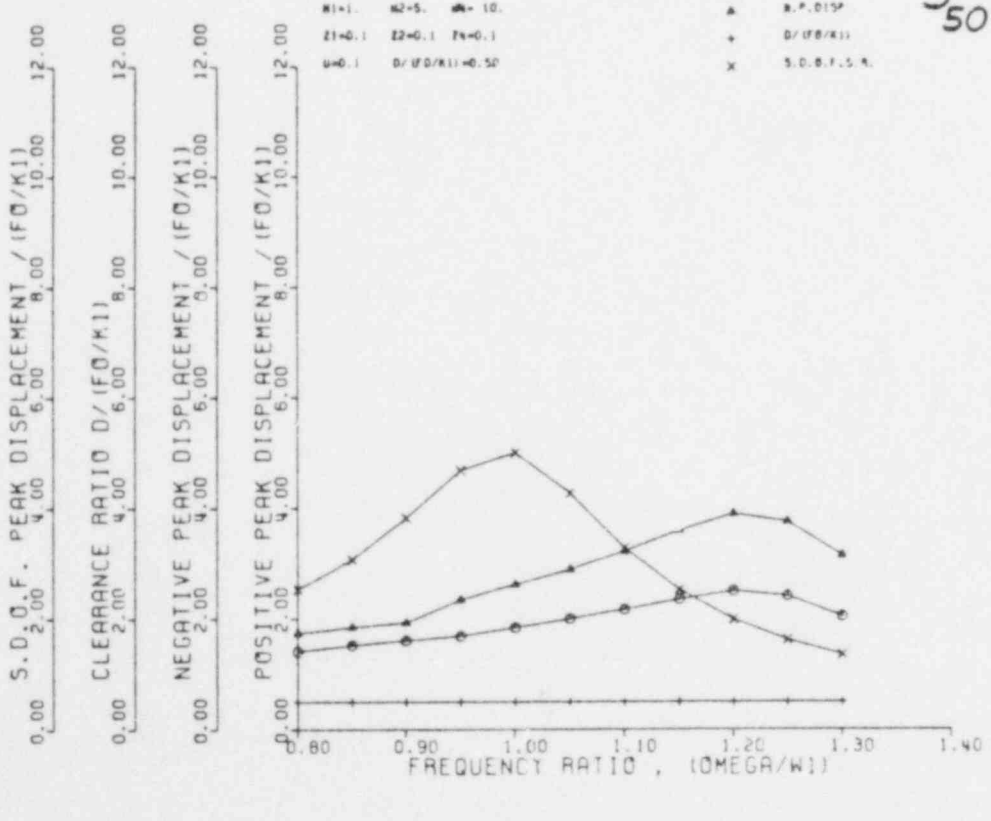

S50

Figure S51

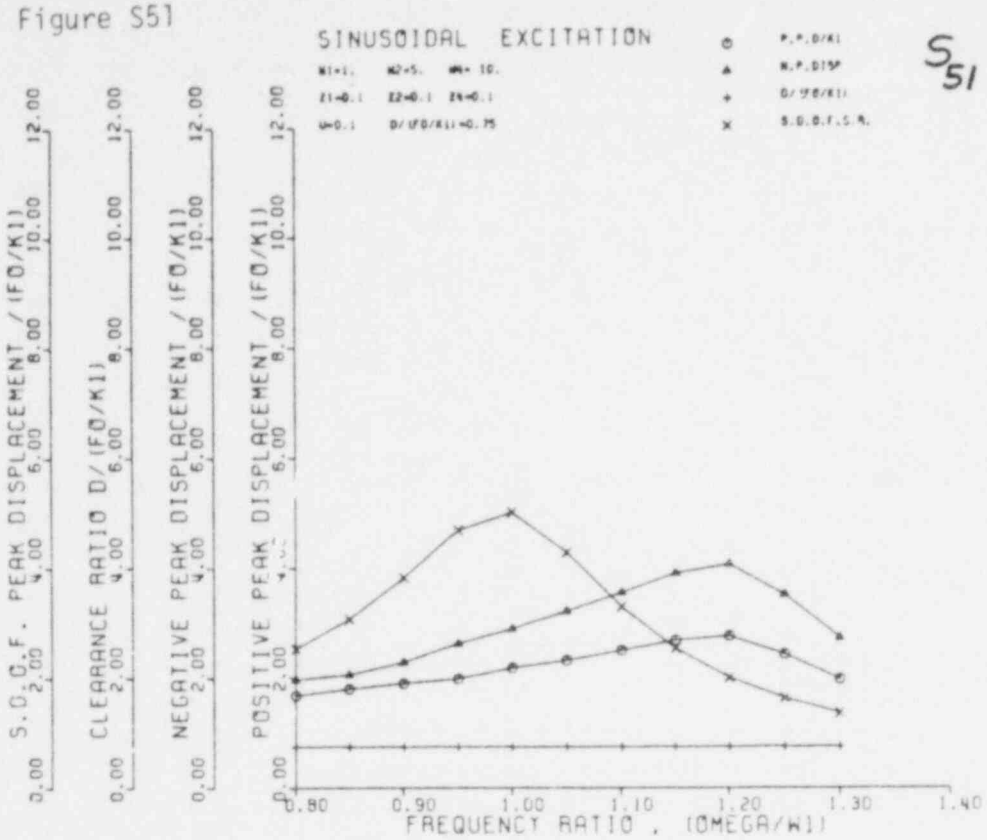

S51

Figure S52

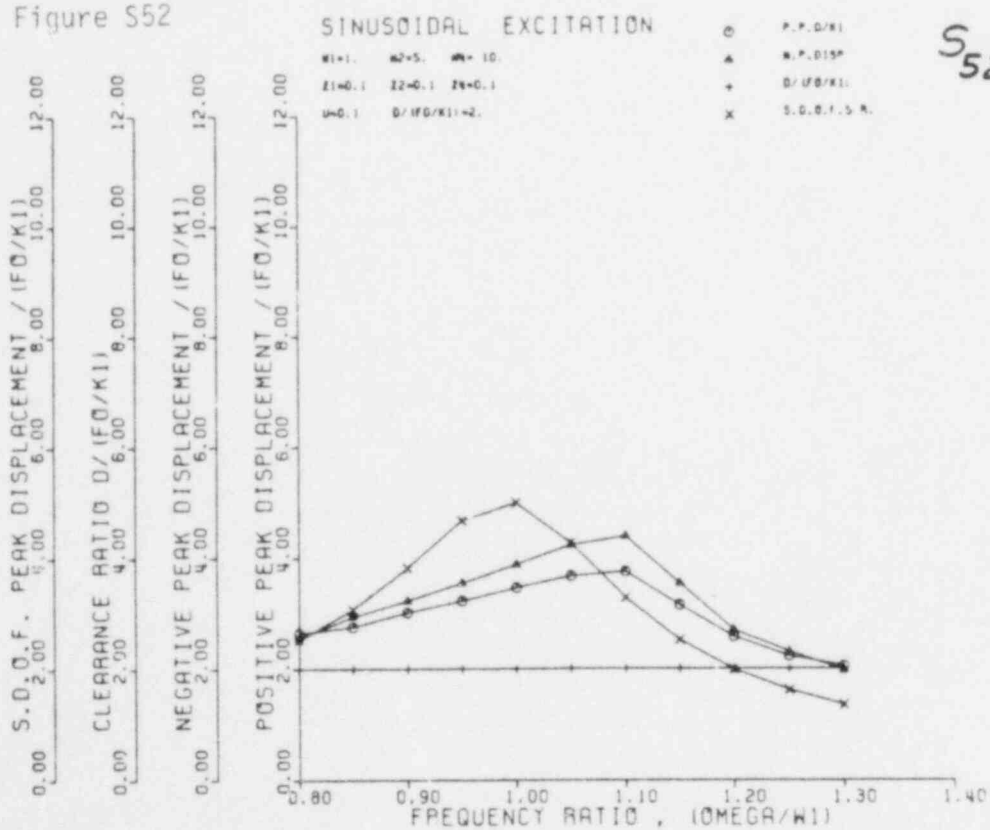

S52

Figure S53

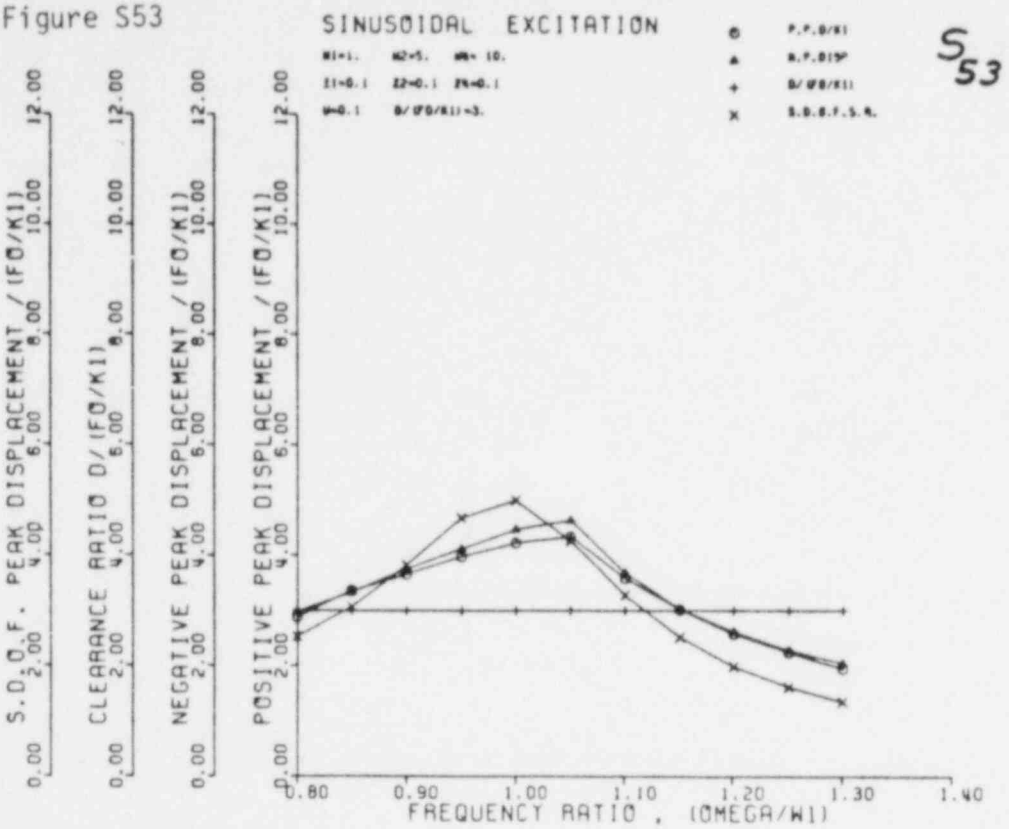

S53

Figure S54

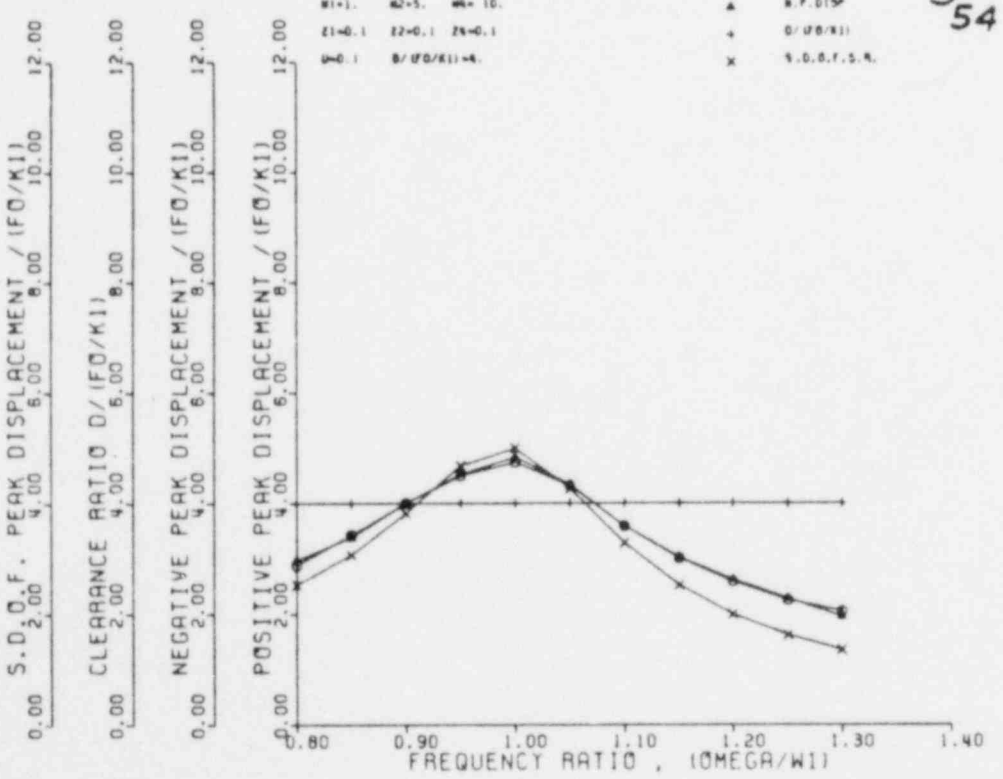

S54

Figure S55

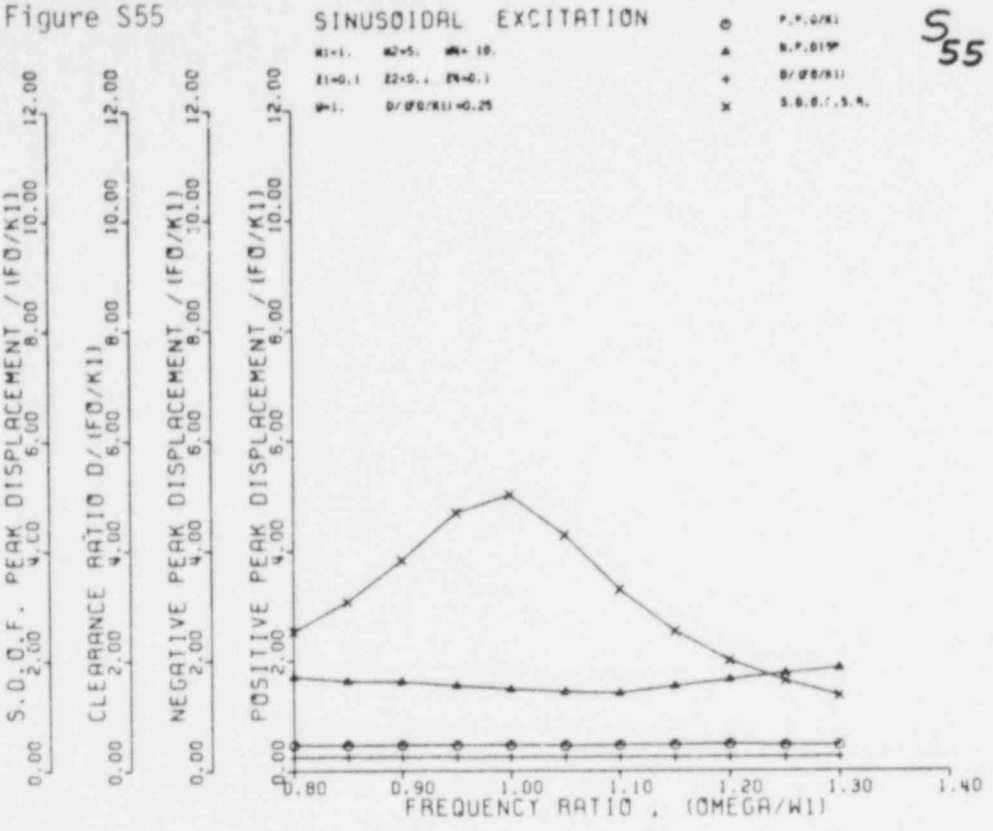

S55

Figure S56

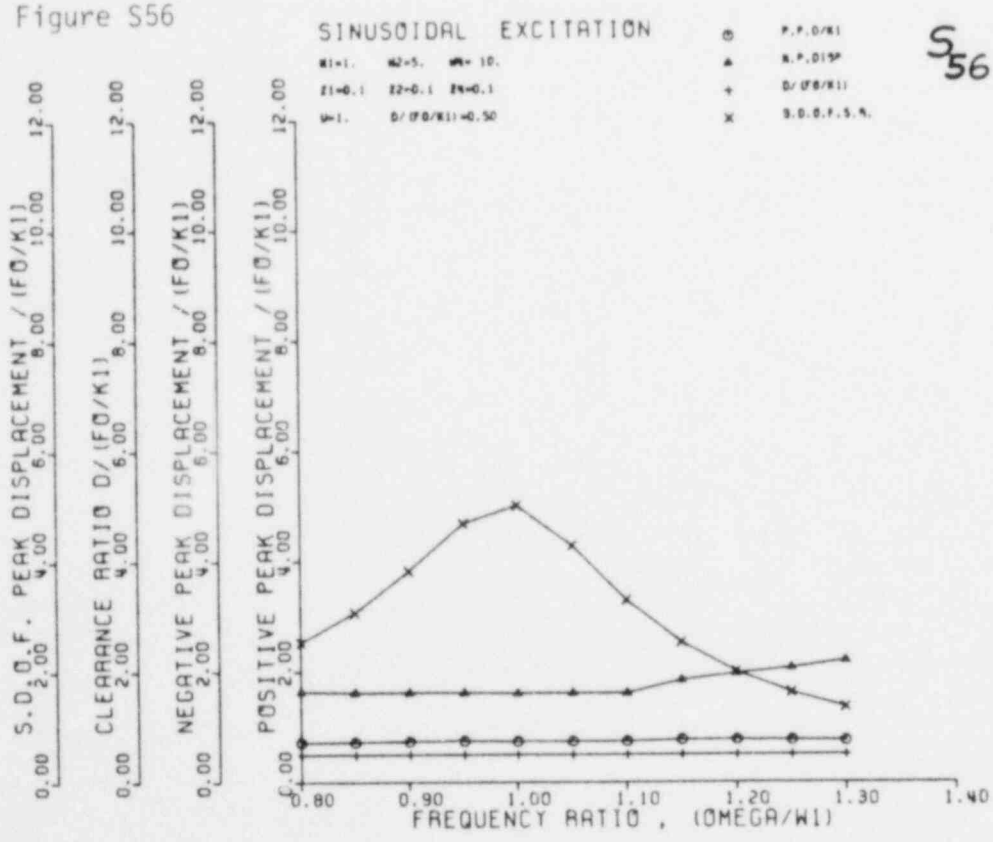

S56

Figure S57

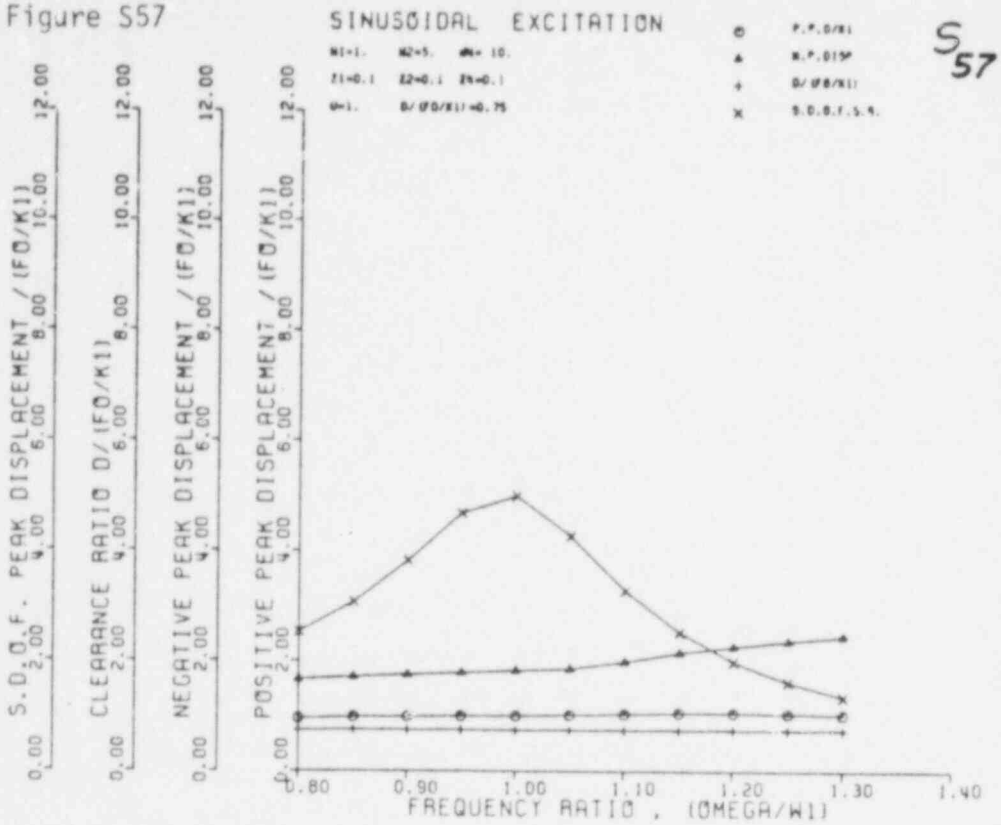

S57

Figure S58

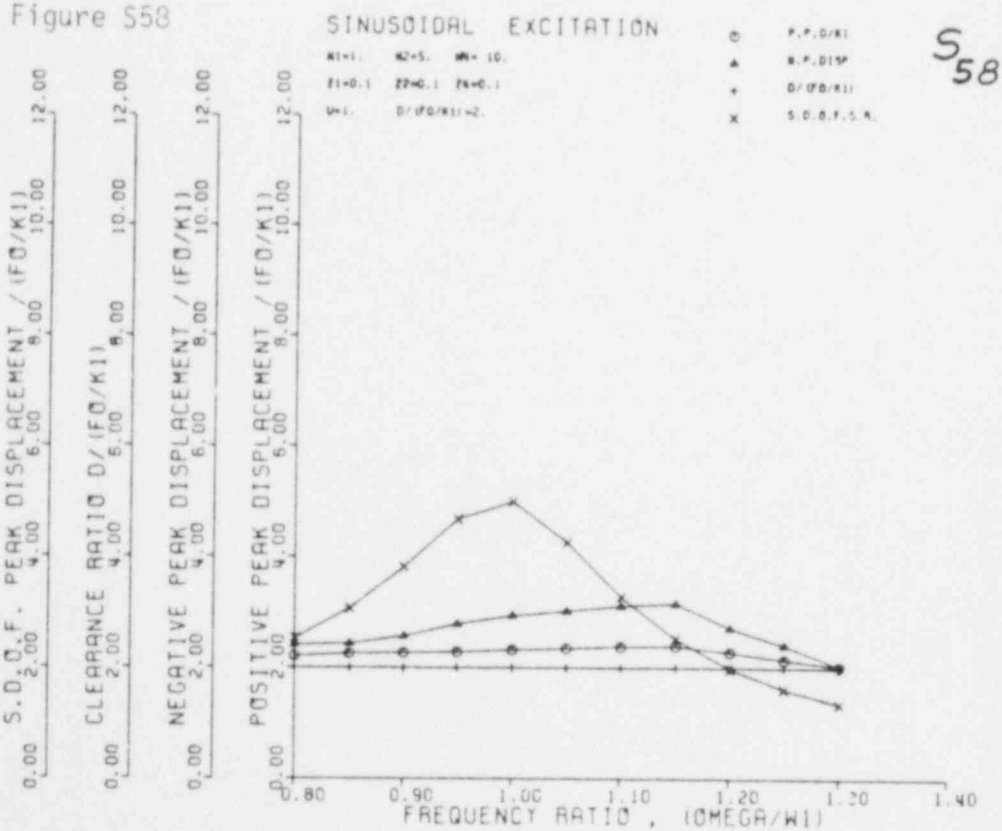

S58

Figure S59

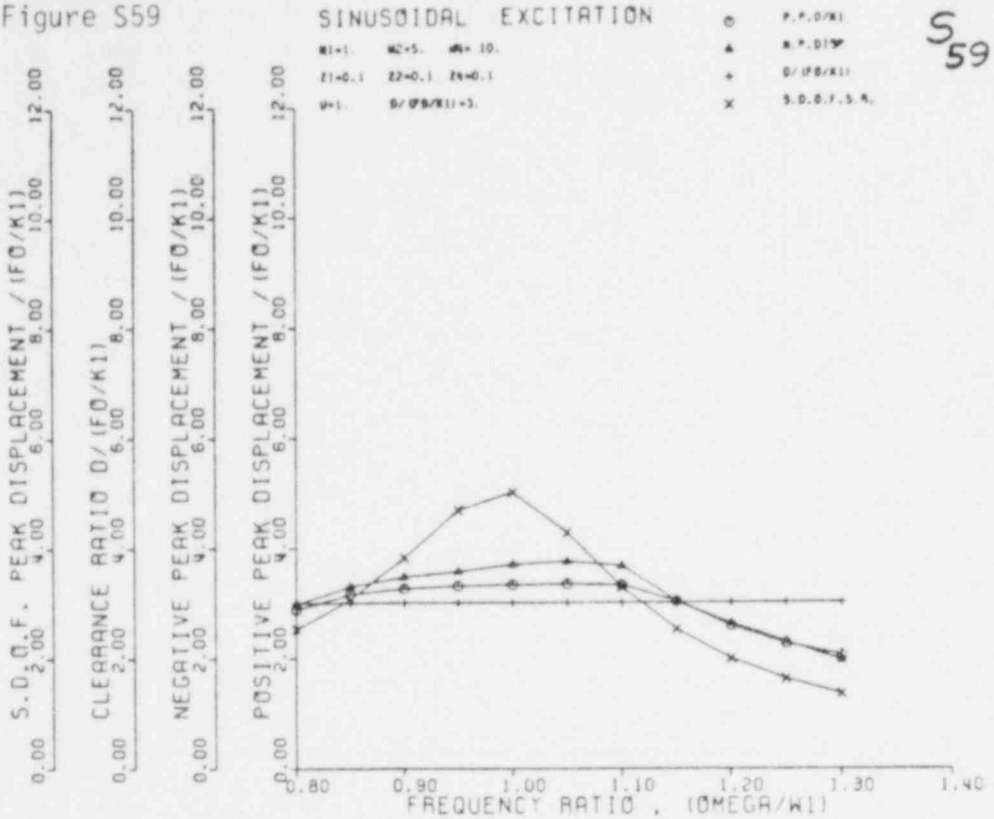

S59

Figure S60

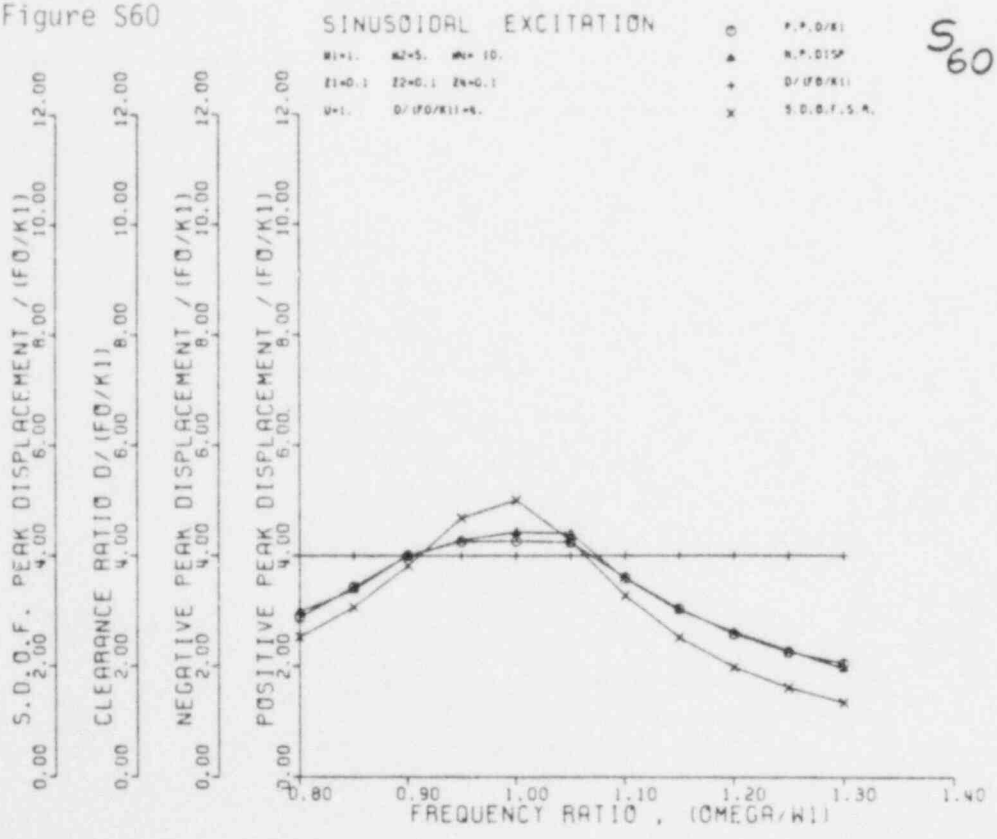

S60

Figure S61

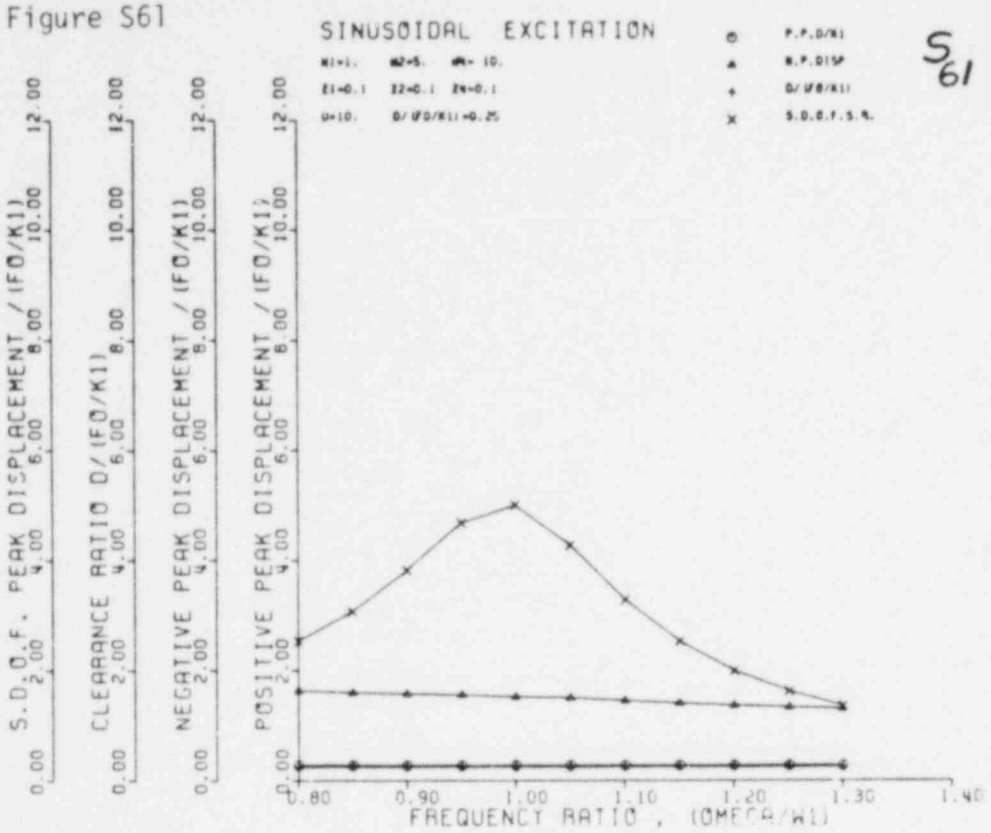

S61

Figure S62

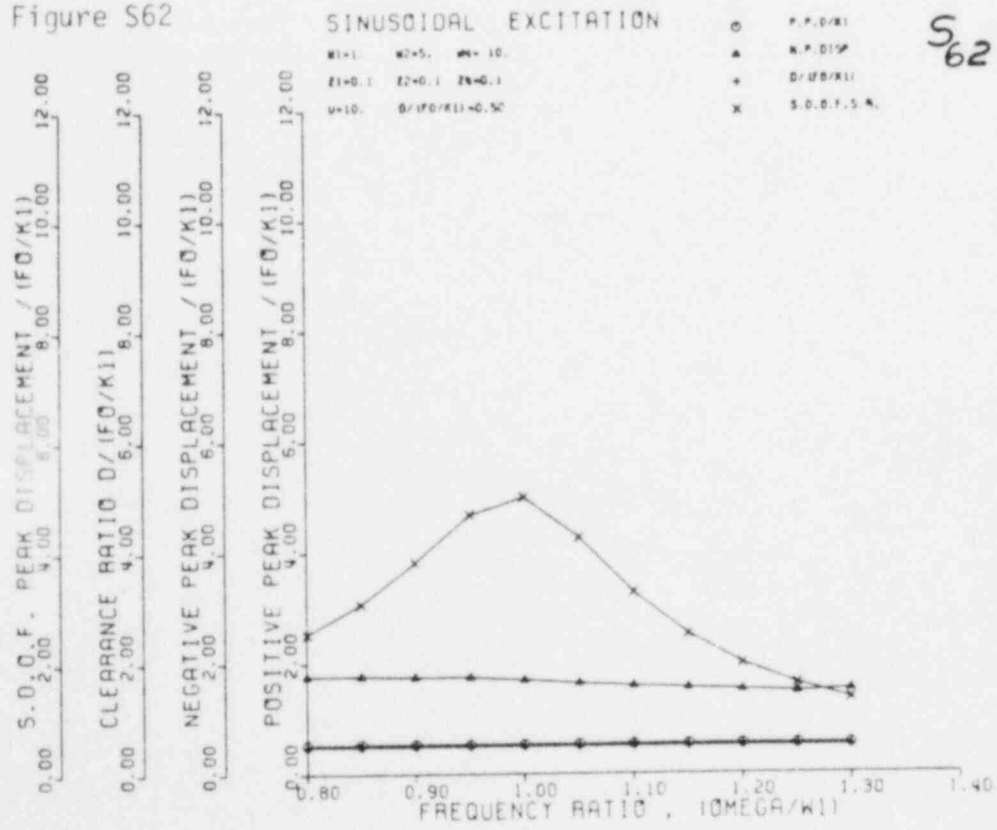

S62

Figure S63

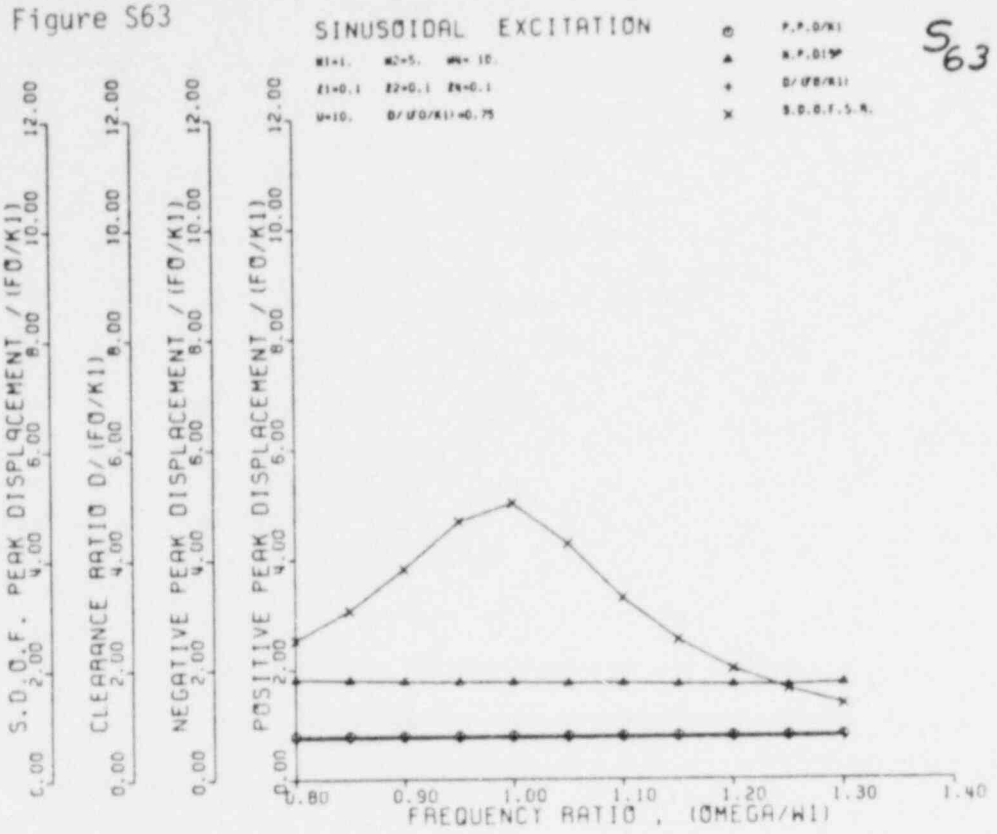

S63

Figure S64

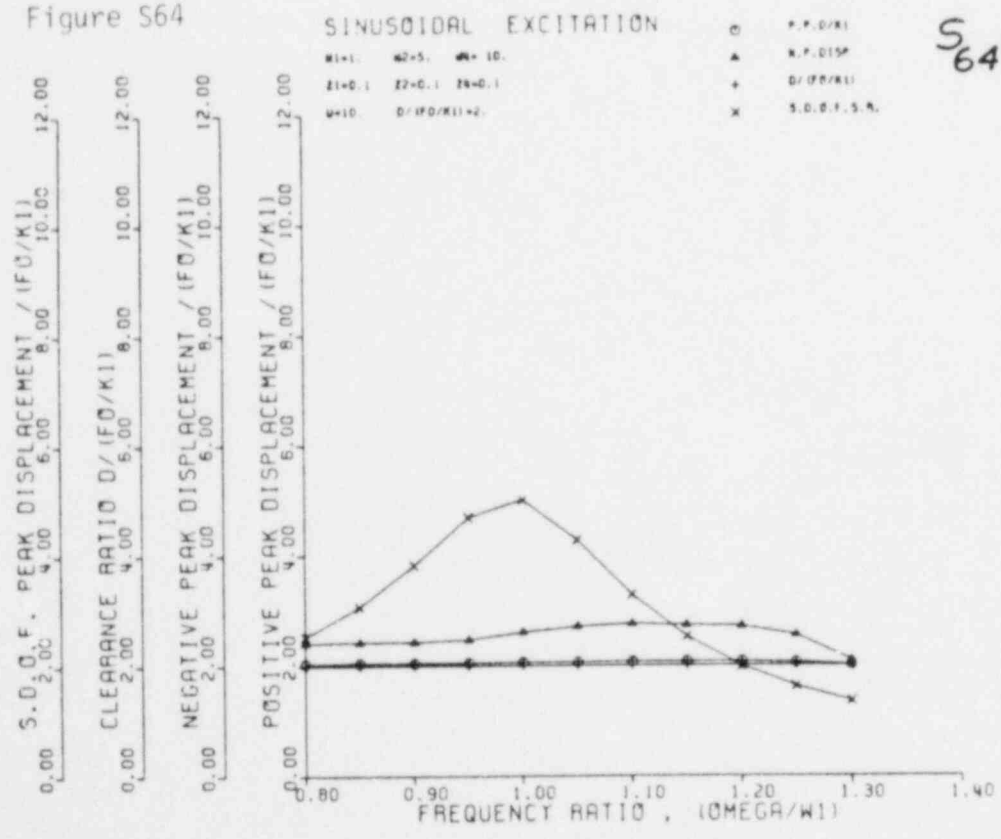

S64

Figure S65

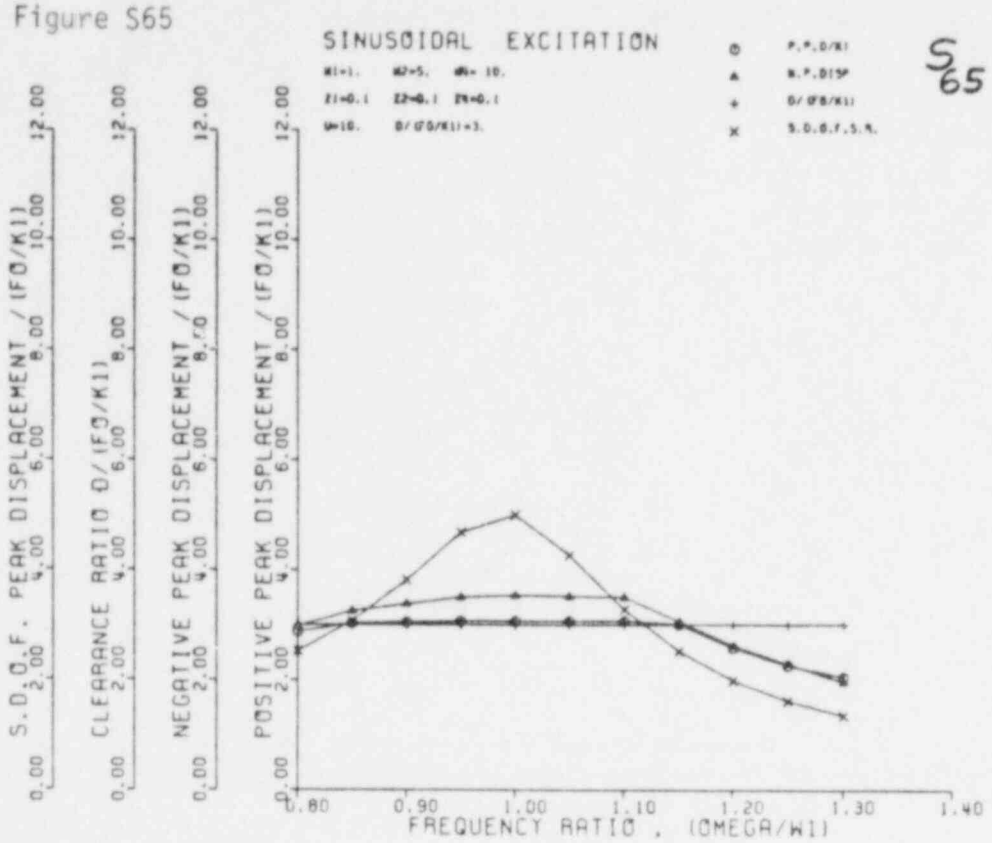

S65

Figure S66

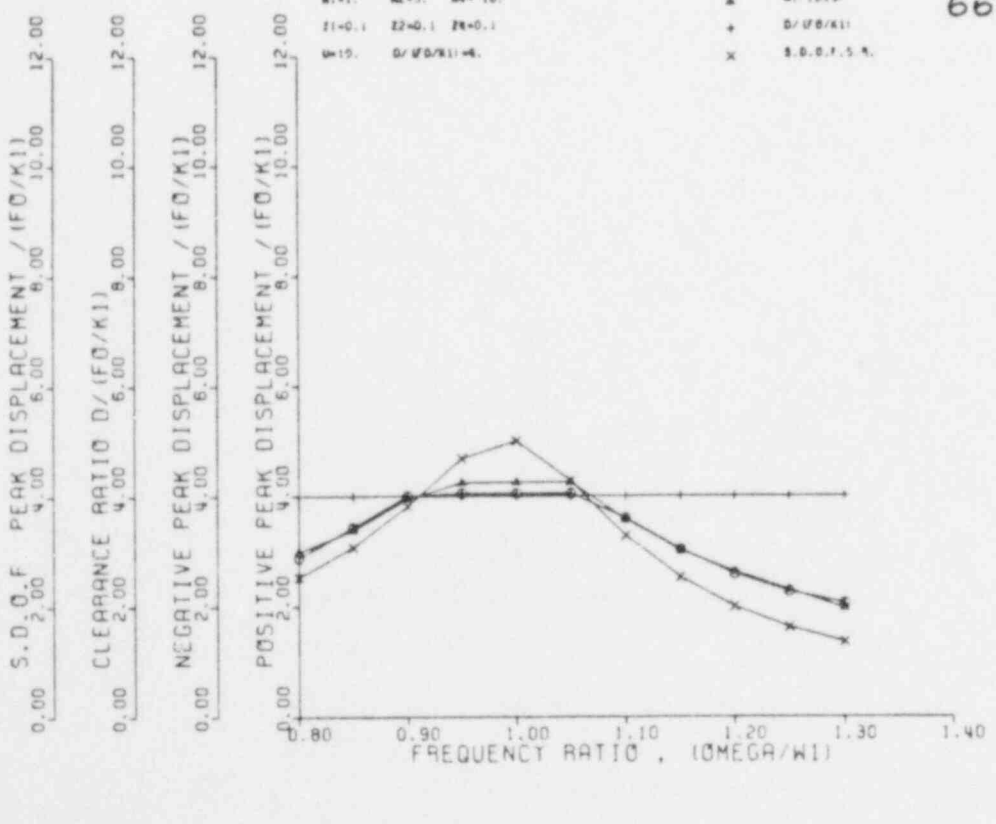

S66

TABLE 4B.1 DATA SUMMARY FOR RESPONSE SPECTRA:

PULSE EXCITATION

$\frac{\omega_4}{\omega_1}$	ζ_4	$D/(F_o/K_1)$	ζ_1	ζ_2	$\mu = \frac{M_2}{M_1}$	$\frac{\omega_2}{\omega_1}$	Page	Plot No.
10.0	0.1	0.4	0.01	0.1	0.1	0.5	4B-31	P55
						1.0	4B-22	P37
						2.0	4B-13	P19
						5.0	4B-4	P1
					1.0	0.5	4B-34	P61
						1.0	4B-25	P43
						2.0	4B-16	P25
						5.0	4B-7	P7
					10.0	0.5	4B-37	P67
						1.0	4B-28	P49
						2.0	4B-19	P31
						5.0	4B-10	P13
			0.1		0.1	0.5	4B-31	P56
						1.0	4B-22	P38
						2.0	4B-13	P20
						5.0	4B-4	P2
					1.0	0.5	4B-34	P62
						1.0	4B-25	P44
						2.0	4B-16	P26
						5.0	4B-7	P8
					10.0	0.5	4B-37	P68
						1.0	4B-28	P50
						2.0	4B-19	P32
						5.0	4B-10	P14

TABLE 4B.1

(Continued)

$\frac{\omega_4}{\omega_1}$	ζ_4	$D/(F_o/K_1)$	ζ_1	ζ_2	$\mu = \frac{M_2}{M_1}$	$\frac{\omega_2}{\omega_1}$	Page	Plot No.
10.0	0.1	0.8	0.01	0.1	0.1	0.5	4B-32	P57
↓	↓	↓	↓	↓	↓	0.1	4B-23	P39
↓	↓	↓	↓	↓	↓	2.0	4B-14	P21
↓	↓	↓	↓	↓	↓	5.0	4B-5	P3
↓	↓	↓	↓	↓	1.0	0.5	4B-35	P63
↓	↓	↓	↓	↓	↓	1.0	4B-26	P45
↓	↓	↓	↓	↓	↓	2.0	4B-17	P27
↓	↓	↓	↓	↓	↓	5.0	4B-8	P9
↓	↓	↓	↓	↓	10.0	0.5	4B-38	P69
↓	↓	↓	↓	↓	↓	1.0	4B-29	P51
↓	↓	↓	↓	↓	↓	2.0	4B-20	P33
↓	↓	↓	↓	↓	↓	5.0	4B-11	P15
↓	↓	↓	0.1	↓	0.1	0.5	4B-32	P58
↓	↓	↓	↓	↓	↓	1.0	4B-23	P40
↓	↓	↓	↓	↓	↓	2.0	4B-14	P22
↓	↓	↓	↓	↓	↓	5.0	4B-5	P4
↓	↓	↓	↓	↓	1.0	0.5	4B-35	P64
↓	↓	↓	↓	↓	↓	1.0	4B-26	P46
↓	↓	↓	↓	↓	↓	2.0	4B-17	P28
↓	↓	↓	↓	↓	↓	5.0	4B-8	P10
↓	↓	↓	↓	↓	10.0	0.5	4B-38	P70
↓	↓	↓	↓	↓	↓	1.0	4B-29	P52
↓	↓	↓	↓	↓	↓	2.0	4B-20	P34
↓	↓	↓	↓	↓	↓	5.0	4B-11	P16

TABLE 4B.1

(Concluded)

$\frac{\omega_4}{\omega_1}$	ζ_4	$D/(F_o/K_1)$	ζ_1	ζ_2	$\mu = \frac{M_2}{M_1}$	$\frac{\omega_2}{\omega_1}$	Page	Plot No.
10.0	0.1	1.2	0.01	0.1	0.1	0.5	4B-33	P59
↓	↓	↓	↓	↓	↓	1.0	4B-24	P41
↓	↓	↓	↓	↓	↓	2.0	4B-15	P23
↓	↓	↓	↓	↓	↓	5.0	4B-6	P5
↓	↓	↓	↓	↓	1.0	0.5	4B-36	P65
↓	↓	↓	↓	↓	↓	1.0	4B-27	P47
↓	↓	↓	↓	↓	↓	2.0	4B-18	P29
↓	↓	↓	↓	↓	↓	5.0	4B-9	P11
↓	↓	↓	↓	↓	10.0	0.5	4B-39	P71
↓	↓	↓	↓	↓	↓	1.0	4B-30	P53
↓	↓	↓	↓	↓	↓	2.0	4B-21	P35
↓	↓	↓	↓	↓	↓	5.0	4B-12	P17
↓	↓	↓	0.1	↓	0.1	0.5	4B-33	P60
↓	↓	↓	↓	↓	↓	1.0	4B-24	P42
↓	↓	↓	↓	↓	↓	2.0	4B-15	P24
↓	↓	↓	↓	↓	↓	5.0	4B-6	P6
↓	↓	↓	↓	↓	1.0	0.5	4B-36	P66
↓	↓	↓	↓	↓	↓	1.0	4B-27	P48
↓	↓	↓	↓	↓	↓	2.0	4B-18	P30
↓	↓	↓	↓	↓	↓	5.0	4B-9	P12
↓	↓	↓	↓	↓	10.0	0.5	4B-39	P72
↓	↓	↓	↓	↓	↓	1.0	4B-30	P54
↓	↓	↓	↓	↓	↓	2.0	4B-21	P36
↓	↓	↓	↓	↓	↓	5.0	4B-12	P18

Figure P1

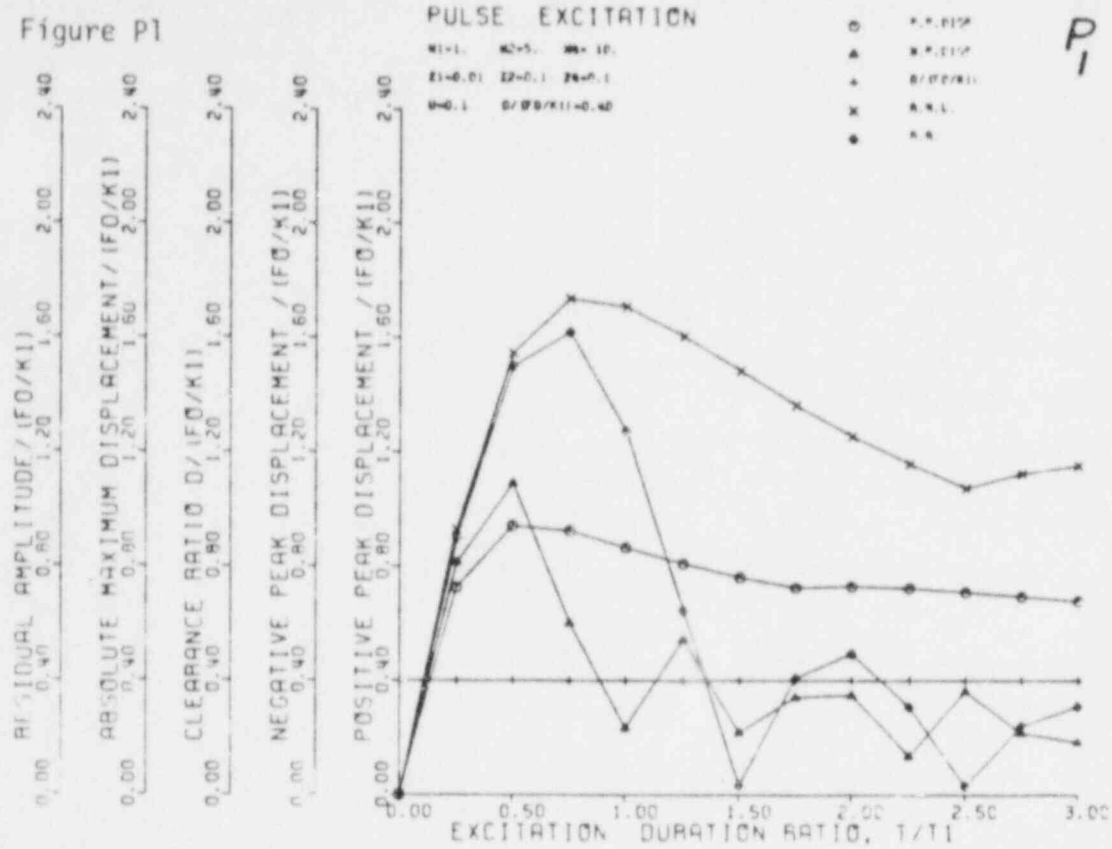

Figure P2

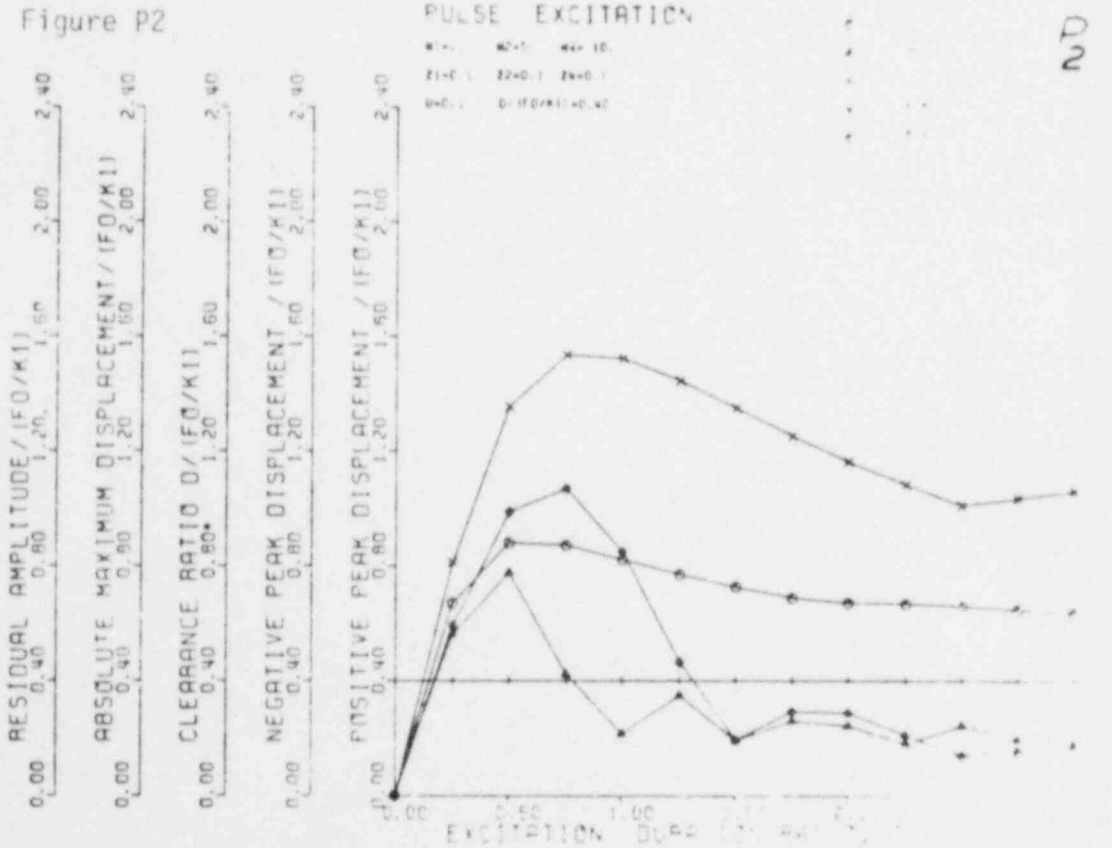

Figure P3

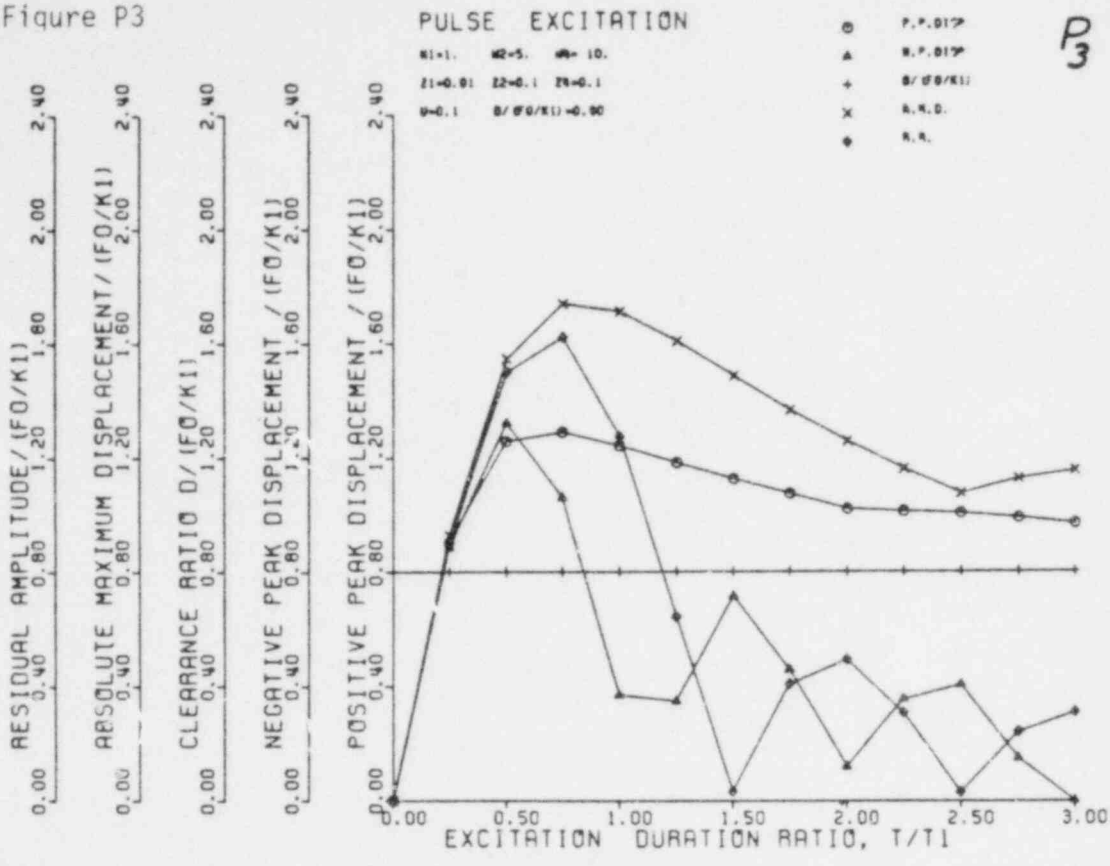

Figure P4

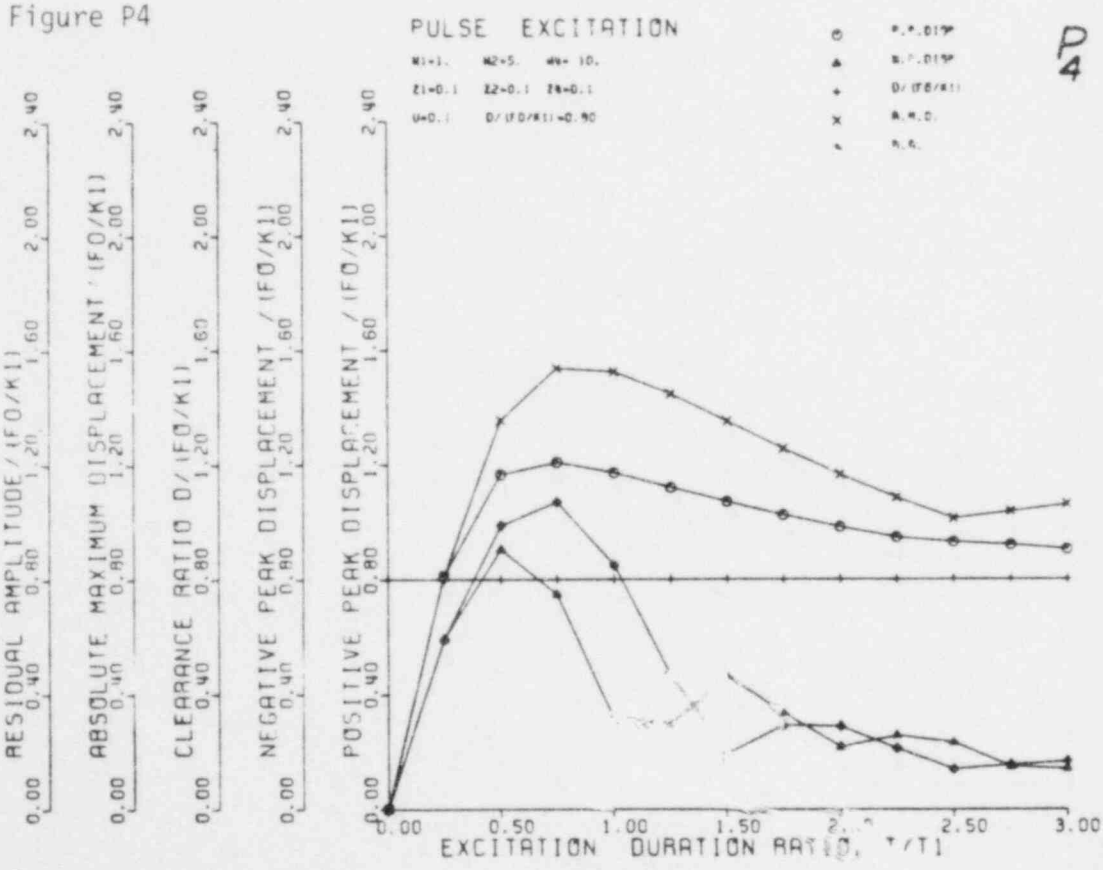

Figure P5

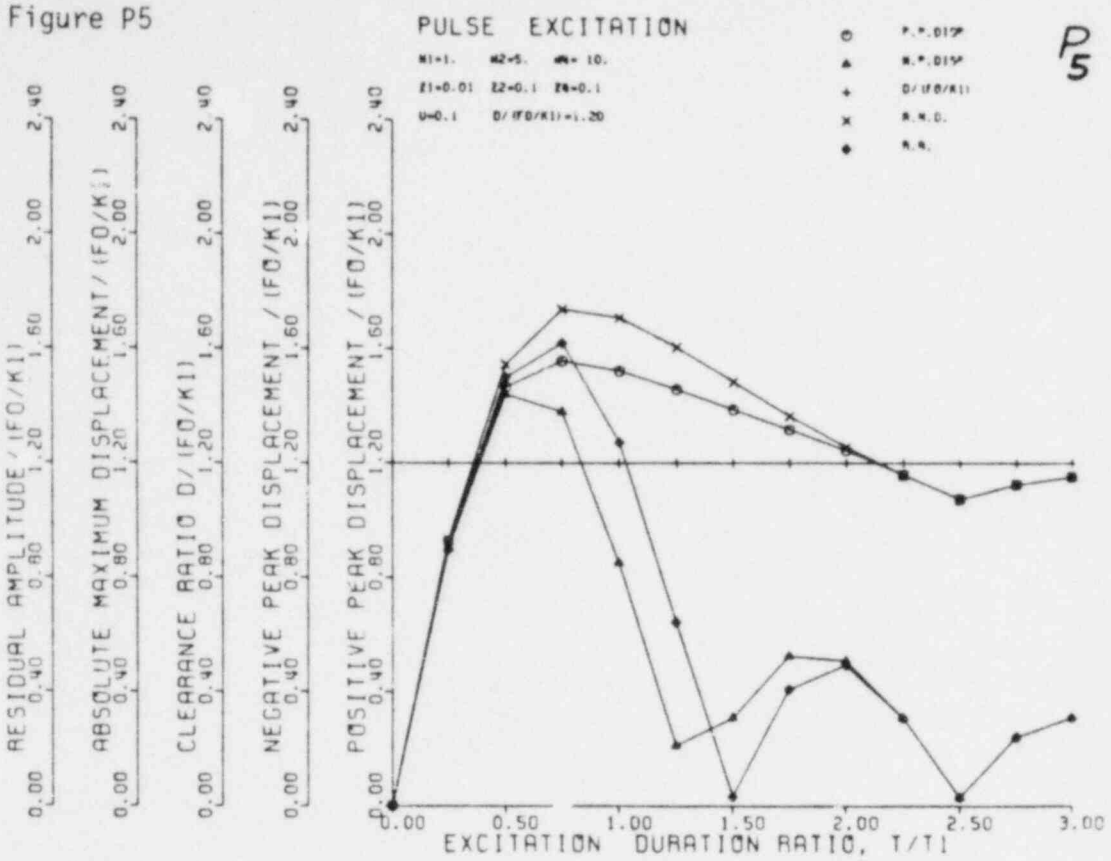

Figure P6

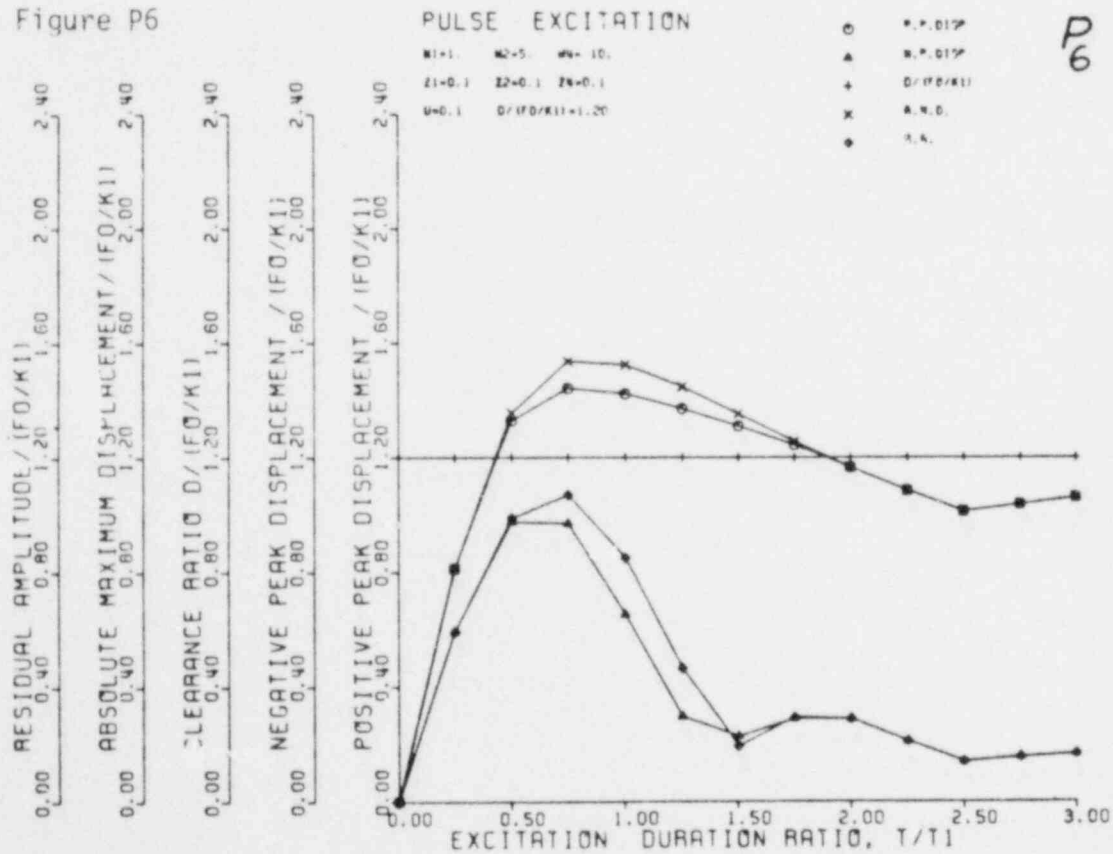

Figure P7

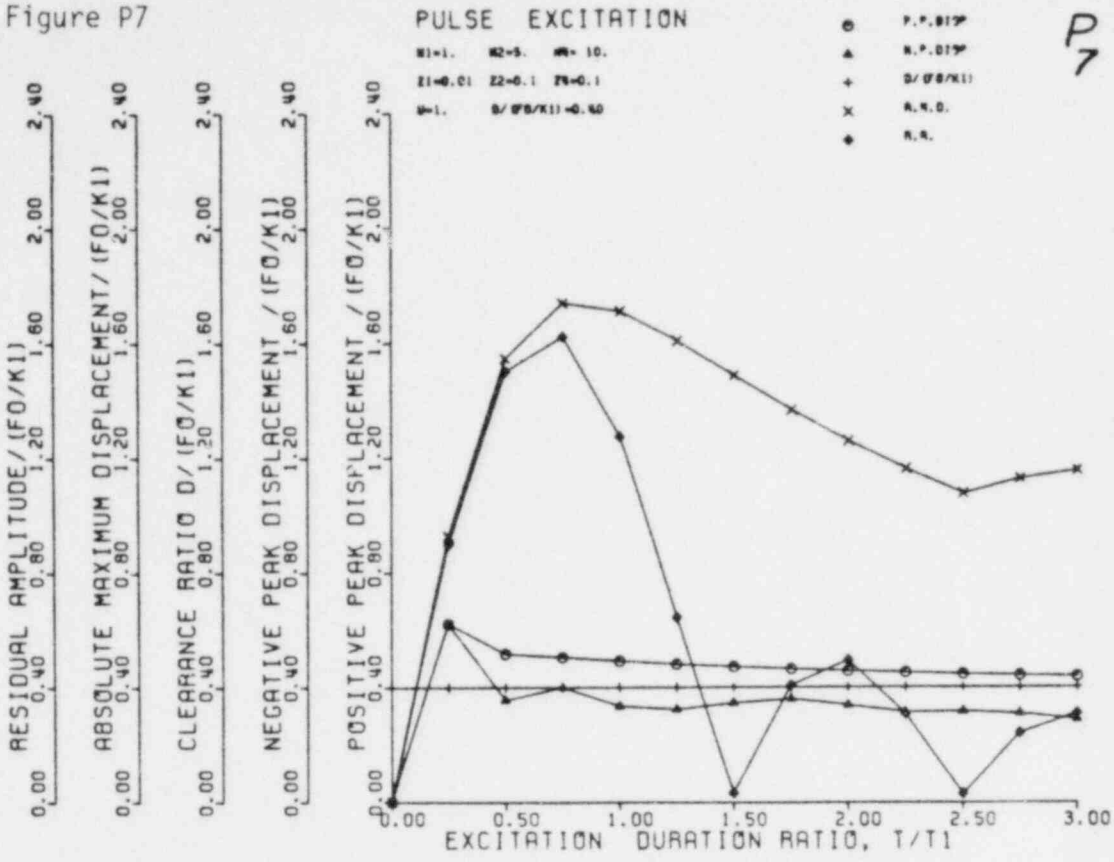

Figure P8

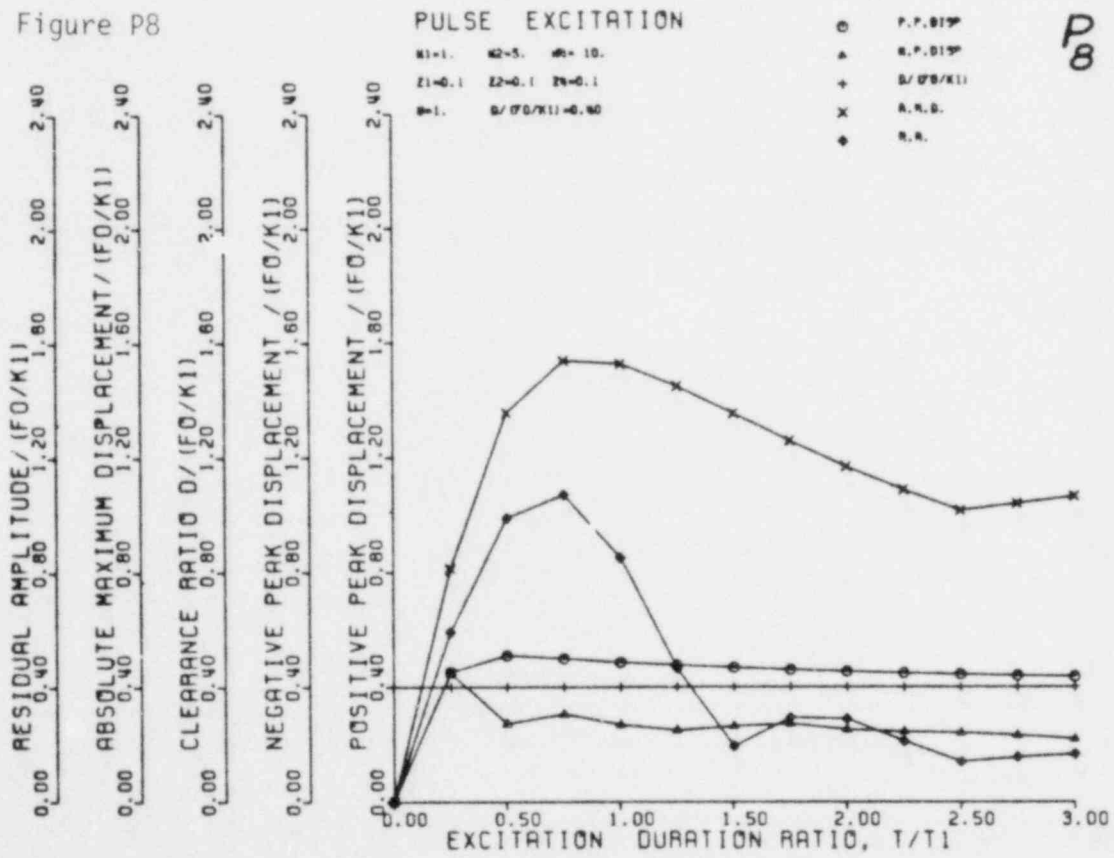

Figure P9

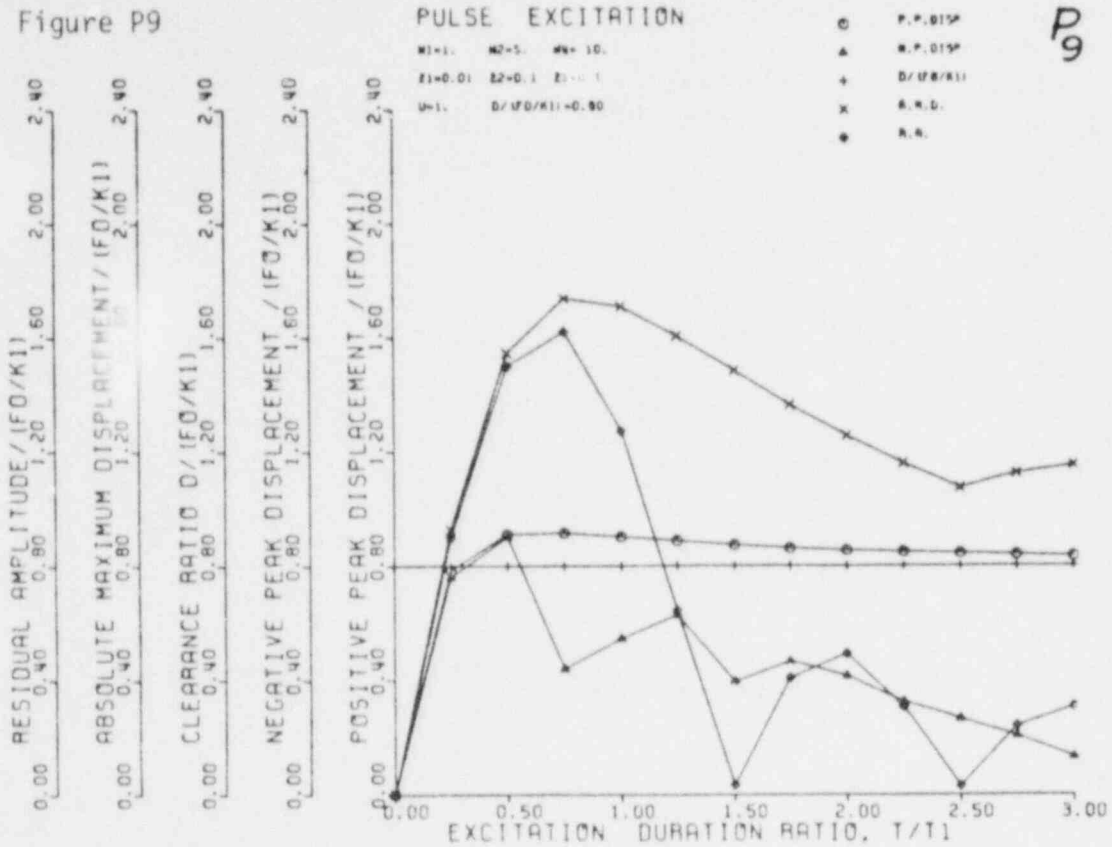

Figure P10

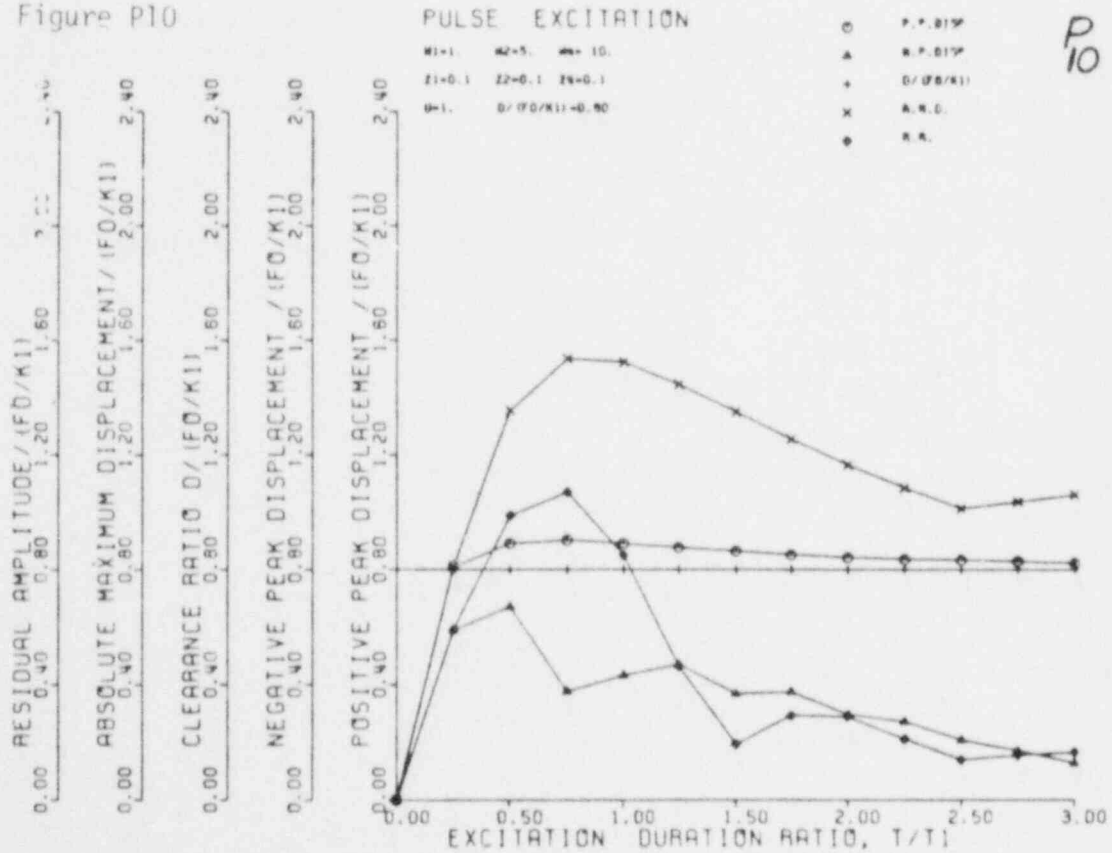

Figure P11

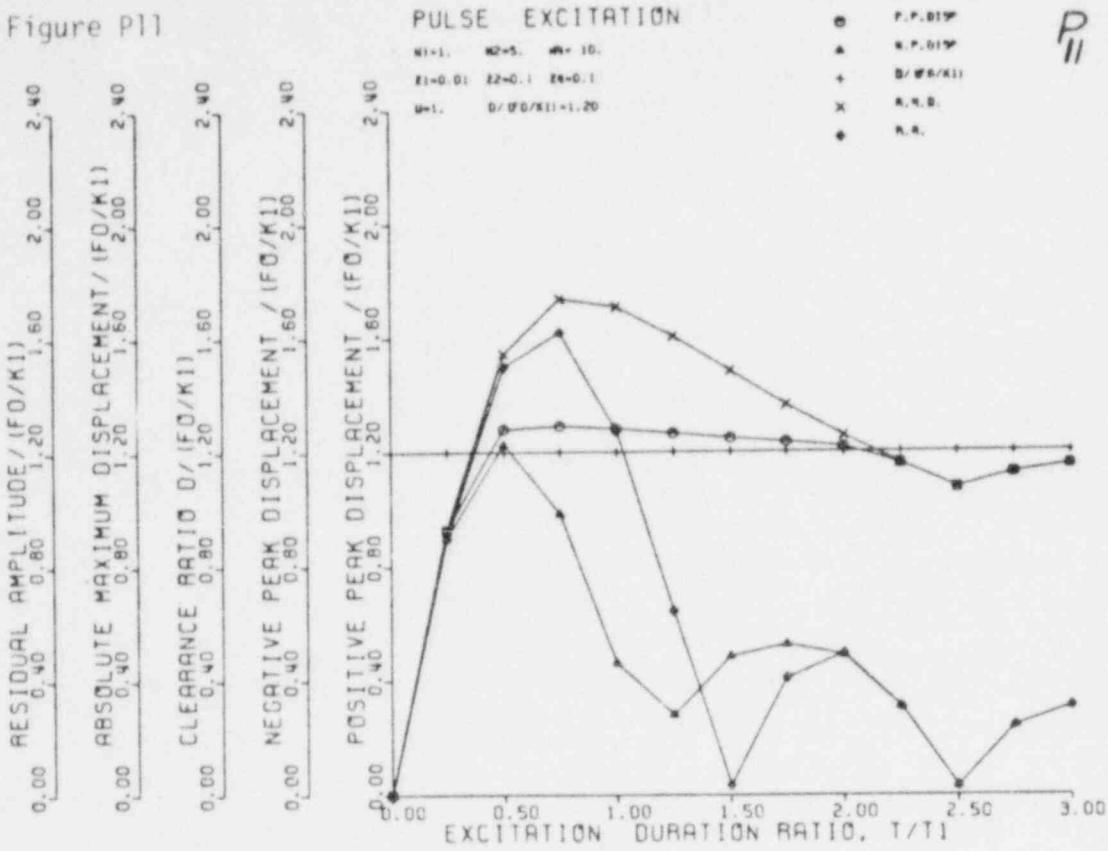

P11

Figure P12

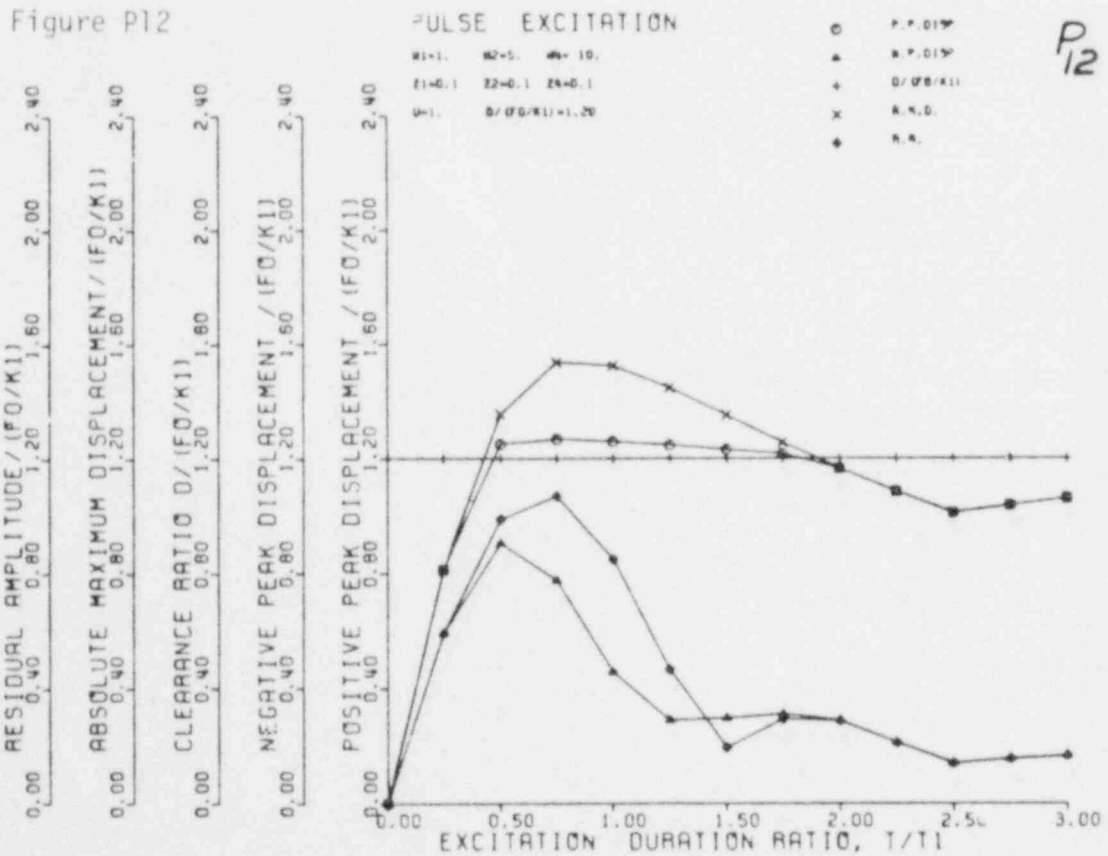

P12

Figure P13

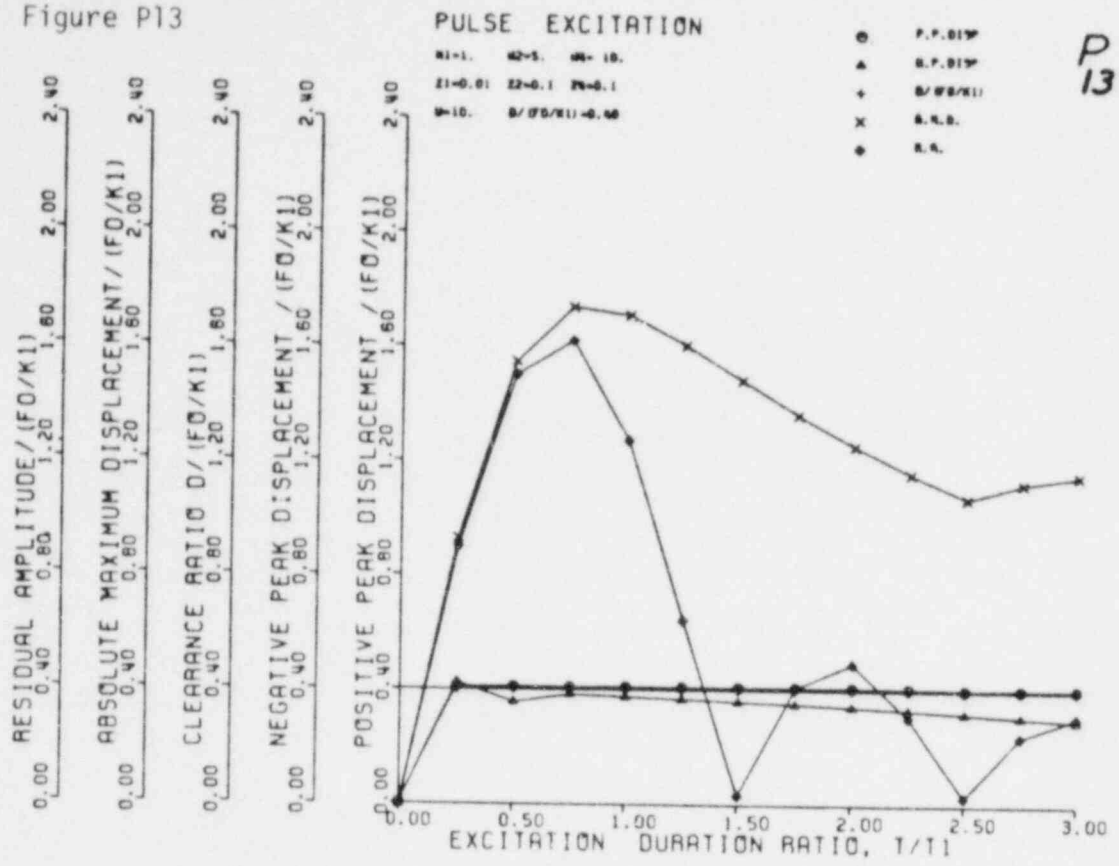

P13

Figure P14

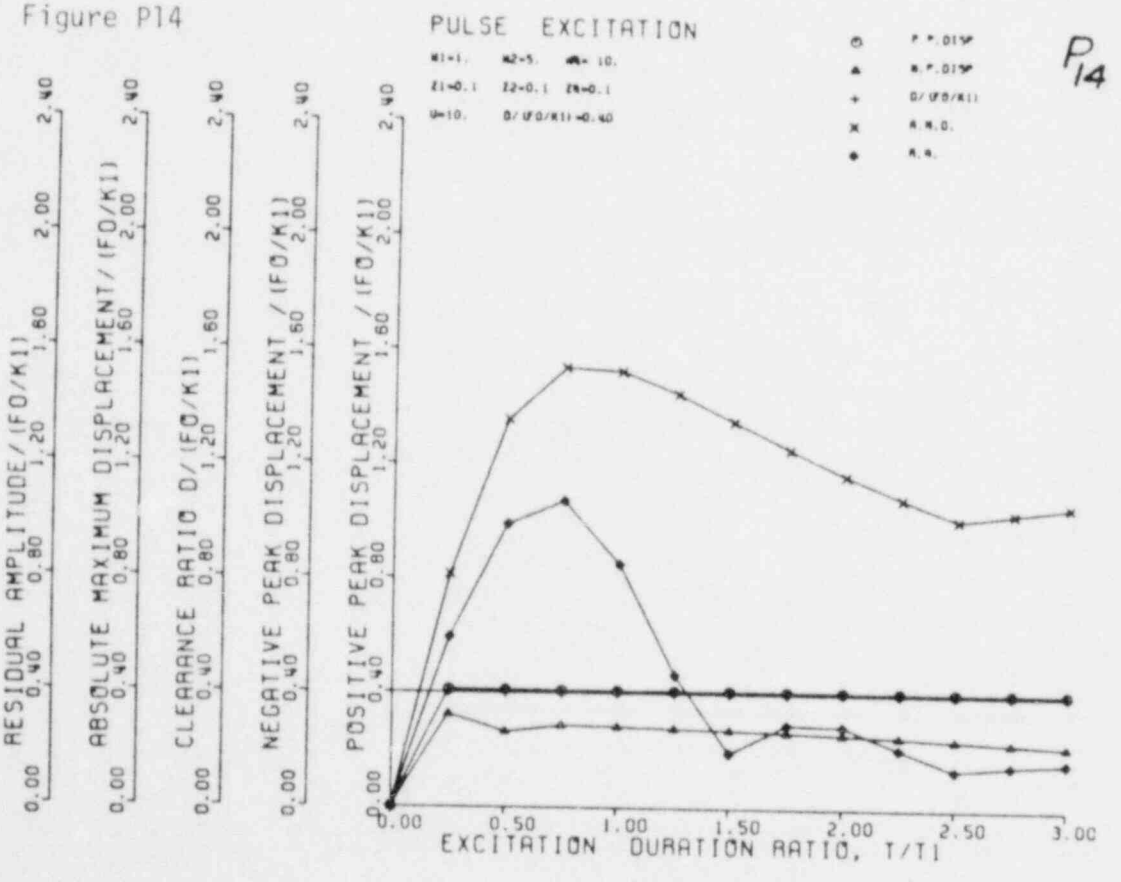

P14

Figure P15

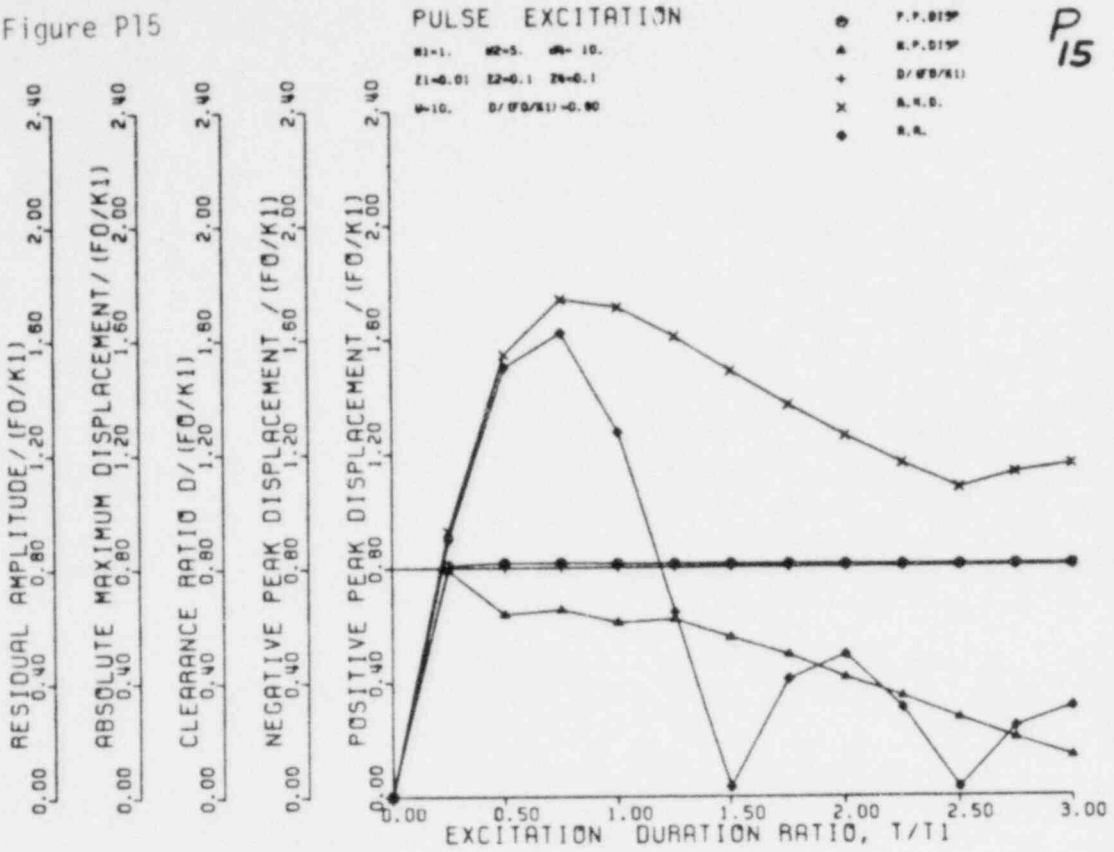

P15

Figure P16

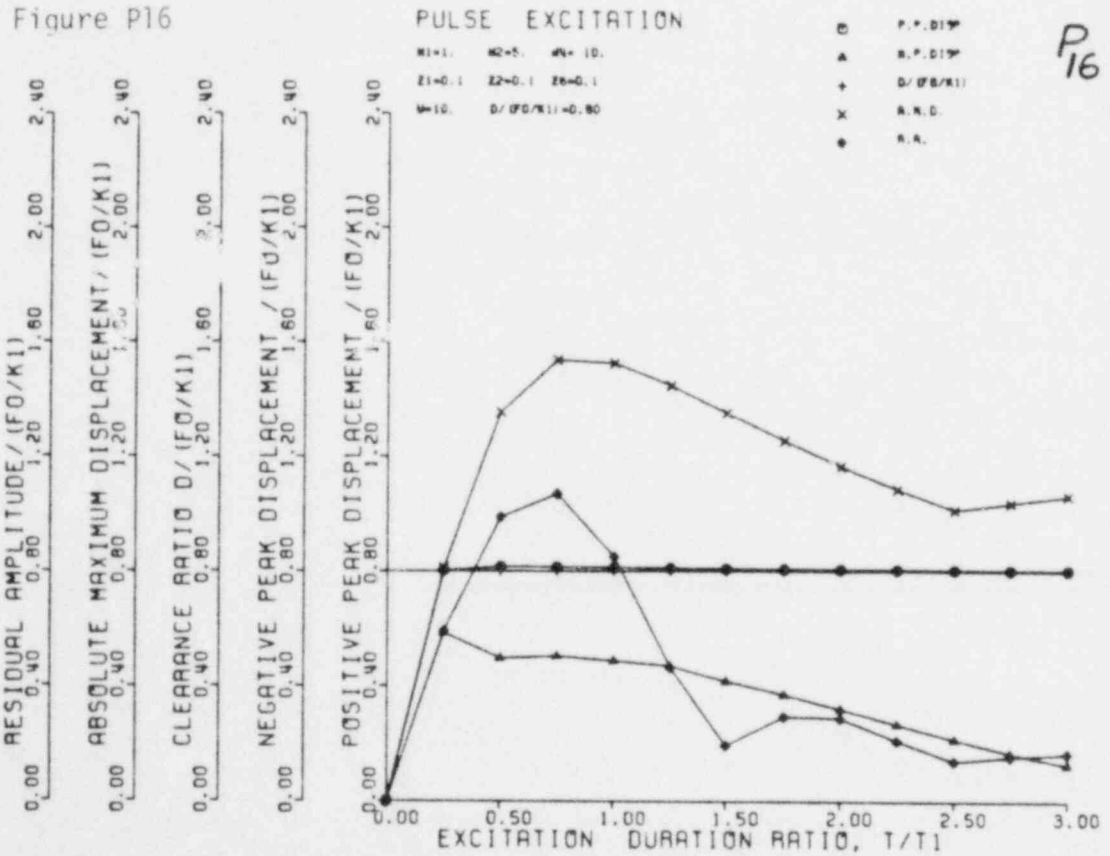

P16

Figure P17

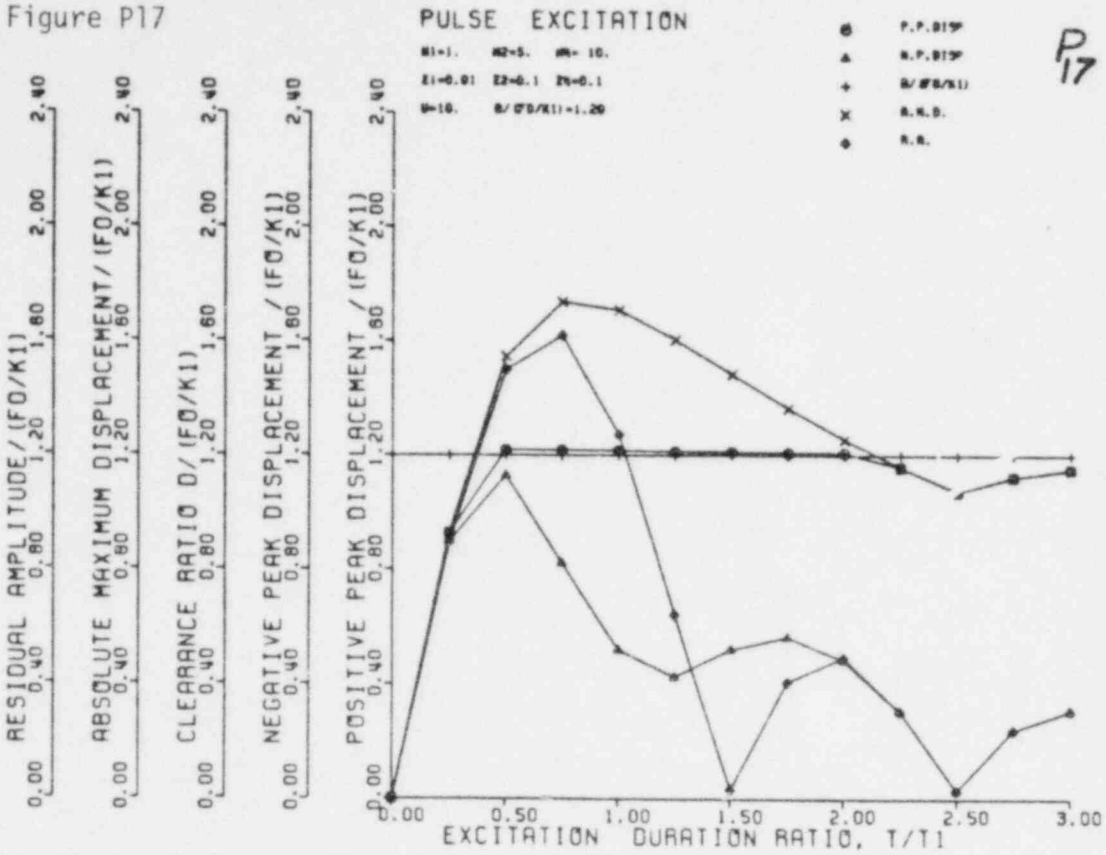

P17

Figure P18

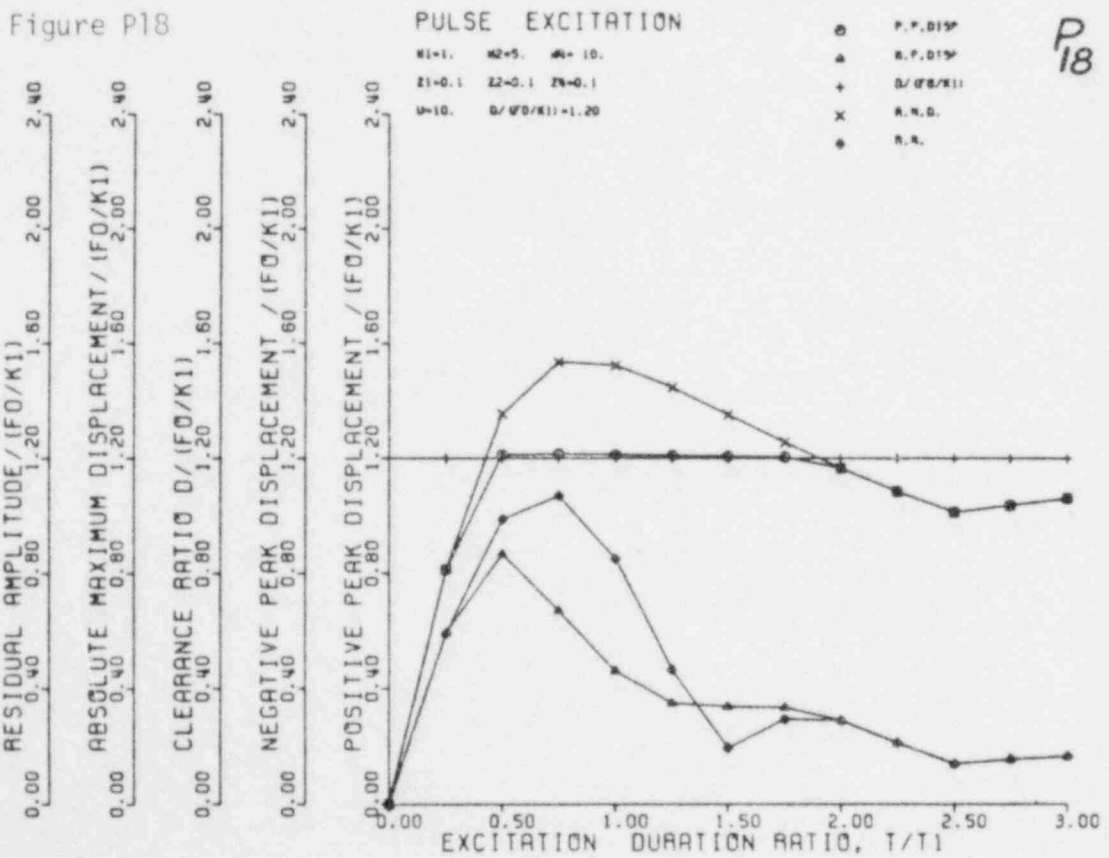

P18

Figure P19

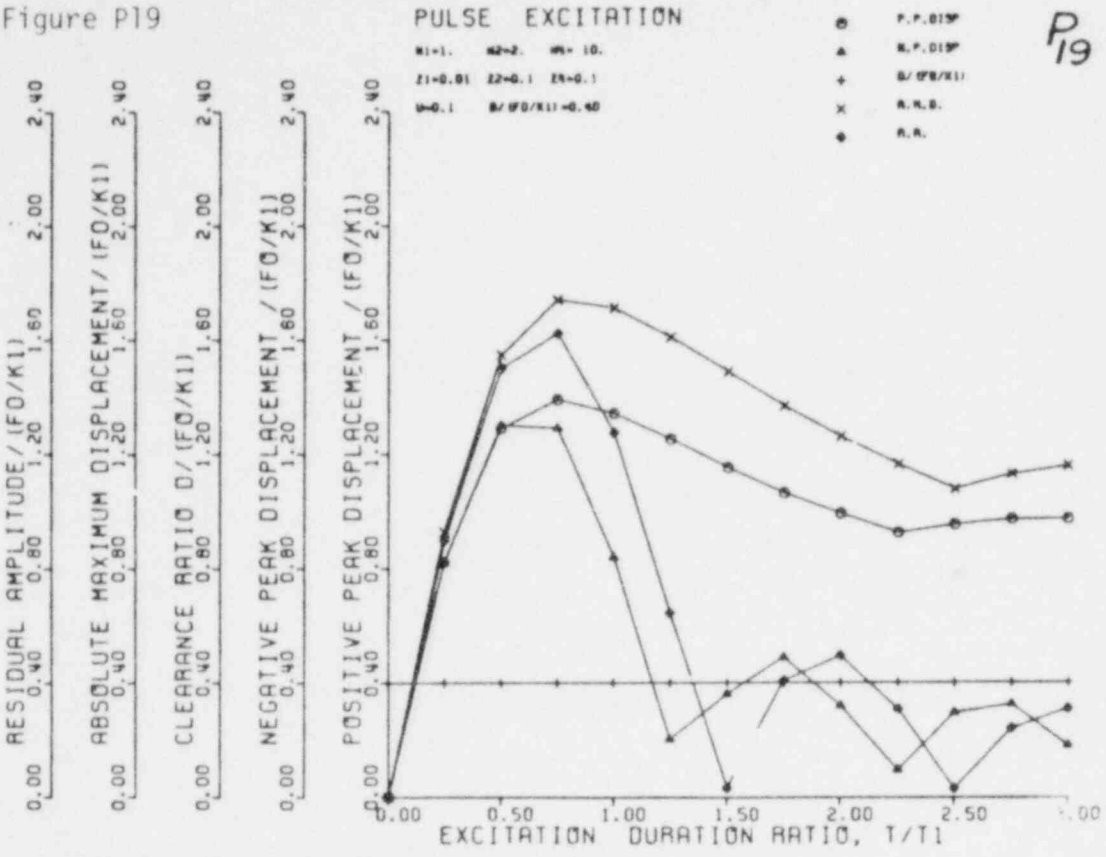

P19

Figure P20

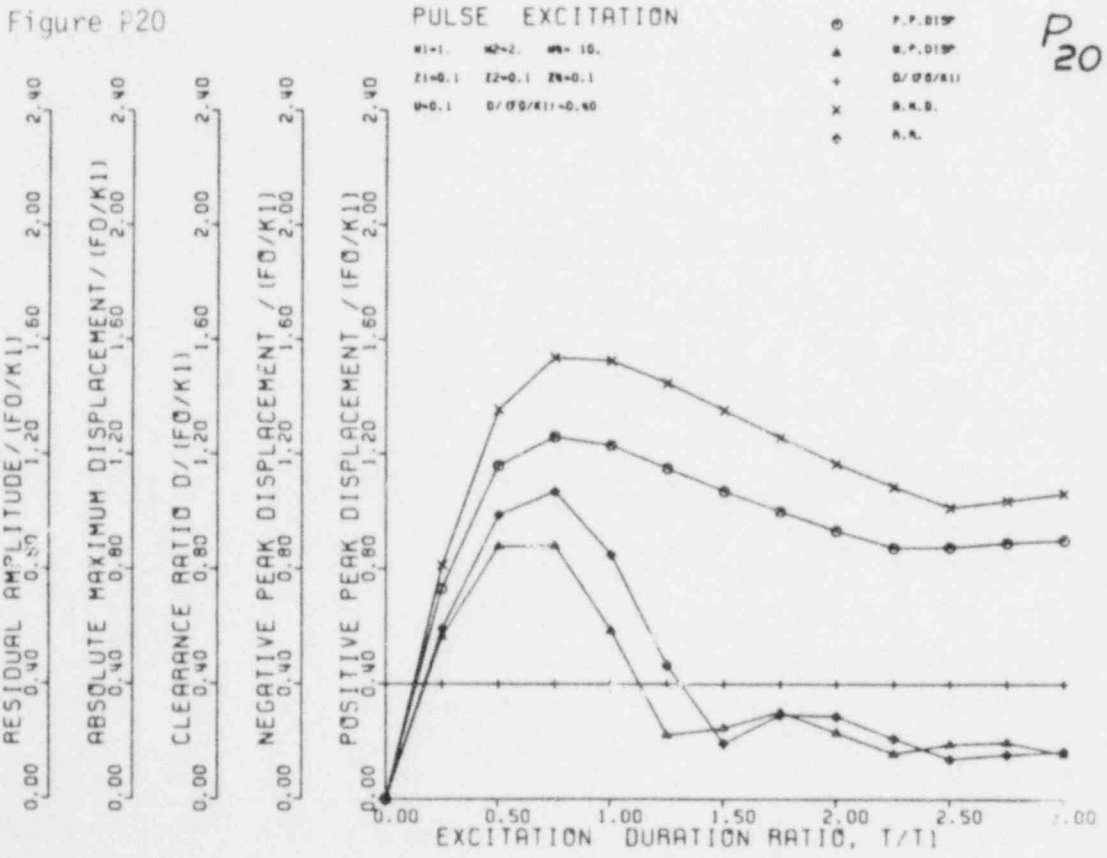

P20

Figure P21

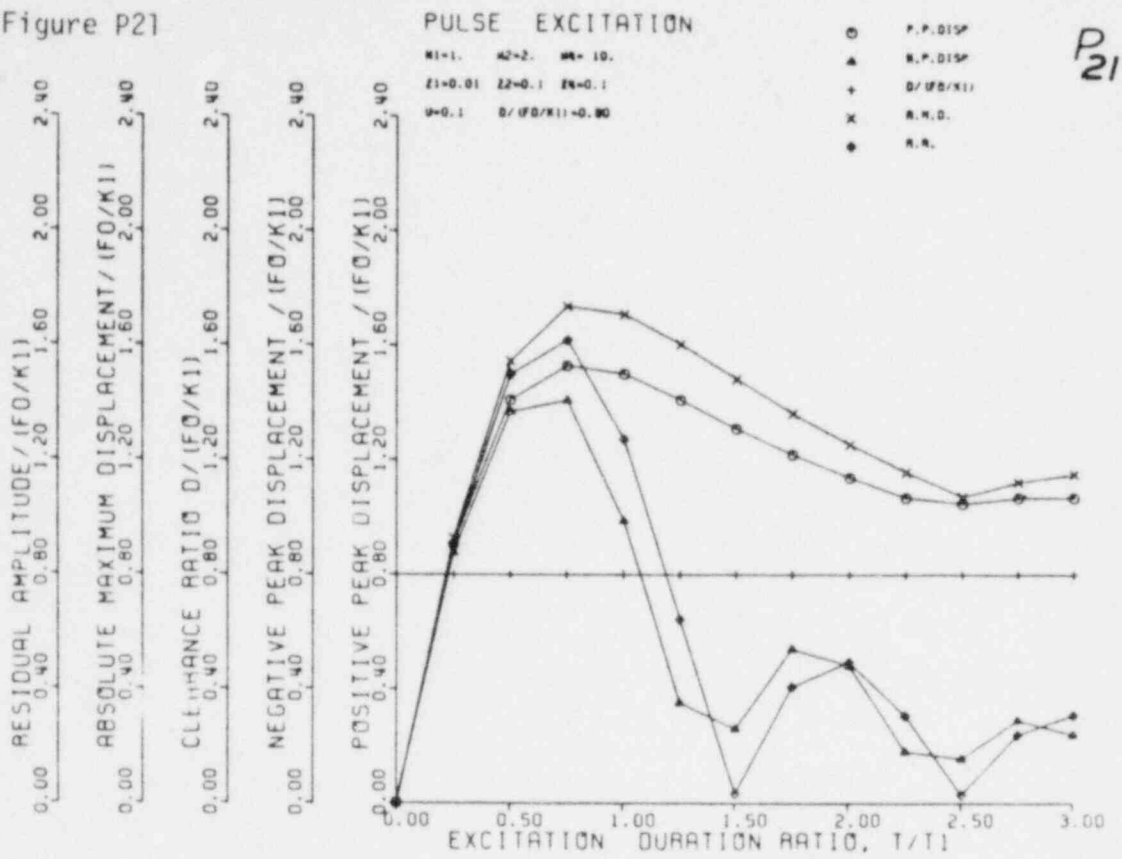

P21

Figure P22

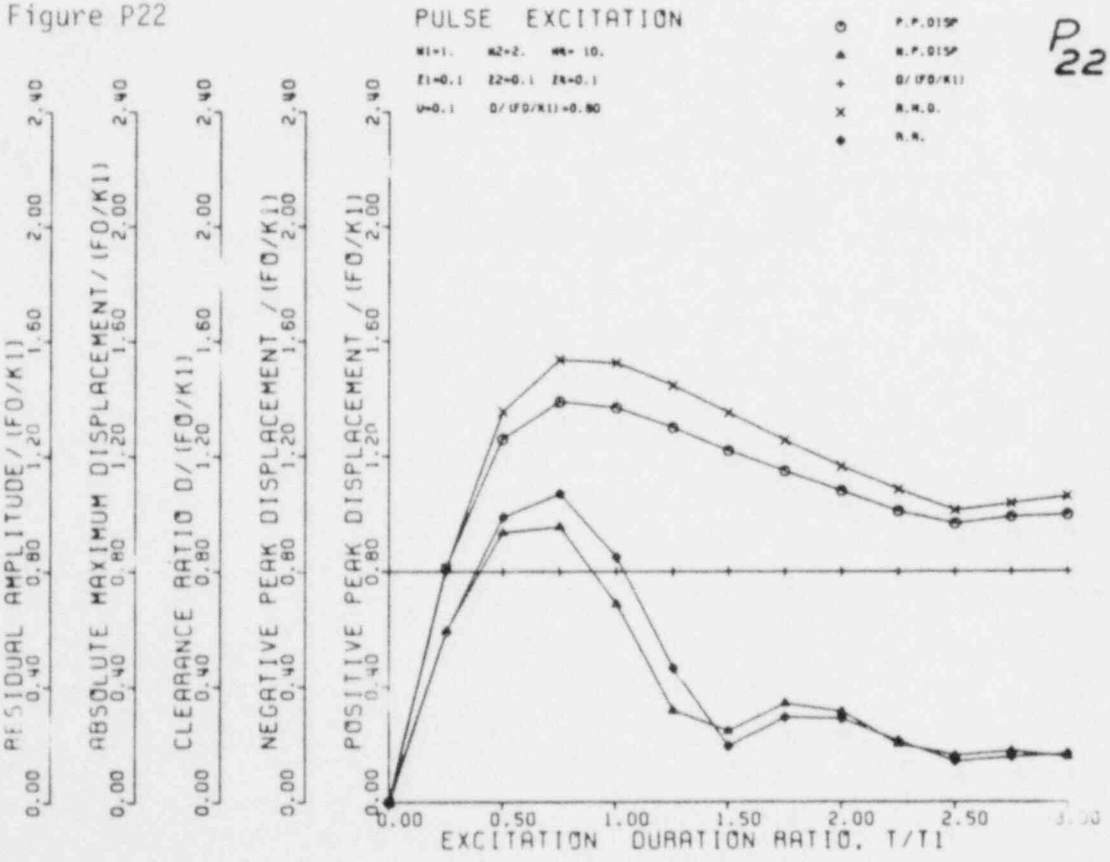

P22

Figure P23

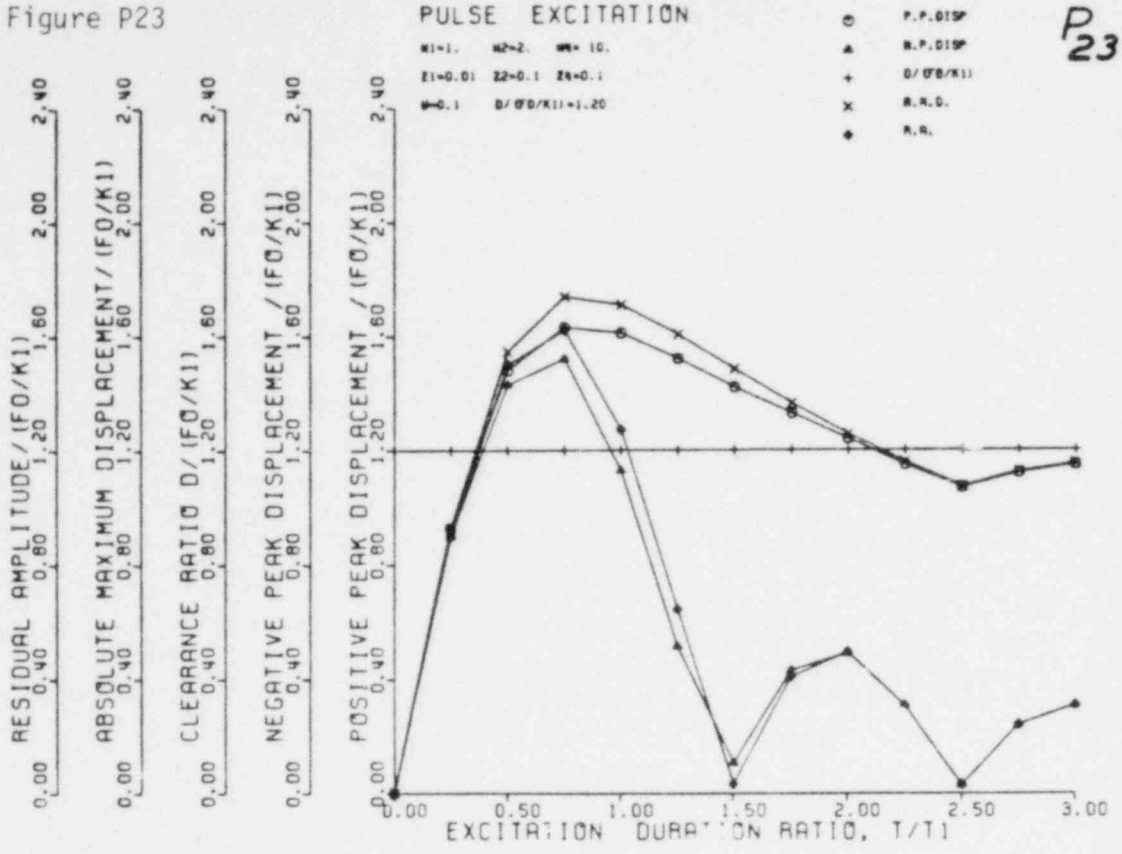

P23

Figure P24

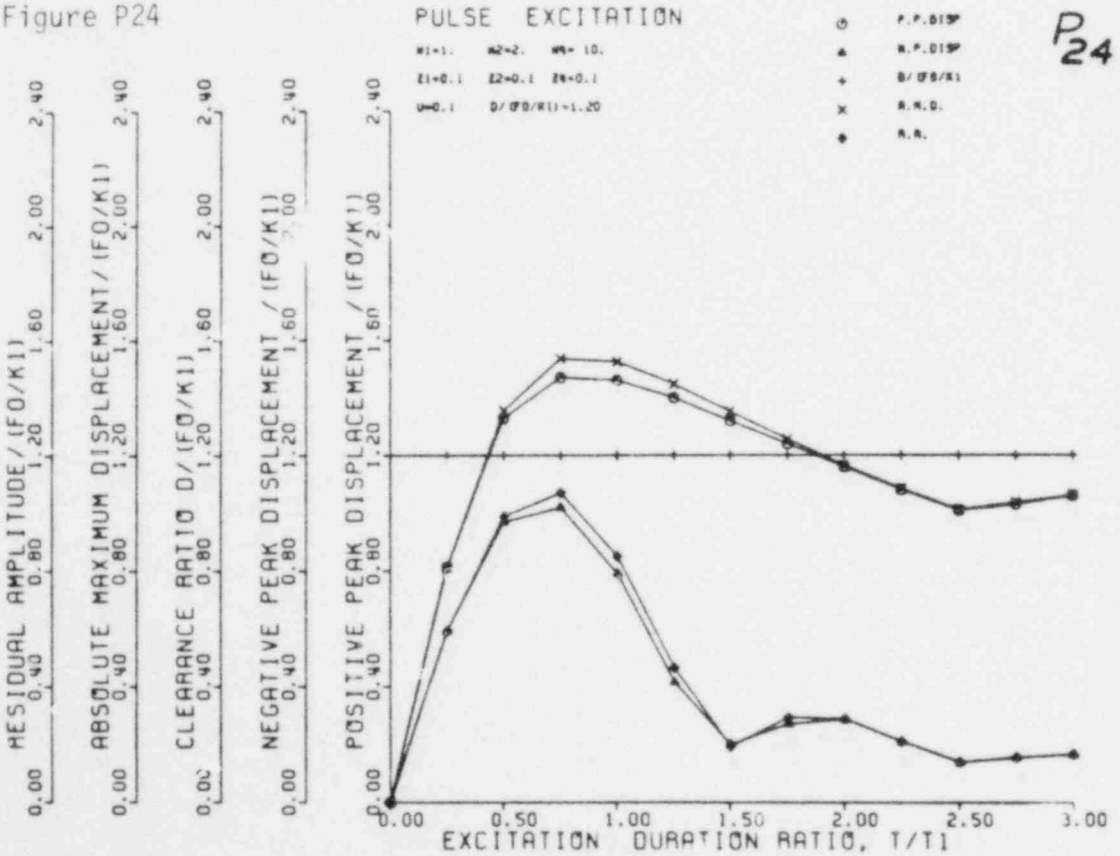

P24

Figure P25

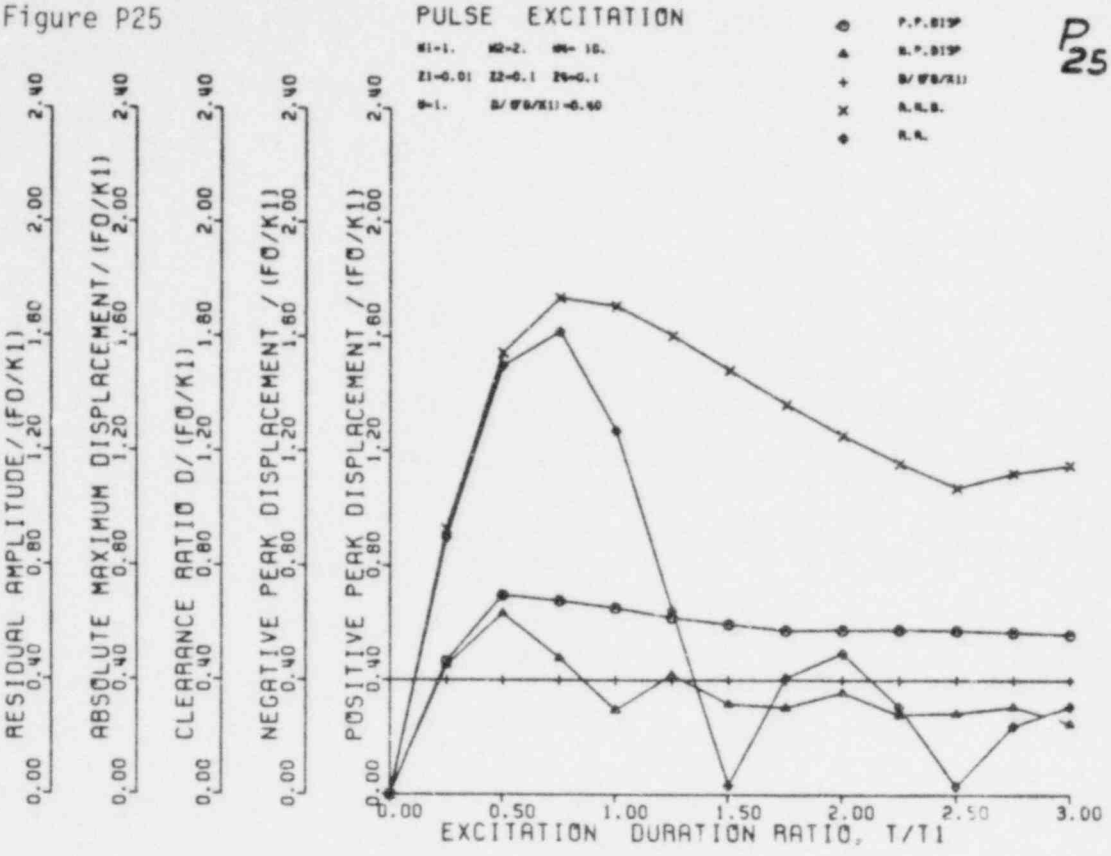

P25

Figure P26

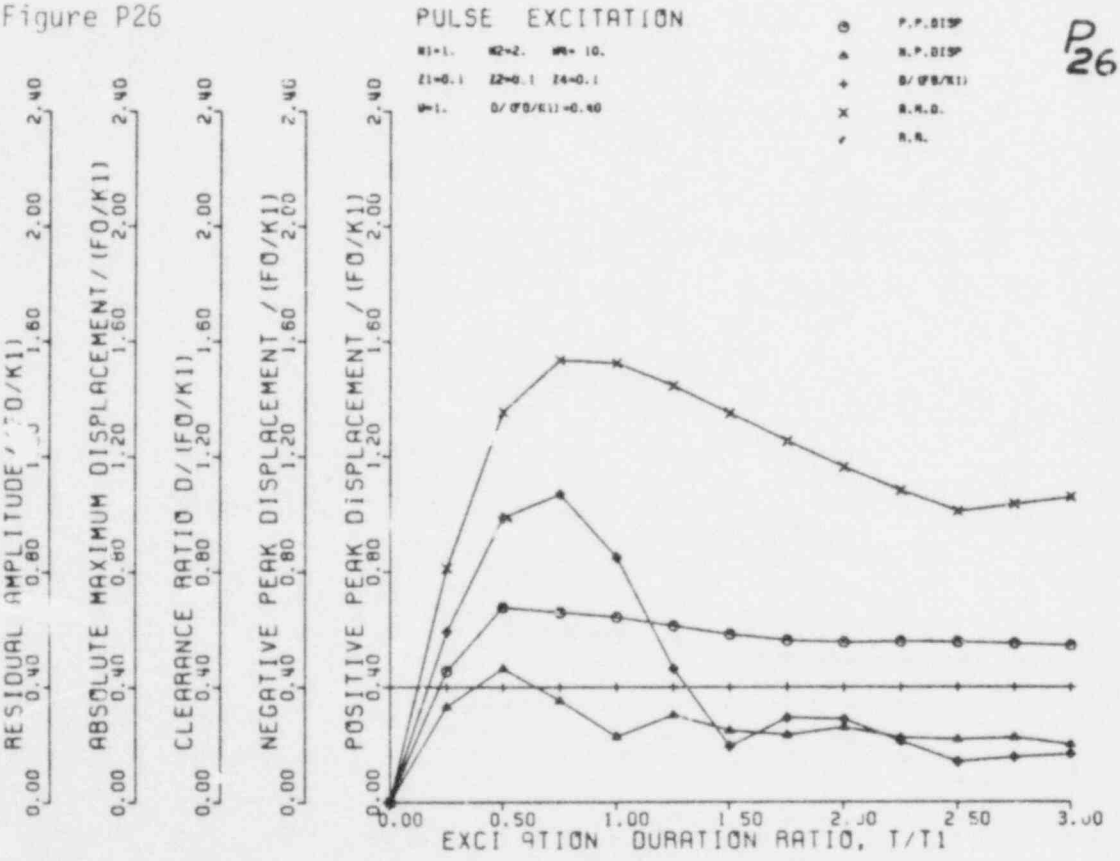

P26

Figure P27

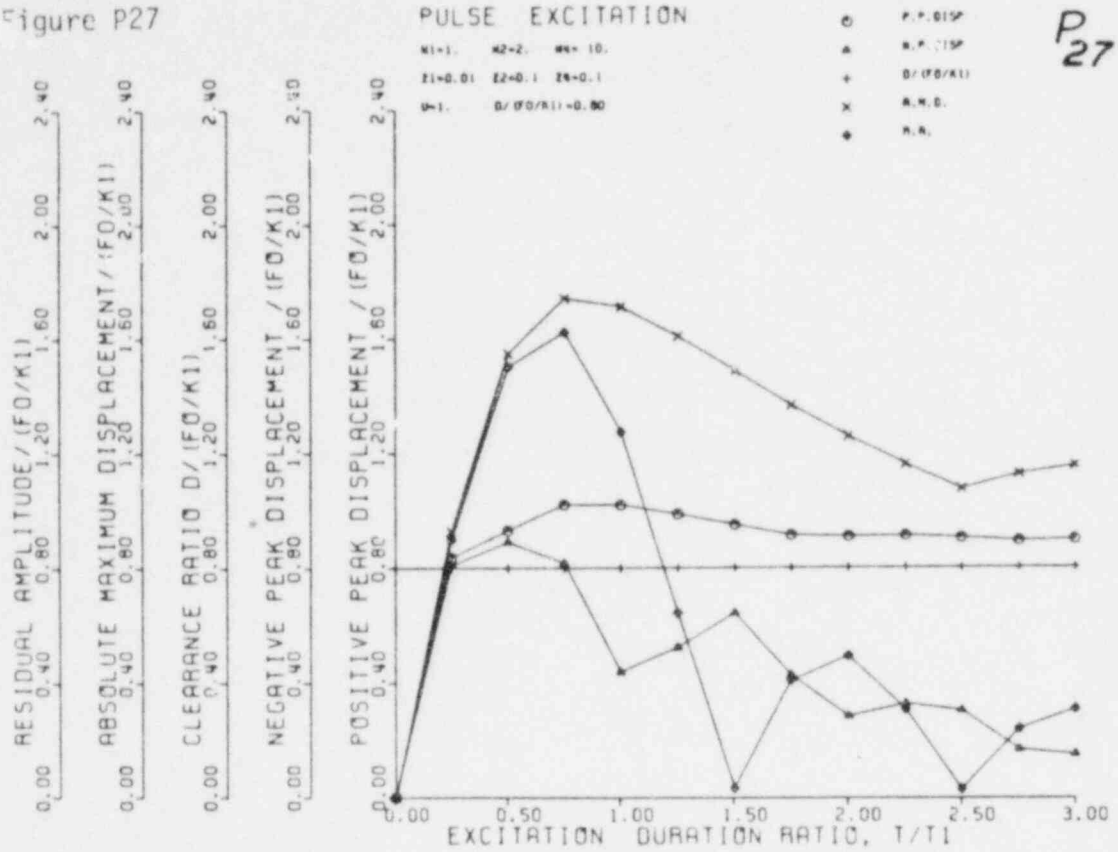

P27

Figure P28

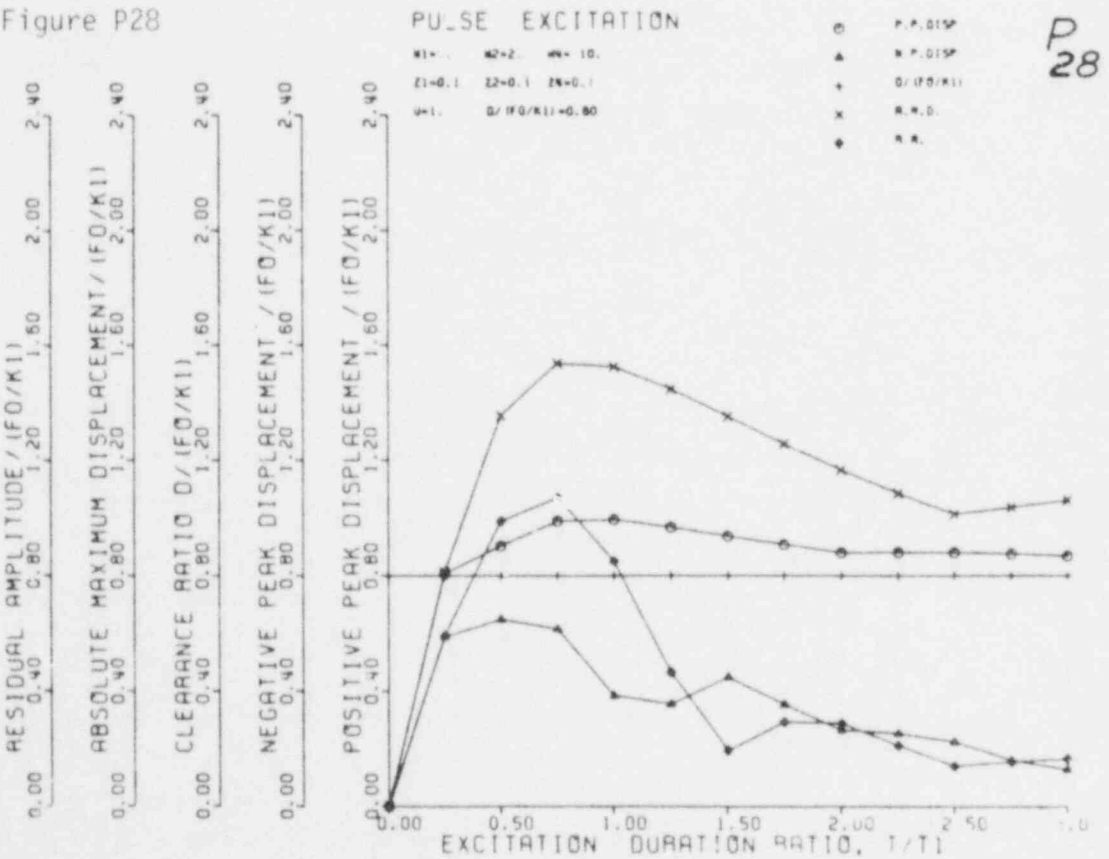

P28

Figure P29

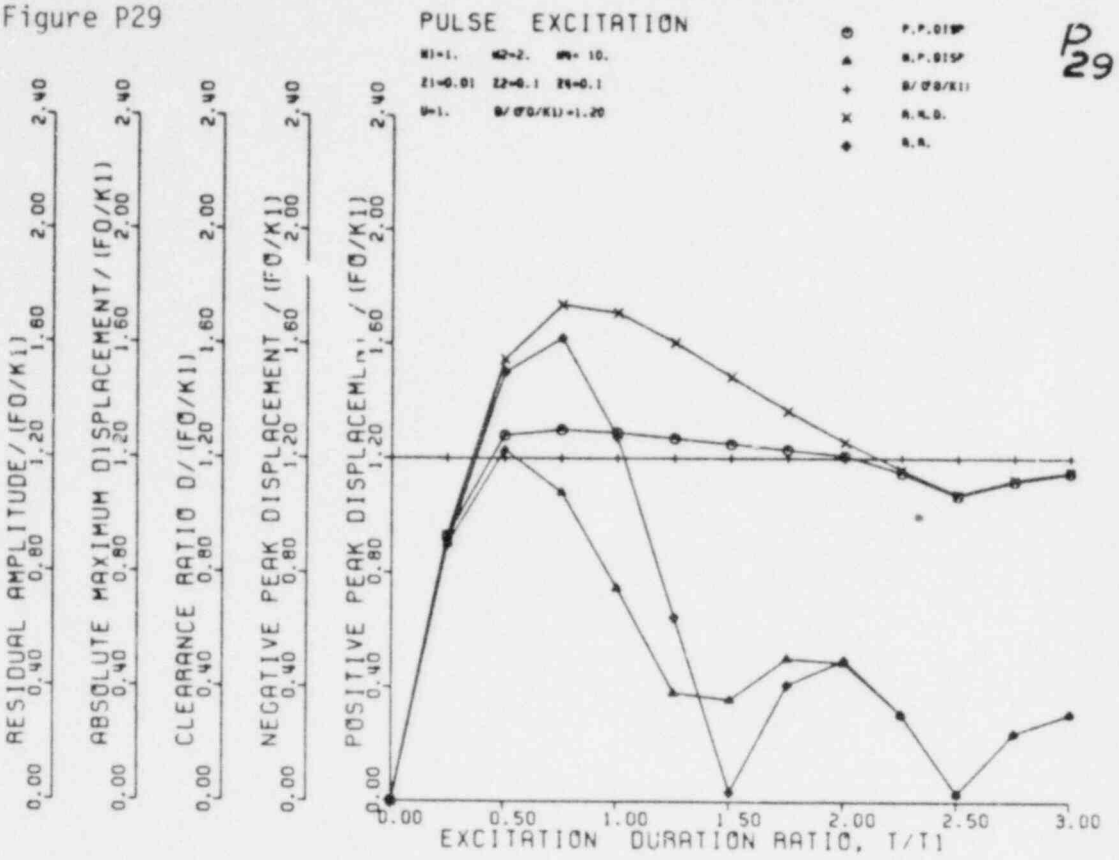

P29

Figure P30

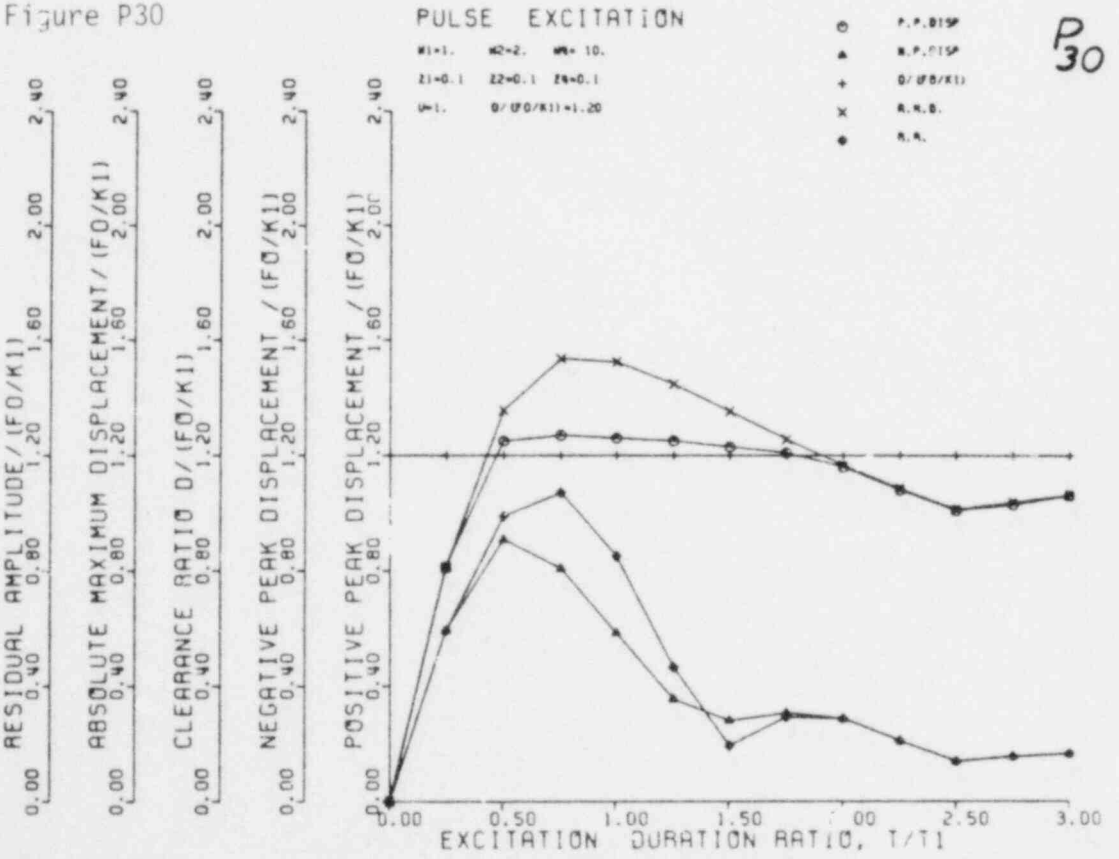

P30

Figure P31

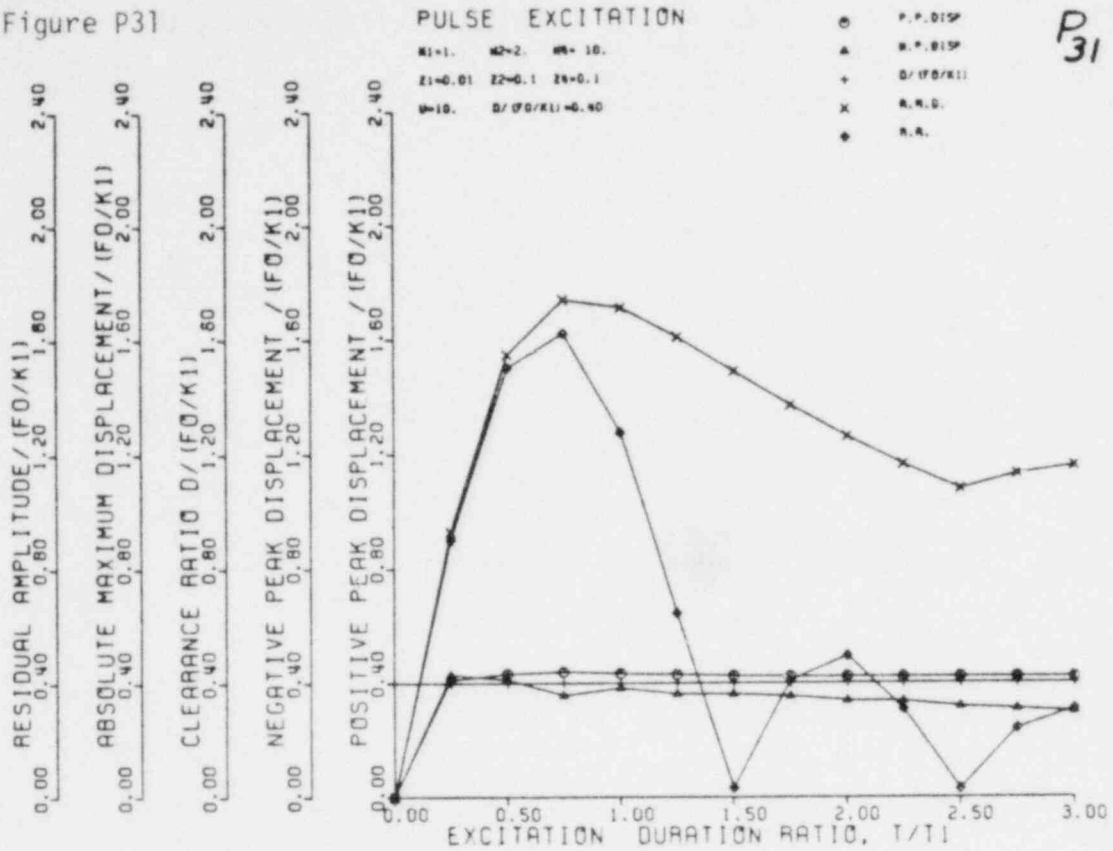

P31

Figure P32

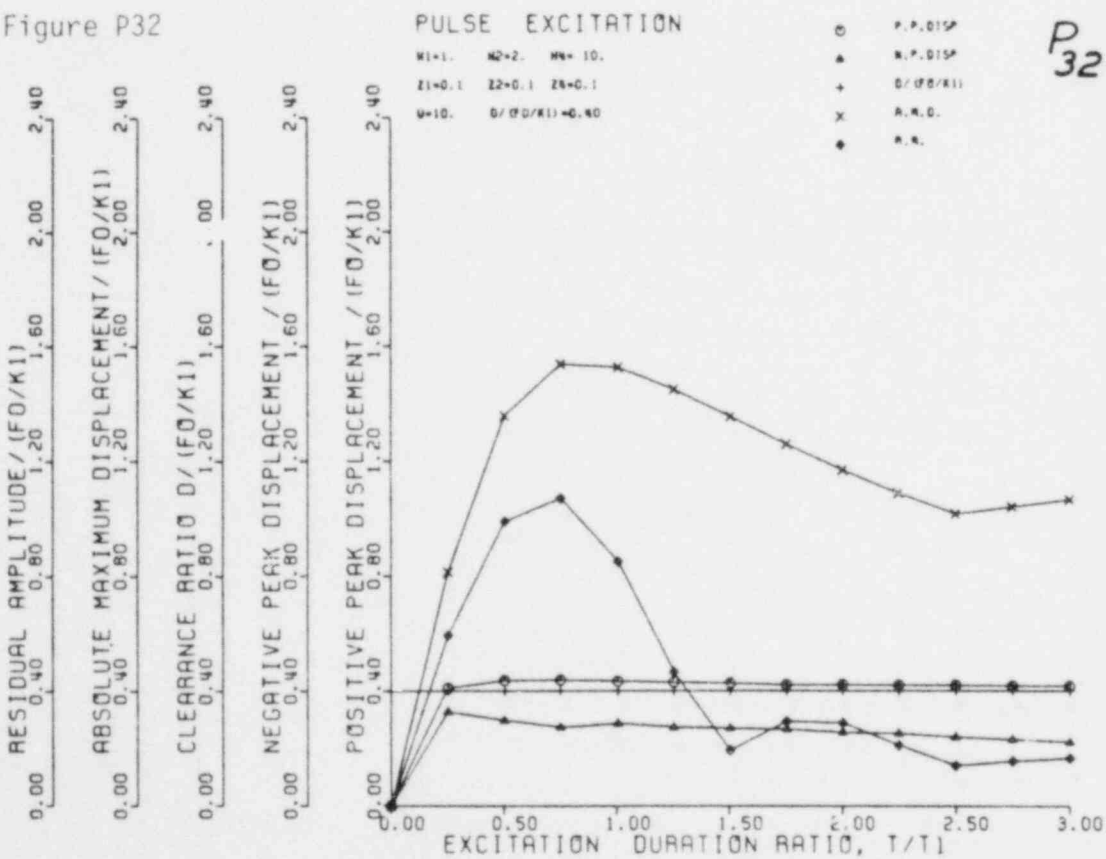

P32

Figure P33

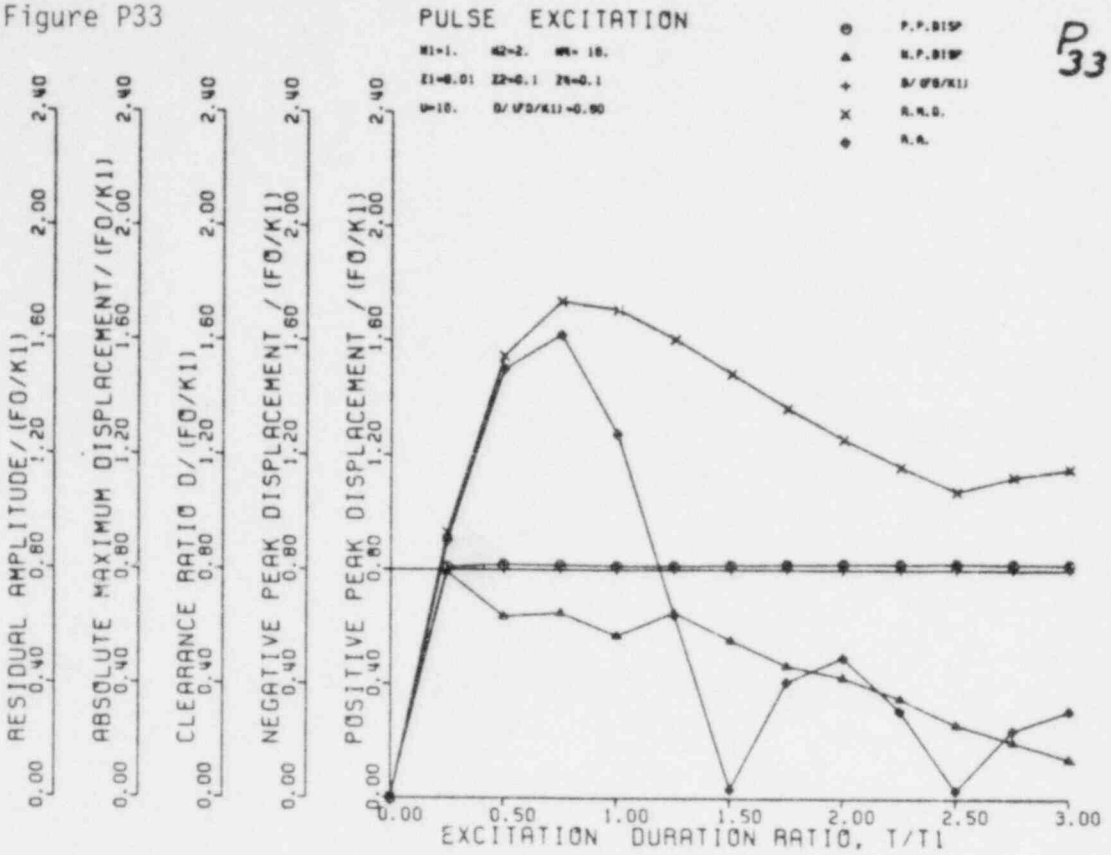

P33

Figure P34

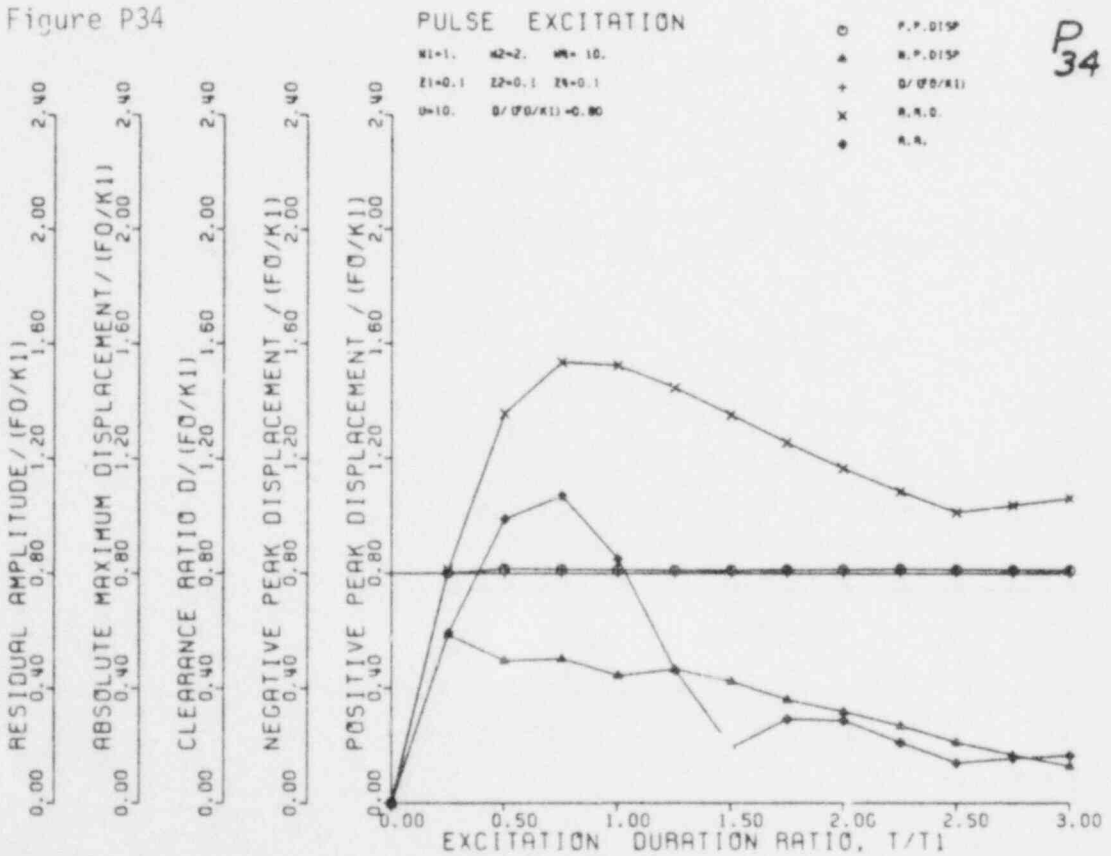

P34

Figure P35

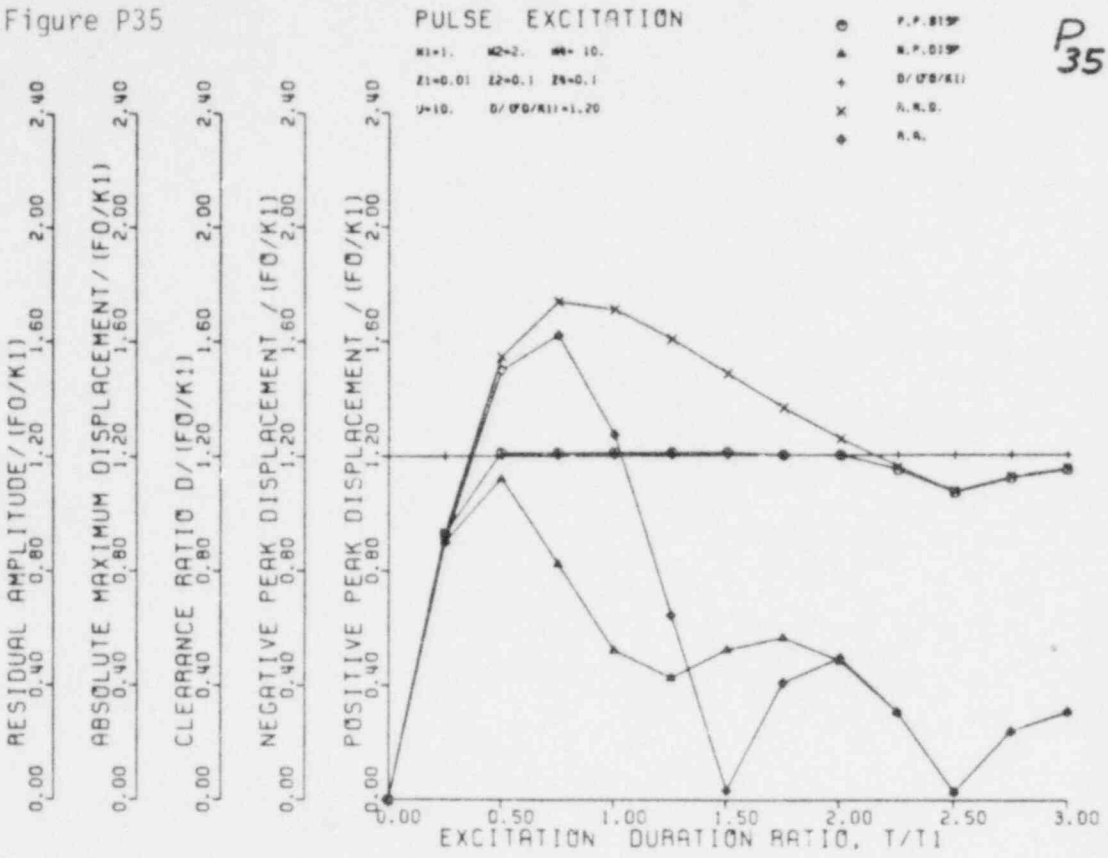

P35

Figure P36

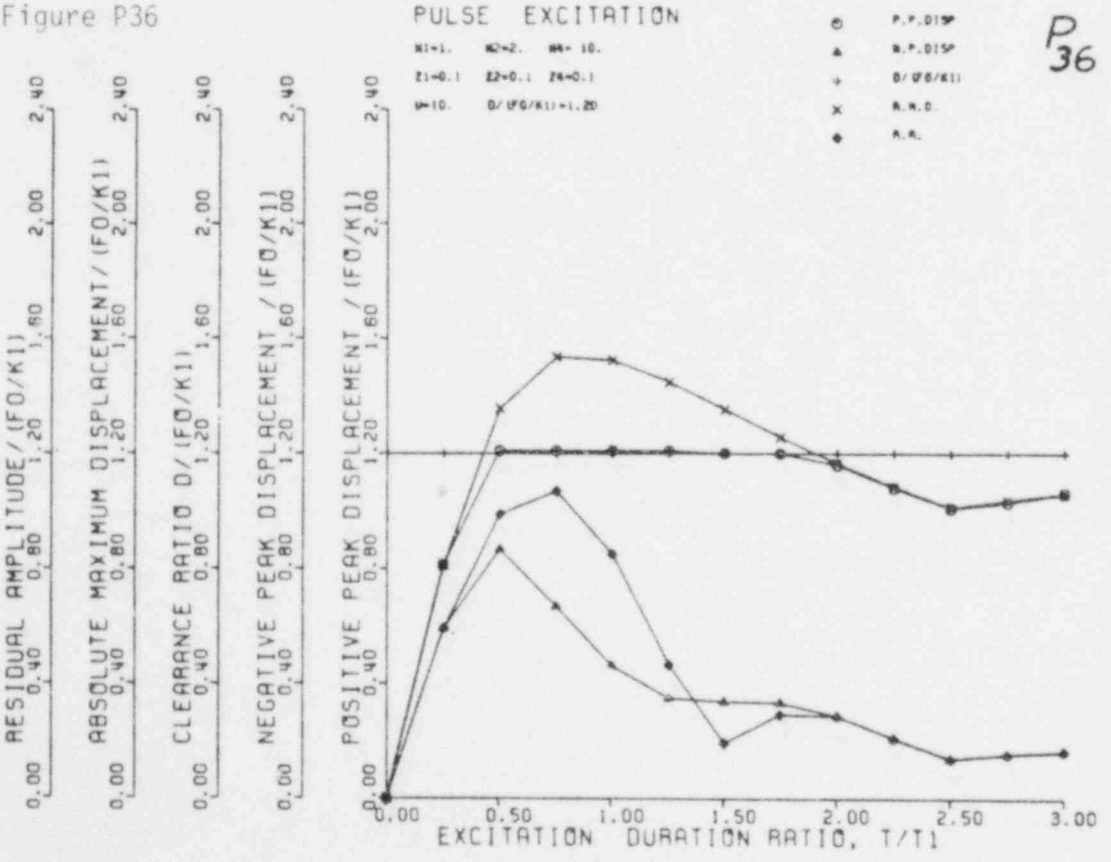

P36

Figure P37

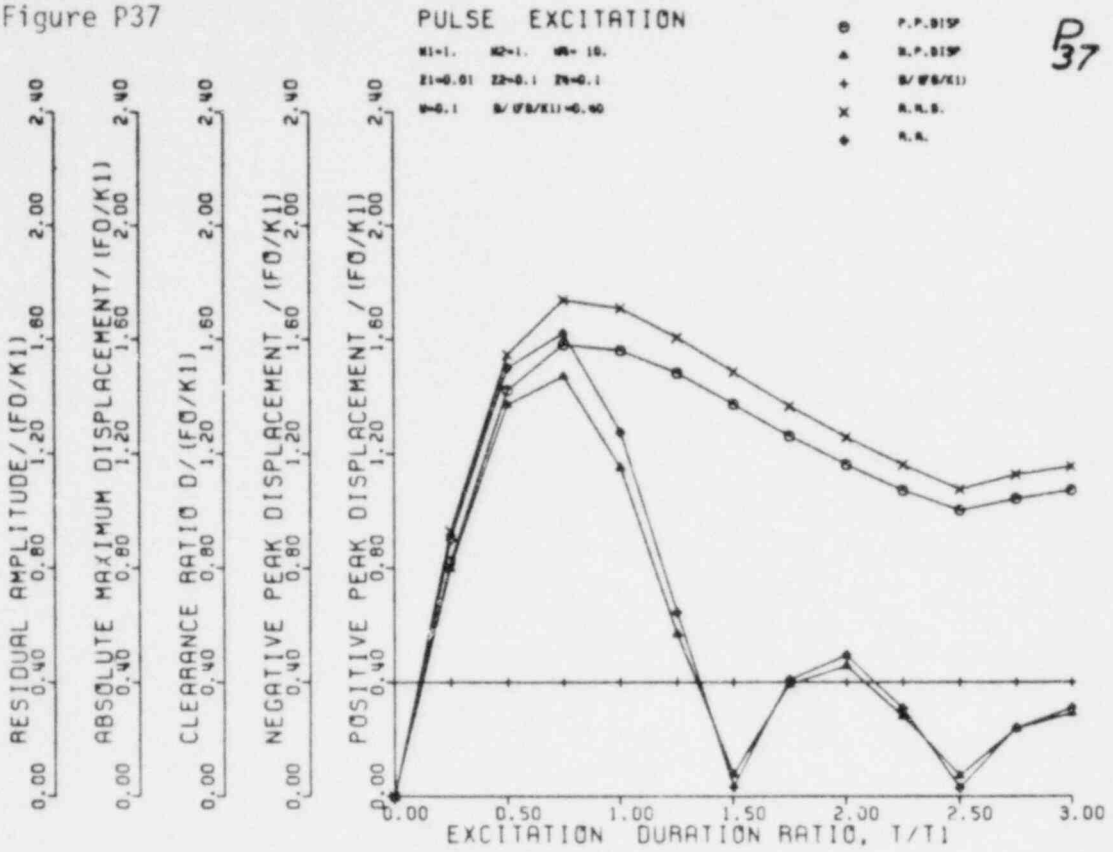

P37

Figure P38

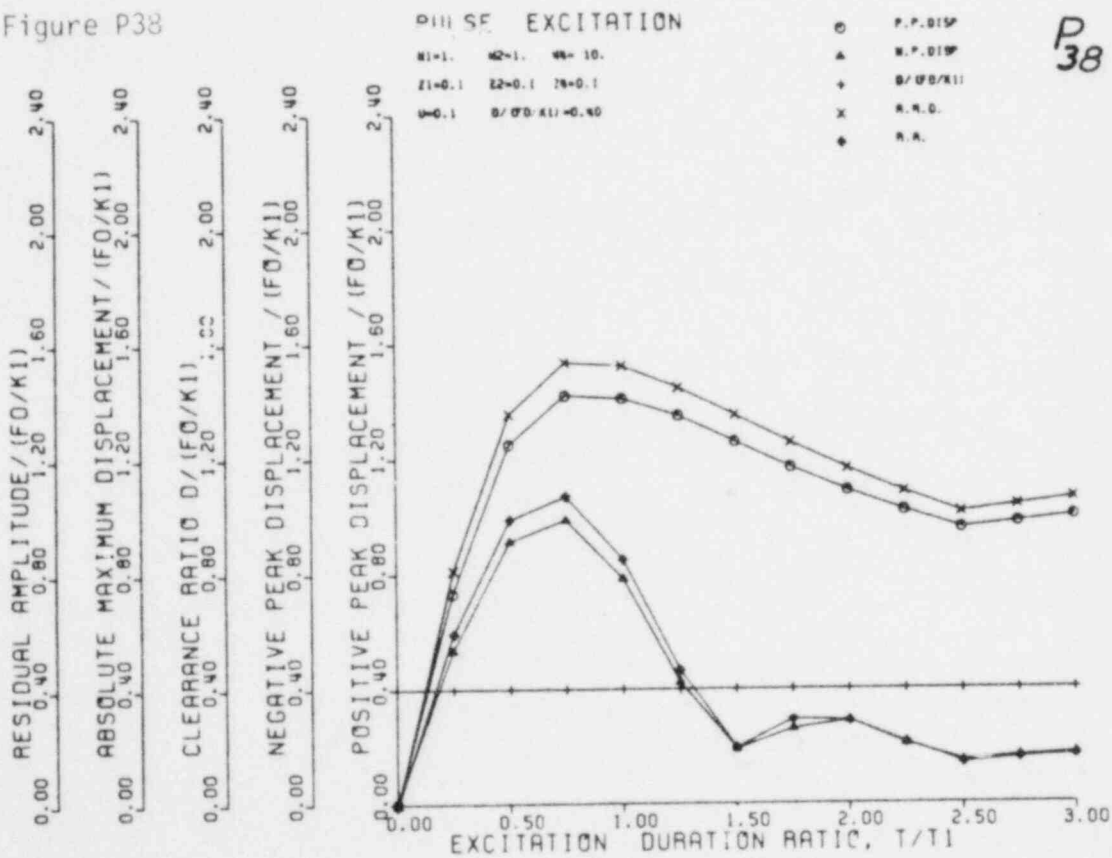

P38

Figure P39

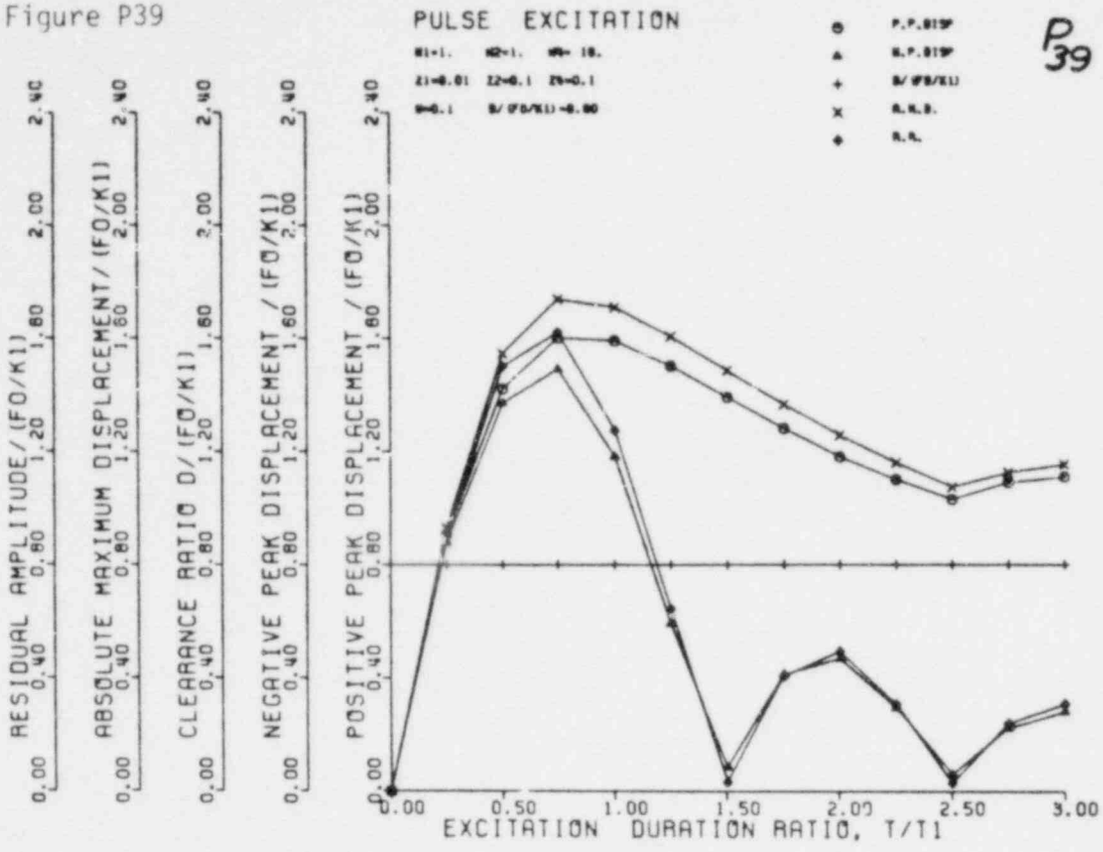

Figure P40

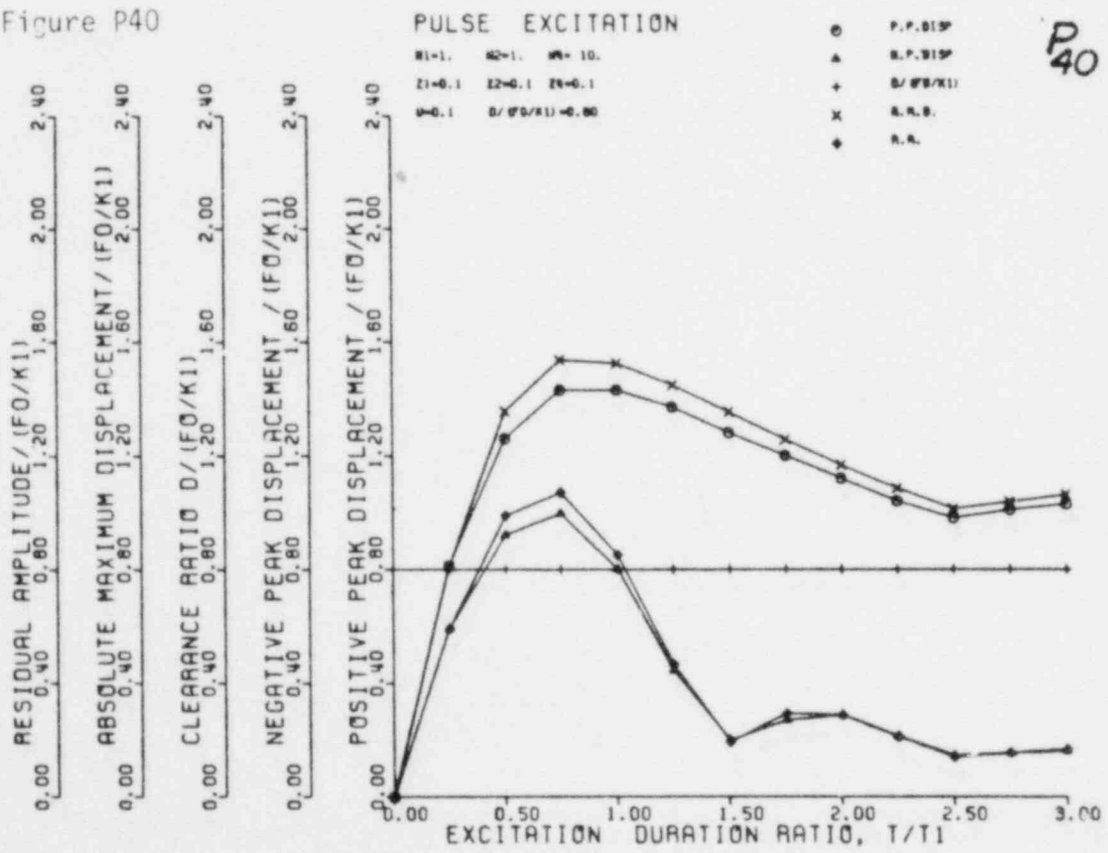

Figure P41

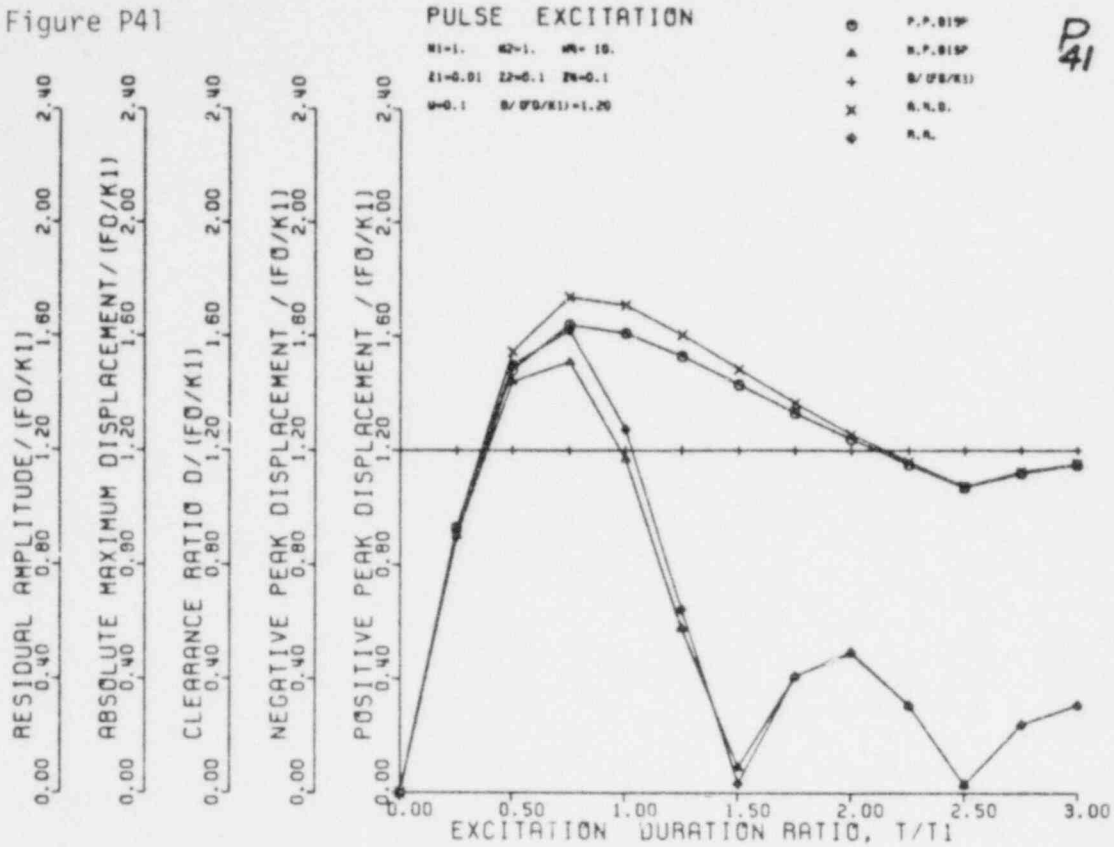

P41

Figure P42

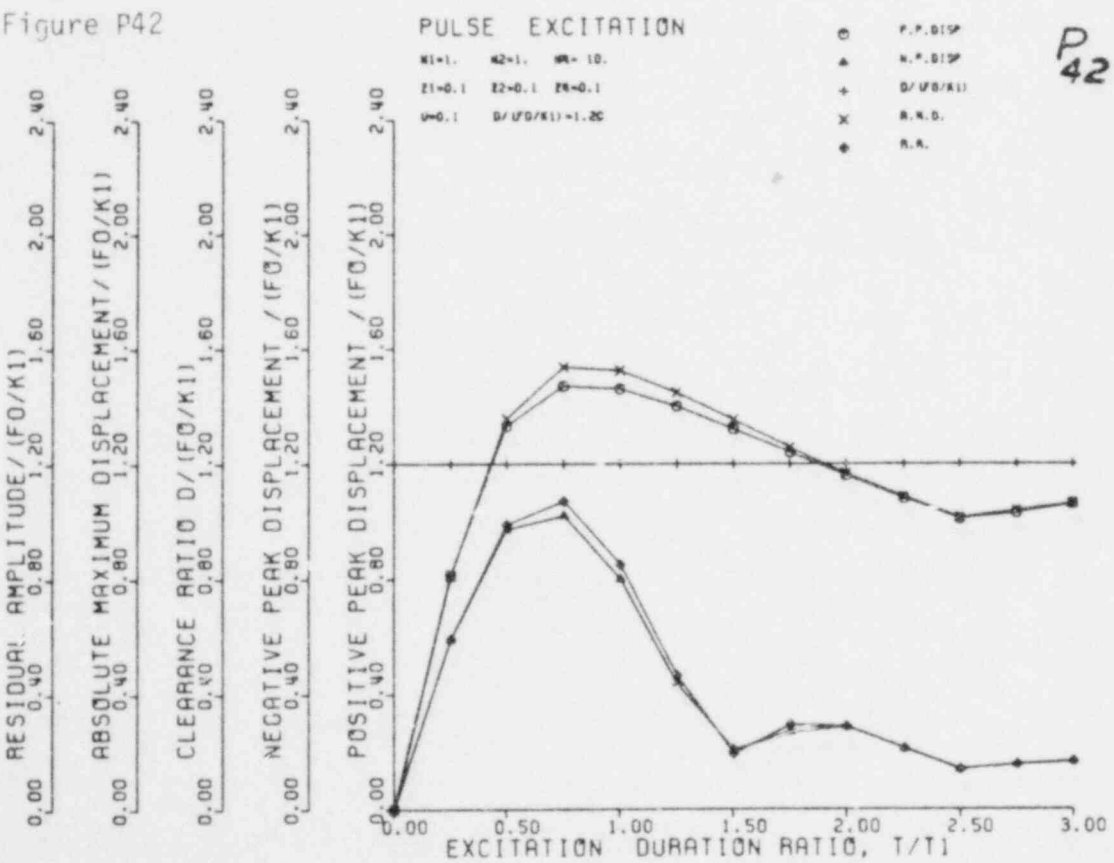

P42

Figure P43

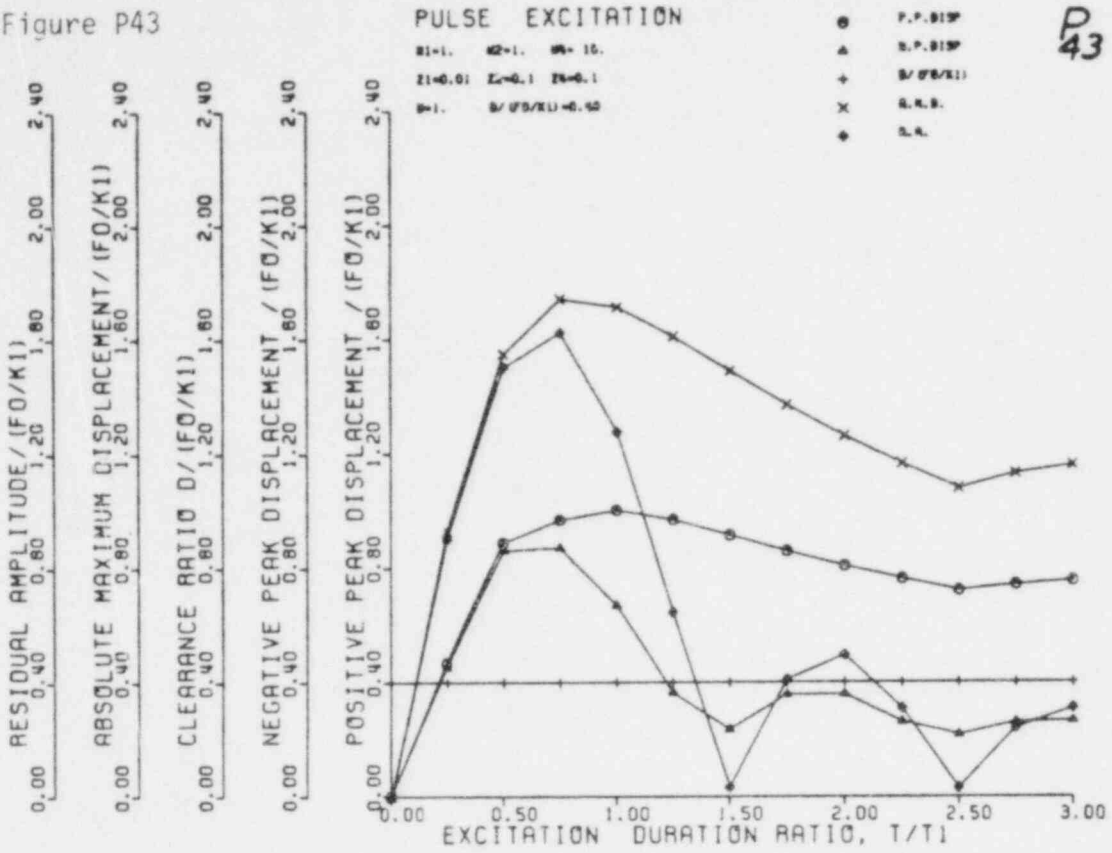

P43

Figure P44

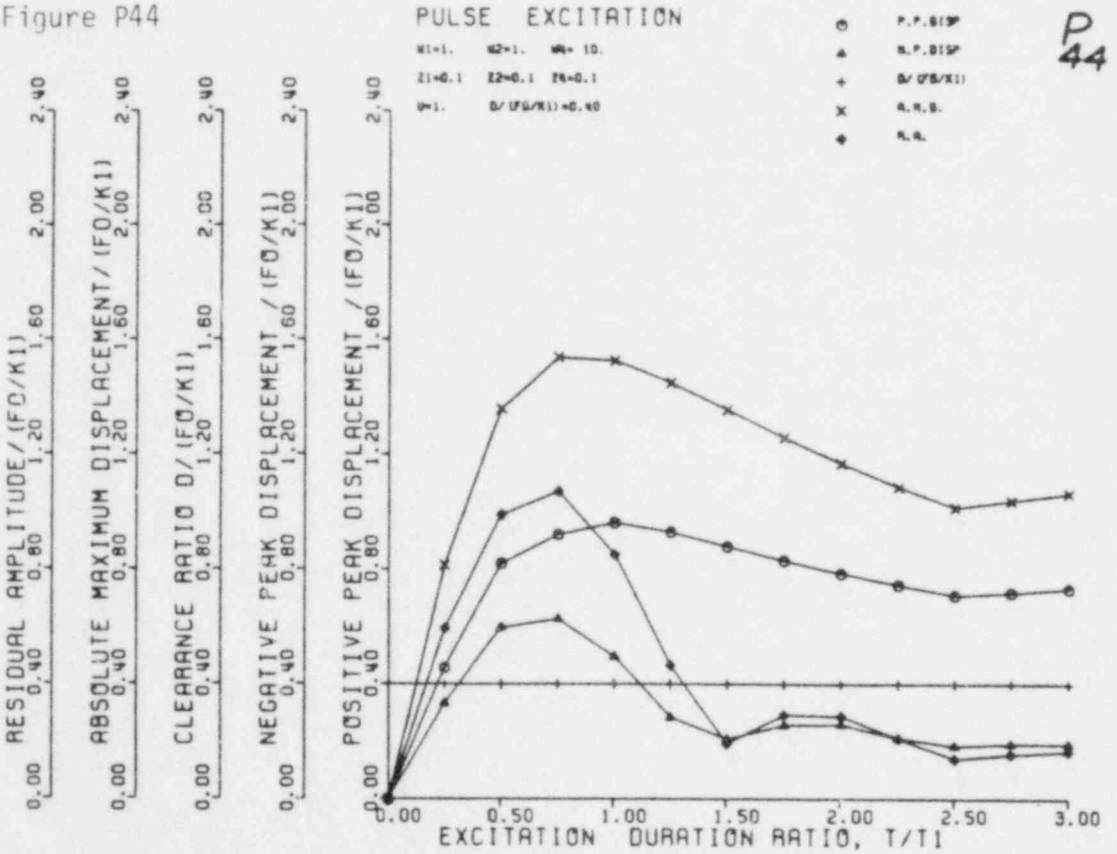

P44

Figure P45

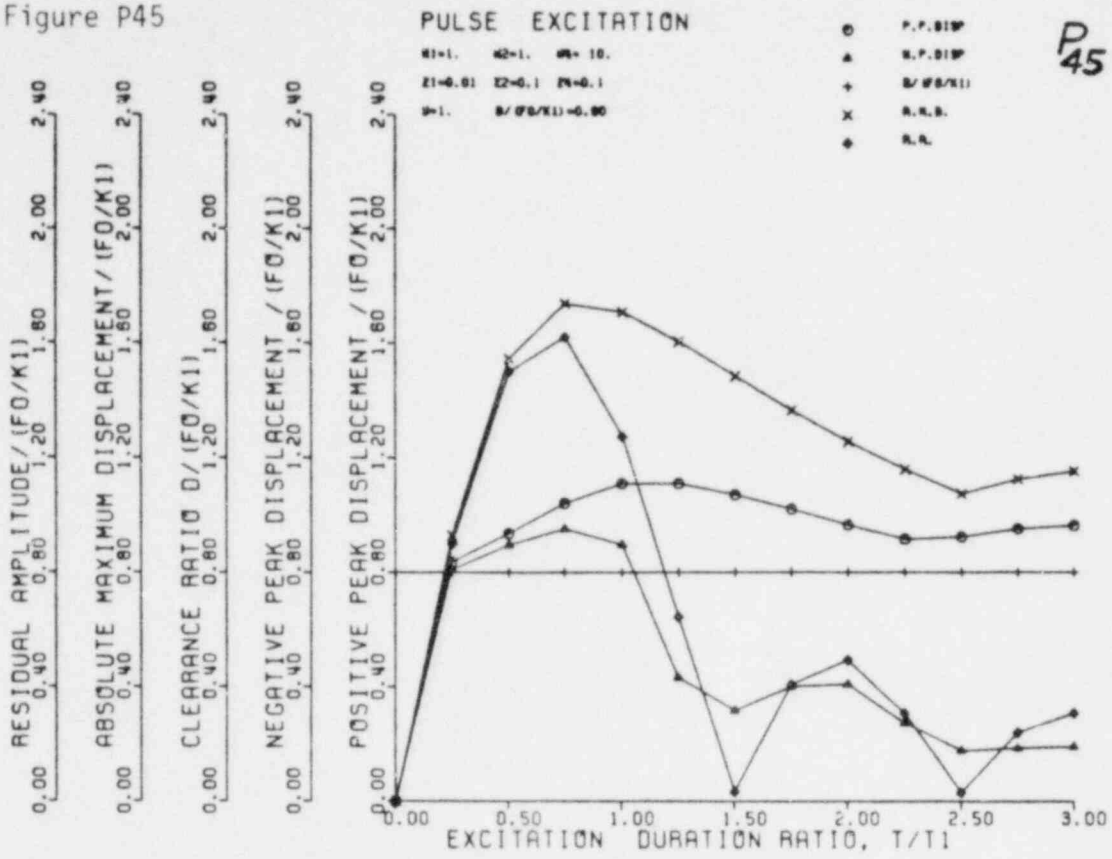

P45

Figure P46

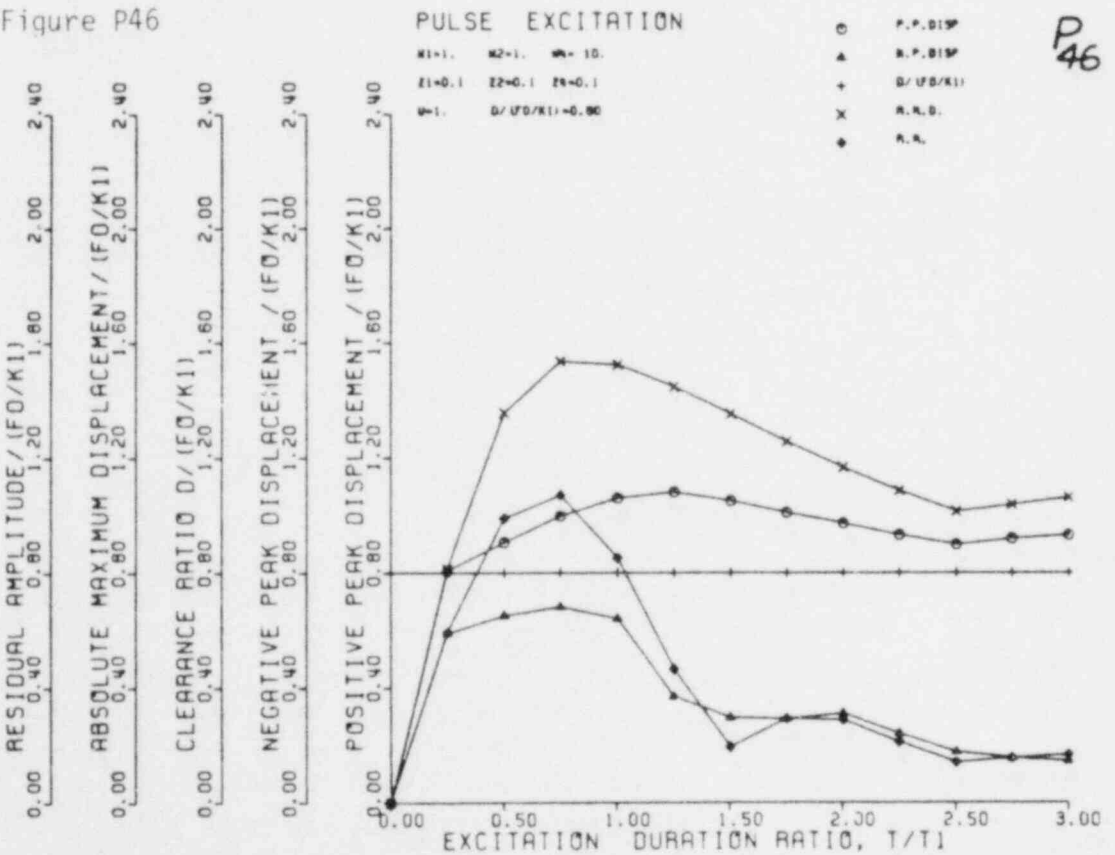

P46

Figure P47

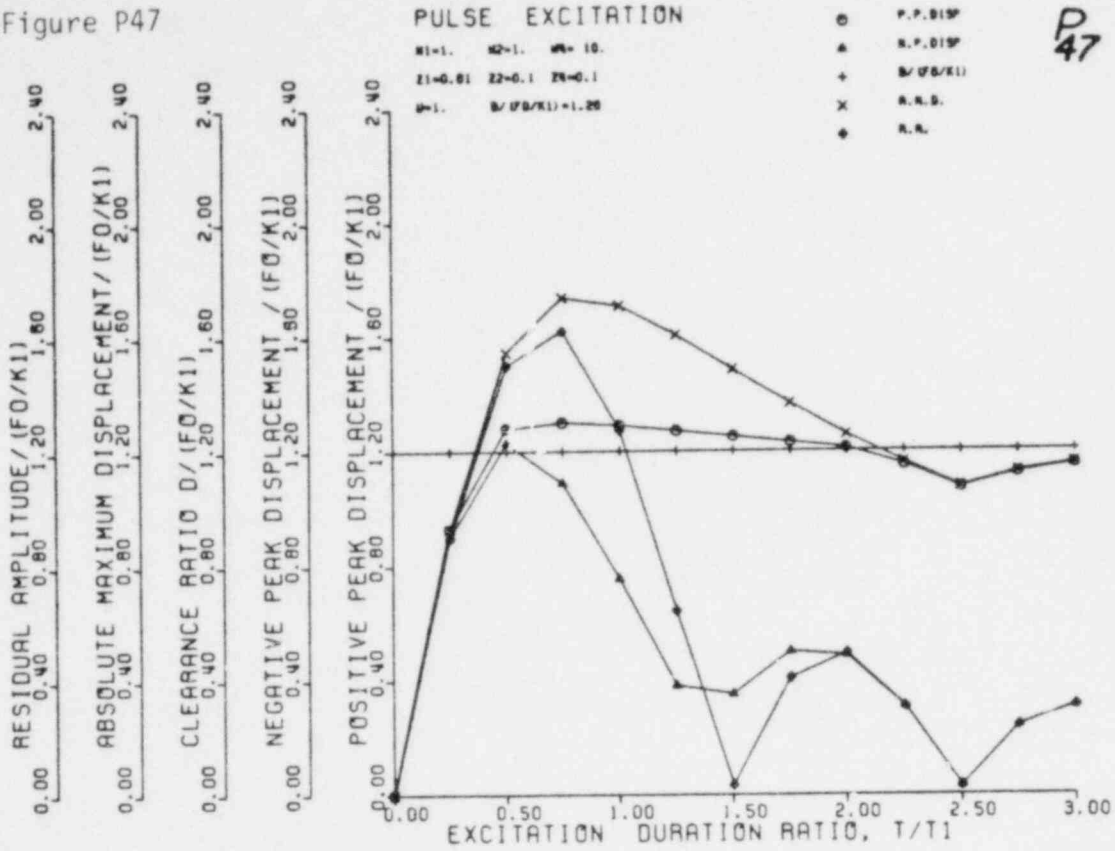

P47

Figure P48

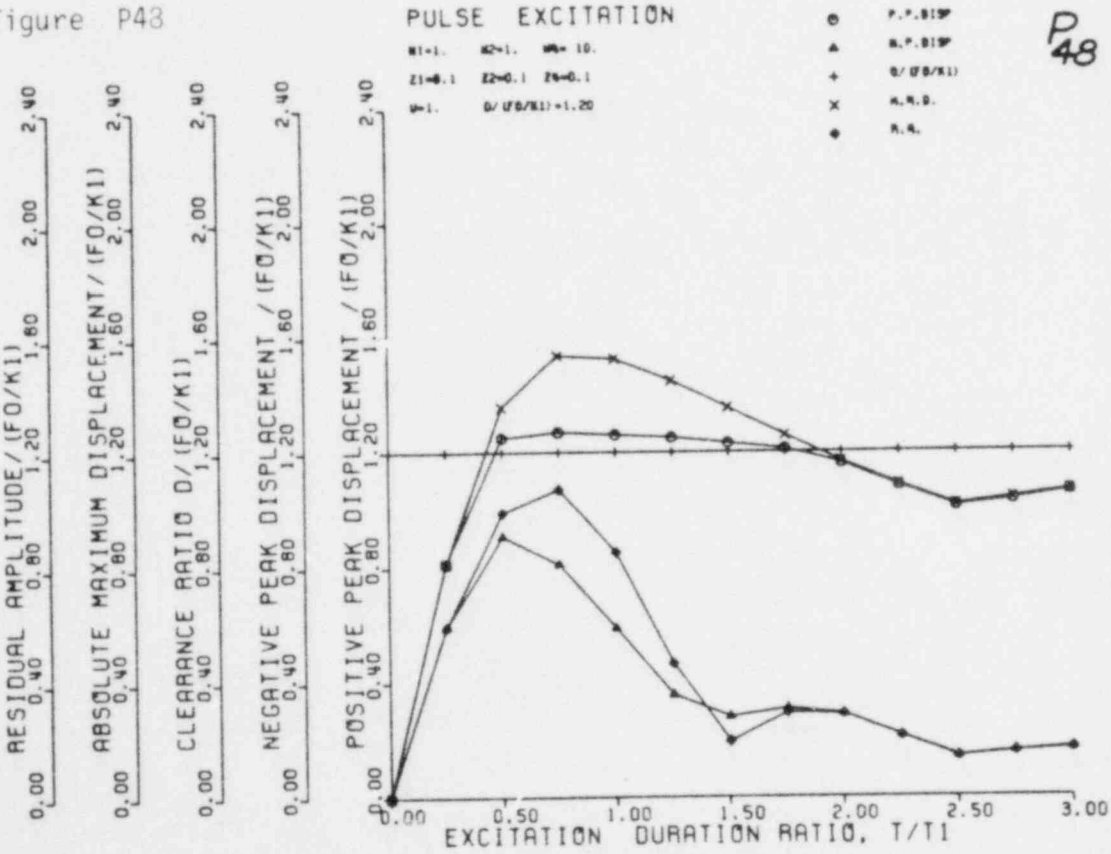

P48

Figure P49

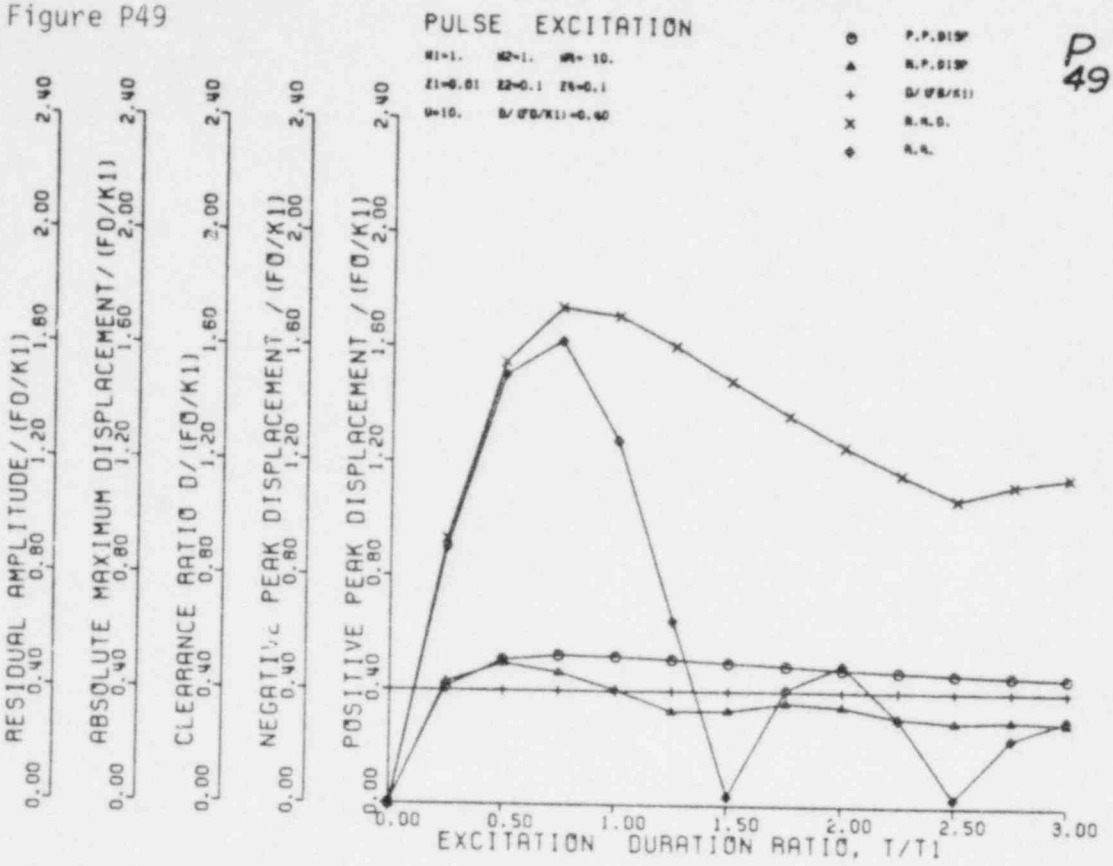

P49

Figure P50

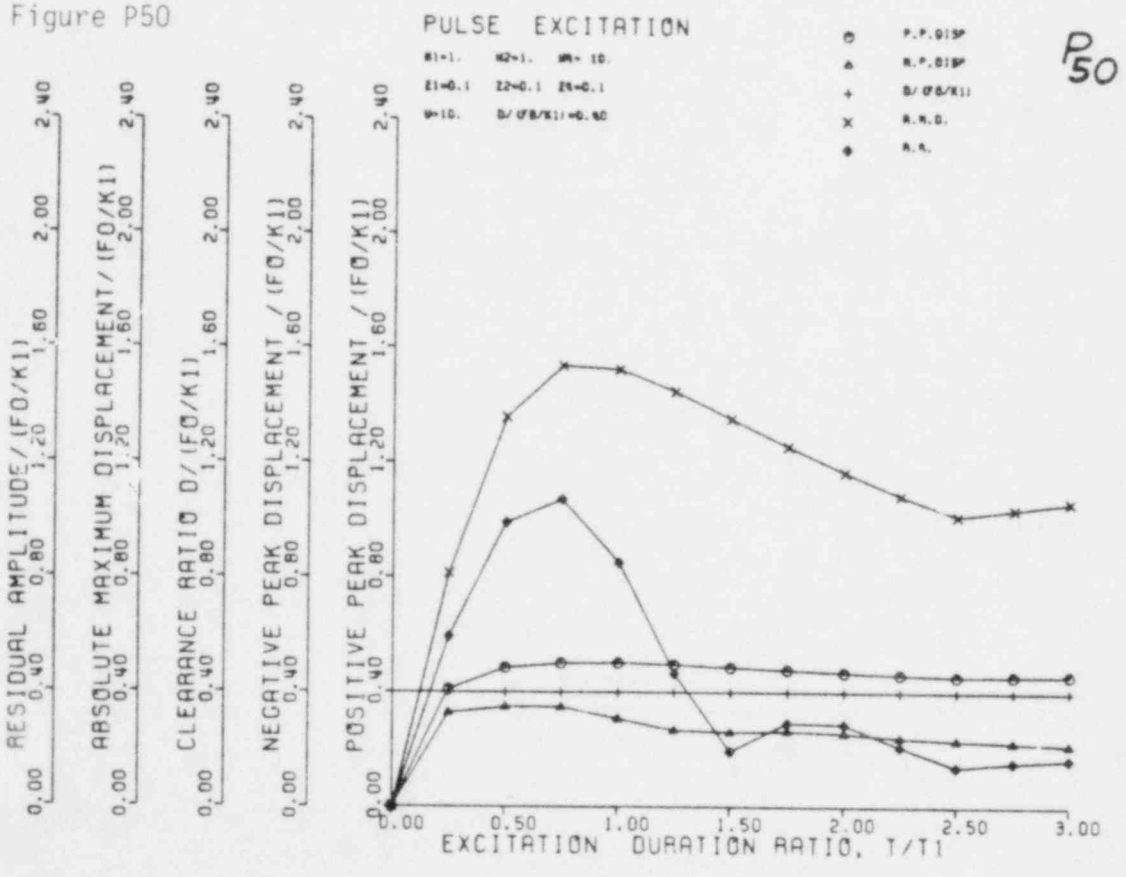

P50

Figure P51

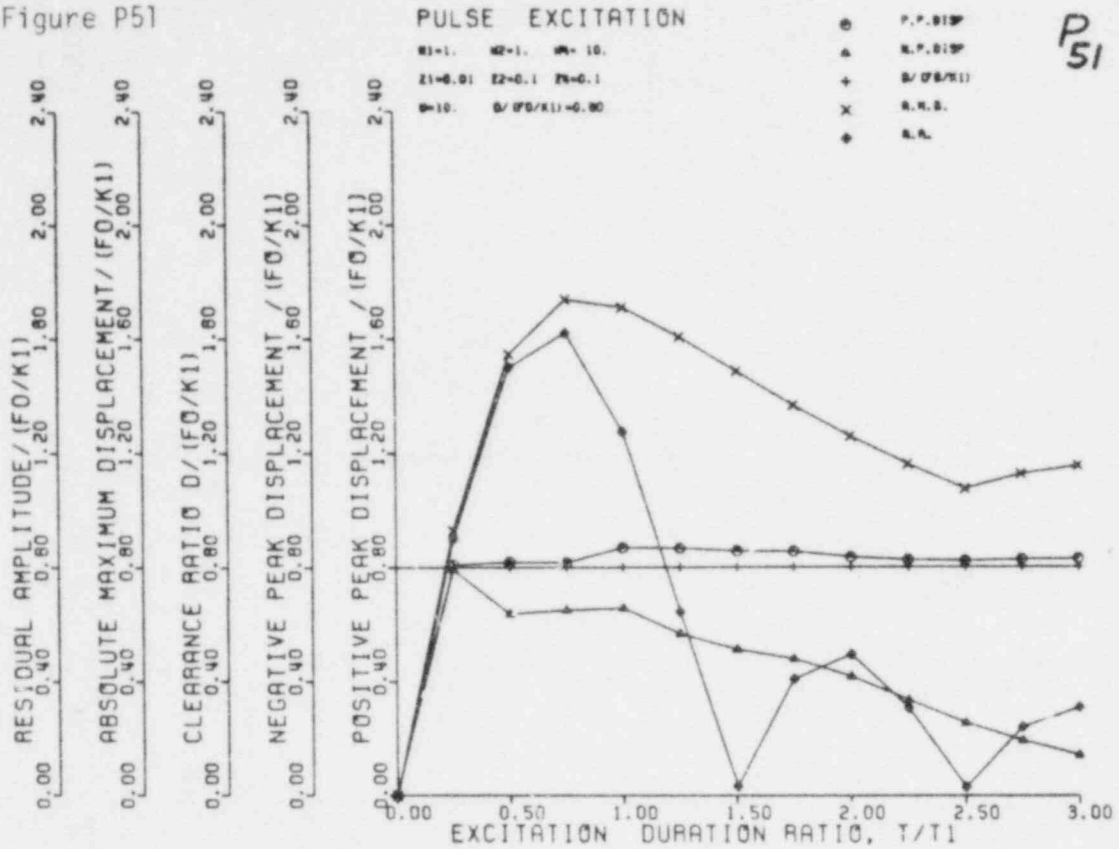

P51

Figure P52

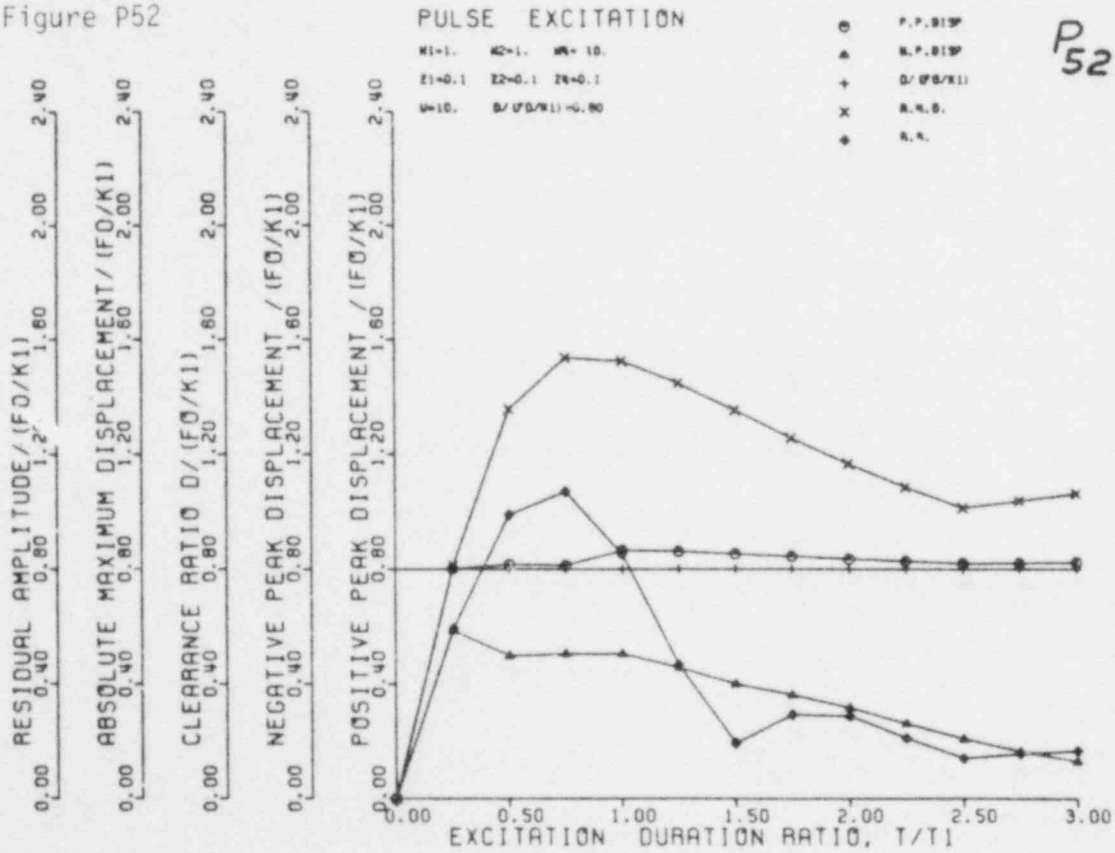

P52

Figure P53

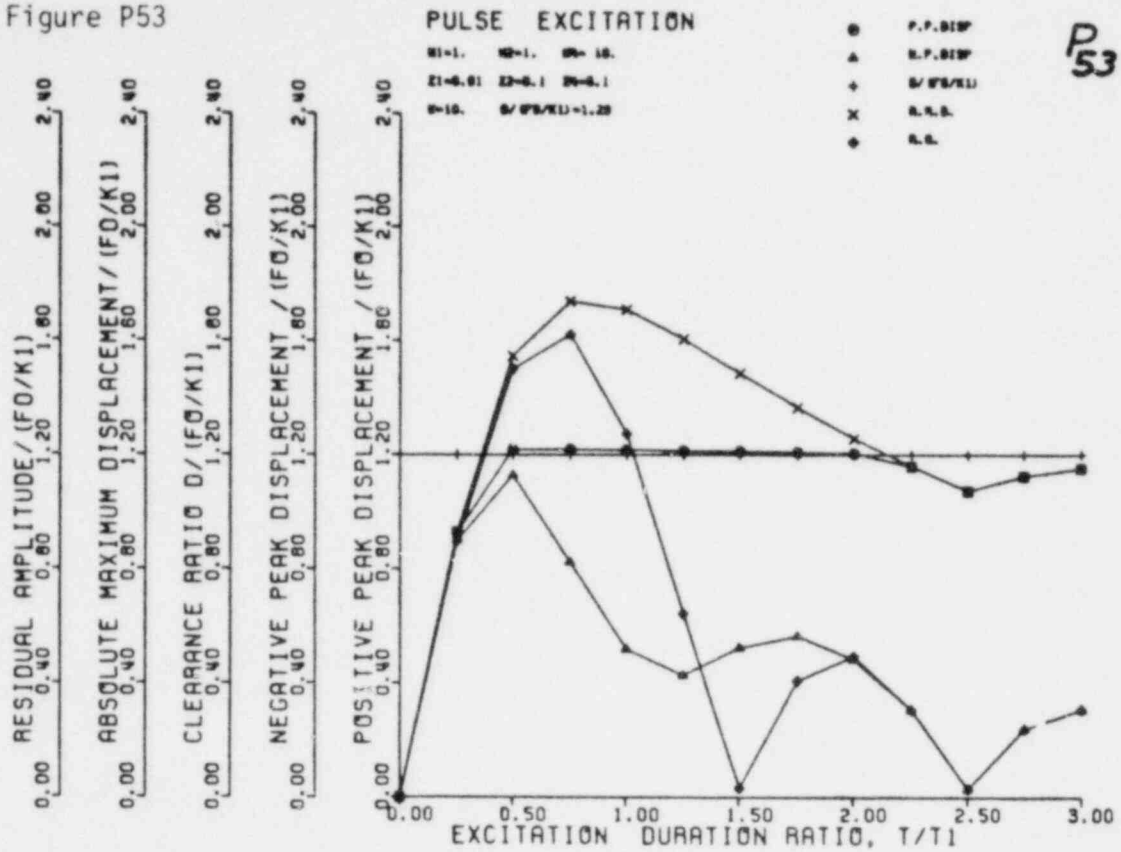

Figure P54

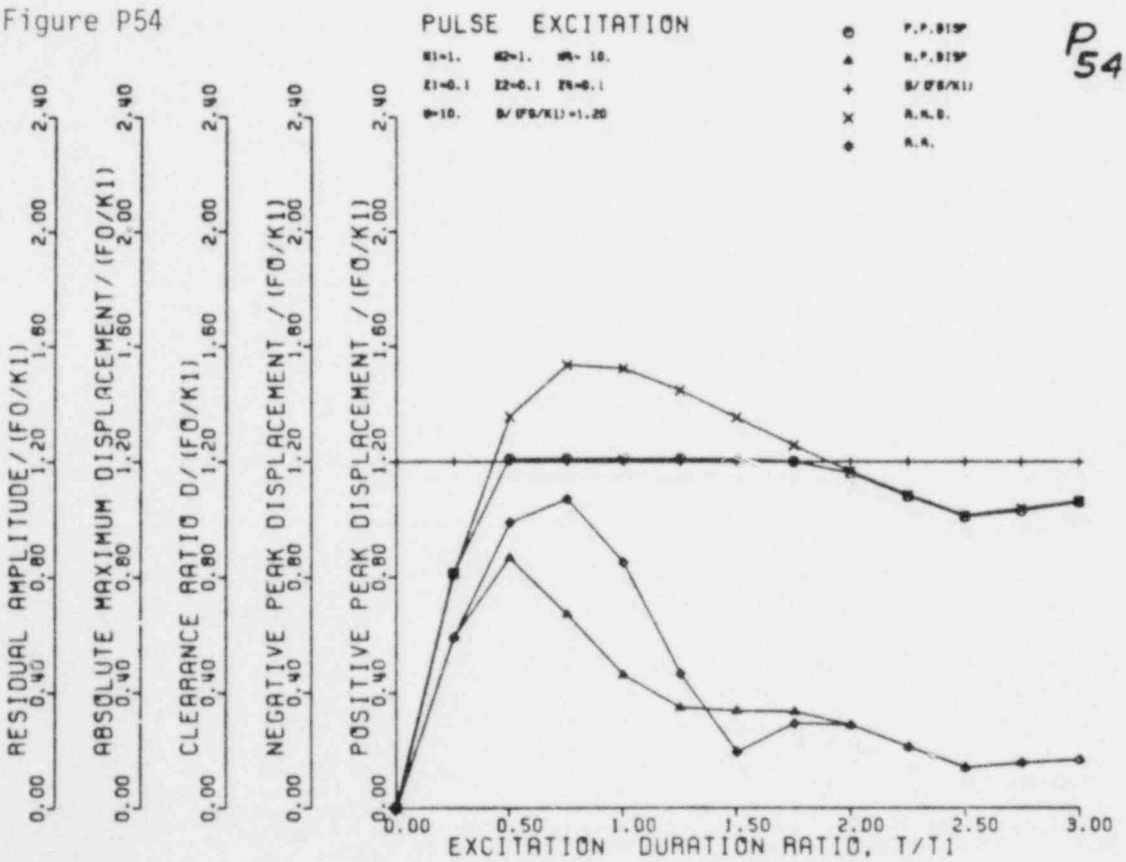

Figure P55

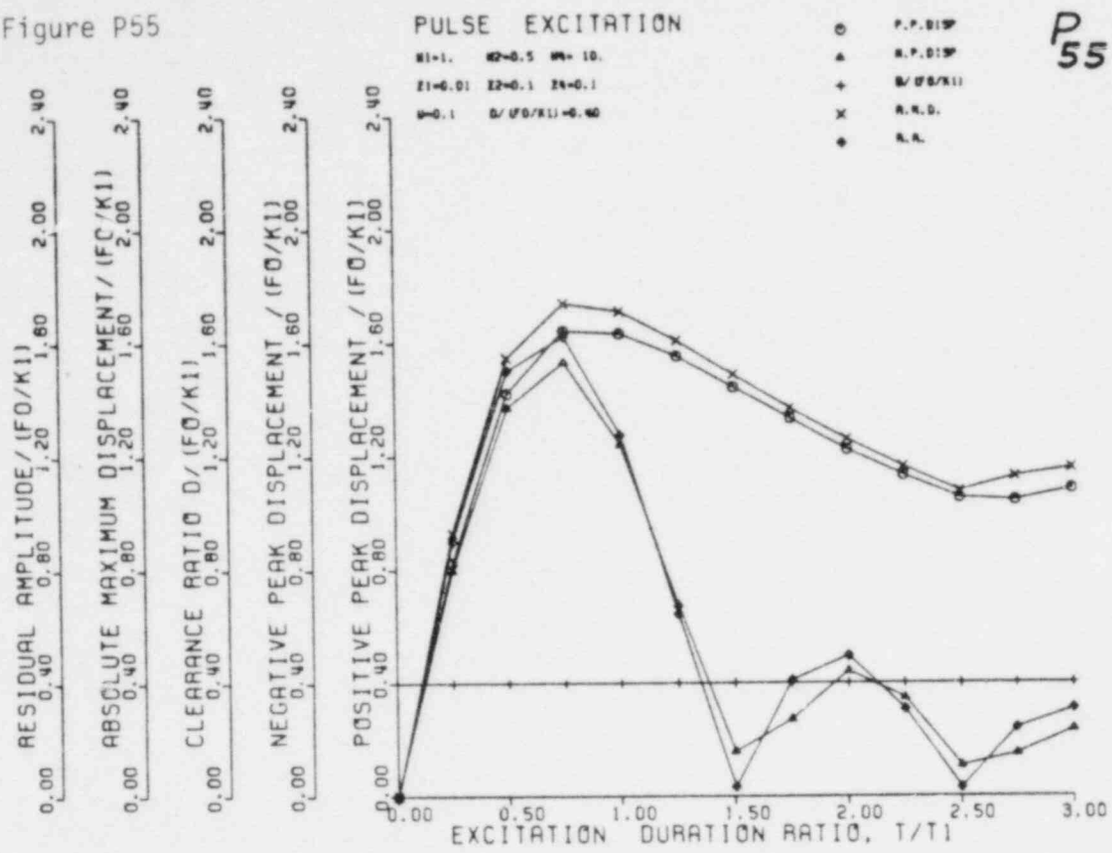

P55

Figure P56

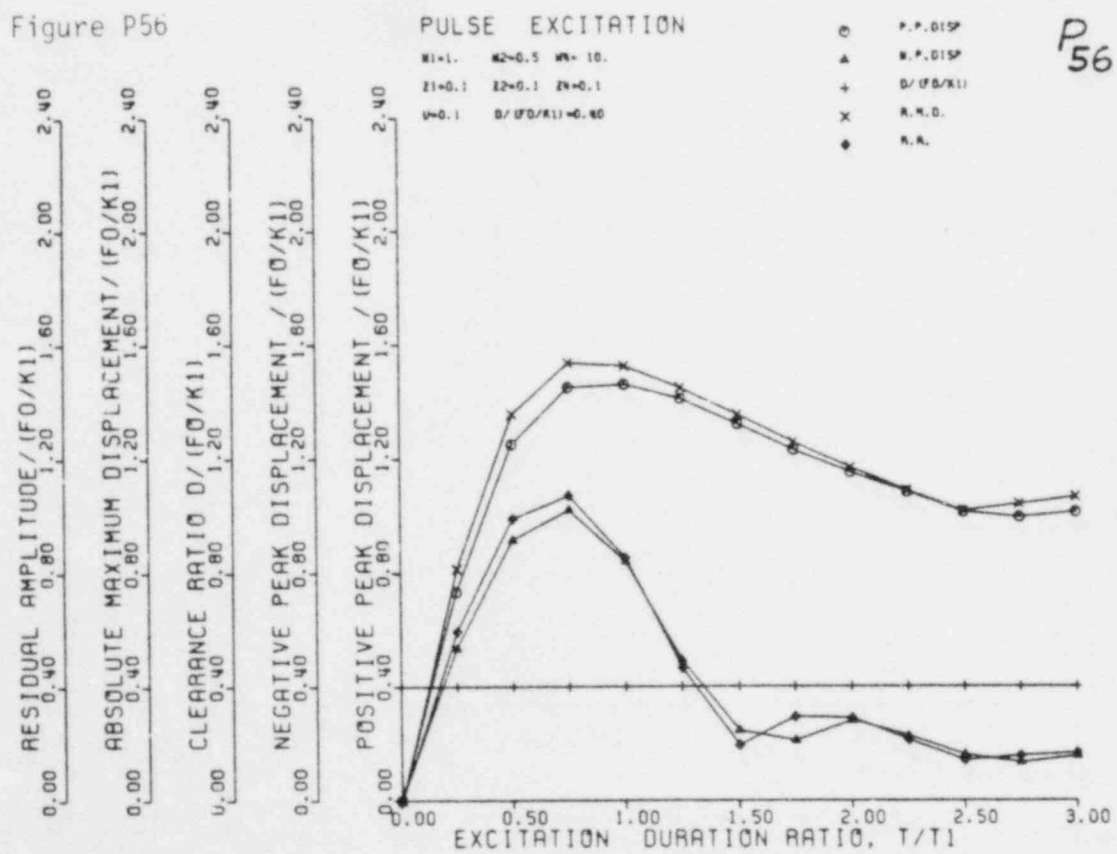

P56

Figure P57

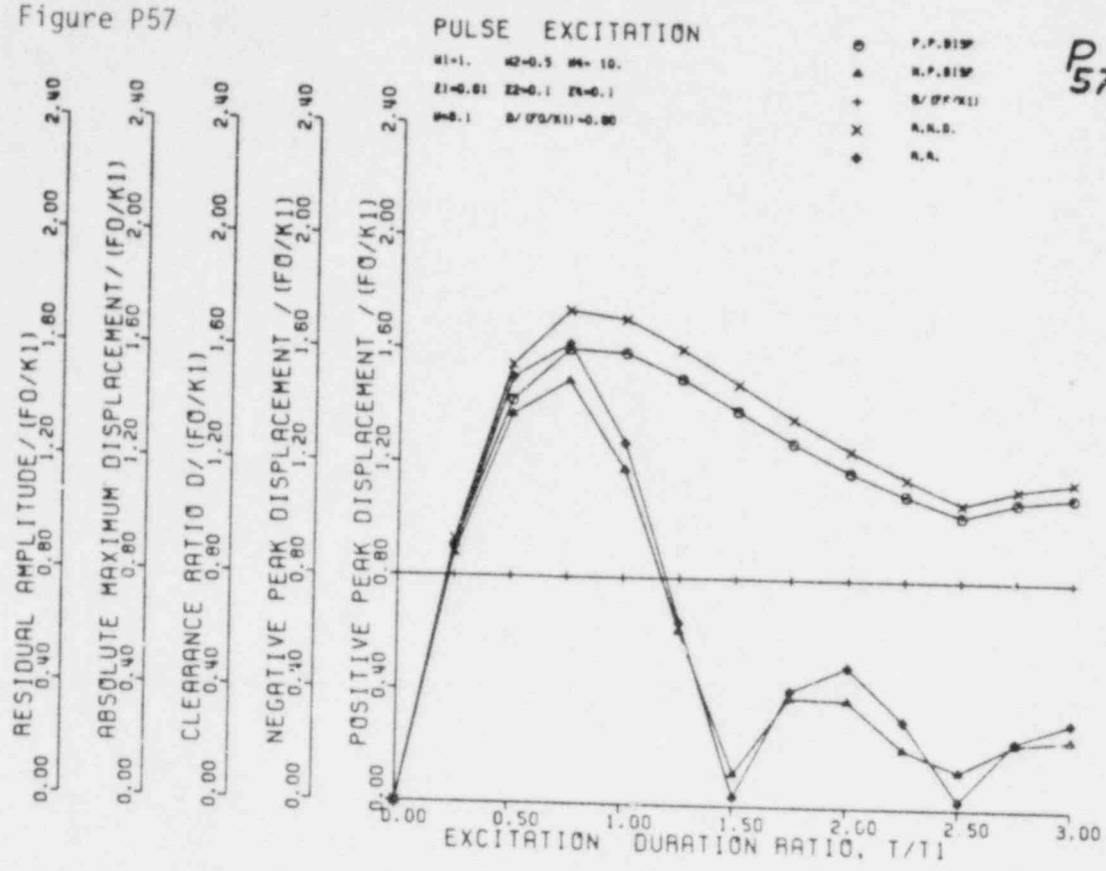

Figure P58

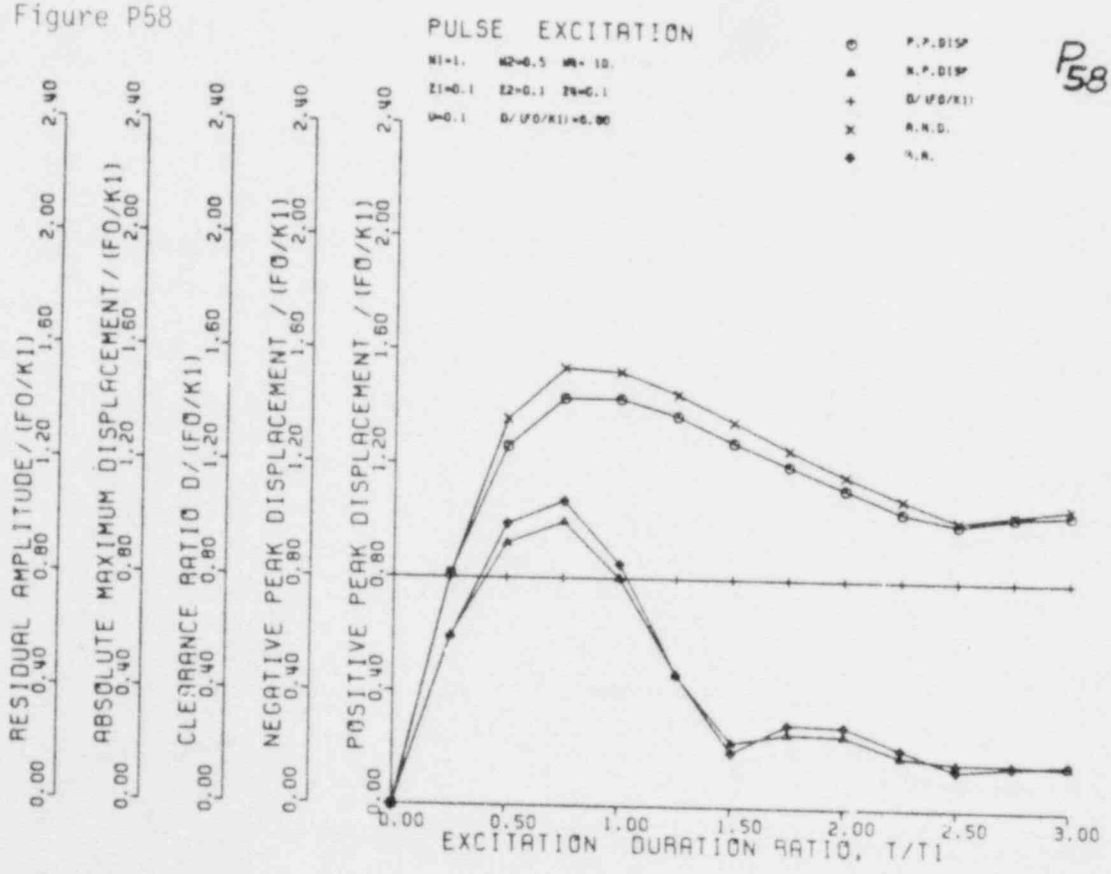

Figure P59

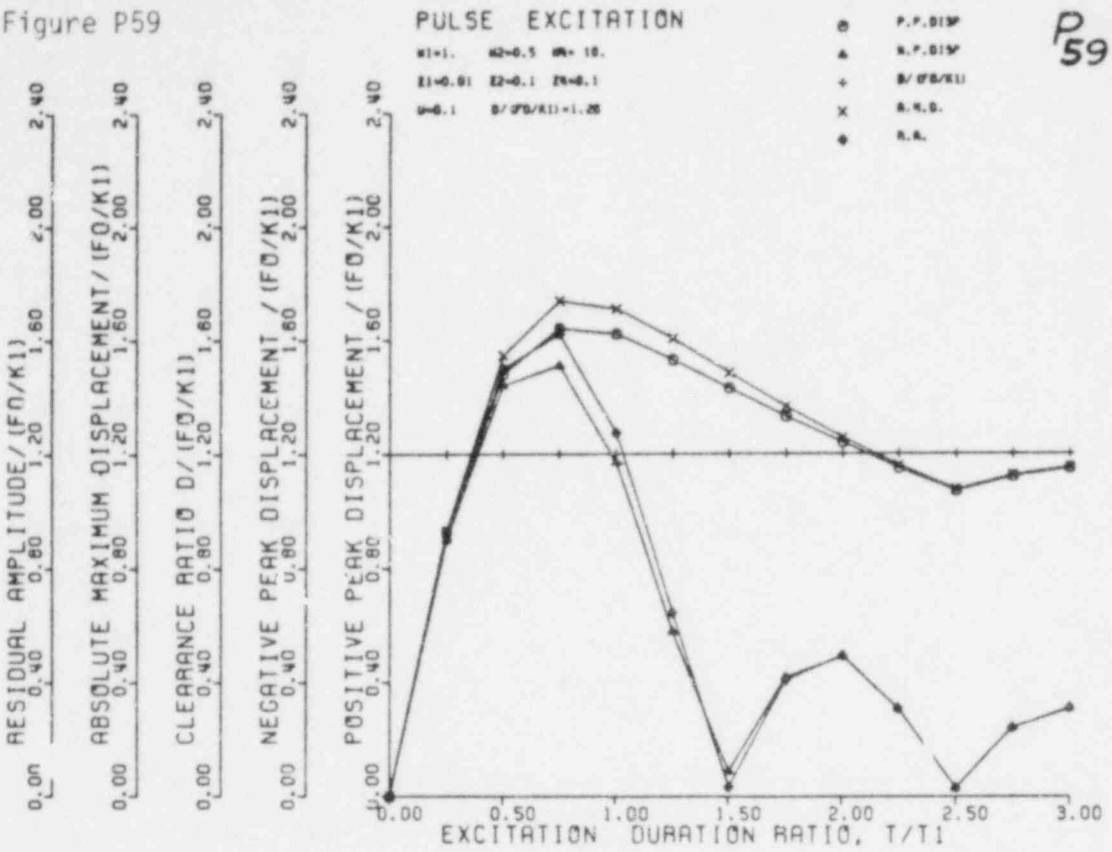

Figure P60

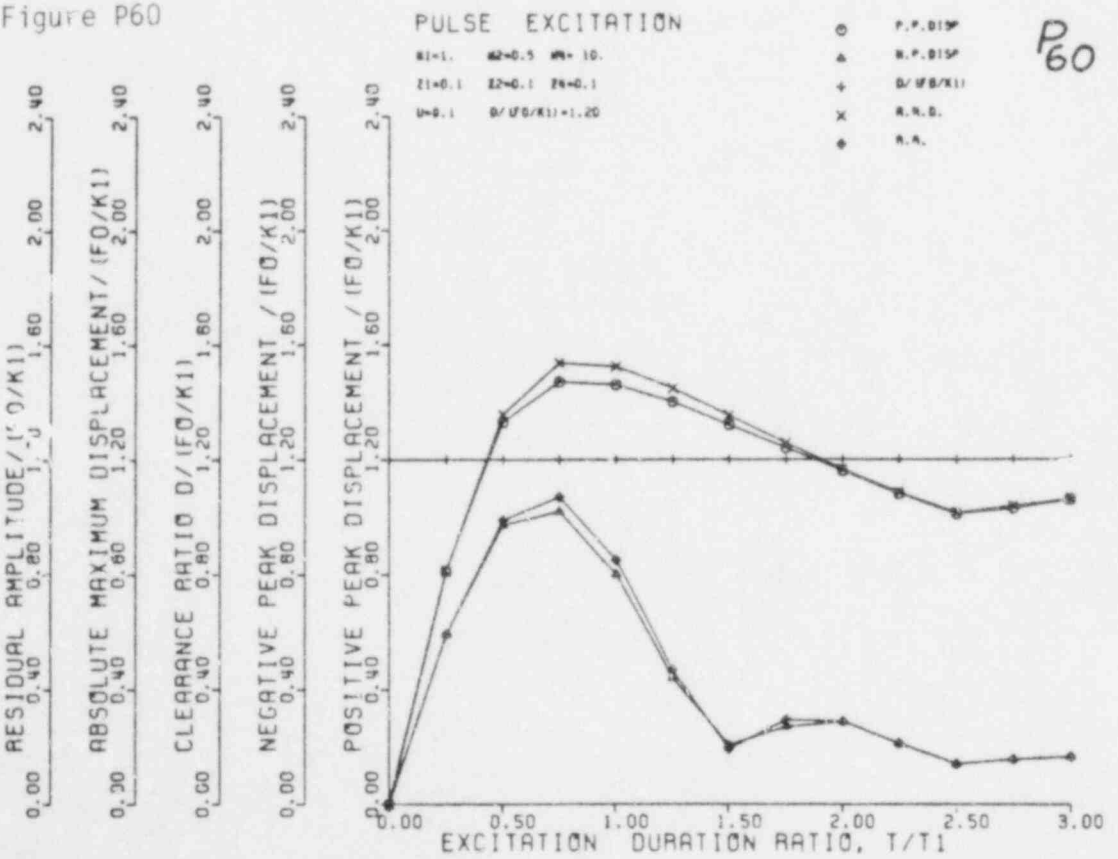

Figure P61

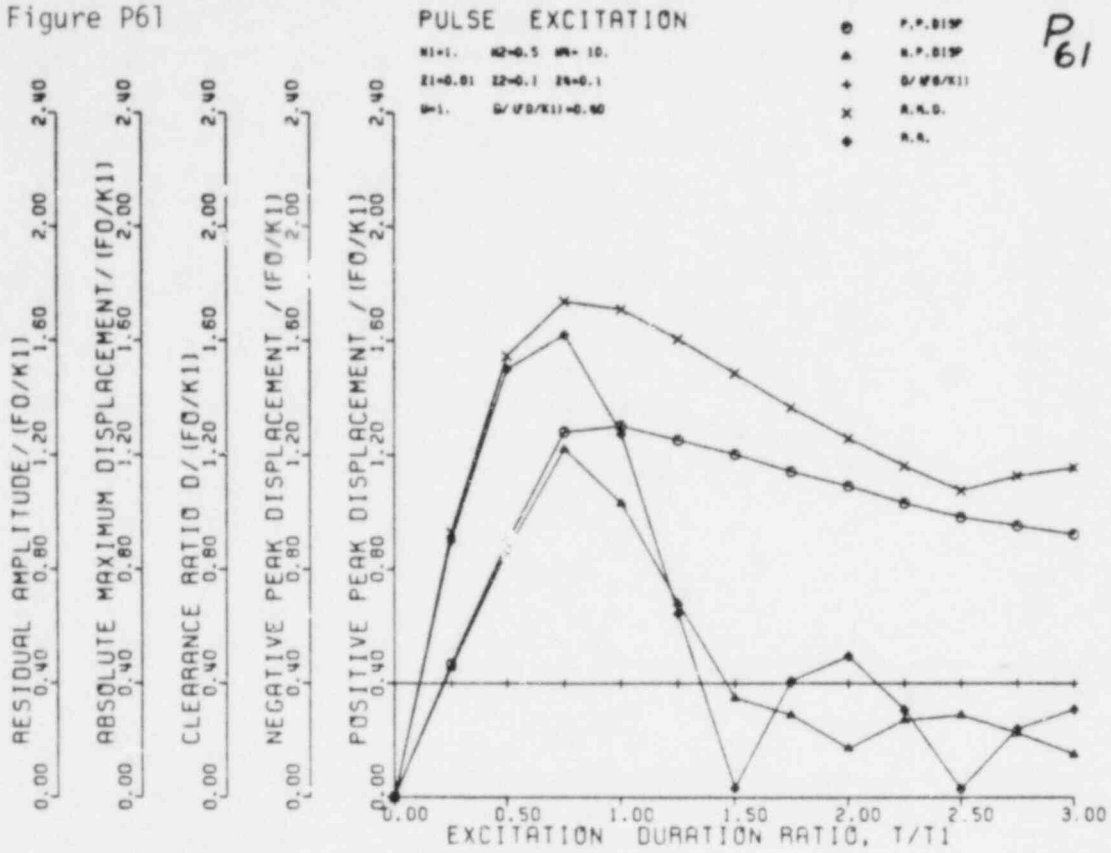

Figure P62

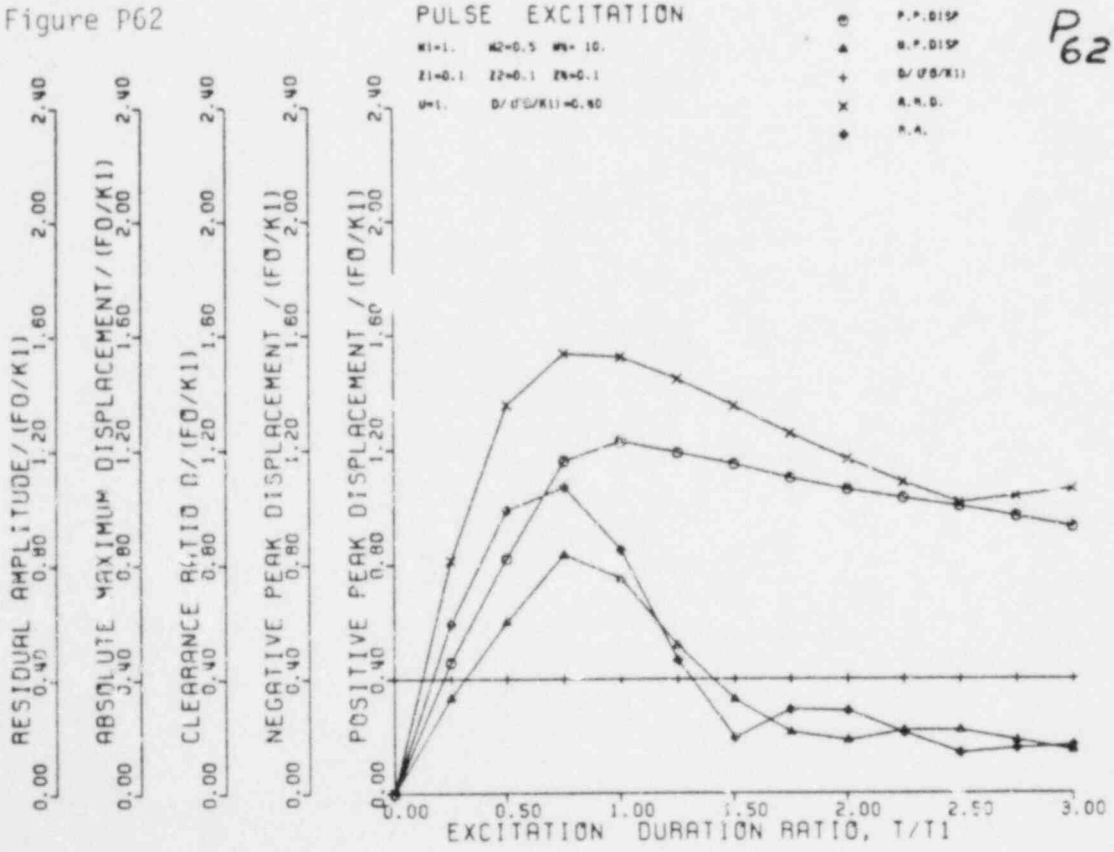

Figure P63

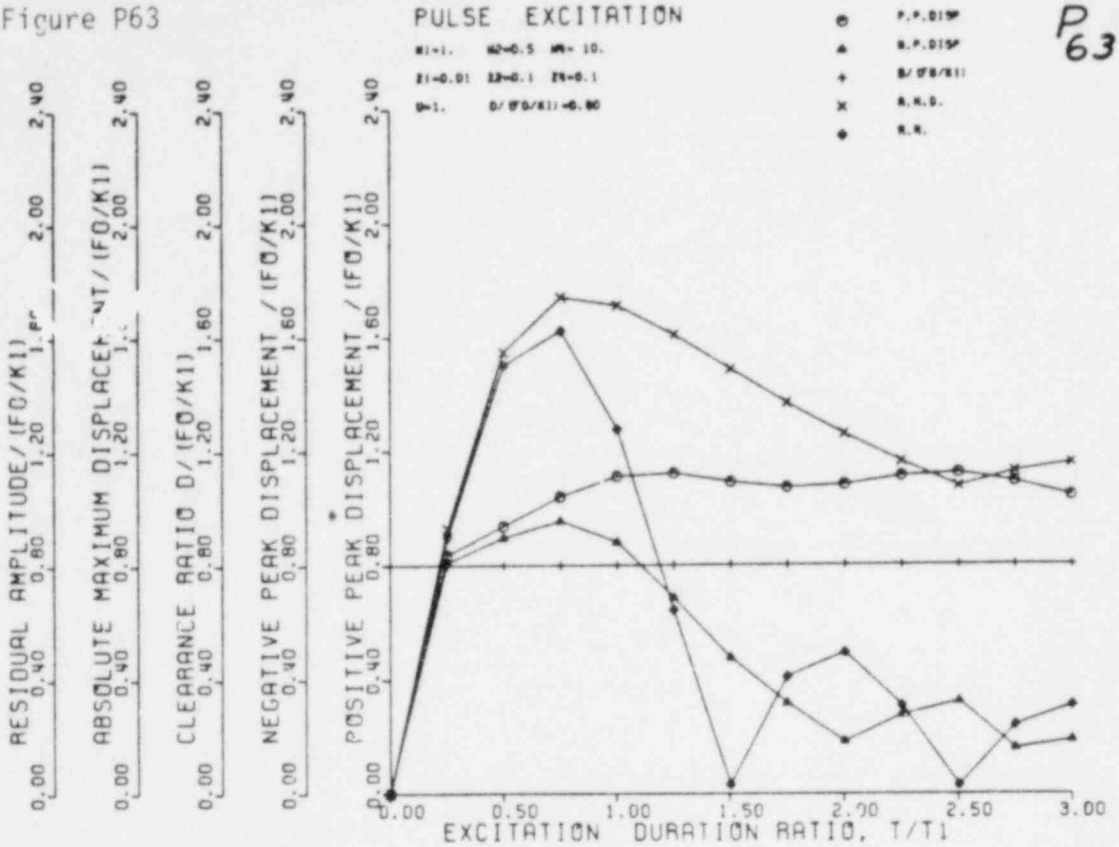

P63

Figure P64

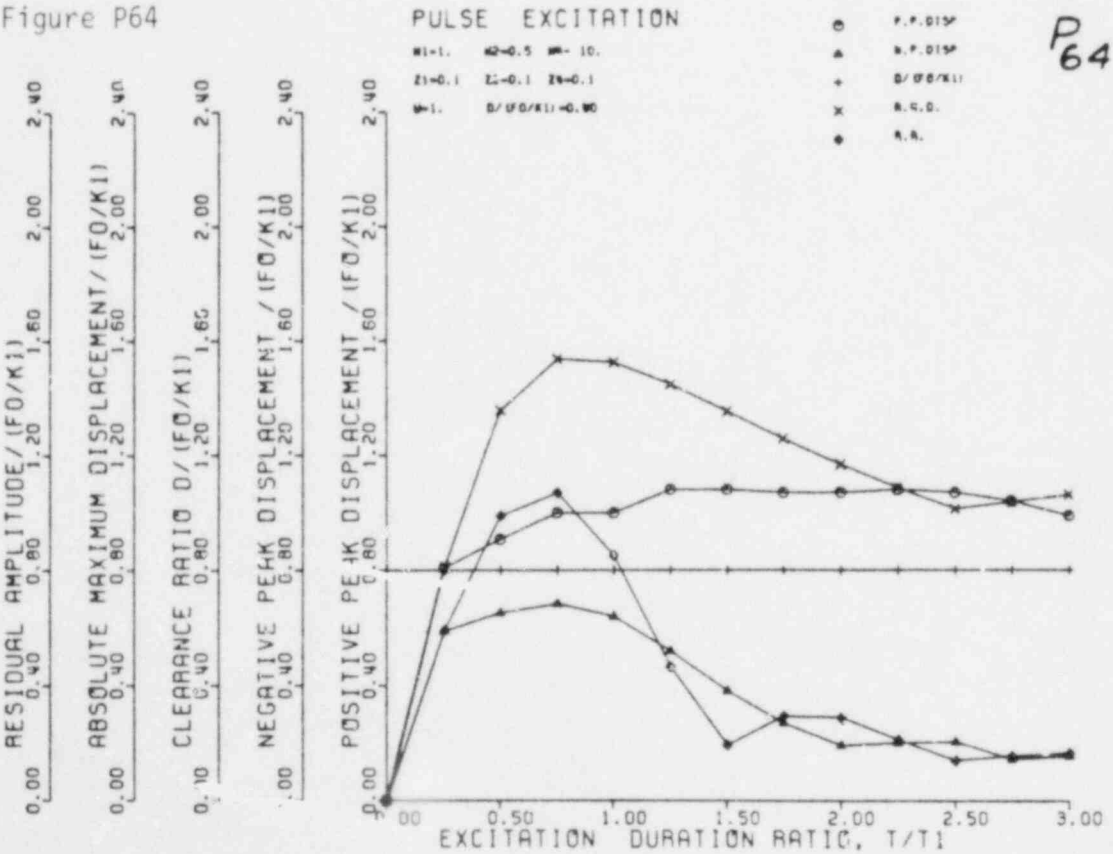

P64

Figure P65

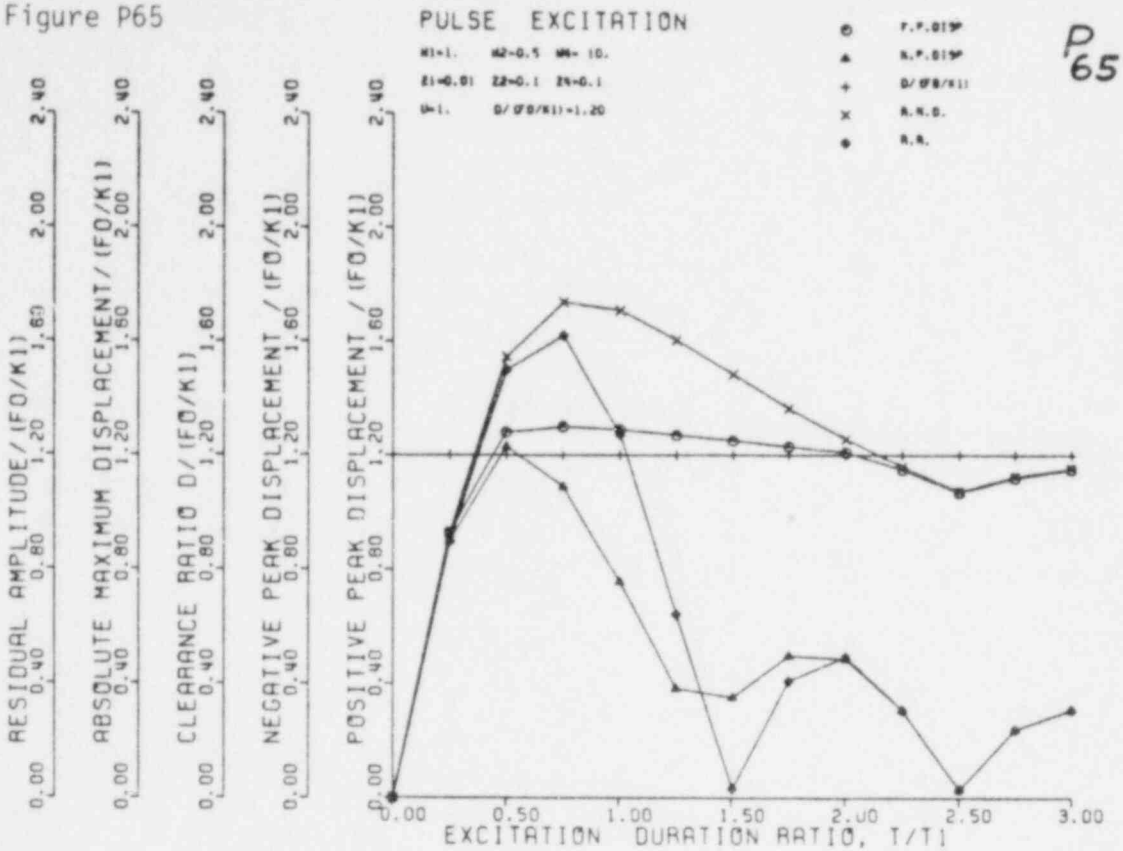

P65

Figure P66

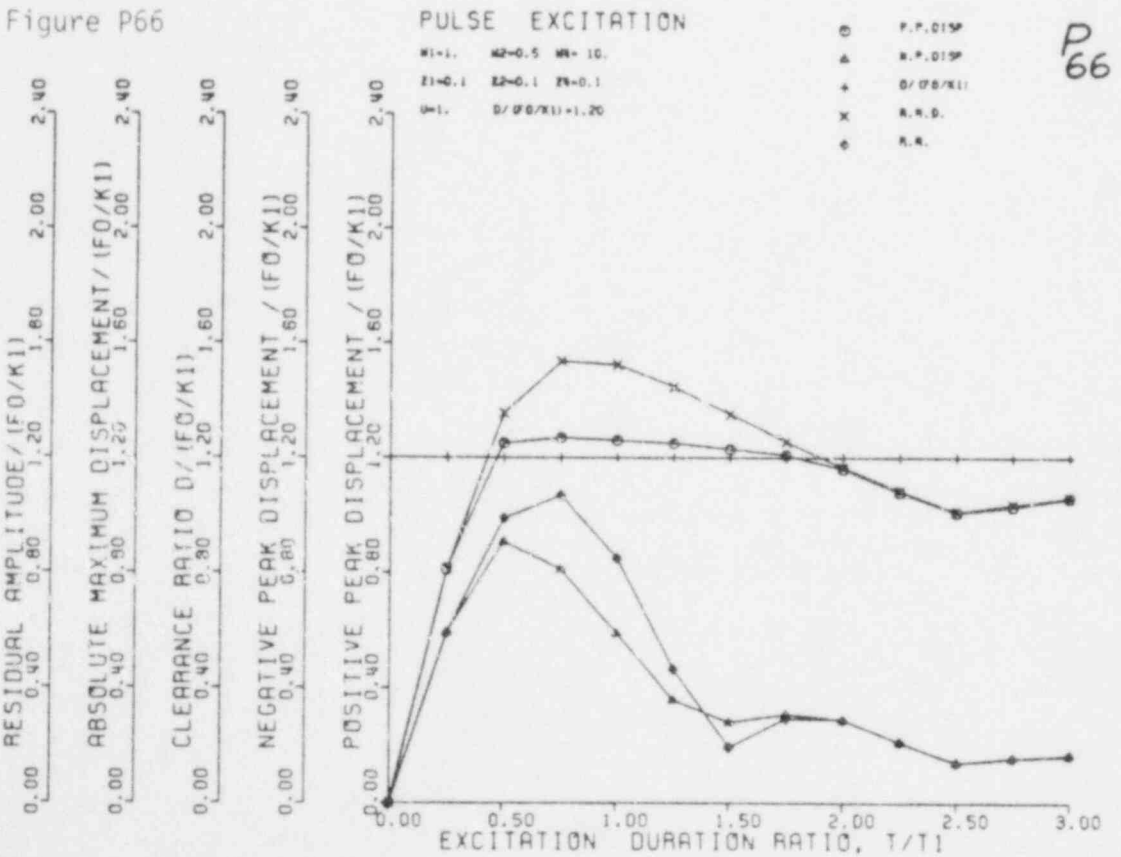

P66

Figure P67

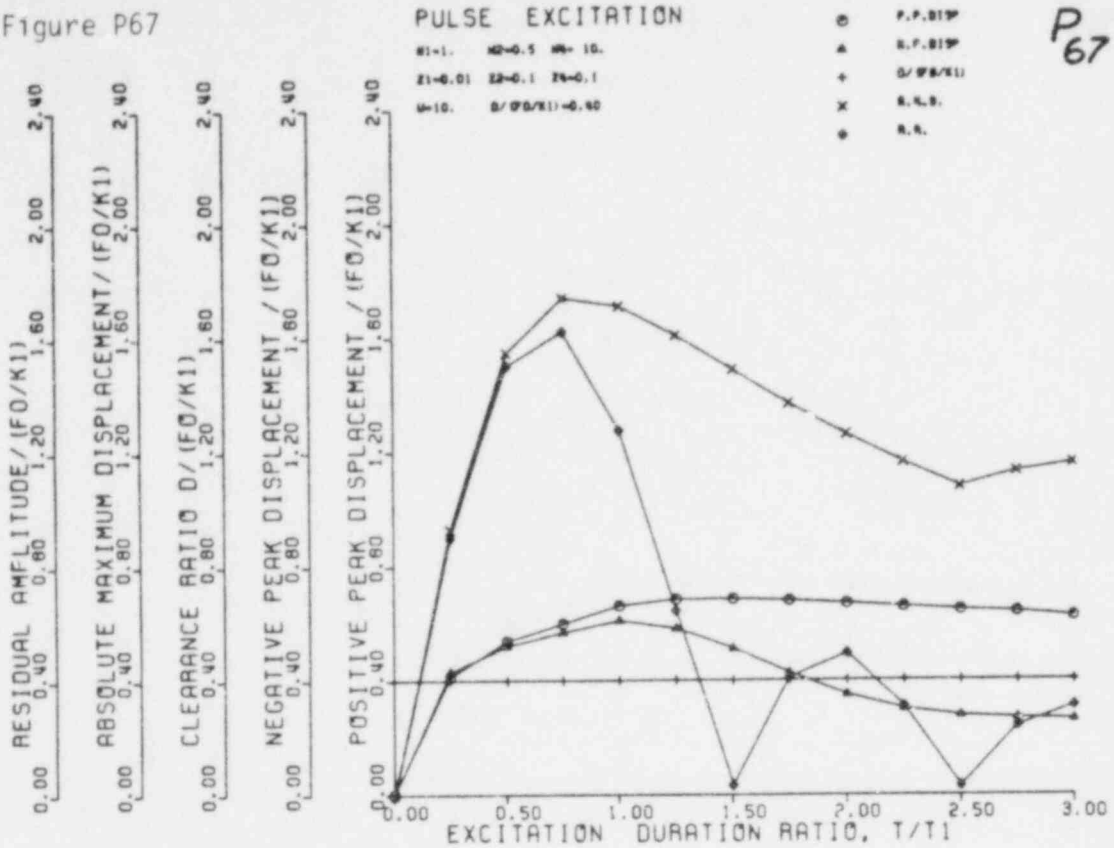

P67

Figure P68

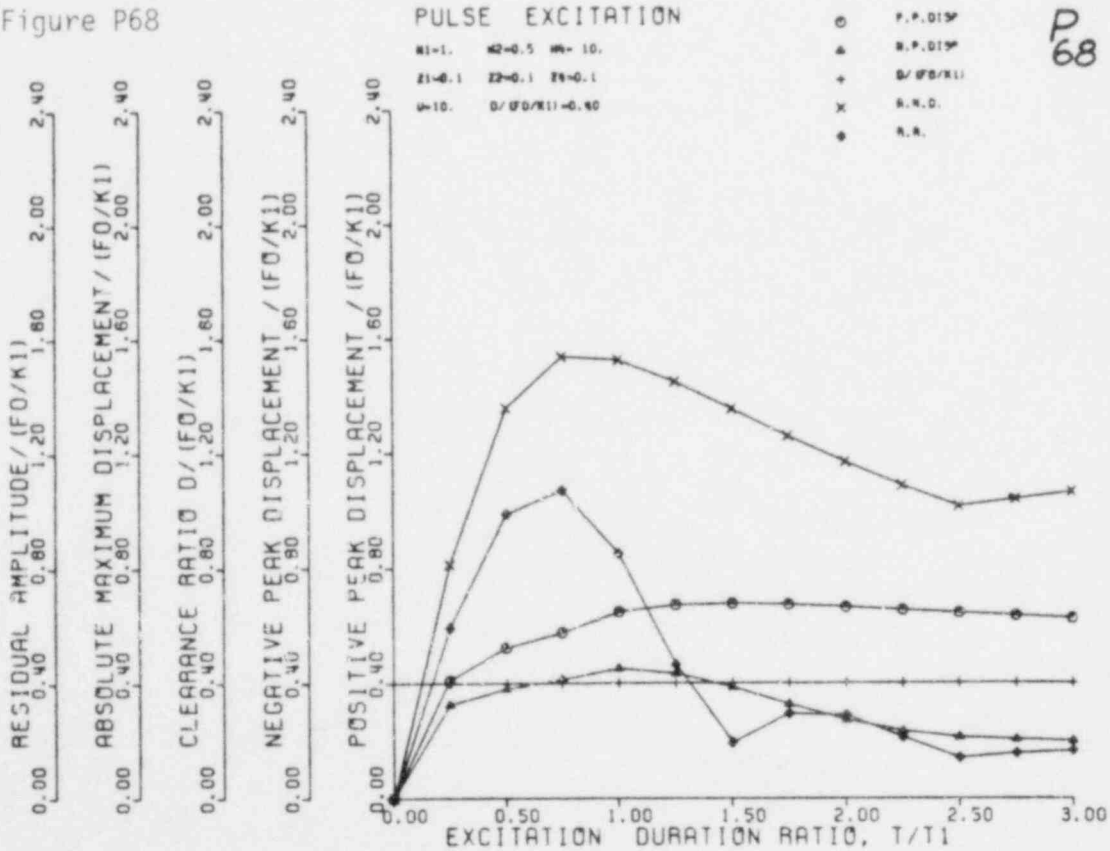

P68

Figure P69

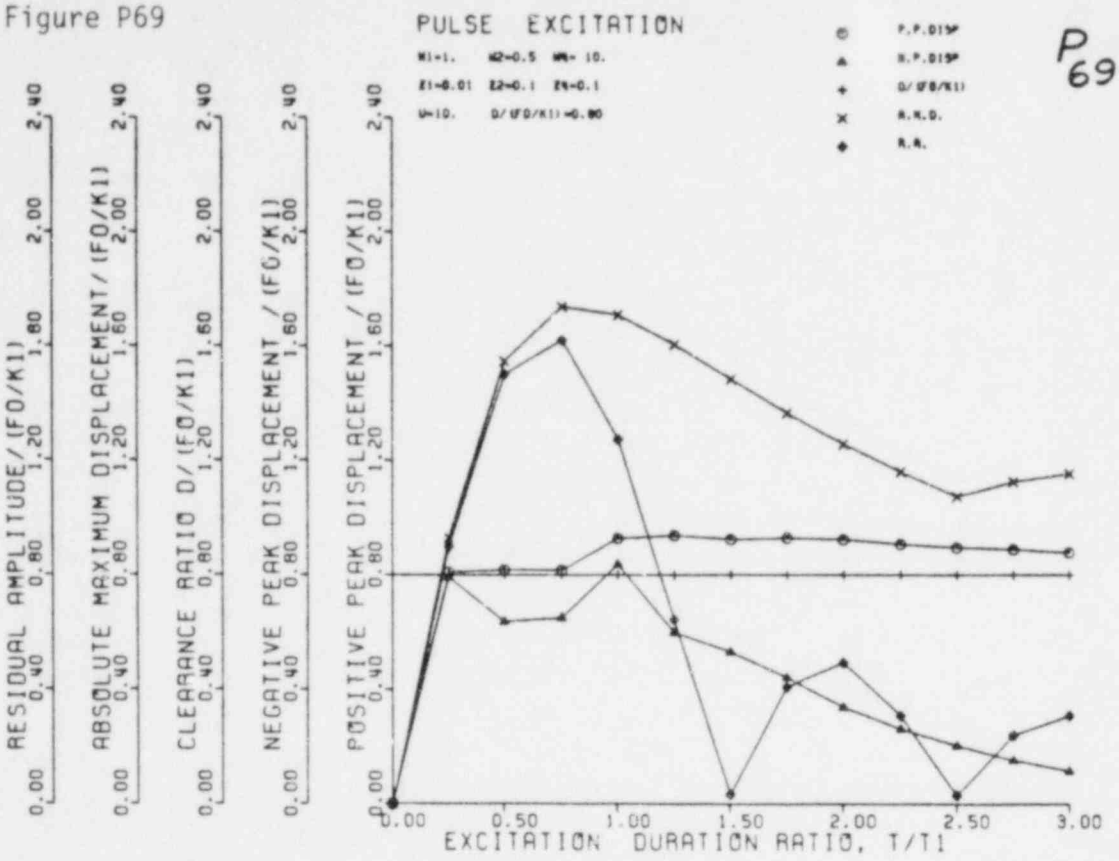

P69

Figure P70

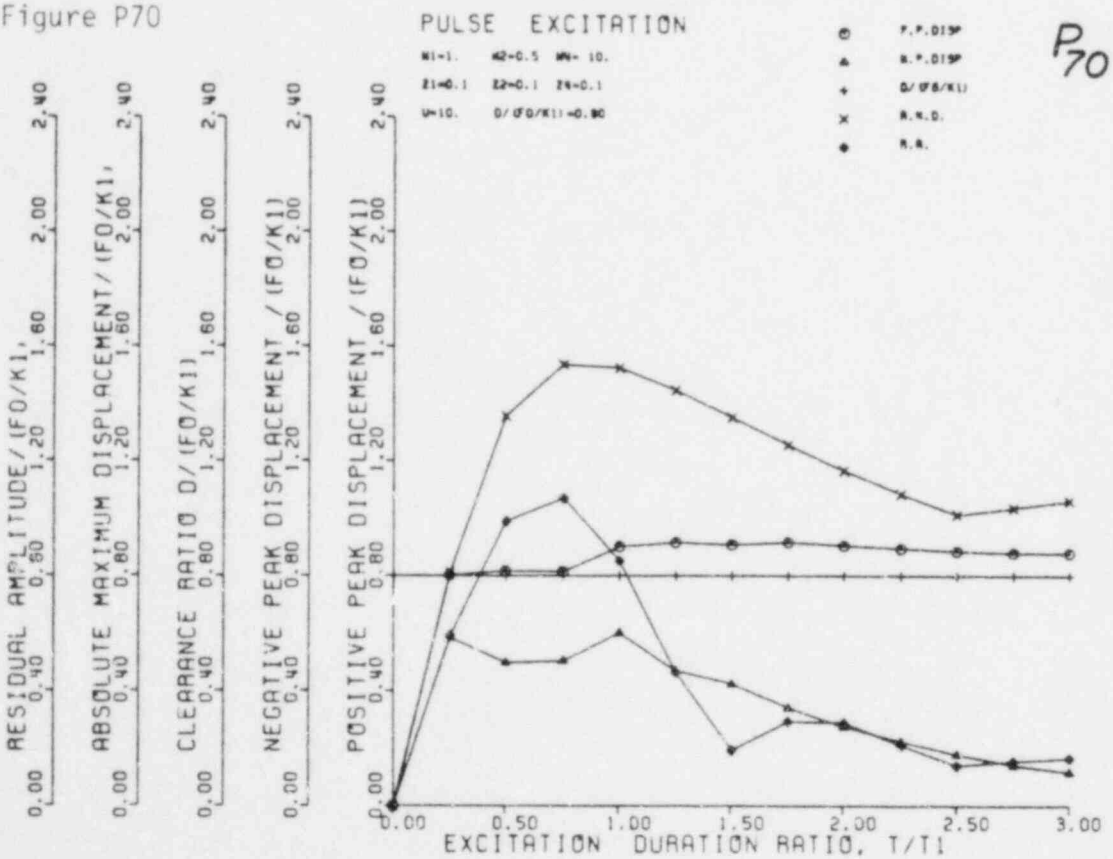

P70

Figure P71

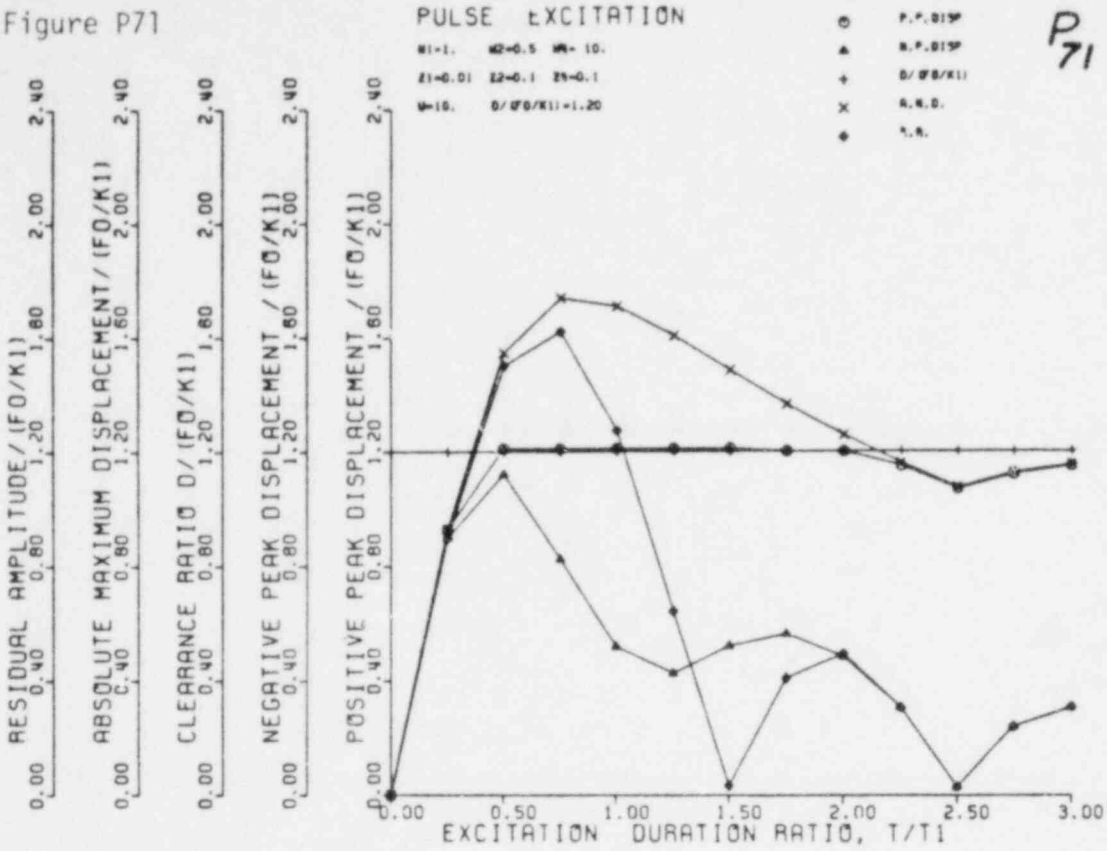

P71

Figure P72

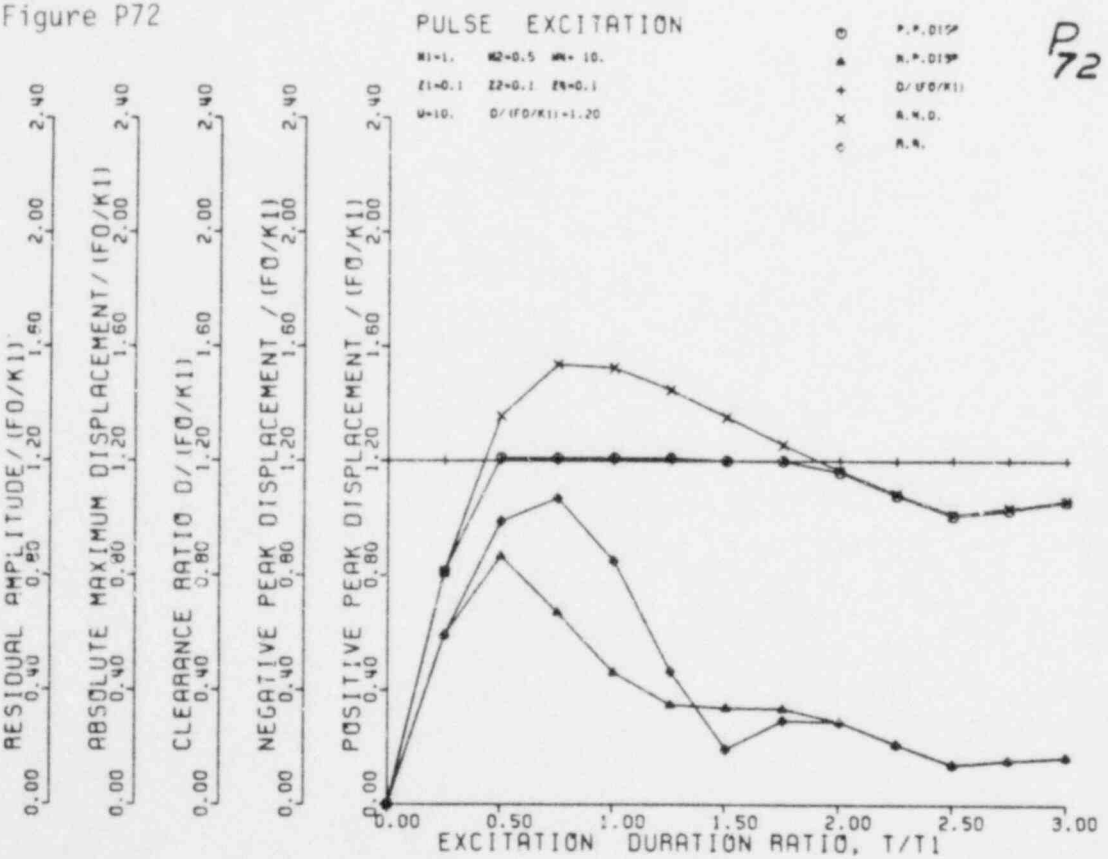

P72

TABLE 4C.1 DATA SUMMARY FOR RESPONSE SPECTRA:

STATIONARY RANDOM EXCITATION

$\frac{\omega_4}{\omega_1}$	ζ_4	D/σ_{x_o}	ζ_1	ζ_2	$\mu = \frac{M_2}{M_1}$	$\frac{\omega_2}{\omega_1}$	Page	Plot No.
10.0	0.1	0.25-2.25	0.01	0.1	0.1,1,10	0.5	4C-5	R7
						1.0	4C-4	R5
						2.0	4C-3	R3
						5.0	4C-2	R1
		0.3-2.85	0.1			0.5	4C-5	R8
						1.0	4C-4	R6
						2.0	4C-3	R4
						5.0	4C-2	R2
		0.25-2.25	0.01		0.1	0.5,1,2,5	4C-6	R9
					1.0		4C-6	R10
					10.0		4C-7	R11
		0.3-2.85	0.1		0.1		4C-7	R12
					1.0		4C-8	R13
					10.0		4C-8	R14
		0.25-2.85	0.01,0.1		0.1	0.5	4C-13	R24
						1.0	4C-12	R21
						2.0	4C-10	R18
						5.0	4C-9	R15
					1.0	0.5	4C-14	R25
						1.0	4C-12	R22
						2.0	4C-11	R19
						5.0	4C-9	R16
					10.0	0.5	4C-14	R26
						1.0	4C-13	R23
						2.0	4C-11	R20
						5.0	4C-10	R17

Figure R1

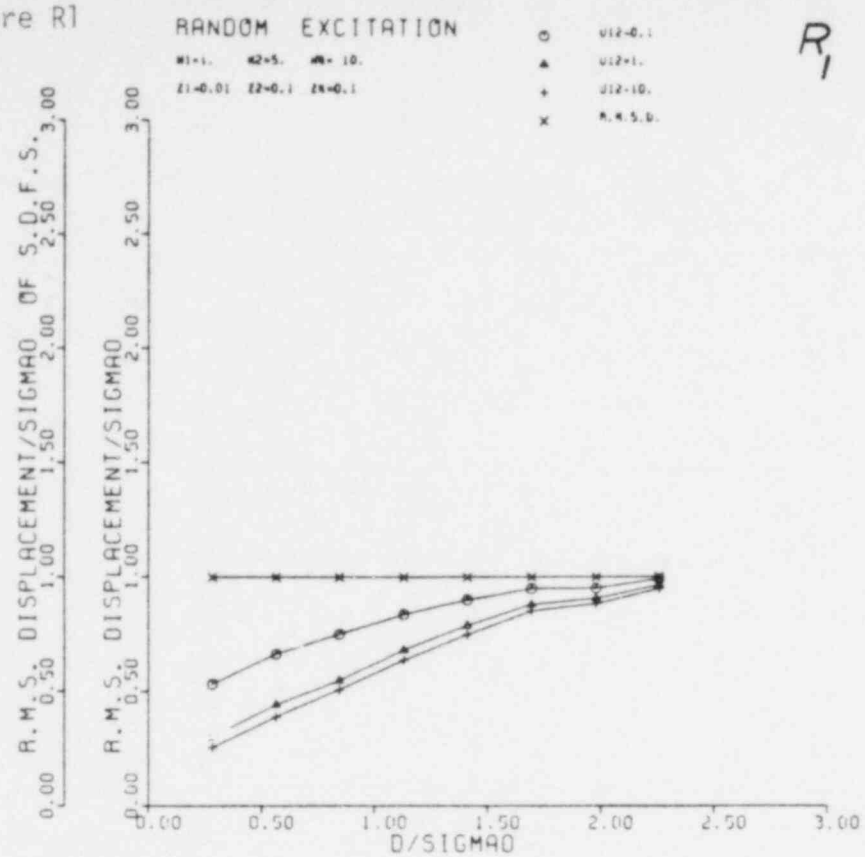

R_1

Figure R2

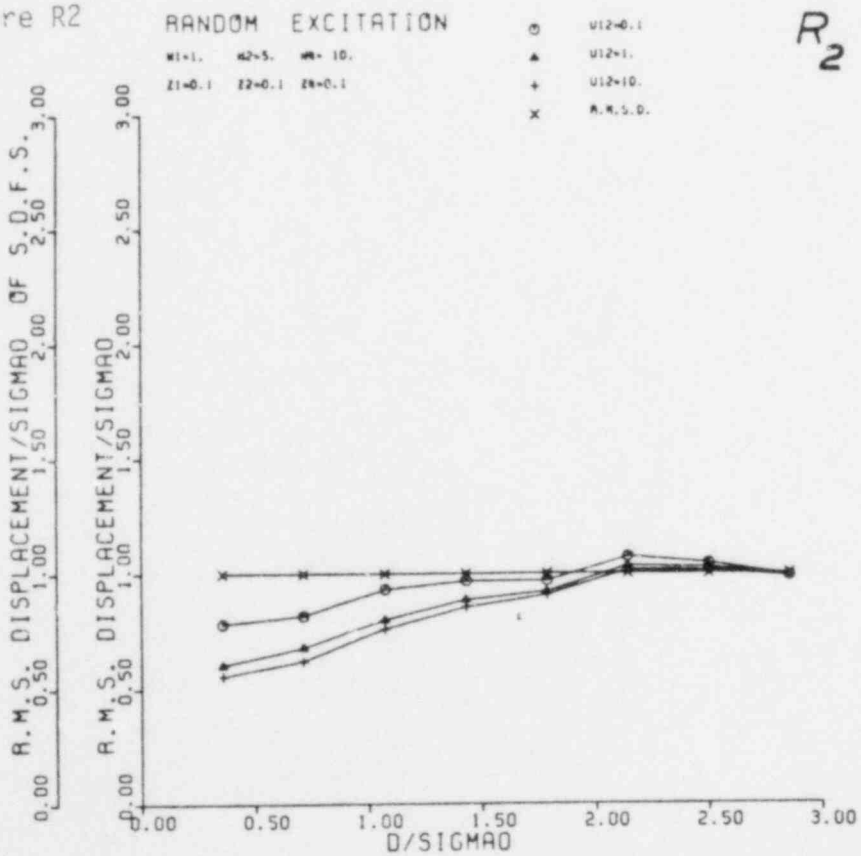

R_2

Figure R3

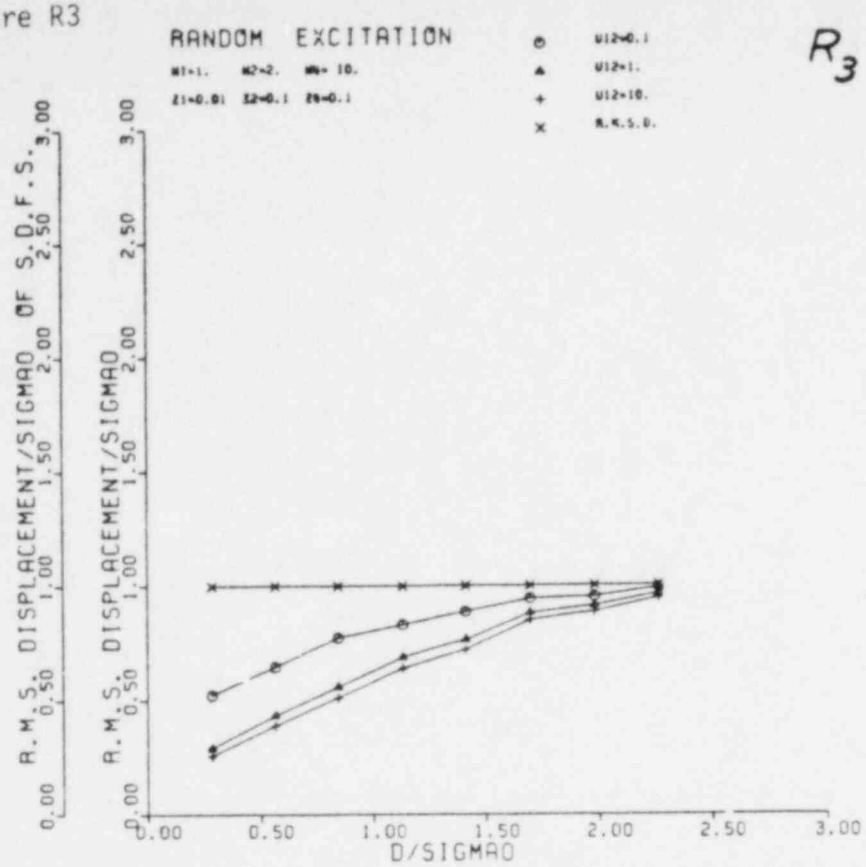

R_3

Figure R4

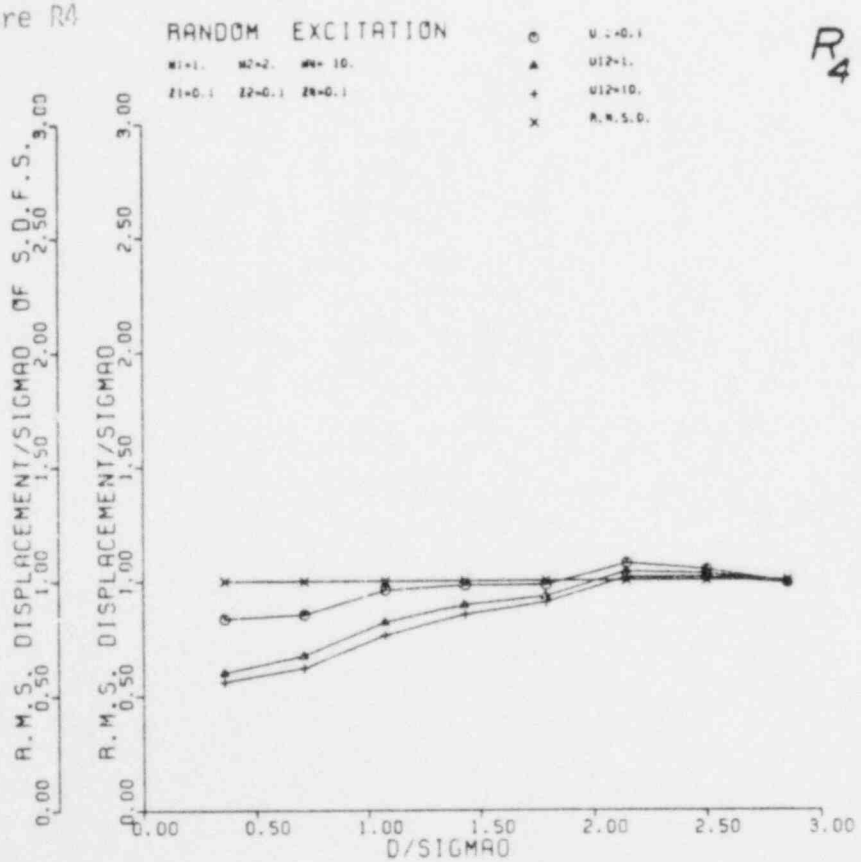

R_4

Figure R5

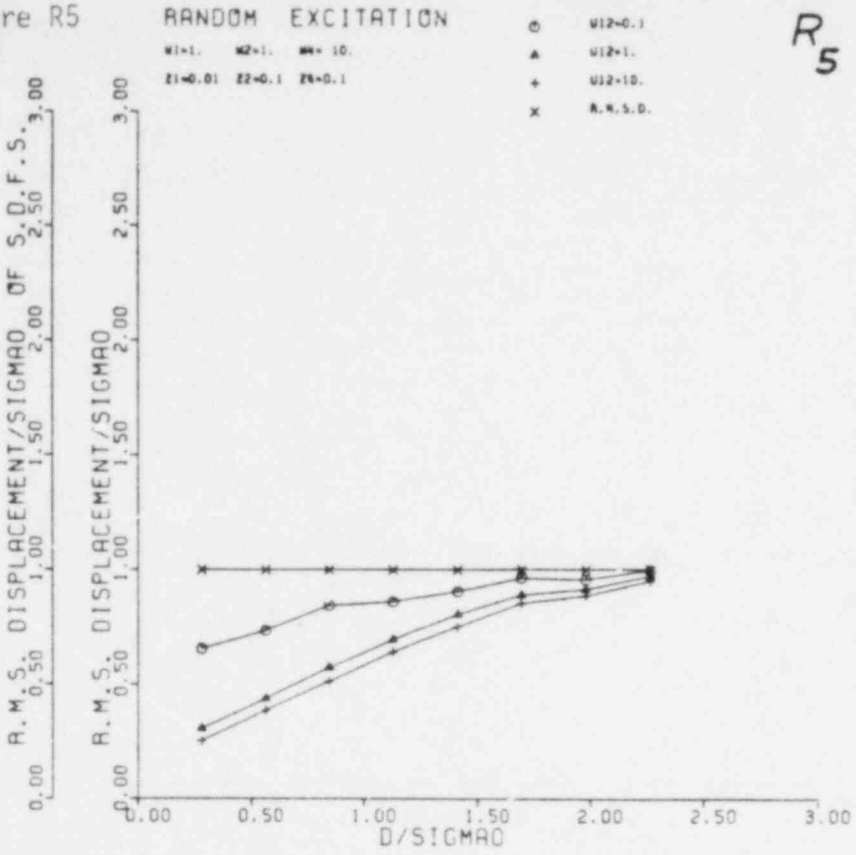

R_5

Figure R6

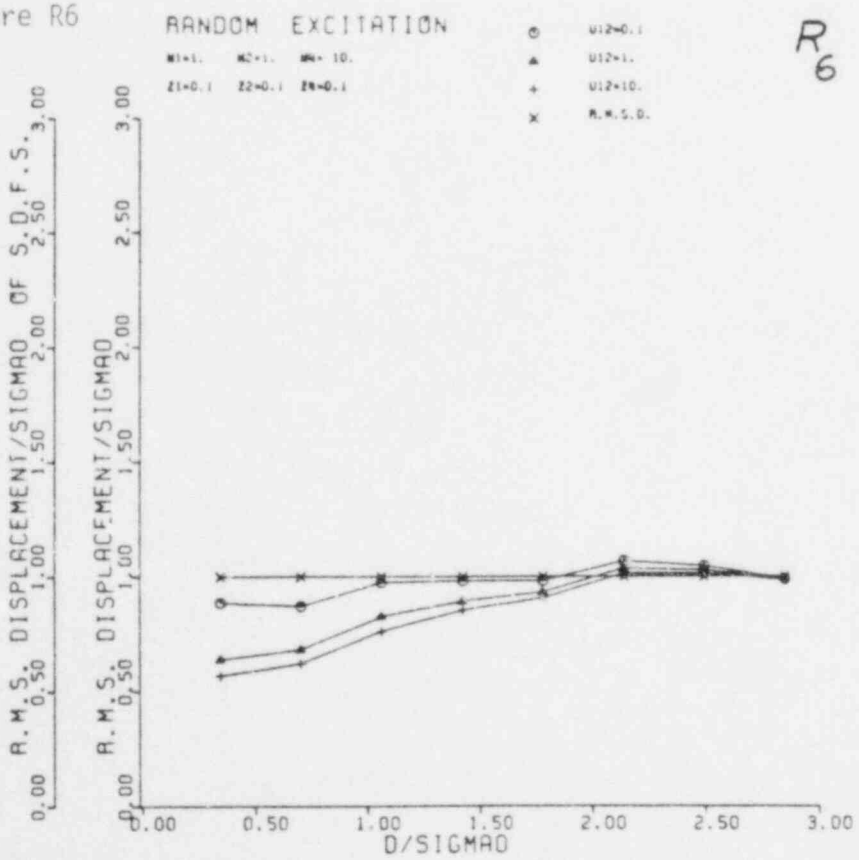

R_6

Figure R7

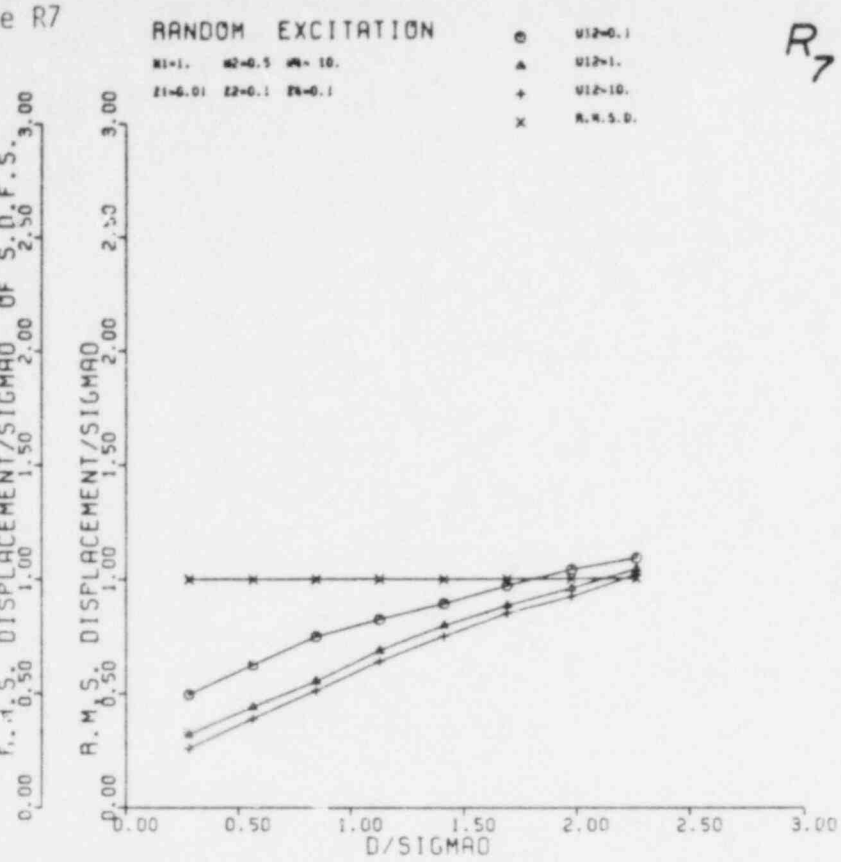

R7

Figure R8

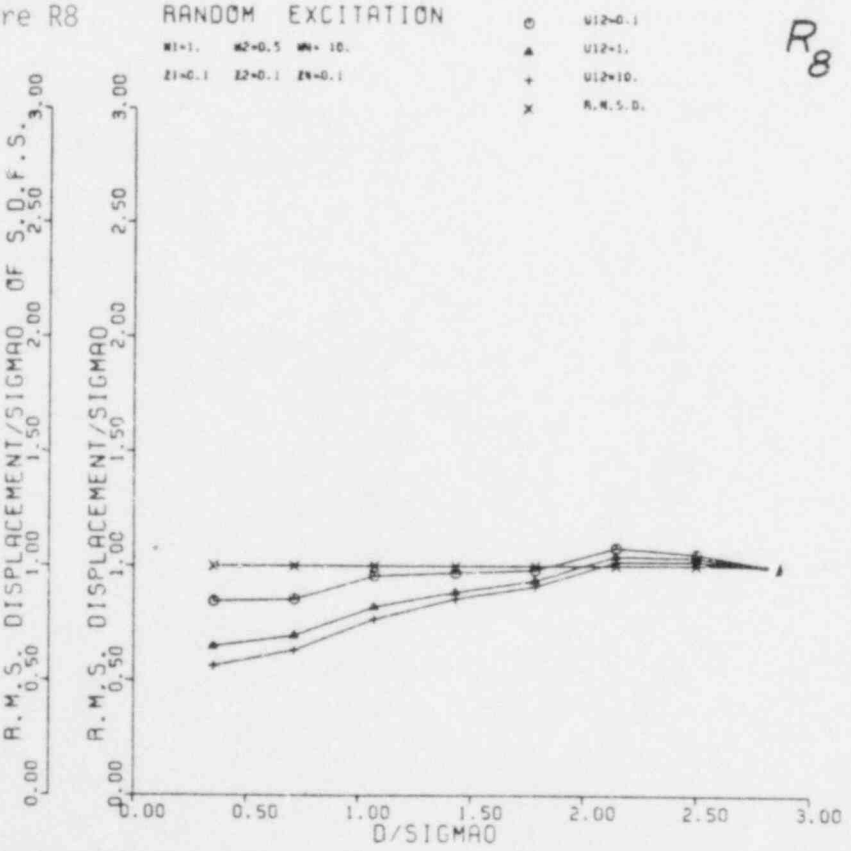

R8

Figure R9

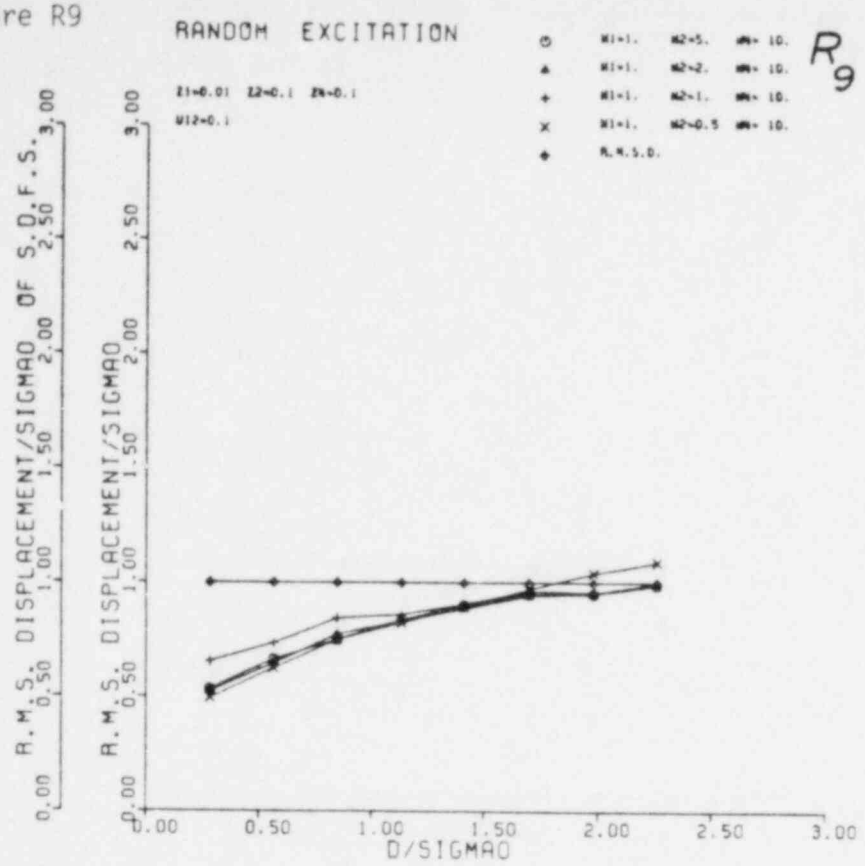

R9

Figure R10

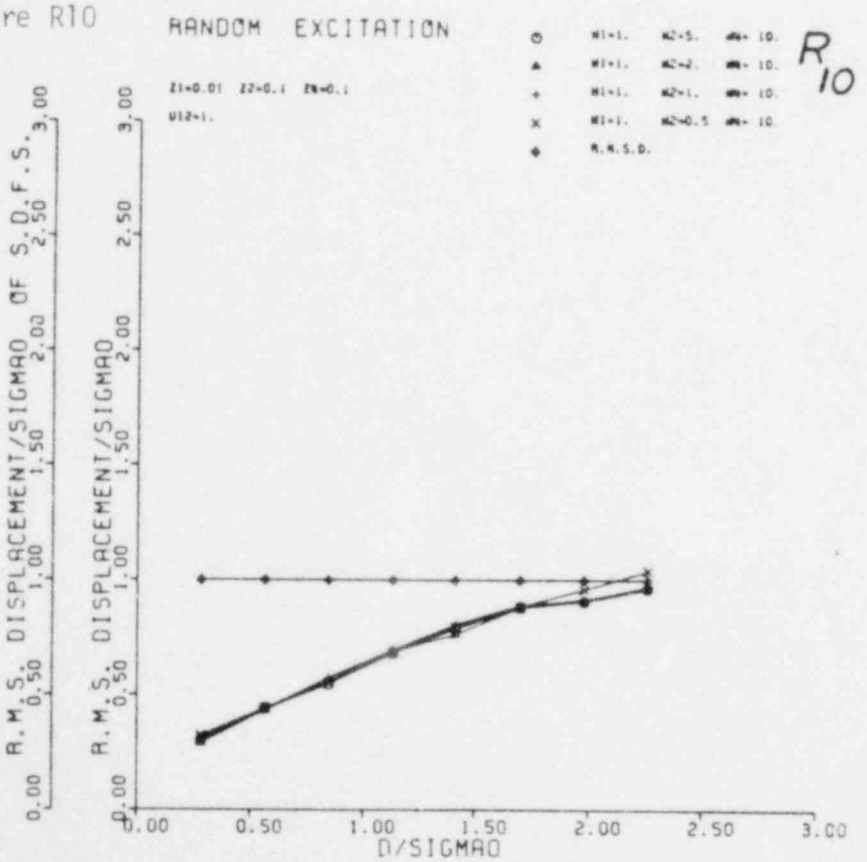

R10

Figure R11

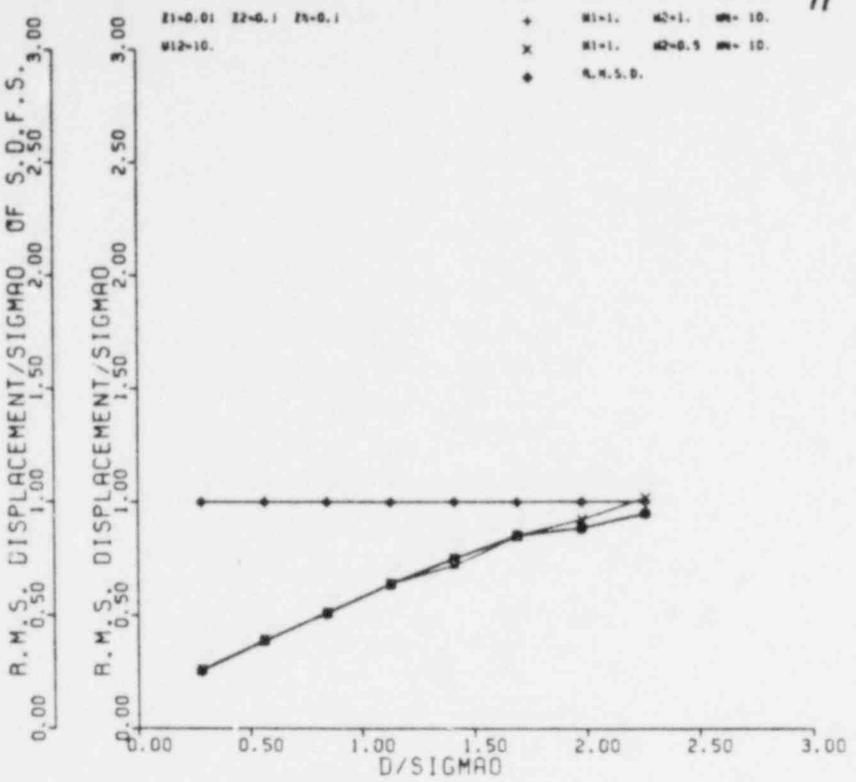

R_{11}

Figure R12

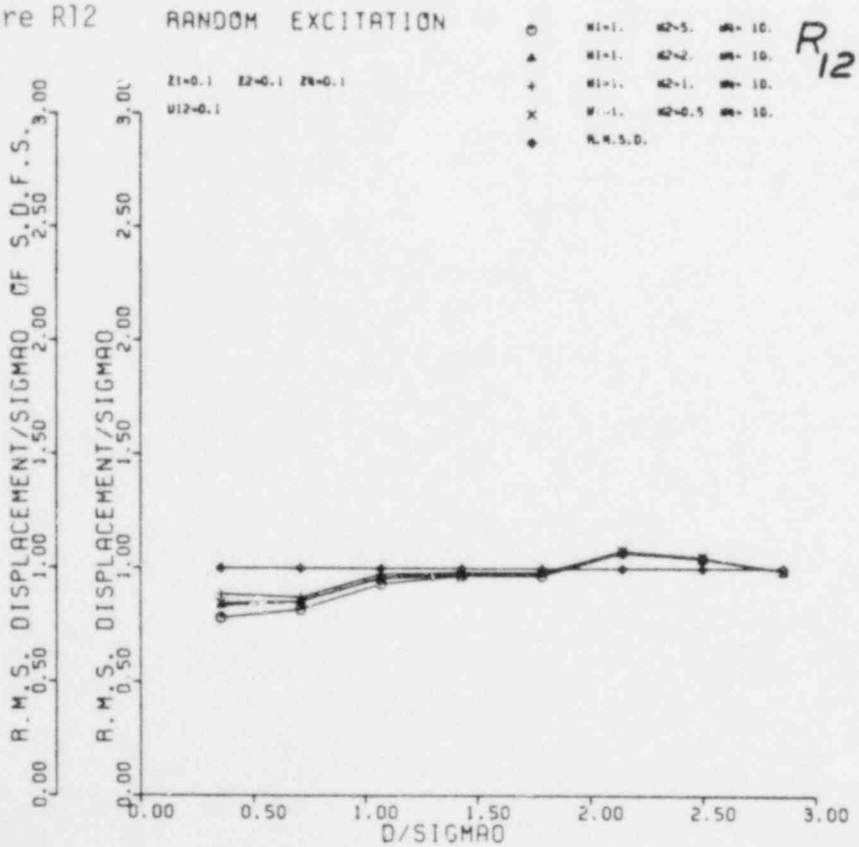

R_{12}

Figure R13

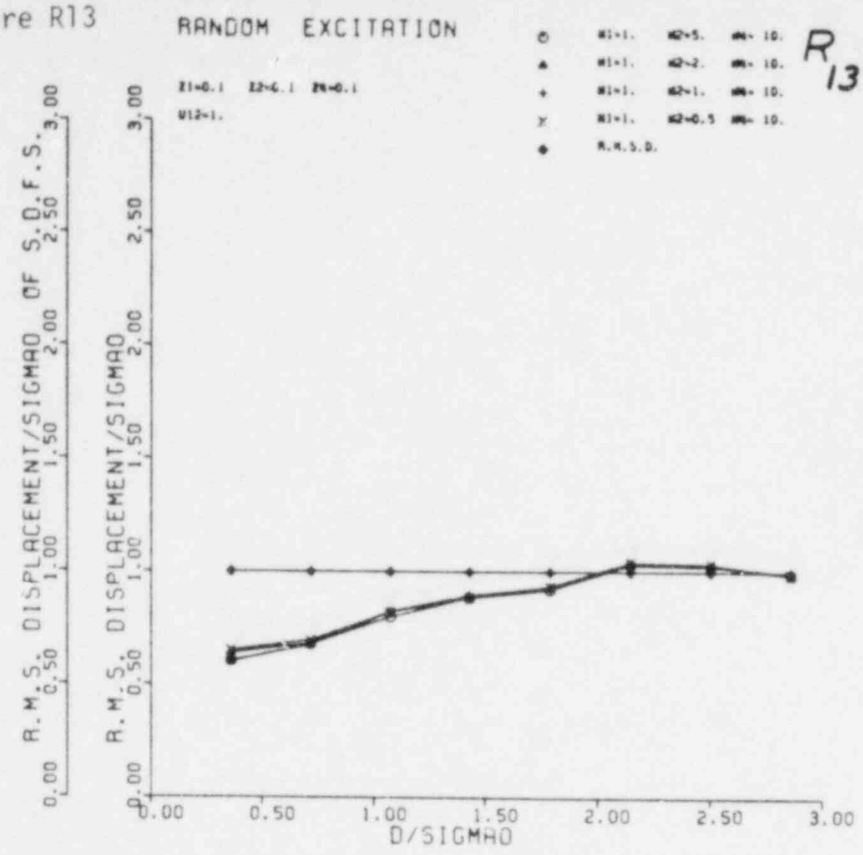

R13

Figure R14

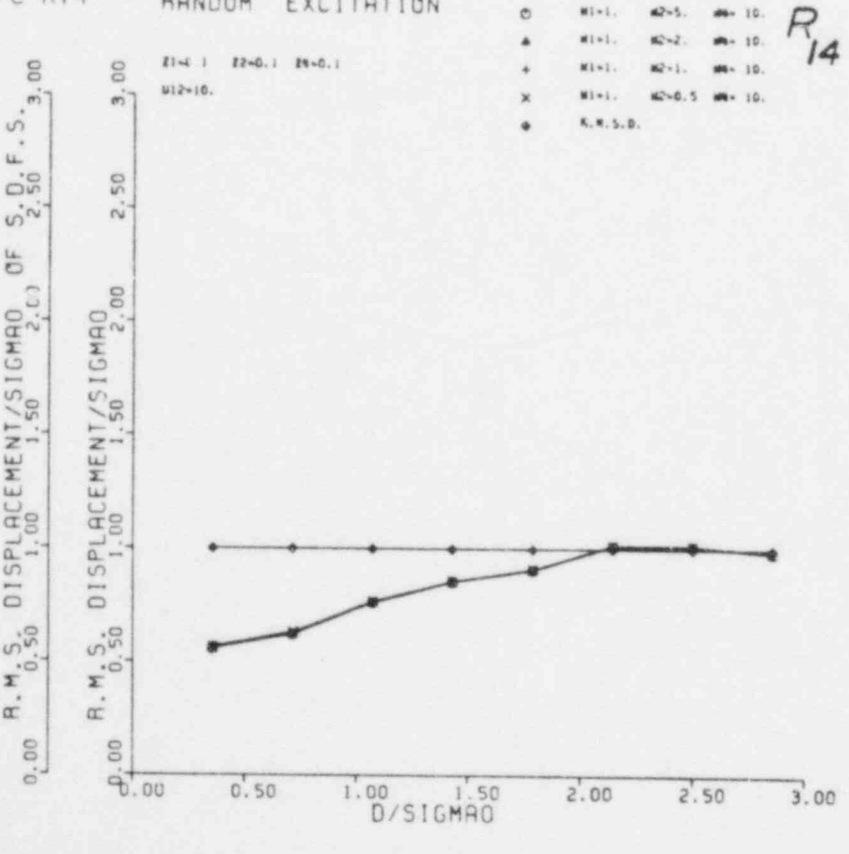

R14

Figure R15

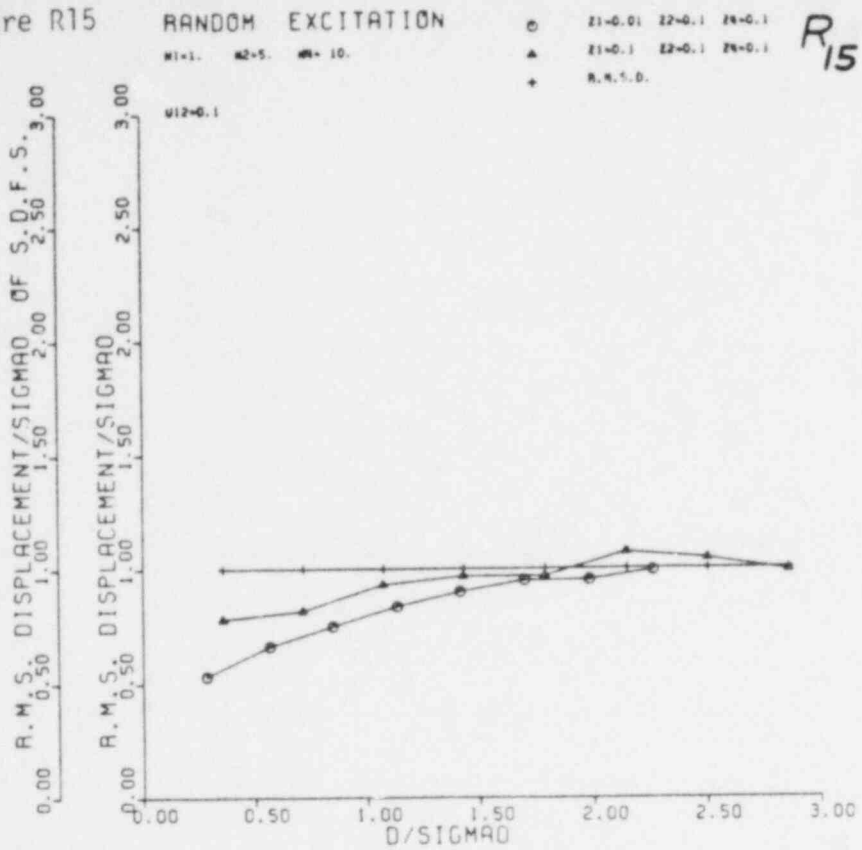

R_{15}

Figure R16

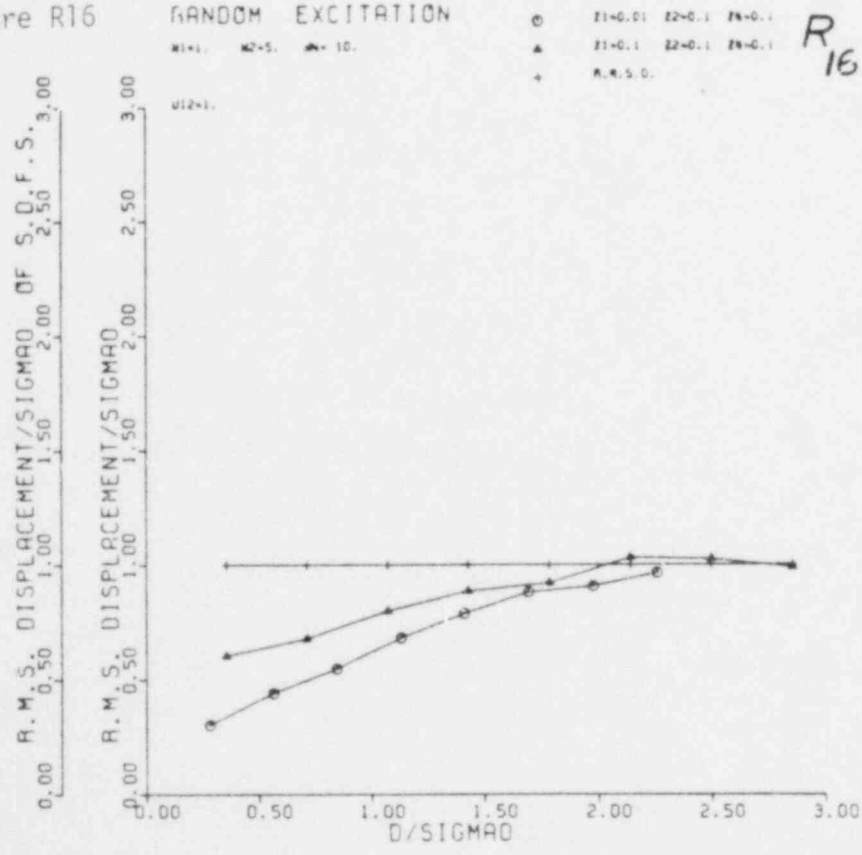

R_{16}

Figure R17

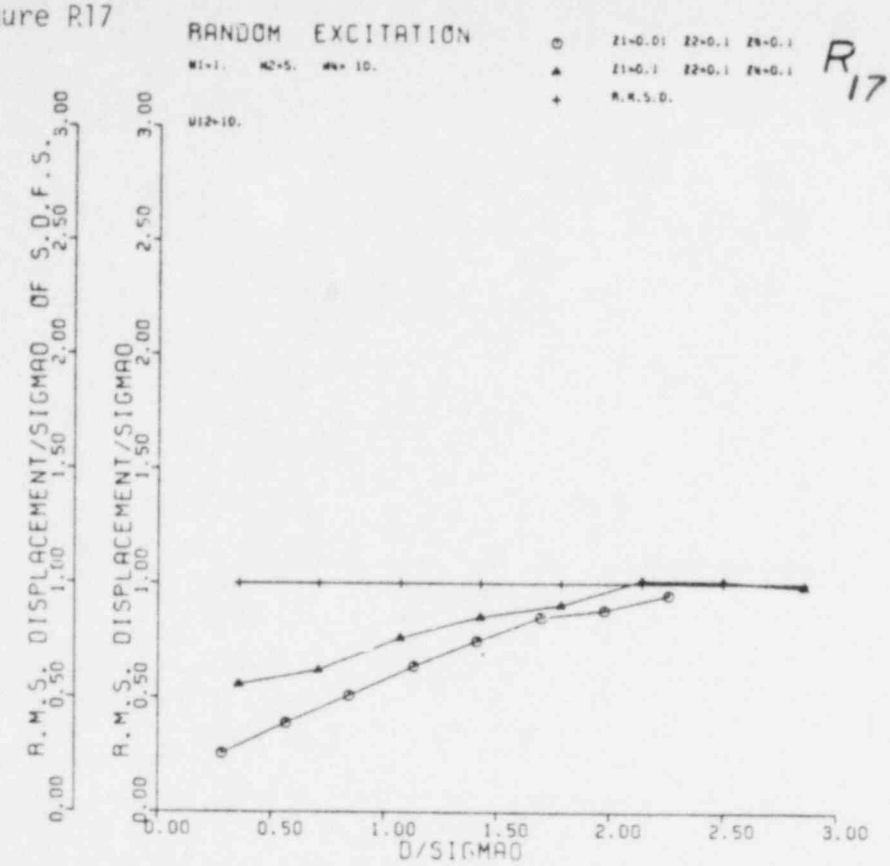

R17

Figure R18

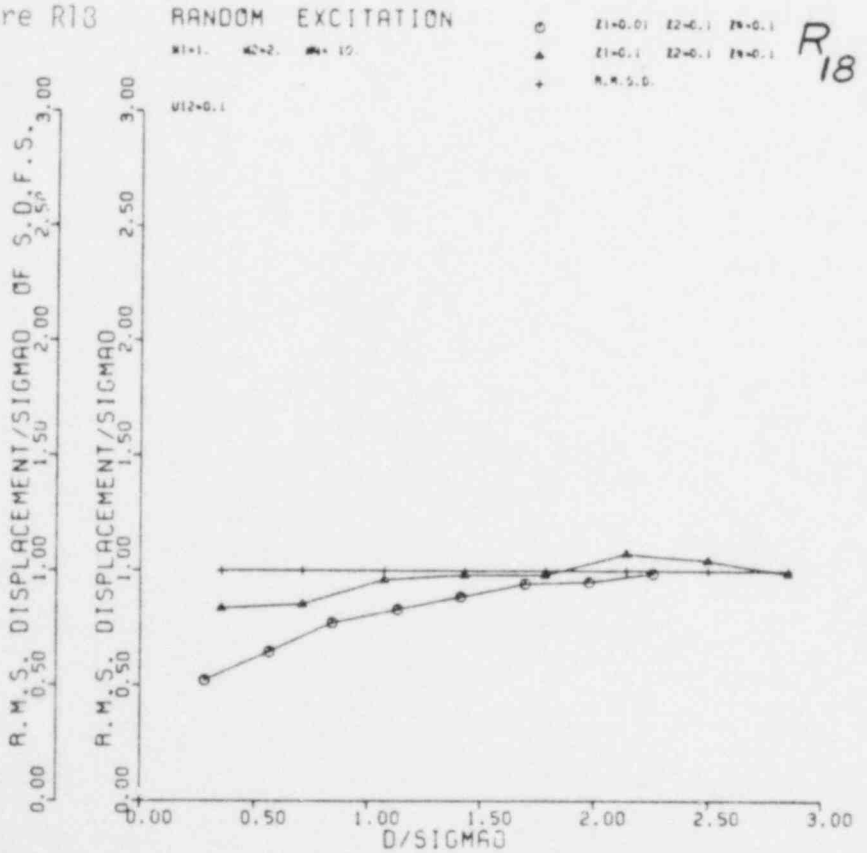

R18

Figure R19

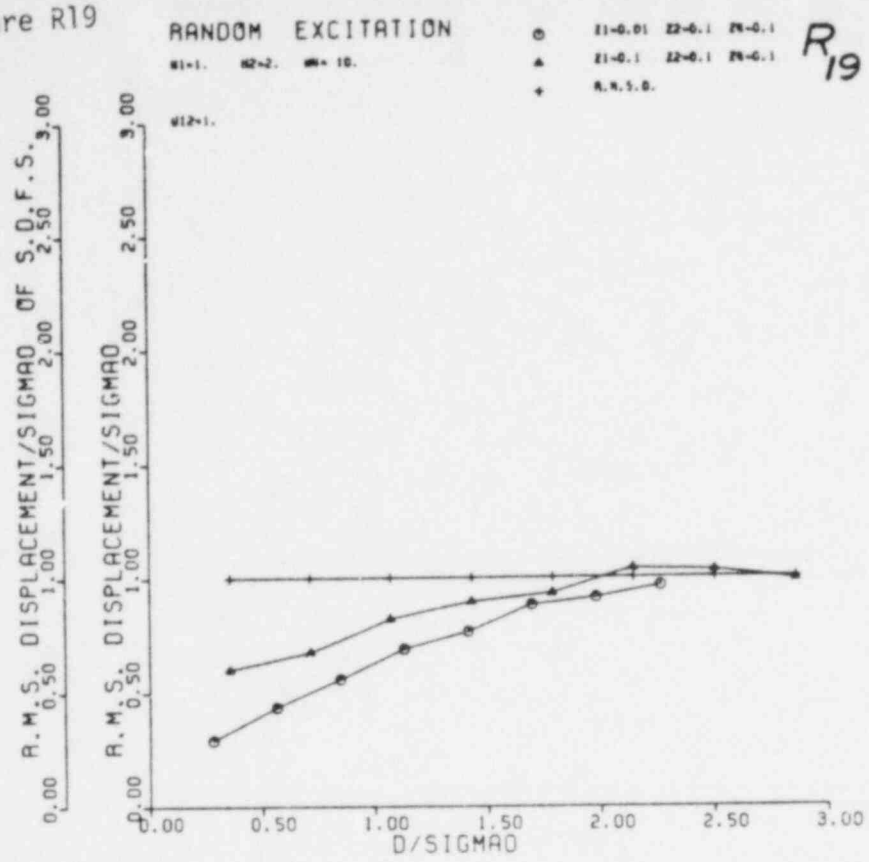

R_{19}

Figure R20

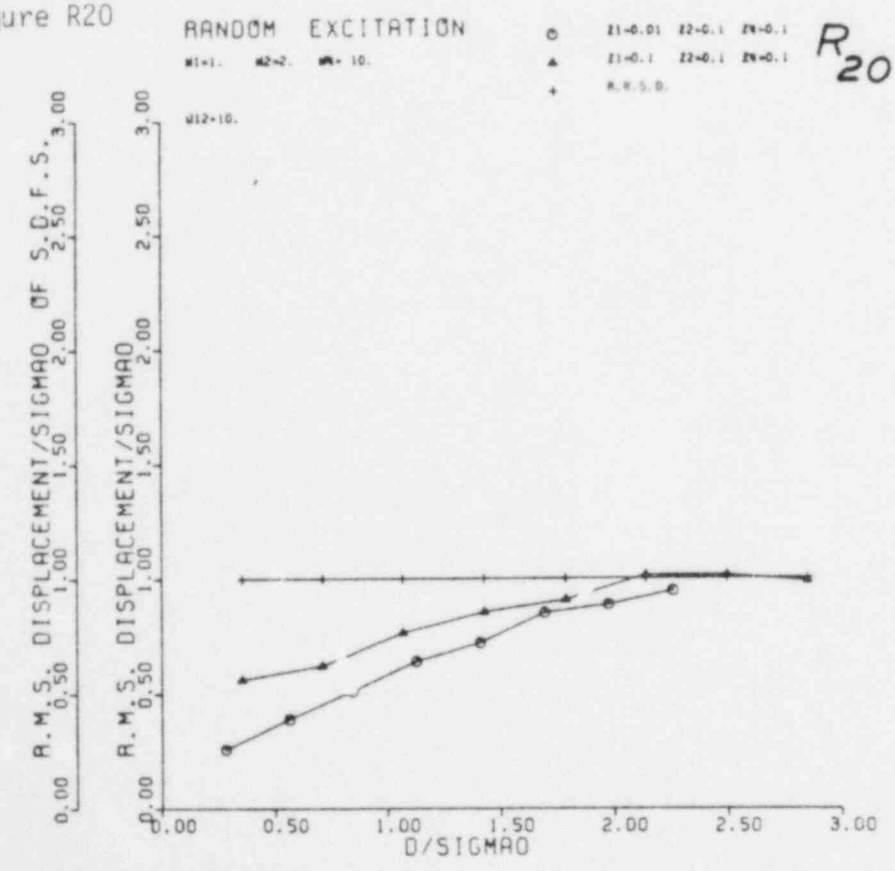

R_{20}

Figure R21

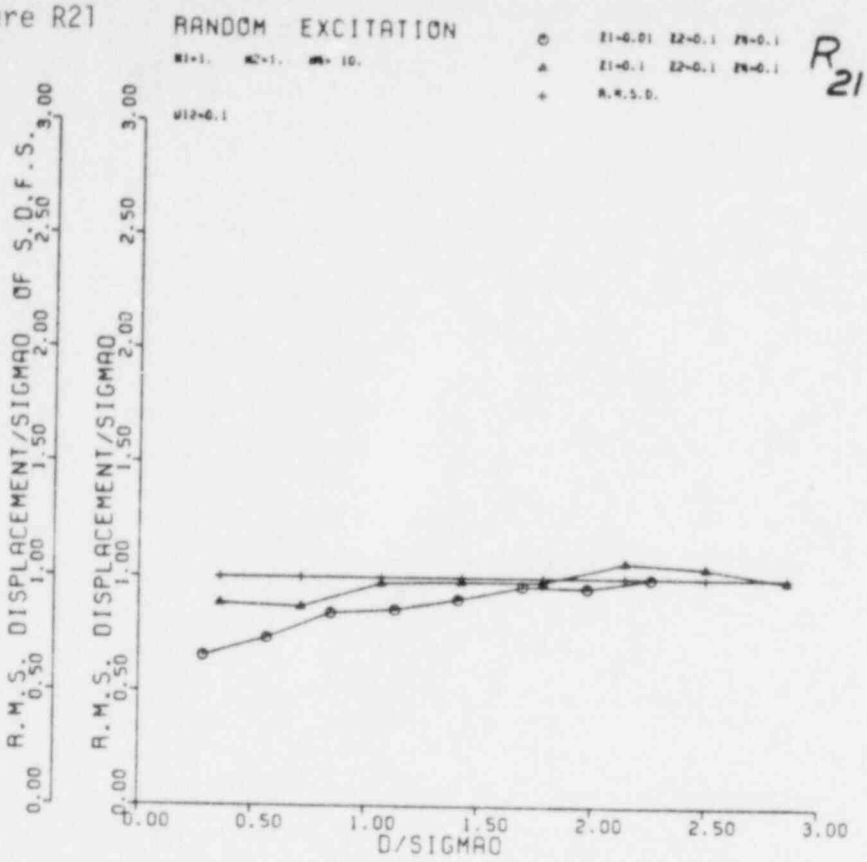

R21

Figure R22

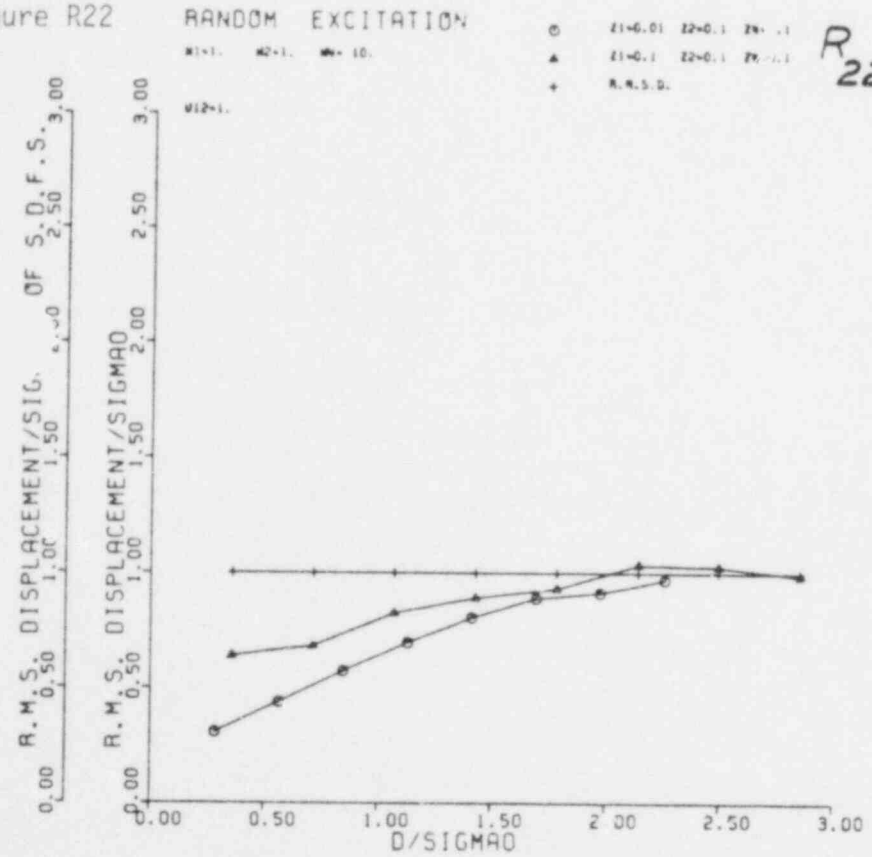

R22

Figure R23

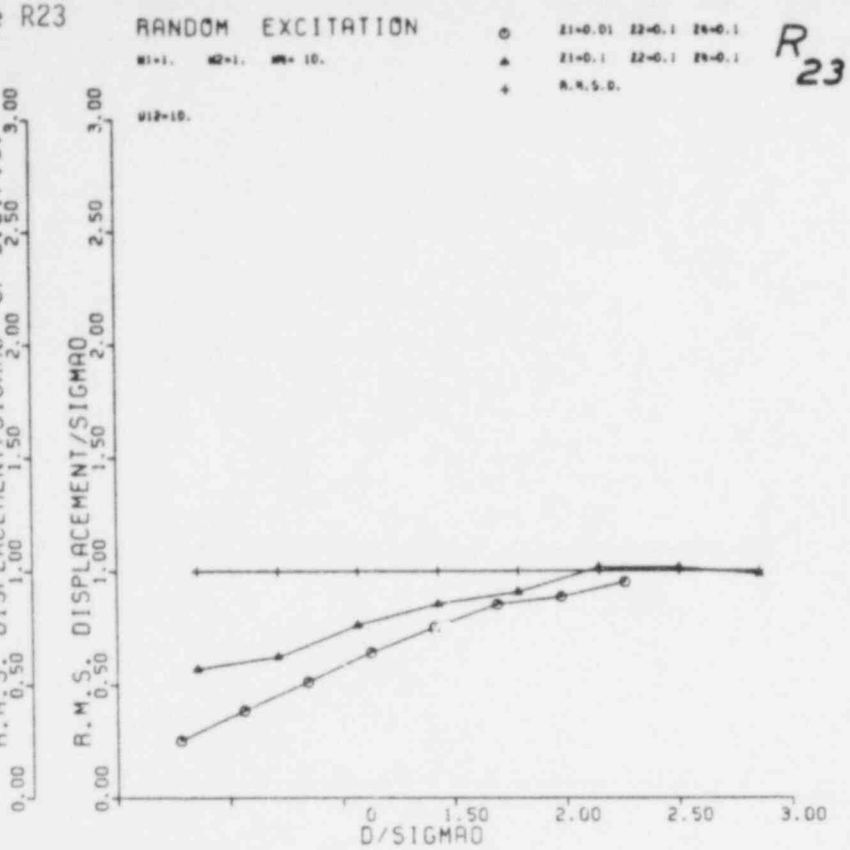

R23

Figure R24

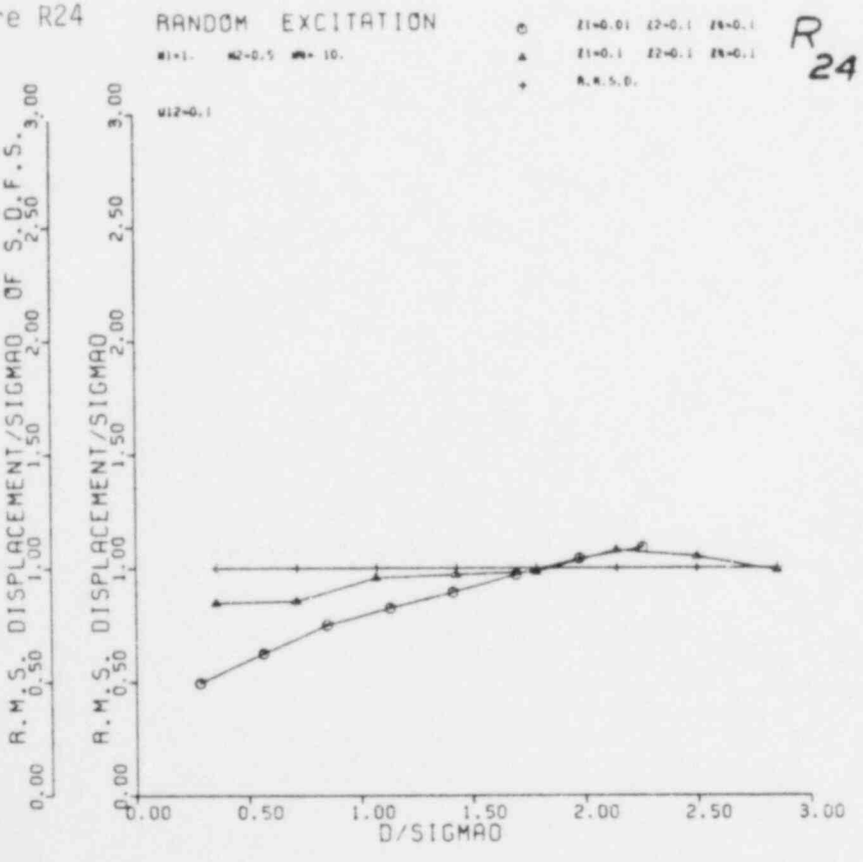

R24

Figure R25

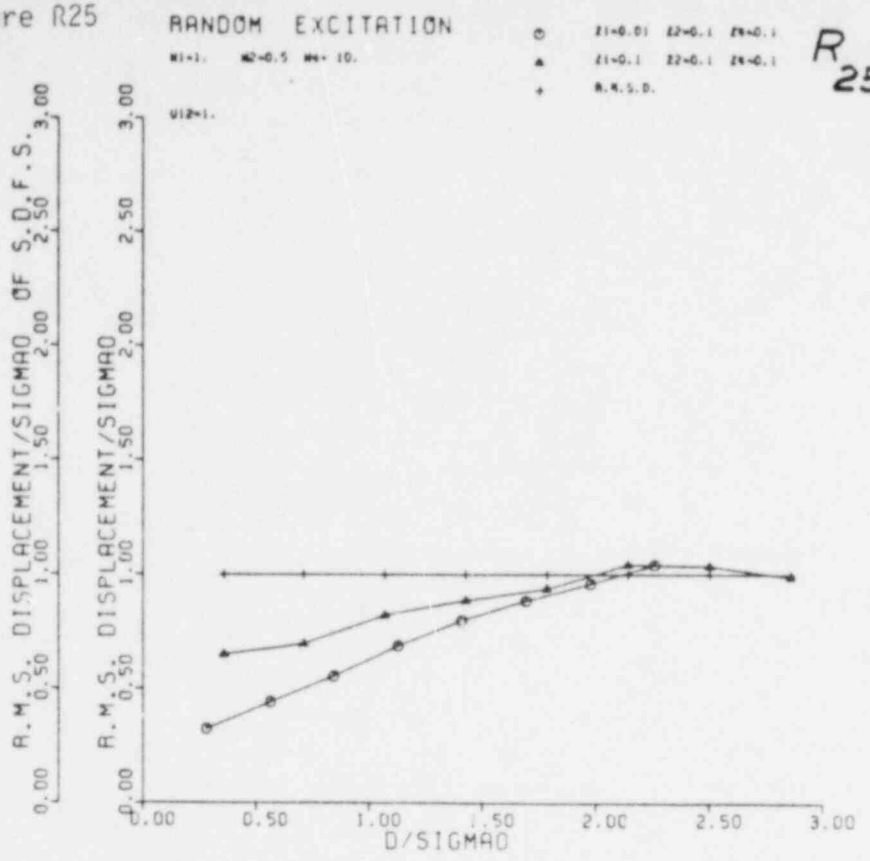

R25

Figure R26

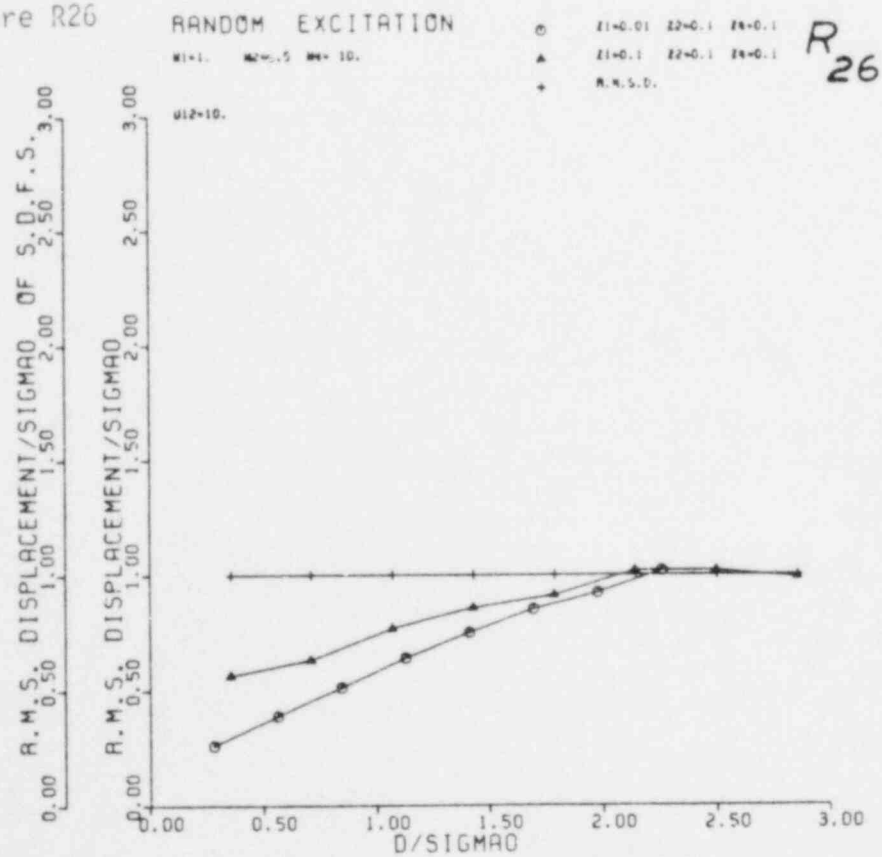

R26

SECTION 5

SUMMARY AND CONCLUSIONS

This report contains a collection of design charts for a class of nonlinear multi-degree-of-freedom systems with gaps under a variety of dynamic loads. The charts are presented in three sections:

- Section 4A contains numerically generated response spectra for the system model when subjected to harmonic excitation. The data are presented in a format that displays dimensionless positive peak response $x_{max}/(F_o/K_1)$ and dimensionless negative peak response $x_{min}/(F_o/K_1)$ versus the dimensionless frequency ratio ω/ω_1.

- Section 4B contains numerically generated response spectra for a half-sine pulse. These data are presented in a format that displays dimensionless peak response versus dimensionless excitation duration ratio τ/T_1.

- Section 4C contains numerically generated response spectra for the system model when subjected to broadband random excitation (i.e., uniform power spectral density). These data are presented in a format that displays dimensionless root mean square displacements, $RSMD/\sigma_{x_o}$, of the primary system M_1 versus the dimensionless gap-size ratio, D/σ_{x_o}, where σ_{x_o} is the RMSD of a primary system with an infinite gap (i.e., a linear SDOF system).

The frequency ratio ω_4/ω_1 and the damping ratio ζ_4, which control the loss of energy during impact, were chosen on the basis of previous research experience and experimental data that are available in the literature (Masri and Ibrahim, 1973). The two parameters that model the impact phenomena remained constant throughout the charts presented in this study.

Review of the response spectra presented in this report, as well as other parametric studies that were performed, allows the following conclusions to be made about parameter trends and their effect on the peak response x_1 of the primary mass of the system model (See Tables 5.1 - 5.8):

(1) Increasing the damping ratio ζ_1 decreases the displacement response x_1.

A review of the response spectra data included in Section 4 shows that, in general, increasing the damping ratio ζ_1 will reduce the displacement response x_1. For a factor of 10 increase (i.e., from 0.01 to 0.10) in damping ζ_1, reductions of 10% to 70%, depending on the values of other system parameters, are observed. Unfortunately, the effect for pulse (half-sine) excitation is not as drastic as that observed for sinusoidal or random excitation since the system does not have sufficient time to mobilize energy dissipation effects before the peak response is reached. For sinusoidal excitation, the reduction in displacement response is also greatly influenced by the frequency ratio ω_2/ω_1 and the mass ratio μ. It is important to note for random excitation, although the absolute RMS displacement response decreases, the plotted ratio RMSD/σ_{x_o}, where σ_{x_o} is the RMSD of the SDOF system with infinite gap-size ratio D/σ_{x_o}, increases.

(2) Increasing the mass ratio μ decreases the displacement response x_1.

Random, sinusoidal, and pulse response spectra data clearly show that for the range of parameters investigated in this report, a tenfold increase in μ (i.e., from 1.0 to 10.0) yields reductions in displacement response x_1 of 15% to 50%

of the theoretical linear SDOF values.

(3) Decreasing the gap-size ratio decreases the displacement response x_1 in both directions.

A reduction of the gap-size ratio (that is, $D/(F_o/K_1)$) for pulse and sinusoidal excitation and D/σ_{x_o} for random excitations will definitely reduce the peak response of the system. Obviously, the maximum displacement response will occur when the gap ratio is infinitely large (i.e., the system has become a linear SDOF oscillator). Harmonic displacement response seems to be more drastically affected by variations in gap-size ratio than are the displacement responses due to pulse or random excitation. It is observed that gap-size ratio reductions of 50% can yield displacement response reductions of 10% to 50%, depending upon other system parameters and type of excitation. Displacement away from target is just slightly different from displacement into target.

(4) The effect of the relative stiffness ω_2/ω_1 depends upon the type of excitation and other system parameters.

A review of response spectra contained in Sections 4A - 4C show that for all the values of stiffness ratios (i.e., ω_2/ω_1 = 0.5, 1,2,5) the random or pulse displacement responses depend on the interaction between the frequency ratio (ω_2/ω_1) and the gap ratio ($D/(F_o/K_1)$). However, for harmonic excitation the relative effect of the stiffness ratio is also dependent upon the excitation frequency ratio ω/ω_1 as well as the gap ratio. For example, Figures S_1, S_{13}, S_{25} and S_{37} clearly show that the positive peak response ratio $x_{max}/(F_o/K_1)$ has an approximately 6%

greater value for $\omega_2/\omega_1 = 2$ than $\omega_2/\omega_1 = 1$ at the excitation frequency $\omega/\omega_1 = 1.2$. On the contrary, for the same system parameter values and an excitation frequency $\omega/\omega_1 = 0.85$ the positive peak response, $x_{max}/(F_o/K_1)$, for $\omega_2/\omega_1 = 1$ has 22.8% greater value than the peak positive $\omega_2/\omega_1 = 2$. Thus, from the above results it can be concluded that hardening of the stiffness ratio ω_2/ω_1 for harmonic excitation does not necessarily imply smaller peak displacement responses over a wide frequency band. Some consideration of the excitation frequency range is suggested, especially for softer ω_2/ω_1 ratios and larger gap ratios.

(5) The secondary system critical damping ratio ζ_2 has little effect on displacement response x_1.

A review of included data shows that, for the range of parameters investigated, little effect is obtained by varying the parameter ζ_2. To save space, only $\zeta_2 = 0.1$ values are presented for the pulse and random excitation library plots (Sections 4B and 4C).

Table 5.1 Effects of System Parameters on Peak Response under Harmonic Excitation
($\omega_4/\omega_1 = 10$, $\zeta_4 = 0.1$, $\zeta_2 = 0.01$, $D/(F_o/K_1) = 1$)

Mass Ratio $\mu = \frac{m_2}{m_1}$	Stiffness Ratio $\frac{\omega_2}{\omega_1}$	Damping Ratio ζ_1	Plot No.	Approximate Peak Values in Range $\omega/\omega_1 = 0.8$ to 1.3			Percentage Peak Reduction Due to Changes in ζ_1		Percentage Peak Reduction Due to Changes in ω_2/ω_1	
				Positive	ω/ω_1	Negative	Positive	Negative	Positive	Negative
0.1	0.5	0.01	S_{37}	10.0	1.15	10.0				
		0.10	S_{39}	3.6	1.10	3.9	64	61		
	5.0	0.01	S_1	10.0	1.3	10.0			0	0
		0.10	S_3	2.9	1.2	4.0	71	60	19	≈0
1.0	0.5	0.01	S_{41}	4.6	1.3	7.2				
		0.10	S_{43}	2.6	1.25	3.4	43	53		
	5.0	0.01	S_5	1.8	1.3	4.5			61	38
		0.10	S_7	1.6	1.3	3.1	11	31	38	9
10.0	0.5	0.01	S_{45}	1.4	1.3	2.7				
		0.10	S_{47}	1.2	1.3	2.2	14	8		
	5.0	0.01	S_9	1.2	1.3	2.4			14	11
		0.10	S_{11}	1.1	1.25	2.2	8	8	8	8

Table 5.2 Effects of System Parameters on Peak Response under Harmonic Excitation
($\omega_4/\omega_1 = 10$, $\zeta_4 = 0.1$, $\zeta_2 = 0.1$, $D/(F_o K_1) = 1$)

Mass Ratio $\mu = \frac{m_2}{m_1}$	Stiffness Ratio $\frac{\omega_2}{\omega_1}$	Damping Ratio ζ_1	Plot No.	Approximate Peak Values in Range ω/ω_1 = 0.8 to 1.3			Percentage Peak Reduction Due to Changes in ζ_1		Percentage Peak Reduction Due to Changes in ω_2/ω_1	
				Positive	ω/ω_1	Negative	Positive	Negative	Positive	Negative
0.1	0.5	0.01	S_{38}	8.73	1.05	9.89				
		0.10	S_{40}	3.47	1.05	3.95	60	60		
	5.0	0.01	S_2	8.18	1.2	10.09			6	2
		0.10	S_4	2.93	1.15	4.02	64	60	16	2
1.0	0.5	0.01	S_{42}	4.64	1.3	6.6				
		0.10	S_{44}	2.59	1.25	3.34	44	49		
	5.0	0.01	S_6	1.5	1.3 Constant	4.09			68	38
		0.10	S_8	1.36	1.3 Constant	2.73	9	33	47	18
10.0	0.5	0.01	S_{46}	1.5	1.3	2.66				
		0.10	S_{48}	1.36	1.3	2.32	9	13		
	5.0	0.01	S_{10}	1.09	Constant	2.32			27	13
		0.10	S_{12}	0.95	Constant	1.98	13	15	30	15

Table 5.3 Effects of System Parameters on Peak Response under Harmonic Excitation ($\zeta_1 = 0.1$, $\zeta_2 = 0.1$, $\omega_2/\omega_1 = 5$, $\omega_4/\omega_1 = 10$)

Mass Ratio $\mu = \frac{m_2}{m_1}$	Clearance Ratio $\frac{D}{F_o/K_1}$	Plot No.	Approximate Peak Values in Range ω/ω_1 = 0.8 to 1.3			Penetration $\frac{X_{max}}{D}$
			Positive	ω/ω_1	Negative	
0.1	0.25	S_{49}	2.45	1.25	3.95	9.8
1.0		S_{55}	0.48	Constant	1.9	1.92
10.0		S_{61}	0.27	Constant	1.64	1.08
0.1	0.5	S_{50}	2.59	1.2	3.95	5.18
1.0		S_{56}	0.55	Constant	2.18	1.1
10.0		S_{62}	0.41	Constant	1.77	1.02
0.1	0.75	S_{51}	2.73	1.2	4.09	3.6
1.0		S_{57}	1.09	Constant	2.45	1.45
10.0		S_{63}	0.82	Constant	1.77	1.09
0.1	1.0	S_3	2.9	1.2	4.0	2.9
1.0		S_7	1.6	1.3	3.1	1.6
10.0		S_{11}	1.1	1.25	2.2	1.1
0.1	2.0	S_{52}	3.82	1.10	4.43	1.91
1.0		S_{58}	2.45	1.15	3.2	1.22
10.0		S_{64}	2.05	Constant	2.73	1.02
0.1	4.0	S_{54}	4.77	1.0	4.77	1.19
1.0		S_{60}	4.3	1.0	4.5	1.07
10.0		S_{66}	4.0	0.95	4.23	1.0

Table 5.4 Effects of System Parameters on Peak Response under Pulse Excitation
($\omega_4/\omega_1 = 10$, $\zeta_\ell = 0.1$, $\zeta_2 = 0.1$, $D/(F_o/K_1) = 0.4$)

Mass Ratio $\mu = \frac{m_2}{m_1}$	Stiffness Ratio $\frac{\omega_2}{\omega_1}$	Damping Ratio ζ_1	Plot No.	Approximate Peak Values in Range $\tau/T_1 = 0.5$ to 3.0			Percentage Peak Reduction Due to Changes in ζ_1		Percentage Peak Reduction Due to Changes in ω_2/ω_1	
				Posi[illegible]	τ/T_1	Negative	Positive	Negative	Positive	Negative
0.1	0.5	0.01	P_{55}	1.63	0.75	1.54				
		0.10	P_{56}	1.44	0.75	1.032	12	33		
	5.0	0.01	P_1	0.95	0.5	1.1			42	2[illegible]
		0.10	P_2	0.86	0.5	0.79	9	28	40	23
1.0	0.5	0.01	P_{61}	1.3	0.75	1.24				
		0.10	P_{62}	1.18	0.75	0.84	9	32		
	5.0	0.01	P_7	0.62	0.25	0.62			52	50
		0.10	P_8	0.5	0.5 0.25	0.46	19	26	58	45
10.0	0.5	0.01	P_{67}	0.67	1.5 1.0	0.61				
		0.10	P_{68}	0.67	1.75 1.0	0.46	0	25		
	5.0	0.01	P_{13}	0.42	0.25	0.42			37	31
		0.10	P_{14}	0.4	0.25	0.32	5	21	40	30

Table 5.5 Effects of System Parameters on Peak Response under Pulse Excitation
($\omega_4/\omega_1 = 10$, $\zeta_4 = 0.1$, $\zeta_2 = 0.1$, $D/(F_c/K_1) = 1.2$)

Mass Ratio $\mu = \frac{m_2}{m_1}$	Stiffness Ratio $\frac{\omega_2}{\omega_1}$	Damping Ratio ζ_1	Plot No.	Approximate Peak Values in Range $\tau/T_1 = 0.5$ to 3.0			Percentage Peak Reduction Due to Changes in ζ_1		Percentage Peak Reduction Due to Changes in ω_2/ω_1	
				Positive	τ/T_1	Negative	Positive	Negative	Positive	Negative
0.1	0.5	0.01	P_{59}	1.66	0.75	1.54				
		0.10	P_{60}	1.49	0.75	1.03	10	33		
	5.0	0.01	P_5	1.57	0.75 0.5	1.46			5	5
		0.10	P_6	1.45	0.75 0.5	0.98	8	33	3	5
1.0	0.5	0.01	P_{65}	1.3	0.5	1.25				
		0.10	P_{66}	1.27	0.75 0.5	0.91	2	27		
	5.0	0.01	P_{11}	1.3	0.5	1.24			0	0
		0.10	P_{12}	1.28	0.75 0.5	0.91	2	27	0	0
10.0	0.5	0.01	P_{71}	1.2	0.5	1.13				
		0.10	P_{72}	1.2	0.5	0.88	0	22		
	5.0	0.01	P_{17}	1.22	0.5	1.14			0	0
		0.10	P_{18}	1.22	0.5	1.14	0	0	0	

Table 5.6 Effects of System Parameters on Peak Response under Random Excitation ($\omega_4/\omega_1 = 10$, $\zeta_4 = 0.1$, $\zeta_2 = 0.1$, $D/\sigma_{x_o} = 0.5$)

Mass Ratio $\mu = \frac{m_2}{m_1}$	Stiffness Ratio $\frac{\omega_2}{\omega_1}$	Damping Ratio ζ_1	Plot No.	$\frac{\sigma}{\sigma_{x_o}}$	Percentage Peak Reduction Due to Changes in ζ_1	Percentage Peak Reduction Due to Changes in ω_2/ω_1
0.1	0.5	0.01	R_7	0.60	30	5
		0.10	R_8	0.86		
	5.0	0.01	R_1	0.63	21	
		0.10	R_2	0.80		7
1.0	0.5	0.01	R_7	0.42	38	0
		0.10	R_8	0.68		
	5.0	0.01	R_1	0.42	33	
		0.10	R_2	0.63		7
10.0	0.5	0.01	R_7	0.36	40	0
		0.10	R_8	0.6		
	5.0	0.01	R_1	0.36	37	
		0.10	R_2	0.57		5

Table 5.7 Effects of System Parameters on Peak Response under Random Excitation
($\omega_4/\omega_1 = 10$, $\zeta_4 = 0.1$, $\zeta_2 = 0.1$, $D/\sigma_{x_o} = 1.0$)

Mass Ratio $\gamma_1 = \frac{2}{1}$	Stiffness Ratio $\frac{\omega_2}{\omega_1}$	Damping Ratio ζ_1	Plot No.	$\frac{\sigma}{\sigma_{x_o}}$	Percentage Peak Reduction Due to Changes in ζ_1	Percentage Peak Reduction Due to Changes in ω_2/ω_1
0.1	0.5	0.01	R_7	0.80	14	0
		0.10	R_8	0.93		
	5.0	0.01	R_1	0.80	11	
		0.10	R_2	0.90		3
1.0	0.5	0.01	R_7	0.63	19	0
		0.10	R_8	0.78		0
	5.0	0.01	R_1	0.63	19	
		0.10	R_2	0.78		
10.0	0.5	0.01	R_7	0.57	24	0
		0.10	R_8	0.75		
	5.0	0.01	R_1	0.57	0	
		0.10	R_2	0.57		24

Table 5.8 Effects of System Parameters on Peak Response under Random Excitation ($\omega_4/\omega_1 = 10$, $\zeta_4 = 0.1$, $\zeta_2 = 0.1$, $D/\sigma_{x_o} = 2.0$)

Mass Ratio $\mu = \frac{m_2}{m_1}$	Stiffness Ratio $\frac{\omega_2}{\omega_1}$	Damping Ratio ζ_1	Plot No.	$\frac{\sigma}{\sigma_{x_o}}$	Percentage Peak Reduction Due to Changes in ζ_1	Percentage Peak Reduction Due to Changes in ω_2/ω_1
0.1	0.5	0.01	R_7	1.05	0	
		0.10	R_8	1.05		
	5.0	0.01	R_1	0.96	7	9
		0.10	R_2	1.035		1
1.0	0.5	0.01	R_7	0.96	4	
		0.10	R_8	1.0		
	5.0	0.01	R_1	0.92	7	4
		0.10	R_2	0.99		1
10.0	0.5	0.01	R_7	0.93	5	
		0.10	R_8	0.98		1
	5.0	0.01	R_1	0.89	10	4
		0.10	R_2	0.99		

SECTION 6

REFERENCES

1. Anderson, J.C., and Masri, S.F., Analytical/Experimental Correlation of a Nonlinear System Subjected to a Dynamic Load, Report No. CE 79-07, University of Southern California, Department of Civil Engineering, Los Angeles, California, June 1979.

2. Anderson, J.C., and Singh, A.K., "Inelastic Response of Nuclear Piping Subjected to Rupture Forces", Trans. ASME, Journal of Pressure Vessel Technology, Vol. 98, Series J, No. 2, May 1976.

3. Bechtel Power Corp., Design for Pipe Break Effects, Topical Report No. BN-TOP-2, May 1974.

4. Biggs, J.M., Introduction to Structural Dynamics, McGraw-Hill, New York, 1964.

5. Crandall, S.H., and Mark, W.D., Random Vibration in Mechanical Systems, Academic Press, New York, 1963.

6. Dokanish, M.A., and Elmadary, M.M., "On the Nonlinear Response of a Relief Valve", Trans. ASME, Journal of Mechanical Design, Vol. 100, No. 4, Oct. 1978, pp. 675-680.

7. Harris, C.M., and Crede, C.E., Shock and Vibration Handbook, second ed., McGraw-Hill, New York, 1961.

8. Lyons, J.L., and Askland, C.L., Lyons Encyclopedia of Valves, Van Nostrand and Reinhold Co., New York, 1975.

9. Masri, S.F., and Ibrahim, A.M., "Stochastic Excitation of a Simple System with Impact Damper", in Earthquake Engineering and Structural Dynamics, Vol. 1, 1973, pp. 337-346.

10. Masri, S.F., and Stott, S.J., Computer Program for a Class of Nonlinear Systems with Gaps under a Variety of Dynamic Loads, Report No. CE 79-10, University of Southern California, Department of Civil Engineering, Los Angeles, California, June 1979.

11. Onesto, A.T., Snubber Sensitivity Study, Report No. EETC-TDR-78-17, Energy Technology Engineering Center, Sept. 1978.

12. University of Southern California, Analytical and Experimental Studies of Nonlinear Systems Modeling and Scaling, NRC Report NUREG-0192-1, U.S.C., Los Angeles, California, 1976.

APPENDIX A

EXAMPLE APPLICATIONS

EXAMPLE 1. PIPING SYSTEM WITH SNUBBERS

The first illustrative example is the analysis of a segment of a typical nuclear piping system, as shown in Figure A1.1, with an installed seismic restraint (i.e., snubber). This system is a representation of a leg of the main steam piping of a nuclear power plant and a typical seismic restraint. The analysis of such a problem requires the following procedures:

(1) Discretization of the piping system and seismic restraint into single-degree-of-freedom systems with physical parameters as shown in Figure A1.2. These single-degree-of-freedom systems are representative of a multi-degree-of-freedom system with a gap (Figure A1.2), where piping is represented by the primary system and the seismic restraint by the secondary system.

(2) Analysis of the dynamic response of this multi-degree-of-freedom equivalent system by use of the response spectra provided in this report for various system characteristics.

Obviously, because of the unavailability of plotted response spectra for all possible system parameters, the use of response spectra is limited to those practical problems in which geometrical and material properties are such that the idealized equivalent system has the same or approximately the same system characteristics for which response spectra are available. If response spectra for the system of interest are not included in Section 4 of this report, the computer code (Masri and Stott, 1979) can be used directly to determine the required response. In this example problem, the procedures of idealizing a system and using response

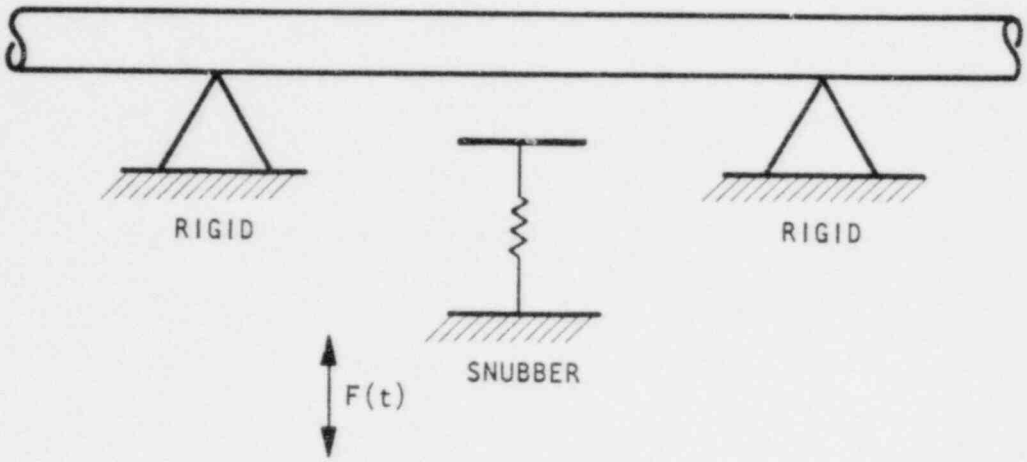

Figure A1.1 Piping with Rupture Restraint

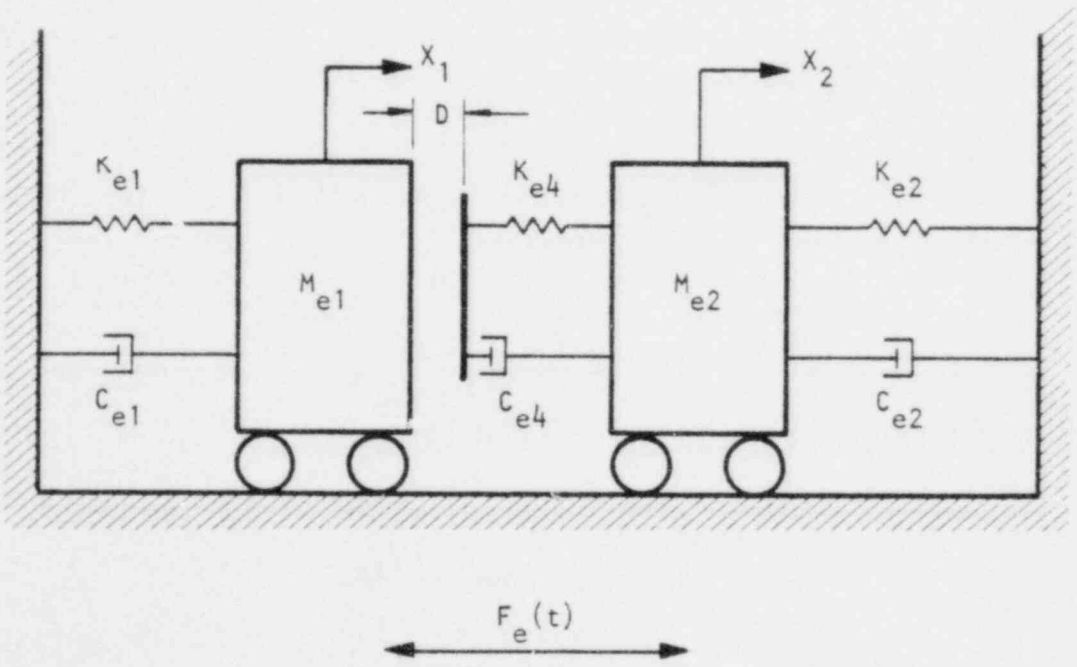

Figure A1.2 Equivalent System - Computer Model

spectra is explained. The material properties were chosen from a typical engineering case (Table A1.1), but the geometrical and loading conditions were chosen such that the final model system would have the same characteristics as a response spectra available from this report.

Idealized System

In order to define an equivalent multi-degree-of-freedom system, it is necessary to evaluate the parameters of that system (M_e, K_e, C_e) as shown in Figure A1.2. Additionally, the load function $F_e(t)$ must be established in order to analyze the system.

A gap of 1 in. was assumed between the pipe and the seismic restraint; an additional spring and viscous dashpot with characteristics K_{e4} and C_{e4} were assumed to be attached in series to mass M_{e2} (equivalent mass of seismic restraint) to include the loss of energy during the impact process. For the seismic restraint, a mass (M_{e2}) equal to 1/10 of the mass of the pipe (M_{e1}) along with a spring constant (K_{e2}) equal to 10^4 lb/in. was assumed. The ratios such as ω_{e2}/ω_{e1} or $D/(F_o/K_{e1})$ were modified to the closest ratios for which the response spectra were available. The building and its foundation were assumed to be rigid so that the ground motion was directly transmitted to the system supports.

The equivalent mass and stiffness for a continuous structure of length L is given by

$$M_e = \int_0^L m\phi^2(x)dx \qquad (1A)$$

where m is the mass/unit length and $\phi(x)$ is the assumed shape function on which the equivalent system is based. For a simply supported beam

Table A1.1

Properties of Pipe

Outside diameter	=	30 in.
Wall thickness	=	1 in.
Weight per unit length (m)	=	32 lb/in.
Young's modulus (E)	=	2.58×10^7 psi
Length of pipe (l)	=	40 feet
Moment of inertia (I)	=	9588 $in.^4$

with a distributed load (i.e., Figure A1.1) the shape function can be written as

$$\phi(x) = \frac{16}{5L^4}\left(L^3x - 2Lx^3 + x^4\right) \tag{2A}$$

Using equations 1A and 2A the equivalent mass is

$$M_e = \int_0^L m\left[\frac{16}{5L^4}\left(L^3x - 2Lx^3 + x^4\right)\right]^2 dx \tag{3A}$$

$$M_e = \frac{256m}{25L^8}\int_0^L\left[L^6x^2 + 4L^2x^6 + x^8 - 4L^4x^4 + 2L^3x^5 - 4Lx^7\right]dx$$

$$M_e = \frac{256m}{25L^8}\left[\frac{L^6x^3}{3} + \frac{4L^2x^7}{7} + \frac{x^9}{9} - \frac{4L^4x^5}{5} + \frac{2L^3x^6}{6} - \frac{4Lx^8}{8}\right]_0^L$$

$$M_e = \frac{256m}{25L^8}\left[\frac{31L^9}{630}\right]$$

$$M_e = 0.504\,(mL) \tag{4A}$$

Define the mass factor by $K_m = \frac{M_e}{M}$, then

$$K_m = \frac{0.504\,(mL)}{(mL)} = 0.504 \tag{5A}$$

In the same manner the load factor K_L can be computed by the following equation:

$$K_L = \frac{\int_0^L p\phi(x)dx}{pL} \tag{6A}$$

where p is load per unit length.

Substituting for $\phi(x)$, then

$$K_L = \frac{\int_0^L p\left[\frac{16}{5L^4}(L^3x - 2Lx^3 + x^4)\right] dx}{pL}$$

$$K_L = \frac{16}{5L^5}\left[\frac{L^3x^2}{2} - \frac{2Lx^4}{4} + \frac{x^5}{5}\right]_0^L$$

$$K_L = 0.64 \tag{7A}$$

For a simply supported beam with uniform section, the spring constant K is

$$K = \frac{384EI}{5L^3} \tag{8A}$$

Thus the equivalent spring constant of a one-degree-of-freedom system is

$$K_e = K_L K = 0.64\left[\frac{384EI}{5L^3}\right] \tag{9A}$$

Using E, I and L from Table A1, then

$$K_{e1} = 0.64\left\{\frac{(384)(2.58 \times 10^7)(9588)}{5[(40)(12)]^3}\right\}$$

or $$K_{e1} = 1.1 \times 10^5 \text{ lb/in.} \tag{10A}$$

and $$M_{e1} = K_m(mL)g \quad \text{where } g = 386.4 \text{ in./sec}^2$$

$$M_{e1} = 0.504[(32)(40)(12)]/386.4$$

$$M_{e1} = 20 \frac{\text{lb. sec}^2}{\text{in.}} \tag{11A}$$

The natural frequency for the equivalent one-degree-of-freedom system mass 1 (M_{e1}) is equal to

$$\omega_{e1} = \sqrt{\frac{K_{e1}}{M_{e1}}} = \sqrt{\frac{1.1 \times 10^5}{20}} = 74.2 \frac{\text{rad}}{\text{sec}} \tag{12A}$$

Assuming $M_{e2} = (\frac{1}{10})M_{e1}$, then the natural frequency for mass 2 (M_{e2}) is

$$\omega_{e2} = \sqrt{\frac{K_{e2}}{M_{e2}}} = \sqrt{\frac{10^4}{2.00}} = 70.7 \frac{rad}{sec} \quad (13A)$$

Consequently, $$\frac{\omega_{e2}}{\omega_{e1}} = \frac{70.7}{74.2} = 0.95 \quad (14A)$$

Since there is no response spectrum available for this exact frequency ratio, $\omega_{e2}/\omega_{e1} = 1$ will be chosen for analysis. The spring constant K_{e4} is chosen such that $\omega_{e4}/\omega_{e1} = 10$ and damping ratios ζ_{e1}, ζ_{e2} and ζ_{e4} are all taken equal to 0.1.

This example will be analyzed for three types of loading: sinusoidal, shock, and stationary random excitation.

Sinusoidal Excitation

Assume the piping is subjected to a motion of the type

$$x = A \sin \omega t \quad (16A)$$

at the supports. Consequently, it then undergoes a uniform acceleration $\ddot{x}$ along the pipe

$$\ddot{x} = -A \omega^2 \sin \omega t \quad (17A)$$

and the equivalent force acting on the equivalent mass M_{e1} is

$$\begin{aligned} F_{e1}(t) &= K_L F(t) \\ &= K_L (m L \ddot{x}) \\ &= K_L (-mLA\omega^2 \sin \omega t) \end{aligned} \quad (18A)$$

If is assumed that $A = -1$ and $\omega/\omega_{e1} = 0.9$, then

$$F_{el}(t) = 0.64 \left\{ - \frac{32}{386.4} (40)(12)(-1) \left[(0.9)(74.2) \right]^2 \right\} \sin \omega t$$

$$F_{el}(t) = (1.135 \times 10^5) \sin \omega t \qquad (19A)$$

and considering, $F_{el} = F_o \sin \omega t$, then

$$\frac{F_o}{K_{el}} = \frac{1.135 \times 10^5}{1.1 \times 10^5} = 1.032 \qquad (20A)$$

The ratio of gap size to equivalent static deflection

$$D/(F_o/K_{el}) = \frac{1.0}{1.032} = 0.969 \approx 1 \qquad (21A)$$

Having all the required values such as mass ratio, stiffness ratio, frequency ratio of the excitation force, and damping ratios, the maximum positive and maximum negative displacements are obtained from the appropriate response spectra curve (Figure A1.3)

$$x_{positive} = x_{negative} = 4.2 \, (F_o/K_{el})$$

Pulse Excitation

Assume a half-sine pulse excitation function with duration $\tau = 0.5T_1$ where T_1 is the period of the equivalent mass-spring system (M_{el}) for the pipe, applied to the supports of the pipe. Similarly, as for the example of sinusoidal excitation, the pipe undergoes a uniformly acceleration x along the beam:

$$x = [-A\omega^2] \sin \omega t \qquad (22A)$$

If $A = -1$, $\omega = \omega_{el}$ and $t \leq 0.5T_1$, the equivalent force is then equal to

$$F_{el} = K_L(m\ddot{Lx}) = 0.64 \left\{ \left(\frac{32}{386.4} \right) (40)(12)(74.2)^2 \right\} \sin \omega t$$

or

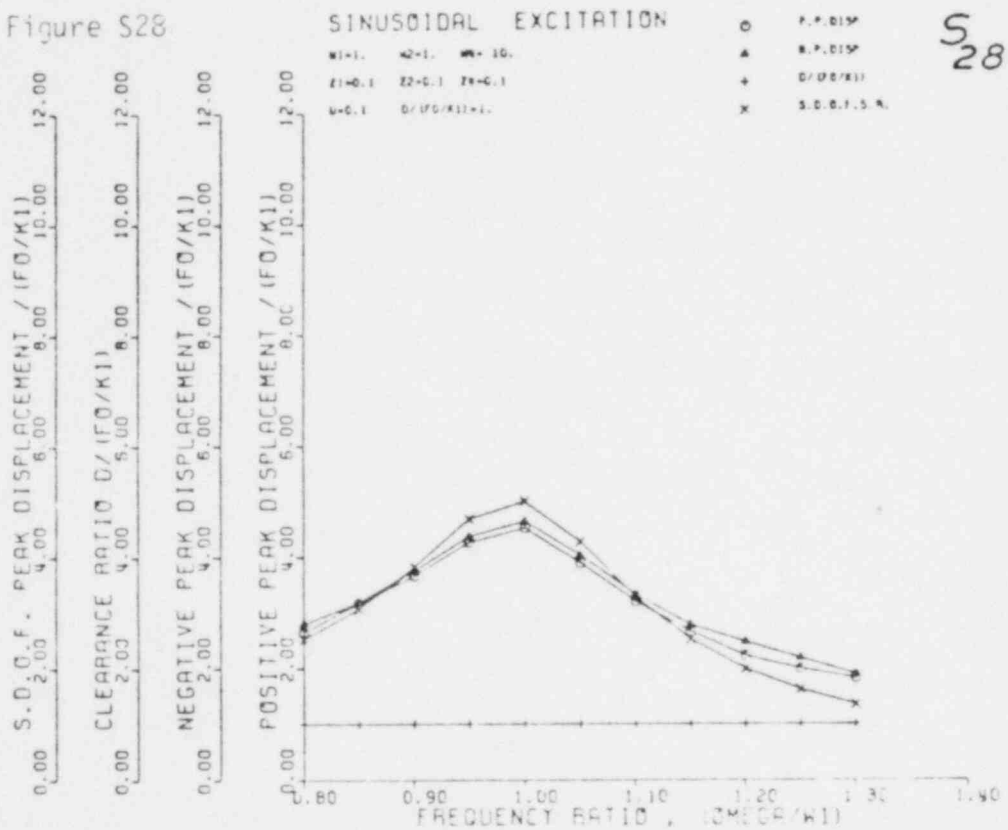

Figure A1.3 Response Spectra: Harmonic Excitation, Example 1
(Section 4A, Figure S28, page 4A-17)

$$F_{el} = (1.4 \times 10^5) \sin \omega t \qquad t \leq 0.5T_1 \qquad (23A)$$

with the resulting $F_o = 1.4 \times 10^5$.

Thus,

$$\frac{F_o}{K_{el}} = \frac{1.4 \times 10^5}{1.1 \times 10^5} = 1.27 \text{ in.}$$

and the gap static delfection ratio is

$$\frac{D}{(F_o/K_{el})} = \frac{1}{1.27} = .787 \approx 0.8 \qquad (24A)$$

Referrring to the response spectrum displayed in Figure A1.4, the positive and negative peak displacements are:

$$x_{1(max)} = 1.26(F_o/K_{el}) \qquad (25A)$$

$$x_{1(min)} = 0.91(F_o/K_{el}) \qquad (26A)$$

Stationary Random Excitation

The pipe would be subjected to a uniformly distributed random acceleration as a result of random excitation at the supports. Assume that the power spectral density of this acceleration is equal to S_o and the excitation has a zero mean value. Then the equivalent single-degree-of-freedom system has a power spectral density equal to

$$S_{el} = K_L^2 S_0 \qquad (27A)$$

Assuming that S_o=1 g^2-sec (g = 386.4 in./sec^2), then the standard deviation of the displacement response of the equivalent single-degree-of-freedom system is

$$\sigma_o = \frac{\pi S_{el}}{2\zeta_{el}\omega_{el}^3} = \frac{(3.14)(0.64)^2(386.4)^2}{(2)(0.1)(74.2)^3} = 1.53 \text{ in.} \qquad (28A)$$

Figure P40

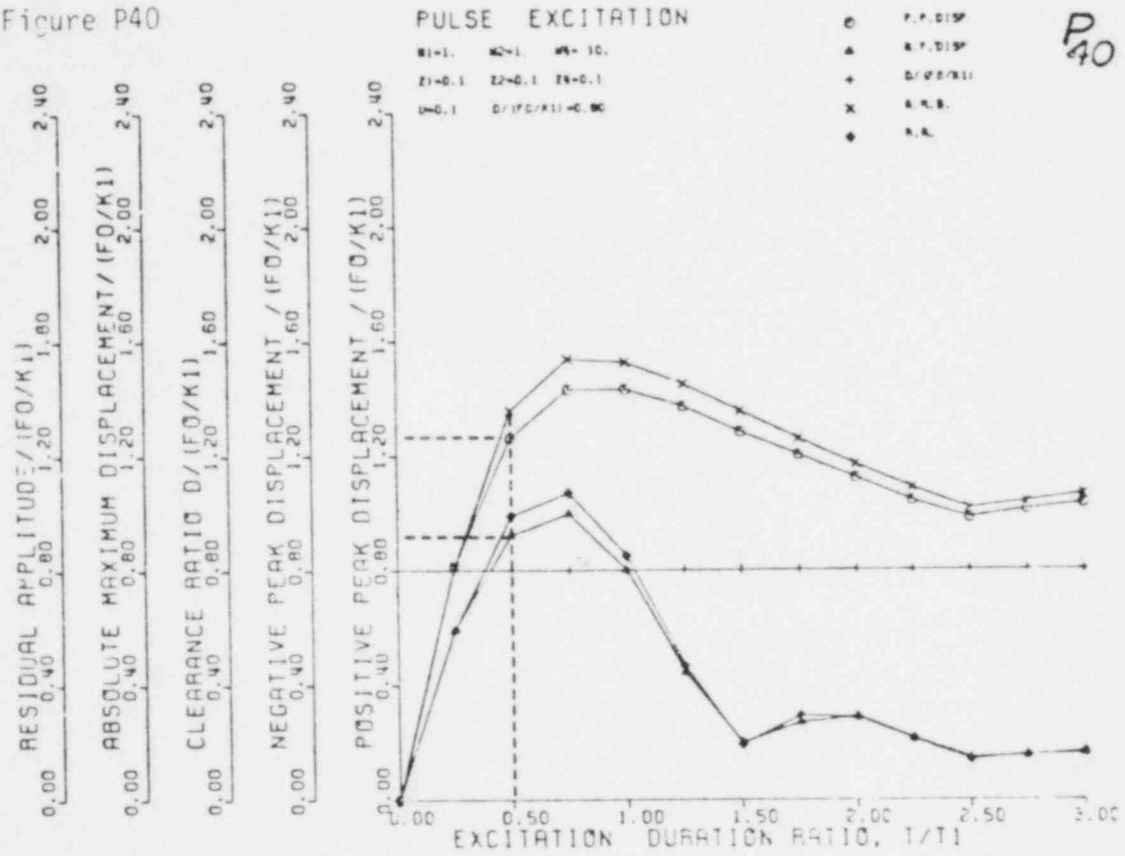

Figure A1.4 Response Spectra: Pulse Excitation (Half-Sine), Example 1 (Section 4B, Figure P40, page 4B-23)

Having values of σ_o, D and other system characteristics, the root mean square response of the equivalent mass (M_{el}) could be obtained from the response spectra (Figure A1.5)

The resulting answer is

$$RMS = 0.85\ \sigma_o \qquad \text{for } D/\sigma_o = 1/1.53 \qquad (29A)$$

which shows that a gap of this size (D = 1) has only a slight effect on the output root mean square displacement response of the primary system (M_{el}).

Figure R6

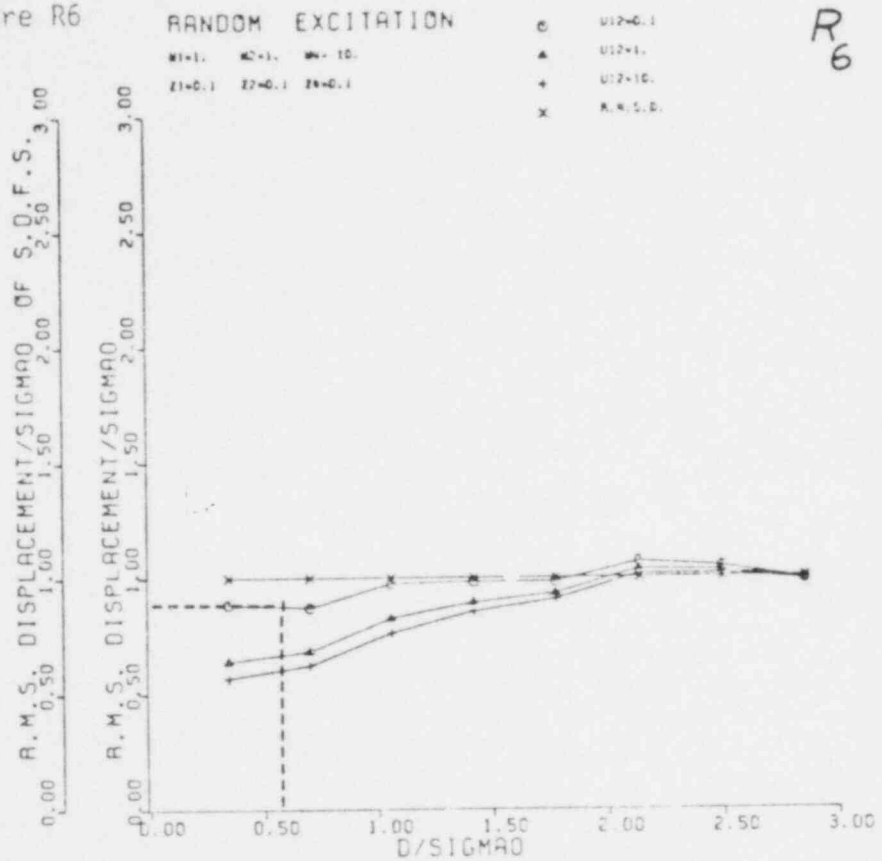

R6

Figure A1.5 Response Spectra: Random Excitation, Example 1
(Section 4C, Figure R6, page 4C-4)

EXAMPLE 2. SPRING-MOUNTED EQUIPMENT

Suppose a machine having a total weight of 2000 lb is mounted on a spring having a modulus of 20 kips/in. and is connected to a dashpot with a damping factor equal to 0.1 of its critical value. Assume that the machine contains a rotating eccentric part with a mass m = 100 lb, and a rotational speed of 600 rpm. To prevent high-amplitude vibration, a motion-limiting stop is placed, as shown in Fig. A2.1, at a distance D from the machine base.

Problem:

Given the above, obtain: (a) the farthest point away from the machine that the motion stopper could be placed in order to reduce the vibration to less than half of its normal magnitude; (b) the percentage of reduction in displacement if the motion stopper is placed 1 in. away from the machine; and (c) the percentage of reduction in displacement if the stiffness of the spring of the motion stopper, placed as in (b) is taken to be the same as the stiffness of the machine.

Solution:

The inertia force generated by the rotating mass is

$$F_1 = m\, r\, \omega_f^2 = \frac{100}{386.4}\,(20)\,(20\pi)^2 = 20{,}433.96 \text{ lb}$$

where $\omega_f = 2\pi\left(\frac{600}{60}\right) = 20\pi$ rad/sec and $r = 20$ in.

The natural frequency of the machine is

$$\omega_1 = \sqrt{\frac{K_1}{M_1}} = \sqrt{\frac{20{,}000}{2000/386.4}} = \sqrt{3864} = 62.16 \text{ rad/sec}$$

Thus, the excitation frequency ratio is

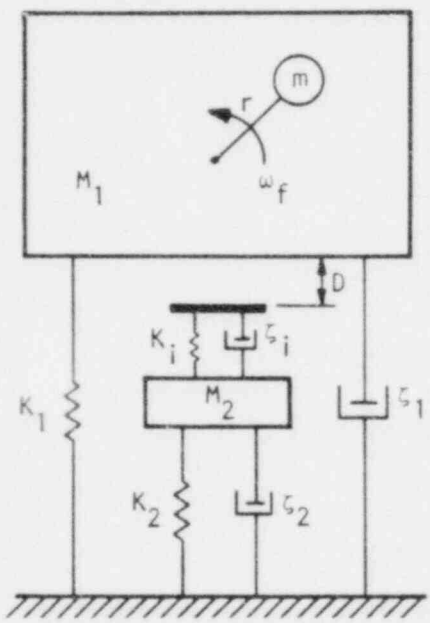

Figure A2.1 Spring-mounted Equipment

$$\frac{\omega_f}{\omega_1} = \frac{62.8}{62.16} = 1.01 \approx 1$$

(a) In the absence of a motion-limiting stop, the maximum displacement, using available spectra for $\zeta = 0.1$, is obtained.

$$x_{max} = 5\left(\frac{F_o}{K_1}\right) = 5\left(\frac{20433.96}{20000}\right) = 5.11 \text{ in.}$$

for $\frac{\omega_f}{\omega_1} = 1$

A study of the applicable spectrum shows that a gap size not greater than $0.5(F_o/K_1)$ would reduce the positive displacement (displacement toward the support) and negative displacement (displacement away from the support) to less than half of its normal value (see Figs. A2.2 and A2.3).

From Fig. A2.2,

$$D = 0.25\left(\frac{F_o}{K_1}\right) = 0.25\left(\frac{20,433.96}{20,000}\right) = 0.255 \text{ in.}$$

and

$$x_{positive} = 1.25\left(\frac{F_o}{K_1}\right) = 1.25\left(\frac{20,433.96}{20,000}\right) = 1.27 \text{ in.}$$

$$x_{negative} = 2.0\left(\frac{F_o}{K_1}\right) = 2.0\left(\frac{20,433.96}{20,000}\right) = 2.0 \text{ in.}$$

Similarly, from Figure A2.3

$$D = 0.5\left(\frac{F_o}{K_1}\right) = 0.511 \text{ in.}$$

$$x_{positive} = 1.8\left(\frac{F_o}{K_1}\right) = 1.83 \text{ in.}$$

$$x_{negative} = 2.5\left(\frac{F_o}{K_1}\right) = 2.55 \text{ in.}$$

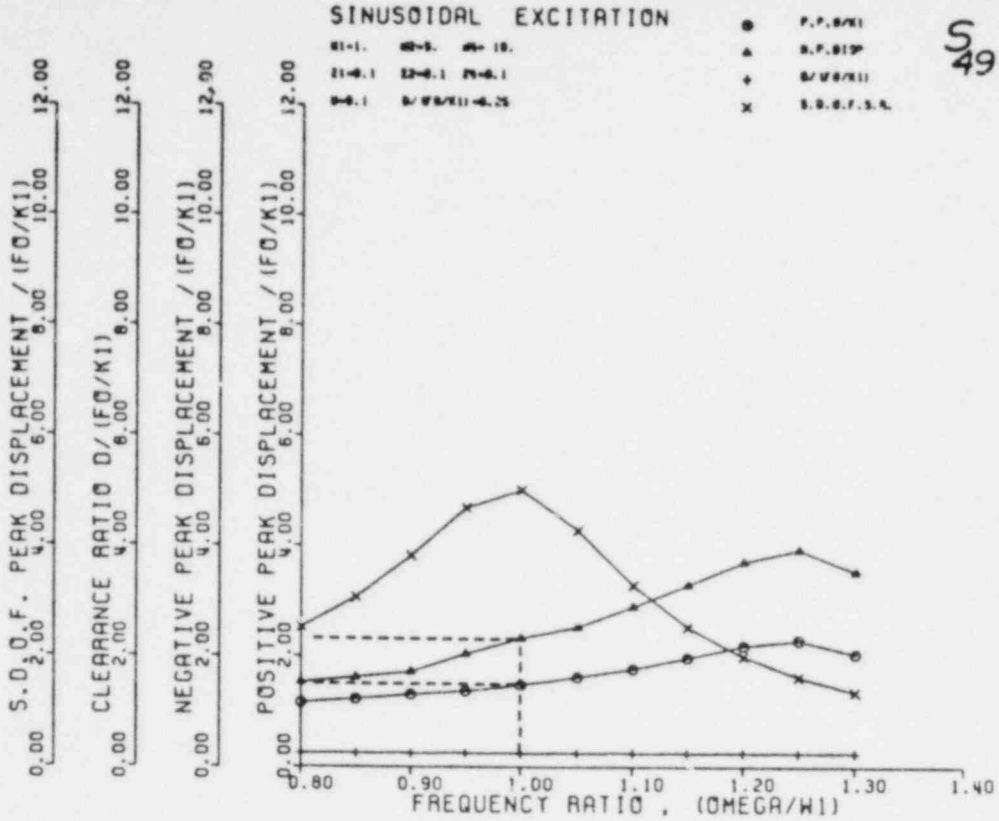

Figure A2.2 Response Spectra: Harmonic Excitation
(Section 4A, Figure S49, page 4A-28)

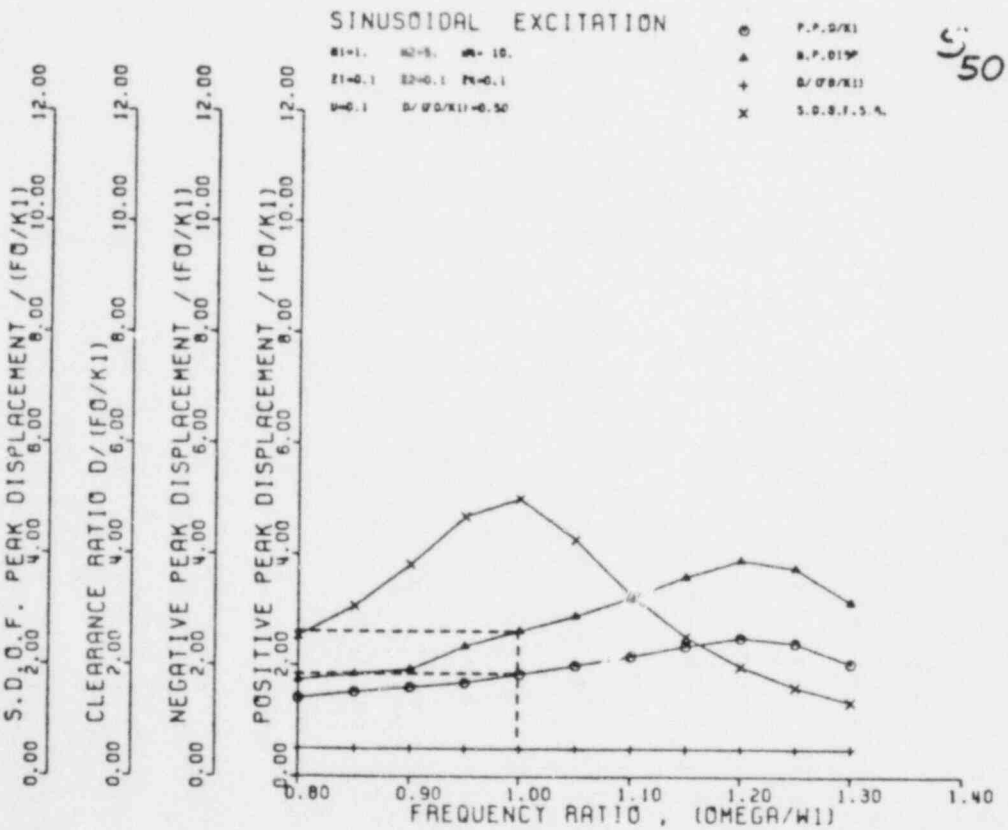

Figure A2.3 Response Spectra: Harmonic Excitation
(Section 4A, Figure S50, page 4A-28)

(b) Using the spectra S_4 (see Fig. A2.4), the maximum positive and negative displacements for D = 1 are obtained.

$$x_{positive} = 2.4\left(\frac{F_o}{K_1}\right) = 2.45 \text{ in.}$$

$$x_{negative} = 2.9\left(\frac{F_o}{K_1}\right) = 2.96 \text{ in.}$$

The percentages of reduction in positive and negative directions are

$$\text{in the positive direction} = \frac{5.11 - 2.45}{5.11} = 52\%$$

$$\text{in the negative direction} = \frac{5.11 - 2.96}{5.11} = 42\%$$

(c) For the case of equal stiffness, i.e. $\omega_2/\omega_1 = \sqrt{K_2/K_1} = 1$, assuming the rest of the parameters to be the same, the spectrum S28 (shown in Fig. A2.5) could be used. The results are

$$x_{positive} = 4.6\left(\frac{F_o}{K_1}\right) = 4.69 \text{ in.}$$

$$x_{negative} = 4.7\left(\frac{F_o}{K_1}\right) = 4.90 \text{ in.}$$

and the percentages of reduction in the positive and negative directions are

$$\text{in the positive direction} = \frac{5.11 - 4.69}{5.11} = 8.20\%$$

$$\text{in the negative direction} = \frac{5.11 - 4.90}{5.11} = 4.10\%$$

Comparison of these values with the corresponding values in (b) of

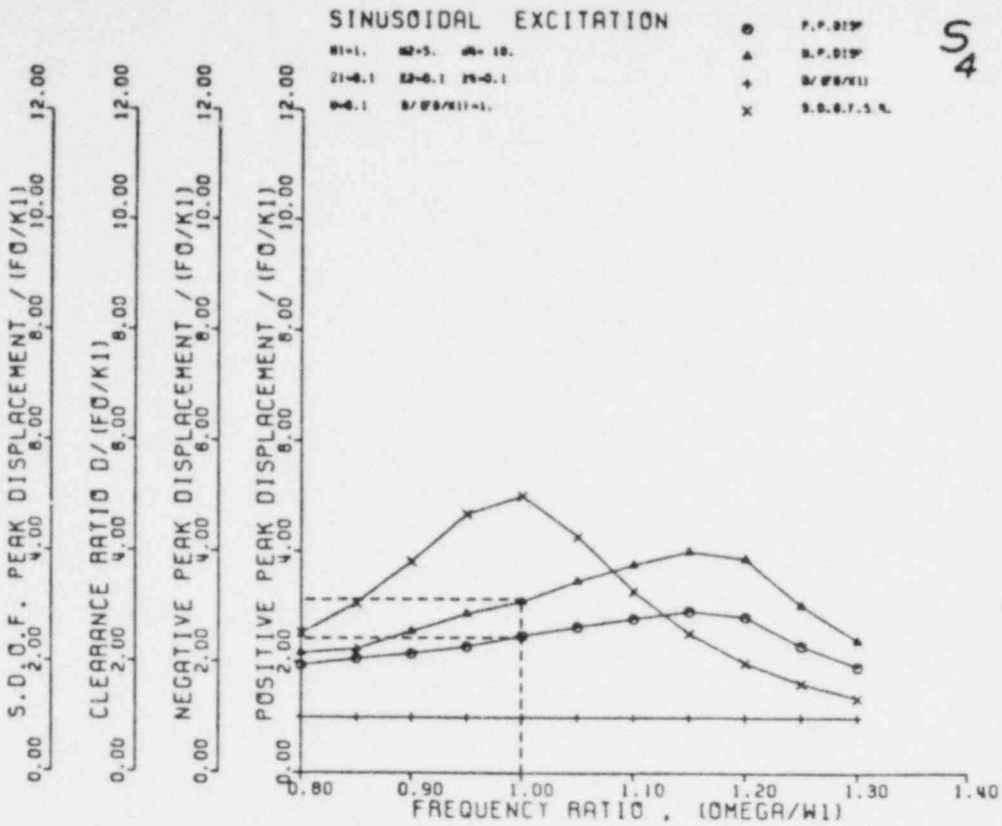

Figure A2.4 Response Spectra: Harmonic Excitation
(Section 4A, Figure S4, page 4A-5)

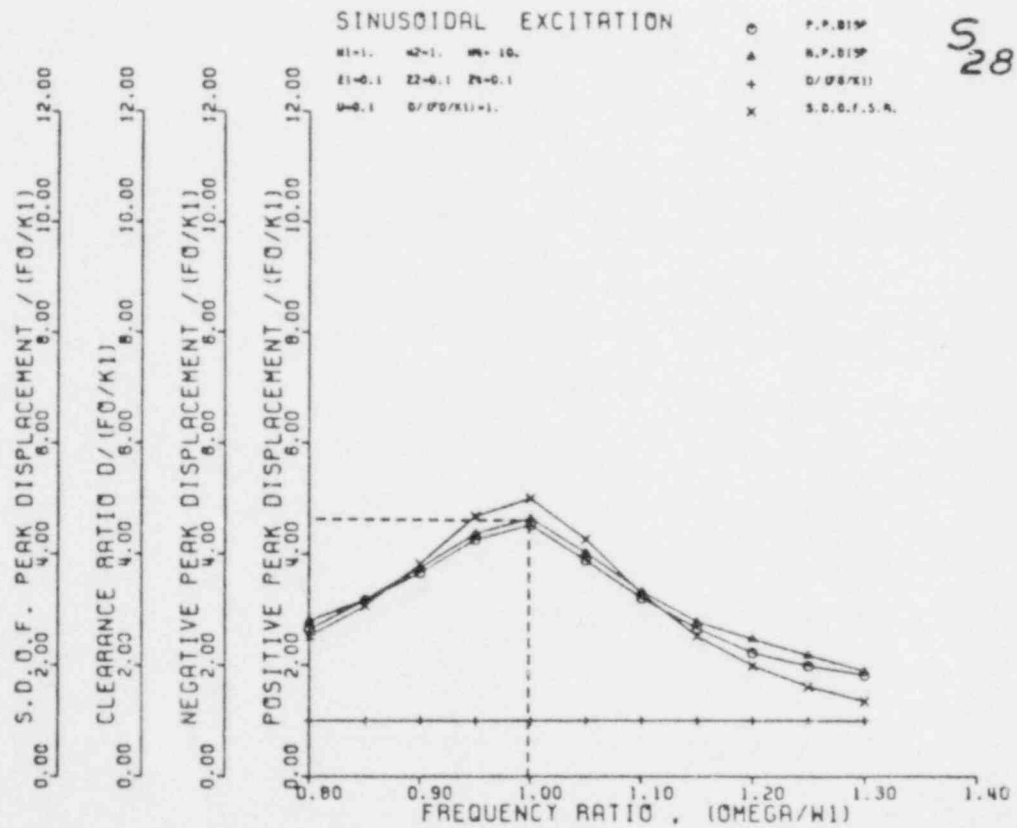

Figure A2.5 Response Spectra: Harmonic Excitation
(Section 4A, Figure S28, page 4A-17)

this example shows the important effect of the stiffness ratio K_2/K_1 in the case of periodic excitation.

EXAMPLE 3. VALVE

Dynamic vibration tests were performed on a valve assembly supplied by the Nuclear Regulatory Commission to USC. Results of a sinusoidal sweep test are shown in Figure A3.1. Here it can be seen that the fundamental frequency of the valve is about 19 Hz. The actual damping in the valve can be estimated by the half-power method.

Peak response = 25

$$\frac{25}{\sqrt{2}} = 17.68 \qquad \text{(i.e., "half-power point")}$$

The frequencies at which the power reduces to half of its maximum are

$$f_1 = 17.5 \quad , \quad f_2 = 20$$

Hence,

$$\zeta = \frac{1}{2}\frac{\Delta\omega}{\omega_n} = \frac{20 - 17.5}{2 \times 19} = 0.07 \approx 0.1$$

Therefore use $\zeta_1 = \zeta_2 = 0.1 = 10\%$

Assume the mass of the valve housing is equal to the mass of the actuator and therefore $\frac{M_2}{M_1} = 1.0$. Also assume that $\omega_2/\omega_1 = 5.0$, which implies that the housing is much stiffer than the valve actuator. If the valve is in the open position and subjected to dynamic excitation, the actuator may vibrate against the valve seat. Furthermore, if the valve opening is taken equal to the static deflection of the actuator $(D/(F_o/K_1) = 1)$, the data summary indicates that spectra chart S8 should be used for the analysis (see Figure A3.2). When the excitation frequency $\omega = 0.95\ \omega_1$, this chart can be used to determine that the maximum positive displacement is $1.28D/(F_o/K_1)$ and the masimum negative

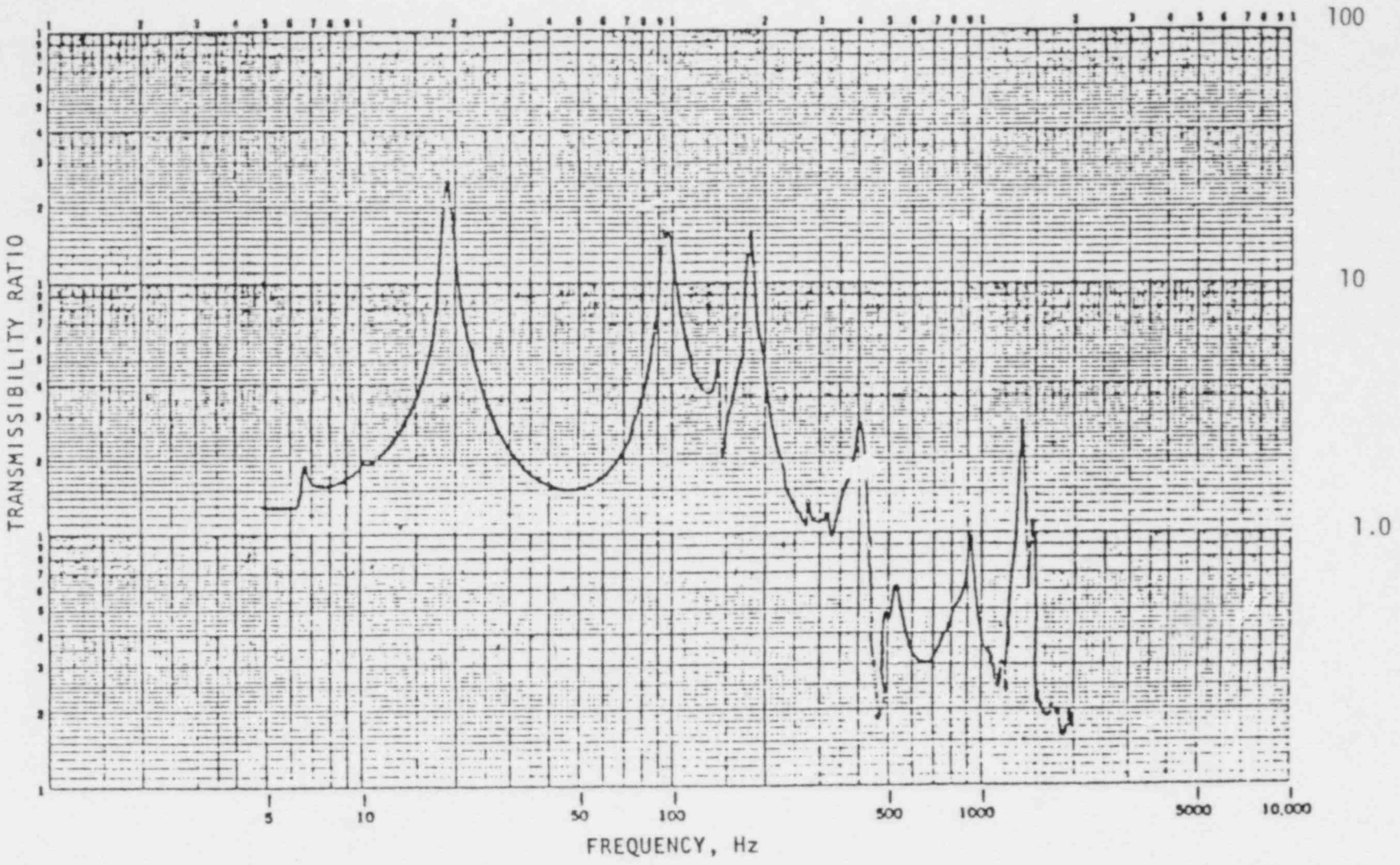

Figure A3.1
Response of Valve

displacement is $2.1D/(F_o/K_1)$. If the static displacement is taken as 0.5 in. ($D/(F_o/K_1) = 0.5$), this results in a positive displacement of 0.64 in. and a negative displacement of 1.05 in. (see Figure A3.3).

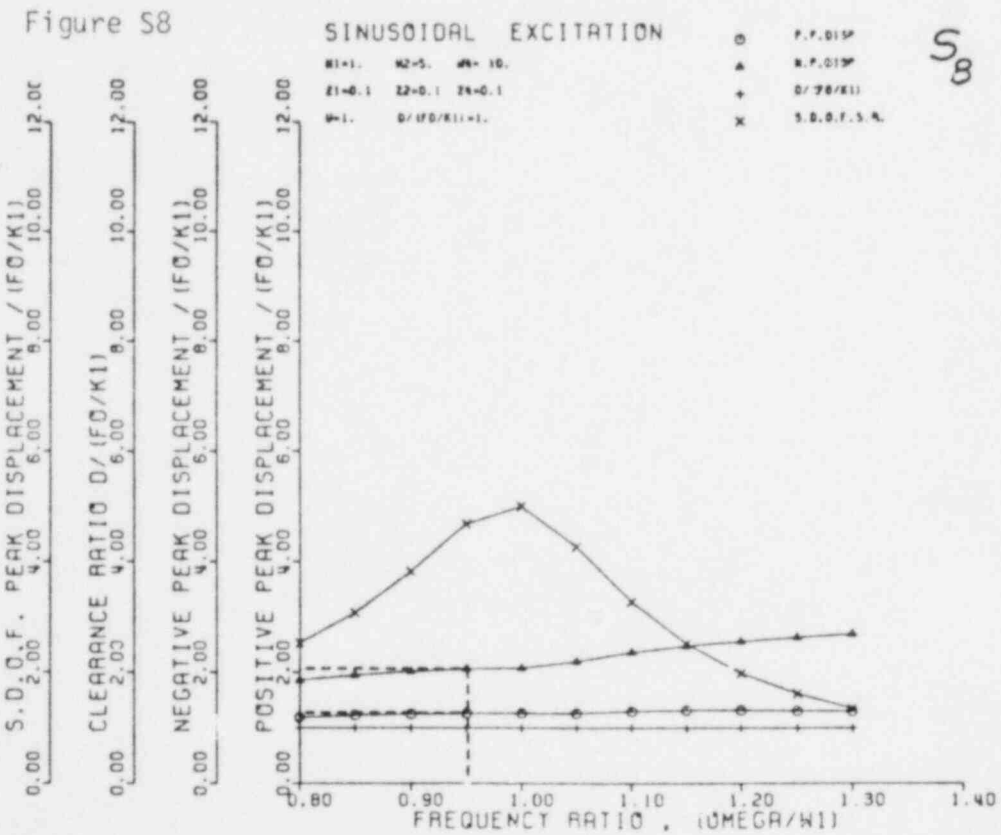

Figure A3.2

Response Spectra: Harmonic Excitation
(Section 4A, Figure S8, page 4A-7)

NRC FORM 335 (7-77)

U.S. NUCLEAR REGULATORY COMMISSION

BIBLIOGRAPHIC DATA SHEET

1. REPORT NUMBER (Assigned by DDC)
NUREG/CR-1067

4. TITLE AND SUBTITLE (Add Volume No., if appropriate)
Design Charts for a Class of Nonlinear Systems with Gaps under a Variety of Dynamic Loads

2. (Leave blank)

3. RECIPIENT'S ACCESSION NO.

7. AUTHOR(S)
J.C. Anderson and others

5. DATE REPORT COMPLETED
MONTH June YEAR 1979

9. PERFORMING ORGANIZATION NAME AND MAILING ADDRESS (Include Zip Code)
Civil Engineering Department
University of Southern California
Los Angeles, CA 90007

DATE REPORT ISSUED
MONTH November YEAR 1979

6. (Leave blank)

8. (Leave blank)

12. SPONSORING ORGANIZATION NAME AND MAILING ADDRESS (Include Zip Code)
General Reactor Safety Research
Nuclear Regulatory Research
Nuclear Regualtory Commission
Washington, D.C. 20555

10. PROJECT/TASK/WORK UNIT NO.

11. CONTRACT NO.
NRC-04-76-262

13. TYPE OF REPORT
Topical

PERIOD COVERED (Inclusive dates)
10/1/78-9/30/79

15. SUPPLEMENTARY NOTES

14. (Leave blank)

16. ABSTRACT (200 words or less)

An analytical investigation is made of the dynamic response of a multi-degree-of-freedom system with a displacement nonlinearity caused by a dead space gap. This class of problem can be used to model some of the mechanical equipment, piping, and components found in nuclear reactor facilities. The problem is discretized mathematically and numerical techniques are used to solve the resulting equations of motion. Displacement response spectra are developed for a variety of system parameters and dynamic loadings that include sinusoidal, random, and half-sine pulse. These response spectra form a library of design charts that provide useful information for designers and engineers.

17. KEY WORDS AND DOCUMENT ANALYSIS
Analytical
Nonlinear
Design
Spectra

17a. DESCRIPTORS
Computer model
Dynamic response
Geometric nonlinearity

17b. IDENTIFIERS/OPEN-ENDED TERMS

18. AVAILABILITY STATEMENT

19. SECURITY CLASS (This report)

21. NO. OF PAGES

20. SECURITY CLASS (This page)

22. PRICE
$